UNCLASSIFIED

UNLIMITED

DRES

CONTRACT REPORT 24-91

ADAPTATION OF A TRACKED VEHICLE PERFORMANCE MODEL NTVPM-85 TO NATO REQUIREMENTS

J.Y. Lee

Vehicle Systems Development Corporation

Ottawa

1991

DEFENCE RESEARCH ESTABLISHMENT SUFFIELD, RALSTON, ALBERTA

"This work was carried out for DRES under contract. The accuracy of the information presented herein is the responsibility solely of the contractor and is NOT to be construed as an Official Department of National Defence position unless so designated by other authorizing documents."

UNCLASSIFIED

CR 24-91

91-0236

VSDC

ADAPTATION OF A TRACKED VEHICLE PERFORMANCE MODEL
NTVPM-85 TO NATO REQUIREMENTS

BY

DR. J. Y. WONG

APRIL 1991

VEHICLE SYSTEMS DEVELOPMENT CORPORATION
OTTAWA, CANADA

ADAPTATION OF A TRACKED VEHICLE PERFORMANCE MODEL NTVPM-85 TO NATO REQUIREMENTS

FINAL REPORT

prepared for

Head

Vehicle Mobility Section

Defence Research Establishment Suffield

Department of National Defence, Canada

prepared by

Dr. J.Y. Wong

Vehicle Systems Development Corporation

Nepean, Ontario, Canada

under Contract

Serial No. W7702-9-R127/01-XSG

April 1991

TABLE OF CONTENTS

FOREWORD

The Vehicle Mobility Section (VMS), Defence Research Establishment Suffield, Canadian Department of National Defence, has entered into an agreement with NATO Panel II/GPE6 to contribute a snow module to the NATO Reference Mobility Model (NRMM). In this connection, VMS has contracted Vehicle Systems Development corporation (VSDC) to examine the feasibility of adapting the Nepean Tracked Vehicle Performance Model NTVPM-85 developed by VSDC to NATO requirements by accepting terrain data obtained using manual penetrometers, such as the Swiss Rammsonde. If this is proved to be successful, it will contribute substantially to NRMM by establishing a snow module for it, thus providing NATO with an important analytical tool for evaluating the over snow performance of tracked vehicles. This report describes the results of such a feasibility study.

The study was performed by Vehicle Systems Development Corporation, under contract (Serial No. W7702-9-R127/01-XSG) to the Canadian Department of National Defence through the Department of Supply and Services. The Principal Investigator was Dr. J.Y. Wong and the project team included Messrs. J. Preston-Thomas, S.T. Chen, and C.S. Smith. The Scientific Authority for the Contract was Dr. G.J. Irwin, Vehicle Mobility Section, Defence Research Establishment Suffield. The Science Contracting Officer was Mr. Don Pickles, Alberta/Northwest Territories Region, Department of Supply and Services.

ACKNOWLEDGEMENTS

Vehicle Systems Development Corporation acknowledges the assistance of Hagglunds Vehicle AB of Sweden in providing some of the vehicle data required for predicting the performance of a BV 206 using the Nepean Tracked Vehicle Performance Model NTVPM described in this report.

SUMMARY

//A study of the correlation between the measured and predicted vehicle performance over undisturbed and preconditioned snow using the Nepean Tracked Vehicle Performance Model NTVPM has been carried out.

It is shown that on undisturbed snow in Fernie, British Columbia, the performance of a BV 206 predicted by NTVPM-85 correlates very well with measured performance obtained in the field. On preconditioned snow, there is also a reasonable correlation between the measured vehicle performance and predicted one using NTVPM-85.

It is found that predictions of vehicle performance made by NTVPM-85 using pressure-sinkage data obtained with the Swiss Rammsonde and with the bevameter are comparable. This indicates that the pressure-sinkage data obtained using the Rammsonde can be used as input to NTVPM-85 for predicting tracked vehicle performance over snow.

It is shown that the latest version of the Nepean Tracked Vehicle Performance Model NTVPM-86, which takes into account fully the characteristics of roadwheel suspension systems, provides improved predictions of vehicle performance over snow where track sinkage is significant.

It is proposed that the computer simulation model NTVPM-85, using pressure-sinkage data obtained by the Rammsonde or the bevameter as input, be recommended to the NATO Panel II/GPE6 as an additional module to the existing NATO Reference Mobility Model for predicting tracked vehicle performance over snow. //

1. INTRODUCTION

The Nepean Tracked Vehicle Performance model NTVPM developed by Vehicle Systems Development Corporation, which currently has two versions: NTVPM-85 and NTVPM-86, is a comprehensive computer simulation model for predicting and evaluating the tractive performance of tracked vehicles over unprepared terrain. Its basic features have been validated over a variety of terrains including mineral terrain, muskeg and snow-covered terrain (Wong, 1986a and 1989a; Wong and Preston-Thomas, 1986 and 1988). NTVPM has been gaining increasingly wide acceptance by industry and governmental agencies. It has been used to assist Hagglunds Vehicle AB of Sweden in the development of a new generation of light armoured fighting vehicle (Combat Vehicle 90), in the further improvement of the performance of the all-terrain vehicle BV 206, and in the evaluation of competing designs for a proposed main battle tank (STRV 2000) for the Swedish Armed Forces (Wong, 1986b and 1989b; Wong and Preston-Thomas, 1989). It has also been used in evaluating the effects of design modifications on the mobility of the main battle tank Leopard C1 for the Canadian Department of National Defence and in the assessment of the mobility of a variety of container handling equipment used by the U.S. Marine Corps (Wong, 1986c, d, and e; Wong and Preston-Thomas, 1987a and c). More recently, it has been employed to assist an Asian company in the evaluation of competing designs for a light armoured fighting vehicle.

Vehicle Mobility Section (VMS) of the Defence Research Establishment Suffield (DRES) of the Canadian Department of National Defence has entered into an agreement with NATO Panel II/GPE6 to contribute a snow module to the NATO Reference Mobility Model (NRMM). It should be noted that currently NRMM can be used to evaluate the tractive performance of off-road vehicles on mineral terrain only, and does not have the capability of evaluating vehicle performance over snow.

The prime objective of the proposed snow module is to provide a user-friendly method for predicting the over snow performance of tracked vehicles using terrain data that can be conveniently obtained in the field. This would also serve, when combined with a geographic snow information system, as a tactical decision aid in the prediction of snow trafficability.

In the light of the objective noted above, VMS has contracted Vehicle Systems Development Corporation to examine the feasibility of adapting the Nepean Tracked Vehicle Performance Model NTVPM-85 to NATO requirements by accepting terrain data obtained using manual penetrometers, such as the Rammsonde. It should be noted that NTVPM-85 currently requires terrain parameters, including the pressure-sinkage and shear strength parameters, obtained using a bevameter as input.

To examine the feasibility of using terrain data obtained with manual penetrometers as input to NTVPM-85 for predicting the performance of tracked vehicles over snow, the following investigations were carried out:

A. The pressure-sinkage relationships of undisturbed and preconditioned snow covers in a test site in Fernie, British Columbia were measured using a Rammsonde cone penetrometer, a bevameter, and Rammsonde cones mounted on the bevameter assembly, and their characteristics were compared. The results of this investigation are described in a report entitled "Measurement and characterization of the pressure-sinkage relationships for snow obtained using a Rammsonde and a bevameter" by Dr. J.Y. Wong, October 1990 (Wong, 1990a).

B. The shear strengths of undisturbed and preconditioned snow covers in the test site were measured using a bevameter shear device and a hand-held shear device, and their characteristics were compared. The results of this study are described in a report entitled "Measurement of the shear strength of snow using a bevameter and a hand-held shear device," by Dr. J.Y. Wong, November 1990 (Wong, 1990b).

C. To facilitate the processing of terrain data obtained using the Rammsonde cone penetrometer, the bevameter and the hand-held shear device, a Terrain Data Analysis Software (TDAS) was developed. A description of this software package is given in a report entitled "User's guide to the VSDC Terrain Data Analysis Software (TDAS)," by C.T. Chen and Dr. J.Y. Wong, November 1990 (Chen and Wong, 1990).

D. Based on the pressure-sinkage data obtained using the Rammsonde cone penetrometer, the bevameter and the Rammsonde cones mounted on the bevameter assembly, as well as the shear strength data obtained using the bevameter shear device, the tractive performance of an all-terrain carrier BV206 over undisturbed and preconditioned snow covers in Fernie, British Columbia was predicted using the Nepean Tracked Vehicle Performance Model NTVPM-85. The predicted performance was compared with the measured one obtained in the same test site by Mining Resource Engineering Limited (MREL), under contract to Vehicle Mobility Section, Defence Research Establishment Suffield. It should be noted that Vehicle Systems Development Corporation did not participate in the field testing of the BV 206 and the processing of vehicle test data.

This report presents the results of a correlation study of the measured tractive performance of the all-terrain carrier BV206 over undisturbed and preconditioned snow covers and the predicted one using NTVPM-85 with terrain data obtained by the Rammsonde cone penetrometer and the bevameter. This study forms the basis for evaluating the adequacy of using terrain data obtained with the Rammsonde cone penetrometer as input to NTVPM-85 for predicting the over snow performance of tracked vehicles.

2. A REVIEW OF THE METHODS FOR PREDICTING TRACKED VEHICLE PERFORMANCE

To provide a proper perspective for the Nepean Tracked Vehicle Performance Model NTVPM-85, upon which the proposed snow module is to be based, a review of some of the methods currently available for predicting tracked vehicle performance is given below.

The track was first conceived in the 18th century, as a "portable railway" and tracked vehicles have been used on a large scale in agriculture, construction, off-road transport, and military operations since the turn of this century. However, for a long period of time, the development and design of tracked vehicles have been, by and large, guided by empiricism and the "cut and try" methodology. As economic and social conditions change with the rapid progress in technology, the "trial and error" approach to off-road vehicle development has become extremely inefficient and prohibitively expensive. Furthermore, new requirements for greater mobility over a wider range of terrain, and growing demands for energy conservation and environmental protection have emerged. This has led to the recognition of the necessity of establishing realistic mathematical models for vehicle-terrain systems that will enable the development and design engineer, as well as the procurement manager, to evaluate a wide range of options and to establish a rational basis for the selection of an optimum vehicle configuration for a given mission and environment.

To be useful to the development and design engineer and to the procurement manager, a mathematical model for tracked vehicle performance should take into account all major vehicle design and operational parameters as well as terrain characteristics. The performance of a tracked vehicle, usually defined by its motion resistance, tractive effort and drawbar pull as functions of slip, is directly related to the normal and shear stress distributions on the track-terrain interface. A central issue in the mathematical modelling of tracked vehicle performance is, therefore, the establishment of the relationship between the interacting forces on the track-terrain interface and vehicle design parameters and terrain characteristics.

A variety of mathematical models for predicting and evaluating tracked vehicle performance, ranging from entirely empirical to totally theoretical, has been developed over the years (Wong, 1989a). In the following a brief review of some of the methods currently in use is presented.

2.1 Empirical Methods

The interaction between an off-road vehicle and the terrain is very complex and difficult to model adequately. To circumvent this difficulty, empirical methods have been developed.

One of the well-known empirical methods for evaluating off-road vehicle performance is that developed by the U.S. Army Engineer Waterways Experiment Station (WES). In developing the method, a series of vehicles of interest were tested in a range of terrains considered to be representative and at the same time terrain conditions were measured using a cone penetrometer. The results of vehicle performance testing and terrain measurements were then empirically correlated, and a model, known as the WES VCI model, was proposed for predicting vehicle performance on fine- and coarse-grained inorganic soils (Rula and Nuttall, 1971). This model forms the basis for the subsequent developments of the AMC-71, AMC-74 and NRMM mobility models.

In the WES model, an empirical equation was established to calculate the mobility index (MI) of a vehicle in terms of certain vehicle design features. For instance, the mobility index for a tracked vehicle is defined as:

$$\text{Mobility Index} = \left[\frac{\text{Contact pressure factor} \times \text{weight factor}}{\text{track factor} \times \text{grouser factor}} + \text{bogie factor} - \text{clearance factor} \right] \times \text{engine factor} \times \text{transmission factor} \quad (2.1)$$

where

$$\text{Contact pressure factor} = \frac{\text{gross weight, lb}}{\text{areas of tracks in contact with ground, in.}^2}$$

Weight factor:

less than 50,000 lb	= 1.0
50,000 to 69,999 lb	= 1.2
70,000 to 99,999 lb	= 1.4
100,000 lb or greater	= 1.8

$$\text{Track factor} = \frac{\text{track width, in.}}{100}$$

Grouser factor:

Grousers less than 1.5 in. high	= 1.0
Grousers more than 1.5 in. high	= 1.1

$$\text{Bogie factor} = \frac{\text{gross weight, lb. divided by 10}}{\text{total number of bogies on tracks in contact with ground} \times \text{area, in.}^2\text{, of one track shoe}}$$

$$\text{Clearance factor} = \frac{\text{clearance, in.}}{10}$$

Engine factor:

$\geq$ 10 hp/ton of vehicle weight	= 1.0
< 10 hp/ton of vehicle weight	= 1.05

Transmission factor: Automatic = 1.0; Manual = 1.05

The mobility index (MI) was then empirically correlated to the vehicle cone index (VCI), which is the minimum soil strength in the critical soil layer defined by the rating cone index (RCI) for fine-grained soils for a specified number of passes of a vehicle, such as 1 pass or 50 passes.

Finally, the values of performance parameters of a tracked vehicle, such as the maximum drawbar pull coefficient, maximum slope negotiable and towed motion resistance coefficient, were empirically determined as functions of vehicle type, number of passes to be completed, and the excess of RCI over VCI (i.e., RCI-VCI) for fine-grained soils (or the cone index (CI) for coarse-grained soils).

Another empirical method for evaluating the mobility of tracked vehicles was suggested by Rowland (1972). He proposed the "mean maximum pressure (MMP)", which is defined as the mean value of the maxima occurring under all the roadwheel stations, as a criterion for evaluating the soft ground performance of off-road vehicles. Empirical equations were derived from vehicle test data for calculating the MMP for different types of track system.

He proposed that for link and belt tracks on rigid roadwheels,

$$MMP = \frac{1.26\ W}{2n_r\, A_l\, b\sqrt{t_t\, D}} \quad kN/m^2 \tag{2.2}$$

and for belt tracks on pneumatic tired road wheels,

$$MMP = \frac{0.5\ W}{2n_r\, b\sqrt{D\, f_t}} \quad kN/m^2 \tag{2.3}$$

W - vehicle weight, kN

n_r - number of wheel stations in one track

A_l - rigid area of link (or belt track cleat) as a proportion of track pitch multiplied by wheel width

b - track or pneumatic tire width, m

t_t - track pitch, m

D - outer diameter of roadwheel or pneumatic tire, m

f_t - radial deflection of pneumatic tire under load, m

To evaluate whether a vehicle with a particular value of MMP will have adequate mobility over a specific terrain, Rowland proposed a set of desired values of the mean maximum pressure for different terrain conditions. Table 2.1 shows the desired values of MMP suggested by Rowland.

Within the context of their intended purposes, the empirical models developed by WES and Rowland are useful in certain types of application. It should be pointed out, however, that strictly speaking, empirical relations are only valid within the specific conditions under which the tests were carried out. Thus, it is by no means certain that empirical relations can be extrapolated beyond the conditions under which they were originally obtained. It appears uncertain, therefore, that an entirely empirical approach could play a useful role in the evaluation of new vehicle design concepts or in the prediction of vehicle performance in new operational environments. Furthermore, an entirely empirical approach is only feasible where the number of variables involved in the problem is relatively small. If a large number of parameters are required to define the problem, then an empirical approach may not be cost-effective.

To provide a more general approach to the prediction and evaluation of tracked vehicle performance, other methods of approach have been developed.

Table 2.1 Desirable Values of Mean Maximum Pressure

Terrain	Mean Maximum Pressure (kN/m^2) Ideal (Multipass Operation)	Satisfactory	Maximum Acceptable (Mostly Trafficable at Single-Pass Level)
Wet fine grained soils			
Temperate	150	200	300
Tropical	90	140	240
Muskeg	30	50	60
Muskeg floating mat and European bogs	5	10	15
Snow	10	25-30	40

2.2 Theoretical Methods

In recent years, attempts have been made to apply the theory of plastic equilibrium, finite element technique, critical state theory and others to the analysis of vehicle-terrain interaction. Among them, the theory of plastic equilibrium is, perhaps, the most developed. One of the examples is the application of the theory of plastic equilibrium to the prediction of the draft of a two-dimensional soil cutting blade. The solution procedures have now been well documented (Hettiaratchi and Reece, 1974).

In the late sixties, an extensive experimental investigation into the physical nature of vehicle-terrain interaction under various operating conditions was carried out by Wong and Reece (1966) and Wong (1967). From the study, it was clearly established that failure zones were developed in dense soils under the action of a vehicle running gear and that there was a close correlation between the failure behaviour of soil and the performance of vehicle running gear. As a result of these findings, attempts have been made to apply the theory of plastic equilibrium to the evaluation of the performance of off-road vehicles (Karafiath and Nowatzki, 1978). The prediction procedure involves the solution of differential equations for the plastic equilibrium of the soil mass in the failure zones, based on the Mohr-Coulomb yield (failure) criterion. To initiate the solution process and to obtain unique solutions to particular problems, certain information on the vehicle-terrain interface, such as the interface friction angle or more generally the direction of the major principal stresses on the interface, must be specified or assumed at the outset. This is one of the most important issues and yet one of the most uncertain parts of the whole methodology.

The application of the theory of plastic equilibrium could provide a better insight into the physical nature of some aspects of the complex phenomenon of vehicle-terrain interaction and could establish a theoretical reference with which the actual performance of cross-country vehicles may be compared under certain idealized conditions. It should be recognized, however, that there are severe limitations to the application of the theory to the prediction and evaluation of vehicle mobility in practice (Wong, 1979).

Firstly, the theory of plastic equilibrium as presently applied is based on the assumption that the terrain behaves like a rigid, perfectly plastic material. This means that the terrain does not deform significantly until the stresses within certain boundaries reach a certain level at which failure occurs. Beyond this point, the strain increases rapidly, while the stress remains constant. Although dense sand and the like may exhibit behaviour close to that of a rigid, perfectly plastic material, a wide range of natural terrains encountered in cross-country operations, such as snow and muskeg, have a high degree of compressibility, and their behaviour does not conform to that of a rigid, perfectly plastic material. Consequently, failure zones in these terrains under vehicular loads do not develop in a manner similar to that assumed in the theory, and the sinkage of vehicle running gear is primarily due to the compression of the terrain and not due to the plastic flow of the terrain material. From a vehicle mobility viewpoint, terrains with a high degree of compressibility are of greater concern to vehicle designers and users than dense sand and the like. Thus, the usefulness of the methodology based on the theory of plastic equilibrium in vehicle mobility study is severely limited in practice. Furthermore, the theory of plastic equilibrium is mainly concerned with the prediction of the maximum load that the vehicle can exert on the terrain without causing failure. Consequently, the deformation of the terrain as a result of the application of load by the vehicle, which is of importance to the evaluation of vehicle performance, cannot be predicted.

Secondly, as mentioned previously, to initiate the numerical procedures to predict the performance of vehicle running gear based on the theory of plastic equilibrium, certain information on the vehicle running gear-terrain interface, such as the interface friction angle, must be specified at the outset. The approaches to specifying the required boundary conditions as presently developed are primarily empirical in nature (Karafiath and

Nowatzki, 1978). Thus, even though an elaborate numerical procedure has been formulated for the evaluation of vehicle mobility, the solutions to any particular problem still heavily rely on either empirical inputs or assumed boundary conditions on the vehicle-terrain interface, some of which do not necessarily have any justifiable theoretical basis.

Because of the problems mentioned above, current methods based on the theory of plastic equilibrium are not capable of providing a practical engineering tool for the evaluation of cross-country vehicle mobility in the field.

Another theoretical approach to the prediction of vehicle performance over unprepared terrain is based on the finite element method (Yong and Fattah, 1976). Applications of this method to the solution of vehicle-terrain interaction problems require either the stress or displacement boundary conditions on the interface to be specified at the outset. As pointed out by Wong (1977), when the stress boundary conditions on the vehicle running gear-terrain interface are specified, the performance of the running gear is completely defined, since performance parameters, such as drawbar pull, motion resistance and input torque to the sprocket or wheel can readily be computed from the specified normal and tangential stresses at the interface using simple integration. Consequently, there is no need whatsoever to follow these approaches to determine the terrain response and then to predict the performance of the running gear. If, on the other hand, displacement boundary conditions at the vehicle-terrain interface are used to initiate the solution process then detailed information on the deformation pattern of the terrain adjacent to the vehicle-terrain interface must be known at the outset, usually through experiments. Thus, in essence, this solution process begins with acquiring terrain deformation data for specifying the displacement boundary conditions as input, then proceeds to the manipulation of the numerical approximation procedures based on the finite element method, and ends up with providing information on terrain response and vehicle performance that could have been directly obtained during the data acquisition phase at the beginning of the solution process.

In a method developed by Karafiath (1984) for predicting the sinkage and motion resistance of tracked vehicles using the finite element technique, the normal pressure distribution on the track-terrain interface is again required as input. This indicates that in general current methods based on the finite element technique do not provide a complete and self-contained procedure for predicting off-road vehicle performance. They do not address the central issue of vehicle performance modelling and the major concern of the development and design engineer, that is, predicting vehicle performance using vehicle design parameters and terrain characteristics as direct inputs. Also, in these models, the design features of the vehicle system, such as, track system configuration, roadwheel arrangements, track design and initial track tension, are not directly taken into account in the analysis of tack-terrain interaction. Furthermore, in many of these theoretical models, the stress-strain relationship and the strain hardening behaviour of the terrain are assumed to be similar to those of metals (Karafiath, 1984). However, very little experimental evidence has so far been produced to support the validity of these assumptions for natural terrains, particularly for marginal terrains where vehicle mobility is of major concern. It appears, therefore, that the usefulness of the theoretical models for off-road vehicle performance developed so far is rather limited in practice, particularly in the development and design processes.

2.3 Methods for Parametric Analysis

One of the better known methods for parametric analysis of tracked vehicle performance is that originally developed by Bekker (1969). In this method, the track in contact with the terrain is assumed to be similar to a rigid footing. If the centre of gravity of the vehicle is located at the mid-point of the contact area, the normal pressure distribution may be taken as uniform, as shown in Fig. 2.1. On the other hand, if the centre of gravity of the vehicle is located ahead or behind the mid-point of the contact area, a sinkage distribution of trapezoidal form may be assumed. Based on the

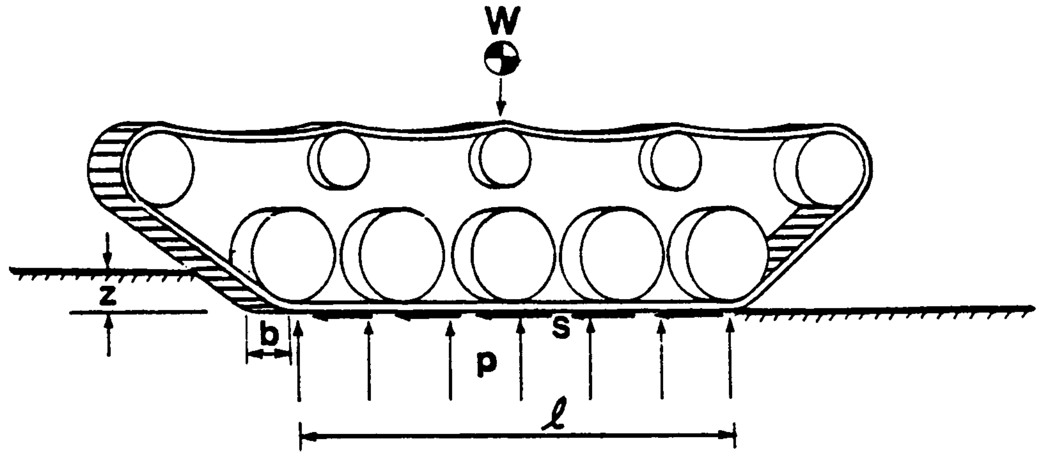

$$p = \frac{W}{2b\ell}$$

$z = f(p)$

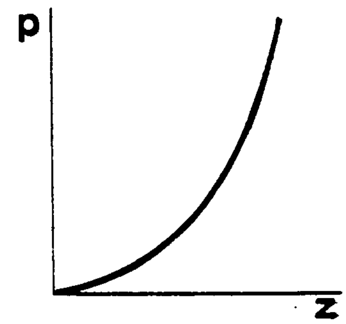

$s = f(p, j)$

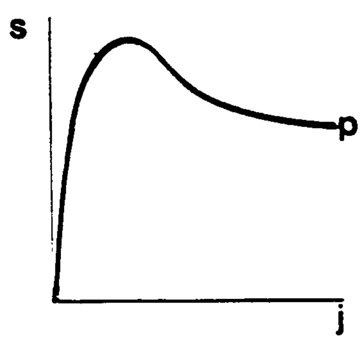

Fig. 2.1 A conventional method for predicting tracked vehicle performance

assumptions mentioned above, and making use of the pressure-sinkage relationship obtained from the bevameter, the sinkage of the track can be predicted.

For a track with uniform contact pressure p, the sinkage z_0 is given by

$$z_0 = \left(\frac{p}{k_c/b + k_\phi}\right)^{1/n} = \left(\frac{W/bl}{k_c/b + k_\phi}\right)^{1/n} \tag{2.4}$$

where b and l are width and contact length of the track, respectively, W is the normal load on the track, and k_c, k_ϕ and n are the pressure-sinkage parameters in the Bekker pressure-sinkage equation (Bekker, 1969).

The motion resistance R_c of the track due to terrain compaction can then be derived from the work done in compacting the terrain and making a rut of depth z_0

$$R_c = \frac{1}{(n+1)\, b^{1/n}\, (k_c/b + k_\phi)^{1/n}} \left(\frac{W}{l}\right)^{(n+1)/n} \tag{2.5}$$

In very soft ground with noticeable sinkage, Bekker suggested that a bulldozing resistance should be taken into account and that it may be estimated using the retaining wall theory of soil mechanics.

To predict the tractive effort, use is made of the shear stress-displacement relationship of the terrain obtained using a bevameter (Fig. 2.1). If the ground pressure is uniformly distributed and the shear stress-shear displacement relationship is described by the simple exponential equation, the tractive effort F of a track can be defined as (Bekker, 1969)

$$F = b\int_0^l \left(c + \frac{W}{bl}\tan\phi\right)\left(1 - e^{-ix/K}\right)dx$$
$$= (Ac + W\tan\phi)\left[1 - \frac{K}{il}\left(1 - e^{-il/K}\right)\right] \tag{2.6}$$

where A is the contact area of the track, c, ϕ and K are cohesion, angle of shearing resistance, and shear deformation modulus, respectively.

From the predicted tractive effort and motion resistance, the drawbar pull as a function of slip and the overall tractive performance of the vehicle can be determined.

Experimental evidence has shown that in general the assumed ground pressure distribution described above is not realistic, particularly for tracked vehicles with high ratios of roadwheel spacing to track pitch designed for high speed operations, such as military vehicles. Ground pressure under these vehicles is usually concentrated under the roadwheels and is far from uniform. Consequently, performance predictions using the method described above will be unrealistic, particularly with respect to sinkage, motion resistance and tractive effort in soft terrain.

In an attempt to improve the prediction of ground pressure distribution under a track, Bekker performed a pioneering theoretical study more than three decades ago (Bekker, 1956). The analysis is intended for the prediction of static ground pressure distribution when the vehicle is at rest. The effect of vehicle weight, track width, roadwheel spacing and the pressure-sinkage relationship of the terrain were taken into account. The study was, however, limited to the analysis of the shape of the track span between two roadwheels, simplified as knife-edge supports, in a terrain with a linear pressure-sinkage relationship. The effect of roadwheel diameter, suspension characteristics and other design factors was not included in the analysis.

In 1981, an improved method for predicting the static ground pressure distribution was developed by Garber and Wong (1981). In the analysis, the major design features of a tracked vehicle, such as the dimensions, spacing and number of roadwheels, vehicle weight, track dimensions, initial track tension, and characteristics of the suspension and track tensioning device, were taken into consideration. The analysis can accommodate terrain with a linear or non-linear pressure-sinkage relationship. Based on a detailed examination of the interaction between the track and the terrain, the interrelationships of vehicle design parameters, terrain conditions, and static ground pressure distribution under a track were established. Figure 2.2 shows the predicted static ground pressure of various tracked vehicles on different types of terrain, obtained using the analytical method developed by Garber and Wong (1981).

It can be seen that the analytical method for predicting the static ground pressure developed by Garber and Wong can serve a useful purpose in differentiating the potential performance of vehicles of different designs and in determining the relative significance of the effects of various vehicle design parameters on ground pressure distribution. It should be pointed out, however, that when a tracked vehicle is in straight line motion, a terrain element under the track is subject to the repetitive loading of consecutive roadwheels. The response of the terrain to repetitive loading should, therefore, be taken into account in predicting the ground pressure distribution under a moving vehicle. Furthermore, for a moving tracked vehicle, shear stresses will be developed on the track-terrain interface. To develop a comprehensive model for predicting the tractive performance of tracked vehicles, these factors should be taken into consideration.

Based on the brief review given above it can be seen that a number of the methods developed so far are either empirical or based upon assumptions that are not necessarily realistic. Therefore, there is a need for the development of a prediction method that takes into account all major factors of vehicle-terrain interaction in a realistic manner. To satisfy this need, a comprehensive mathematical model has been developed

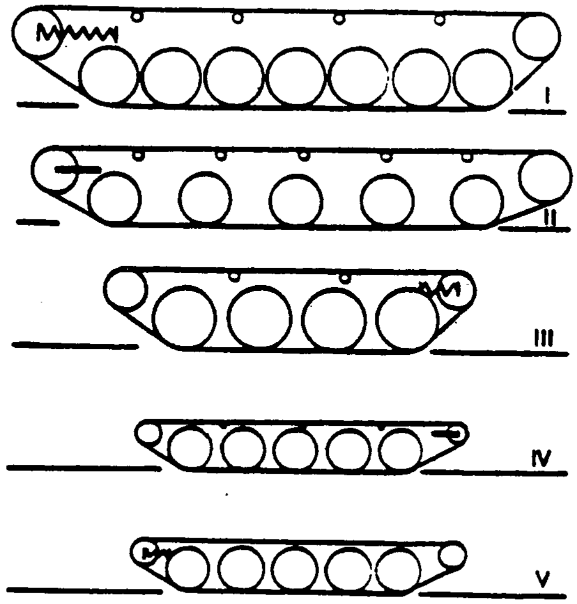

Schematic views of the track systems under consideration.
(I) The tensioning wheel is located in the front.
(II) The tensioning wheel is located in the front and fixed.
(III) The tensioning wheel is located in the rear.
(IV) The tensioning wheel is located in the rear and fixed.
(V) The tensioning wheel is located in the front.

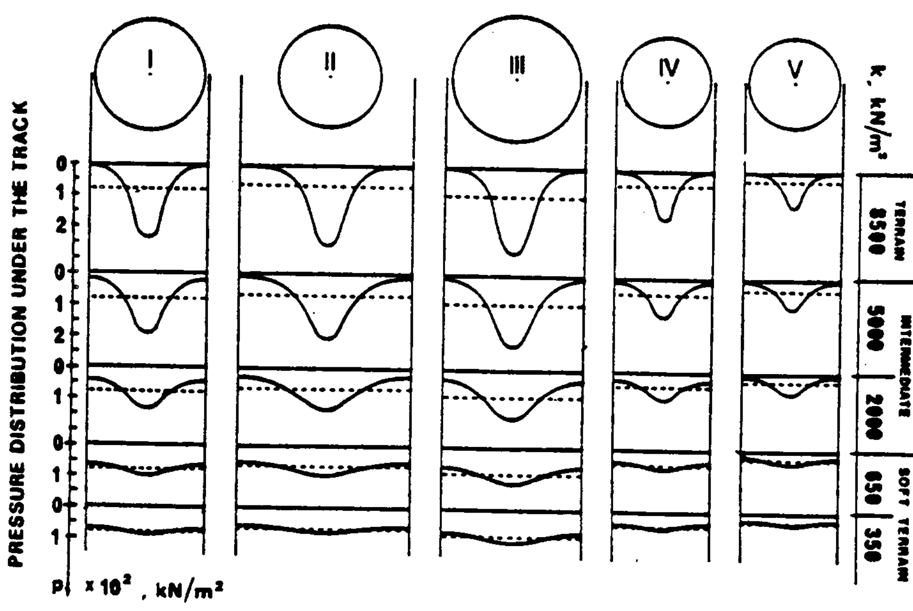

Fig. 2.2 Static normal pressure distribution under various track systems over different terrains

by Wong et al (Wong, 1986a, 1989a; Wong, Garber and Preston-Thomas, 1984; Wong and Preston-Thomas, 1986, 1988).

3. BASIC FEATURES OF THE NEPEAN TRACKED VEHICLE PERFORMANCE MODEL NTVPM

Based on the review given in the preceding section, it appears that most of the methods developed previously for predicting the performance of tracked vehicles are either of empirical nature or based upon assumptions that are not necessarily realistic. With a growing demand for improved mobility over a wider range of terrains in resource and transportation industries and in military operations, there is an increasing need for a comprehensive and yet realistic mathematical model to guide the development and design of tracked vehicles to meet new requirements.

To be useful to the development and design engineer, as well as the procurement manager, a mathematical model for tracked vehicle performance should take into account all major vehicle design parameters and terrain characteristics. A model, referred to as the Nepean Tracked Vehicle Performance Model NTVPM, that satisfies these requirements has been developed (Wong, 1986a, 1989a; Wong and Preston-Thomas, 1986, 1988). It takes into account all major design parameters of the vehicle, including the track system configuration, number of roadwheels, dimensions of roadwheels, roadwheel spacing, track dimensions, initial track tension, track longitudinal elasticity, suspension characteristics, location of the centre of gravity, vehicle belly (hull) shape, and sprocket, idler and supporting roller arrangements. Terrain characteristics, such as the pressure-sinkage and shearing characteristics and the response to repetitive loading, are also taken into consideration. The model can be used to predict the normal and shear stress distributions on the track-terrain interface, and the external motion resistance, tractive effort, drawbar pull and tractive efficiency of the vehicle as functions of track slip. It can be employed to evaluate the tractive performance of single unit tracked vehicles as well as two-unit tracked vehicles with articulated steering. The basic features of the model have been verified by means of full-scale tests made with instrumented vehicles on various types of terrain, including mineral terrain, muskeg and snow.

The model is particularly suited for the evaluation of competing designs and for the examination of the effects on performance of design modifications and changing operating environment. It can play a significant role in the following:

A) optimization of tracked vehicle design;

B) evaluation of tracked vehicle candidates for a given mission and environment;

C) proper interpretation of vehicle test results.

The basic approach to the development of the model is outlined below.

3.1 Terrain Input for the Simulation Model

To develop a realistic model for tracked vehicle performance, the mechanical behaviour of the terrain, which forms an integral part of the input, should be measured under loading conditions similar to those exerted by a tracked vehicle. Among the various terrain measuring techniques currently available, the bevameter technique pioneered by Bekker (1969) appears to provide a close approximation to the loading conditions of a tracked vehicle. Accordingly, in the development of the simulation model NTVPM terrain data measured with a bevameter was used. The bevameter is designed to perform two basic types of test. One is the plate penetration test and the other is the shear test. To reduce the uncertainty in extrapolating terrain data measured by the bevameter to the prediction of the performance of full-size vehicles, the size of the test piece used in the plate penetration test should be comparable to that of the contact area of a track link. Also, the shear ring used to perform the shear test should be made as large as practicable. Based on the pressure-sinkage relationship obtained from plate penetration tests, vehicle sinkage and motion resistance can be predicted. On the other hand, based on the results of shear tests, the tractive effort-slip characteristics and the maximum traction of a vehicle may be estimated. Since an element of the terrain under a moving track is subject to the repetitive loading of consecutive roadwheels, the responses of the terrain to repetitive loading are also taken into account in the simulation model.

In summary, the Nepean Tracked Vehicle Performance Model NTVPM requires the following terrain data as input:

A. pressure-sinkage relationships;

B. shear strengths and shear stress-shear displacement relationships;

C. responses of the terrain to repetitive loadings.

3.2 Approach to the Development of the Simulation Model

When a tracked vehicle rests on a hard surface the tracks lie flat on the ground. In contrast, when the vehicle travels over a deformable terrain the normal load applied through the track system causes the terrain to deform. The track segments between the roadwheels take up load, and as a result they deflect and have the form of a curve, as shown in Fig. 3.1. The actual length of the track in contact with the terrain between the front and rear roadwheels increases in comparison with that when the track rests on a firm ground. This causes a reduction in the sag of the top run of the track and a change in track tension. Furthermore, the passage of each consecutive roadwheel will usually cause additional sinkage, and the vehicle may assume a nose-up attitude.

It should also be pointed out that when a tracked vehicle is travelling in a straight line, an element of the terrain beneath the track is first subject to the load applied by the leading roadwheel. When the leading roadwheel has passed, the load on the terrain element is released. Load is reapplied as the second roadwheel rolls over it. A terrain

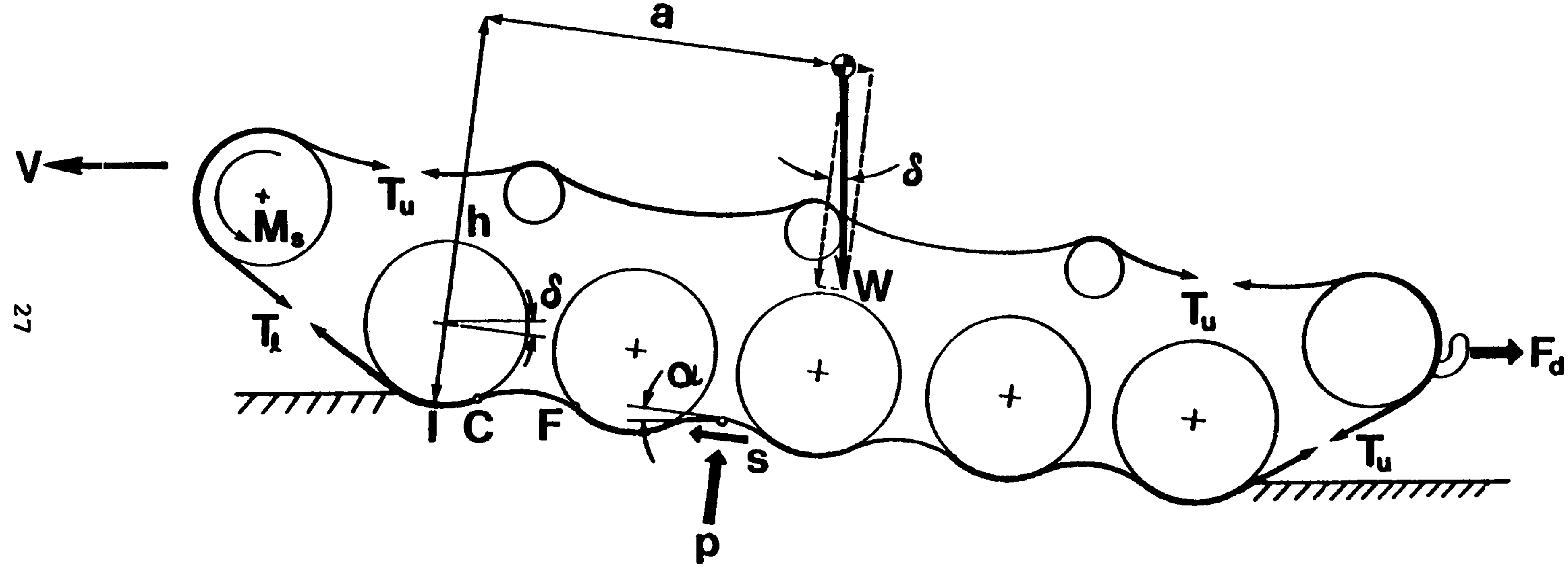

Fig. 3.1 Forces acting on a track system

element under the track is thus subject to the repetitive loading of consecutive roadwheels. The loading-unloading-reloading cycle continues until the rear roadwheel of the vehicle has passed over it. To predict the normal pressure distribution under a moving tracked vehicle, the pressure-sinkage relation and the response to repetitive loading of the terrain, as discussed in the preceding section, must be known.

When the terrain characteristics are known, the prediction of the normal pressure distribution is reduced to the determination of the shape of the deflected track in contact with the terrain. To achieve this, the mechanics of track-terrain interaction has to be examined.

In an initial model known as CTVPM developed under the auspices of the Canadian Department of National Defence in 1984, the following assumptions were made in the analysis of track-terrain interaction (Wong, Garber and Preston-Thomas, 1984):

A. The track is equivalent to a flexible belt. This assumption is considered to be reasonable for rubber-belt type tracks and for link tracks with relatively short track pitch designed for high-speed operations, such as those used in combat vehicles;

B. The track is inextensible;

C. In determining the sinkage of the track under the roadwheels, the effects of the independent suspension of the roadwheels are neglected. This means that the roadwheels are rigidly connected to a common bogie frame and that the sinkage of the first roadwheel together with the attitude of the track system defines the sinkages of subsequent roadwheels. The vehicle body is assumed to be suspended by springs attached to the bogie frame.

In 1985, under the auspices of Vehicle Systems Development Corporation, Nepean, Ontario, Canada, an improved computer simulation model known as NTVPM-85 was developed (Wong, 1986a, f, Wong and Preston-Thomas, 1986). In this model, the track is no longer assumed to be inextensible, and the track longitudinal elasticity, which is defined as the tension per unit longitudinal strain of the track, is taken into account. The track longitudinal elasticity affects the tension distribution in the track and as a result influences the performance of the vehicle to a certain extent over marginal terrain.

Over highly compressible terrain, such as deep snow, the track sinkage may be greater than the ground clearance of the vehicle. If this occurs, the belly (hull) of the vehicle will be in contact with the terrain surface and will support part of the vehicle load. This will reduce the load carried by the tracks and will adversely affect the traction of the vehicle. Furthermore, the belly contact will give rise to an additional drag component - the belly drag. The problem of belly contact is of importance to vehicle mobility. Quite often the reduction in traction and the increase in the total drag due to belly contact will lead to immobilization of the vehicle. In NTVPM-85, the characteristics of belly-terrain interaction are taken into account.

Further developments in the modelling of track-terrain interaction have been carried out by Vehicle Systems Development Corporation since 1986, resulting in the formulation of a new model known as NTVPM-86 (Wong and Preston-Thomas, 1988, Wong, 1989a). In this model, the roadwheels are no longer assumed to be rigidly connected, and the characteristics of the independent suspension of the roadwheels are fully taken into account. Furthermore, the non-linear tension-elongation characteristics of the track link have been taken into consideration. Figure 3.2 shows the measured relationships between the tension and elongation of the track links of a US main battle tank, a European main battle tank, a US military logistic vehicle, a European light armoured fighting vehicle, and a US armoured personnel carrier. The inclusion of the non-linear tension-elongation relationship of the track makes NTVPM-86 even more realistic. Furthermore the algorithms that implement the mathematical model on computers have been greatly improved, as compared with CTVPM and NTVPM-85.

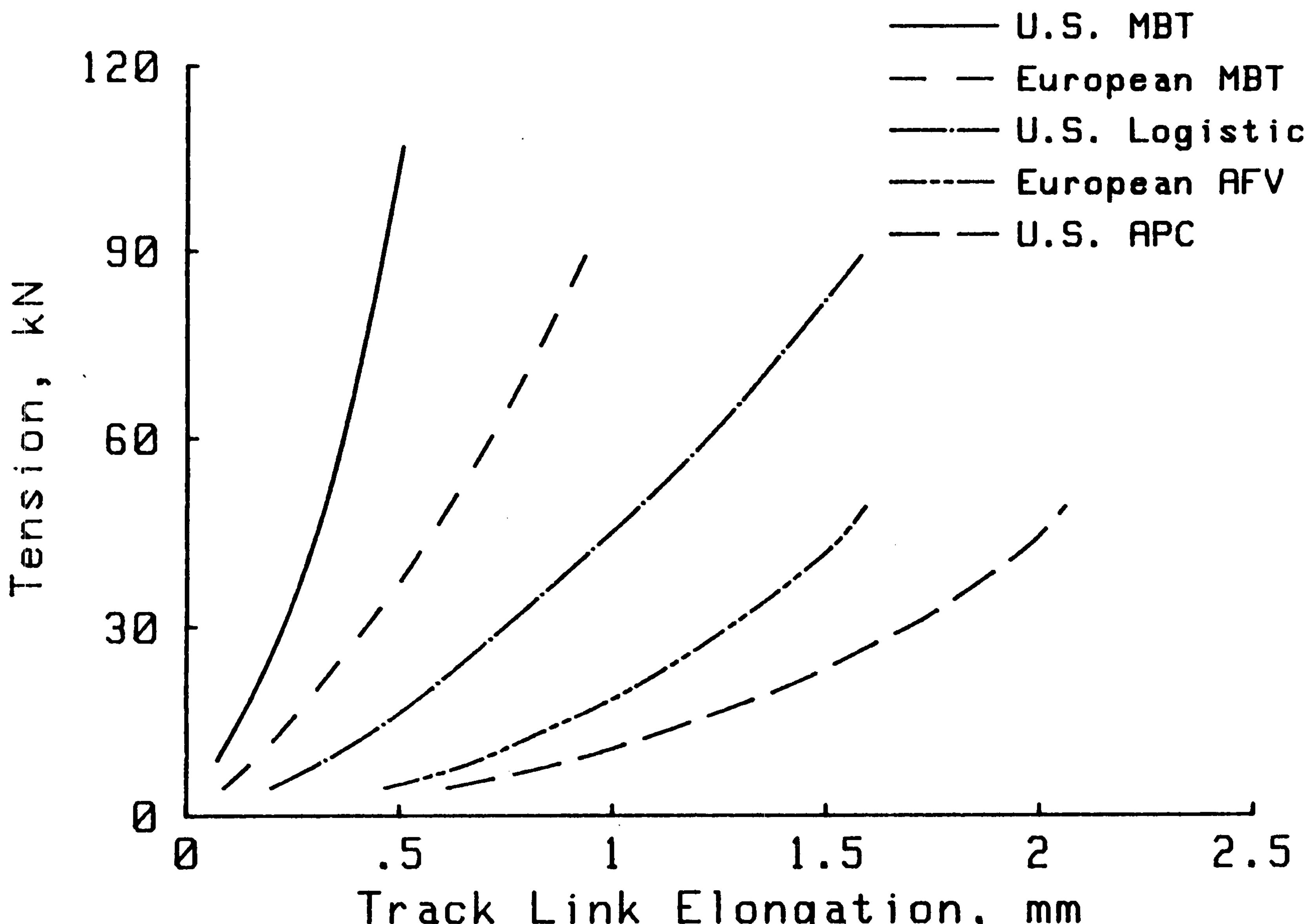

Fig. 3.2 Tension-elongation relationships for various types of track link

Based on the assumptions for the respective models, the mechanics of track-terrain interaction is analyzed, and a set of equations for the equilibrium of the forces and moments acting on the track system, and for the evaluation of the overall track length are derived. They establish the relationship between the shape of the deflected track in contact with the terrain and vehicle design parameters and terrain characteristics. The solution to this set of equations defines the sinkages of the roadwheels, the trim angle of the vehicle, the track tension and the track shape in contact with the ground. From these, the normal pressure distribution under a moving tracked vehicle can be determined.

To predict the shear stress distribution under the track, the shear stress-shear displacement relationship of the terrain and its response to repetitive shearing are used as input to the analysis of the characteristics of track-terrain shearing. The shear displacement developed under a flexible track as a function of slip can be determined through a kinematic analysis of the track based on the concept of slip velocity (Wong, 1978). From these, the shear stress distribution under a moving track can be predicted.

After the normal pressure and shear stress distributions have been determined, the external motion resistance, thrust and drawbar pull as functions of slip can then be predicted. The external motion resistance is calculated by integrating the horizontal component of the normal pressure over the contact area, while the thrust is determined by integrating the horizontal component of the shear stress over the entire track-terrain interface. The drawbar pull is obtained by subtracting the external motion resistance from the thrust.

In should be reiterated that in NTVPM-85, the roadwheels are assumed to be rigidly connected with a common bogie frame and that the vehicle body is assumed to be suspended with springs attached to the bogie frame. This type of arrangement is similar to that in some tracked vehicles used in construction industry and agriculture. NTVPM-86, on the other hand, takes into account the characteristics of the independent suspension of the roadwheels. Torsion bar, hydropneumatic and other types of independent suspension systems can be modelled.

A detailed description of the Nepean Tracked Vehicle Performance Model NTVPM, including both NTVPM-85 and NTVPM-986, is presented by Wong (1989a).

3.3 Experimental Substantiation of the Basic Features of the Simulation Model

To validate the basic features of the model, the normal pressure and shear stress distributions and the drawbar pull-slip characteristics of a tracked vehicle (an M113A1 armoured personnel carrier) were predicted over a variety of terrains, including sandy, organic (muskeg) and snow-covered terrains (Wong, 1989a). The tractive performance of the test vehicle over these terrains was also measured (Wong, 1989a).

Figure 3.3 shows a typical record of the parameters monitored during a test, which include ground contact pressure on various locations of the track link, distance as measured by the fifth wheel, sprocket revolutions, vehicle body and roadwheel displacements, time and drawbar pull.

The measured normal pressure on the rubber pad of the track and the drawbar pull-slip curves of the test vehicle over various types of terrain are shown in Figs. 3.4-3.7 and Figs. 3.8-3.10 respectively. The predicted normal pressure on the rubber pad of the track and the predicted drawbar pull-slip curves of the vehicle are also shown in the figures.

A comparison of the measured performance of the test vehicle and the predicted one using the simulation model NTVPM is made and described below.

1. Comparisons between the predicted normal pressure distributions obtained using the computer simulation model NTVPM-85 and the measured ones

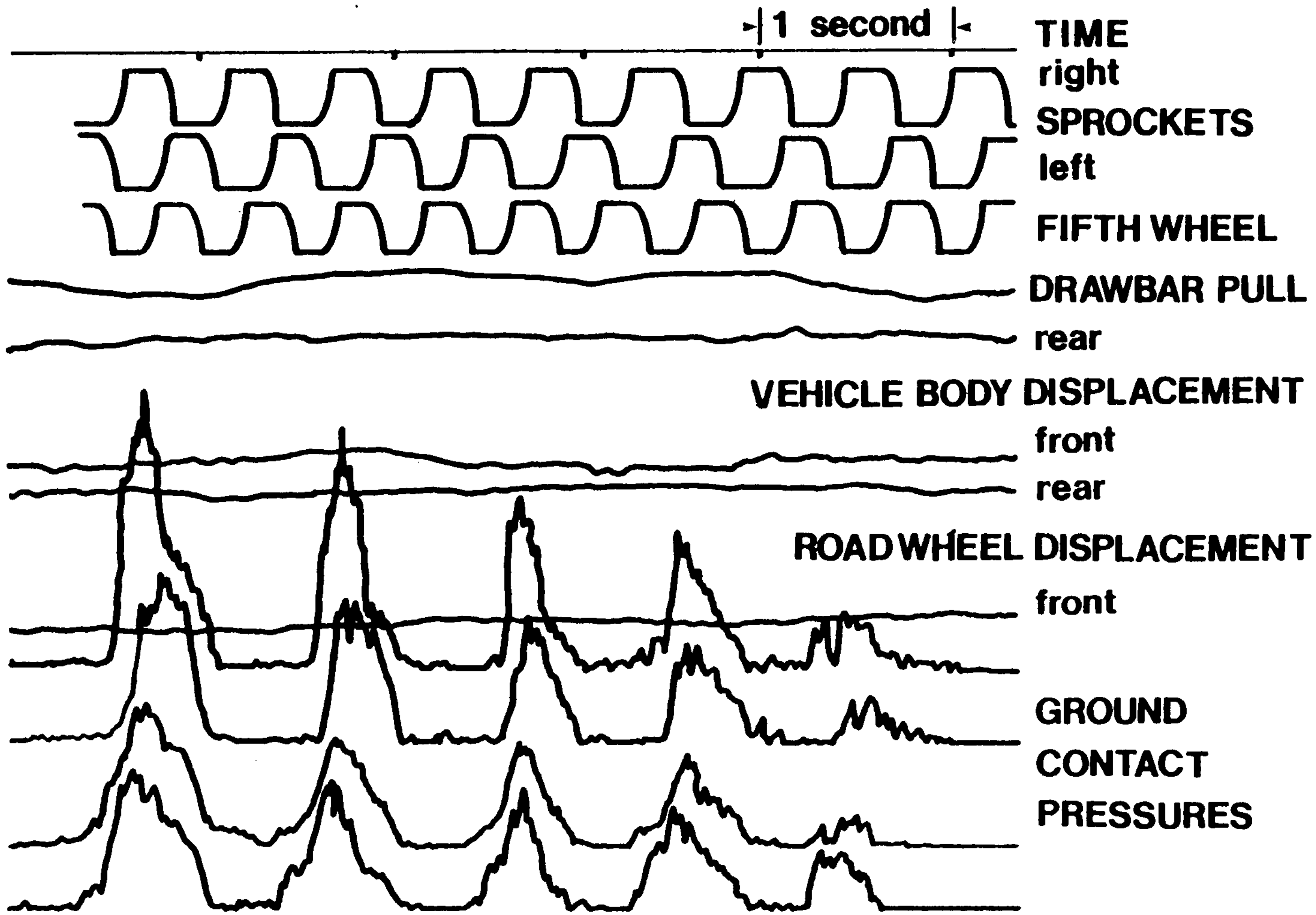

Fig. 3.3 An Oscillograph Record Showing the Parameters Monitored during Field Testing of an M113

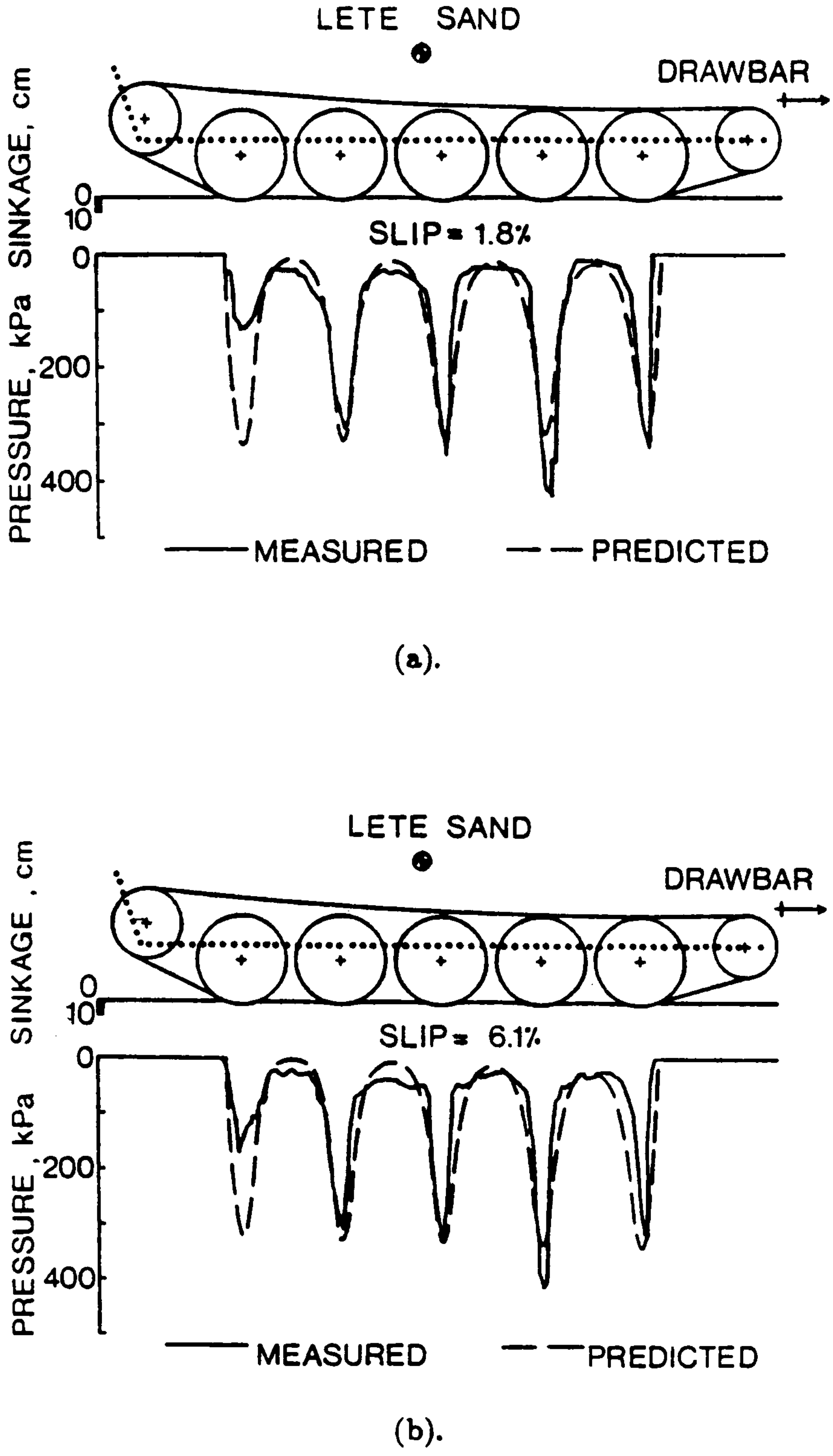

Fig. 3.4 Predicted and measured normal pressure under the track pad over LETE sand at (a) 1.8% and (b) 6.1% slip.

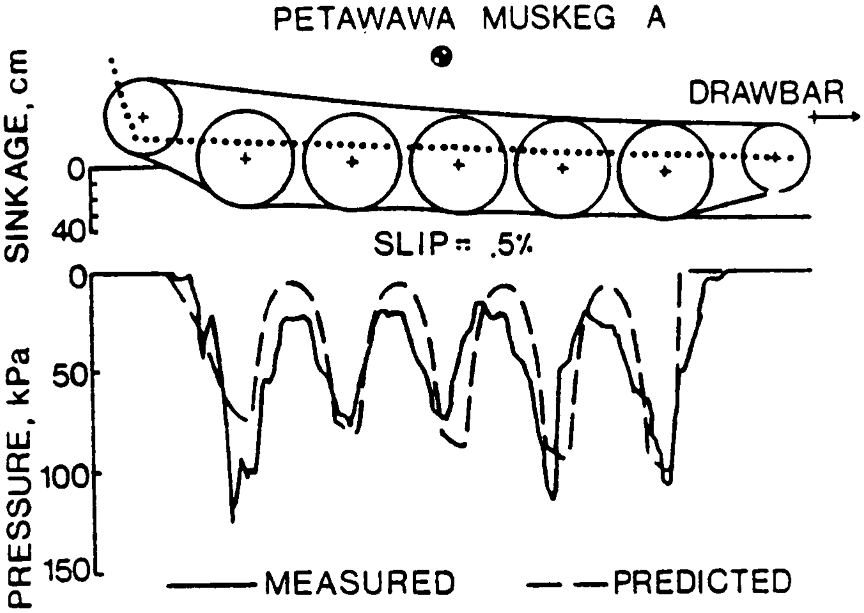

(a).

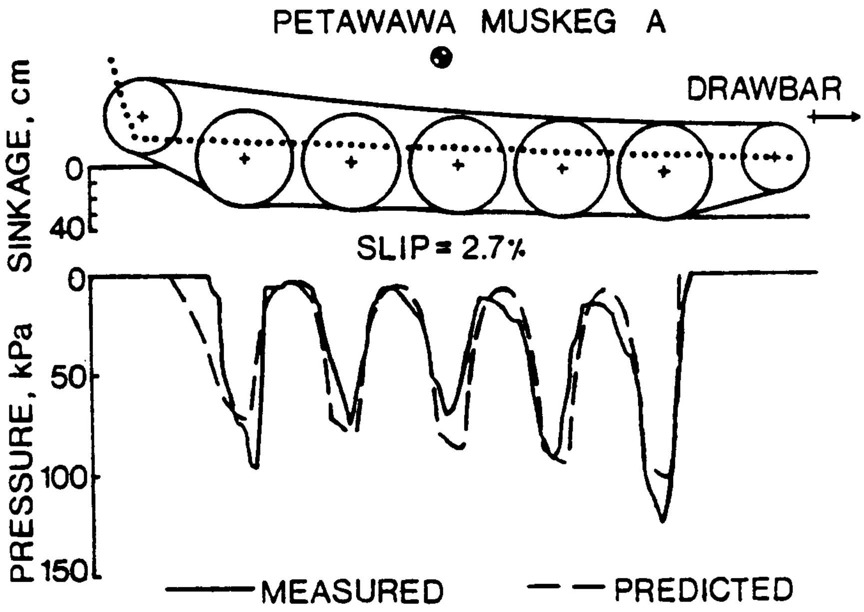

(b).

Fig. 3.5 Predicted and measured normal pressure under the track pad over Petawawa muskeg A at (a) 0.5% and (b) 2.7% slip.

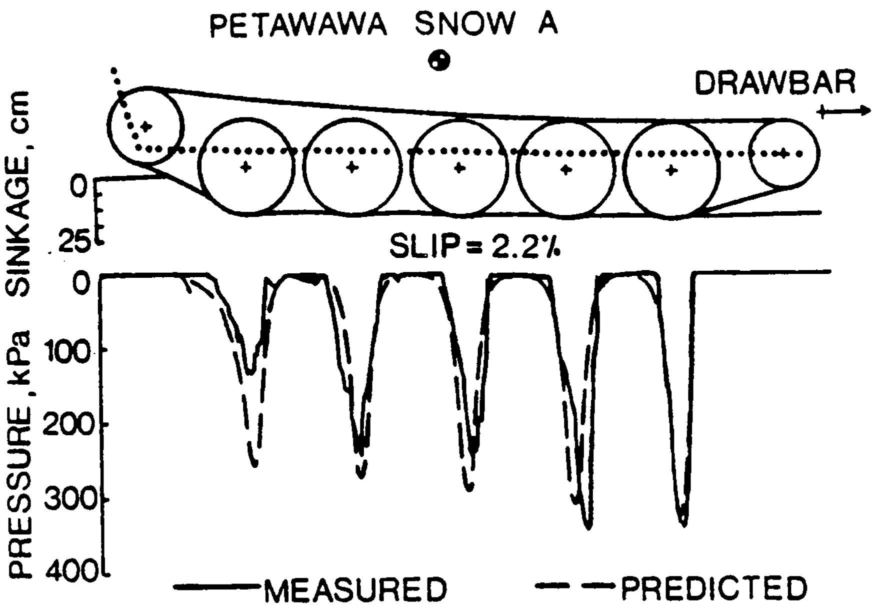

(a).

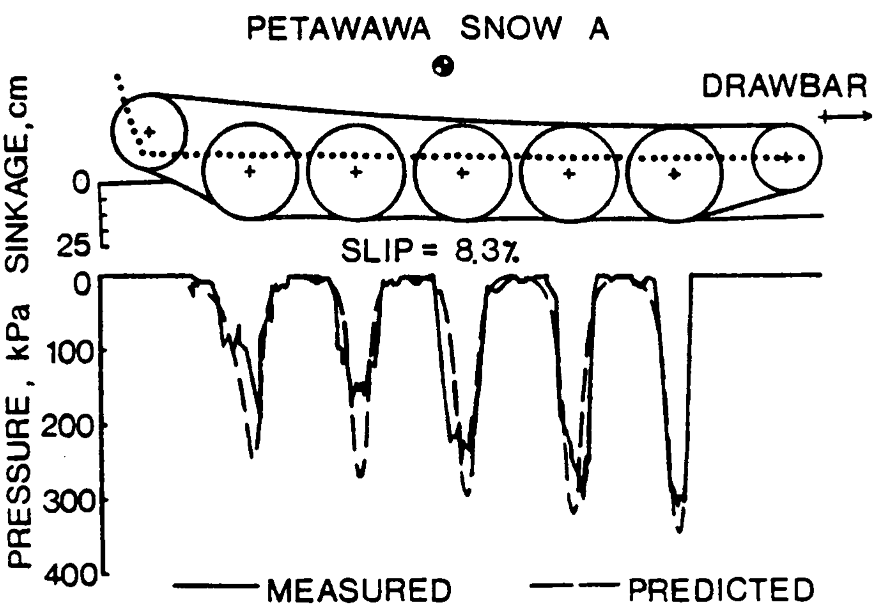

(b).

Fig. 3.6 Predicted and measured normal pressure under the track pad over Petawawa snow A at (a) 2.2% and (b) 8.3% slip.

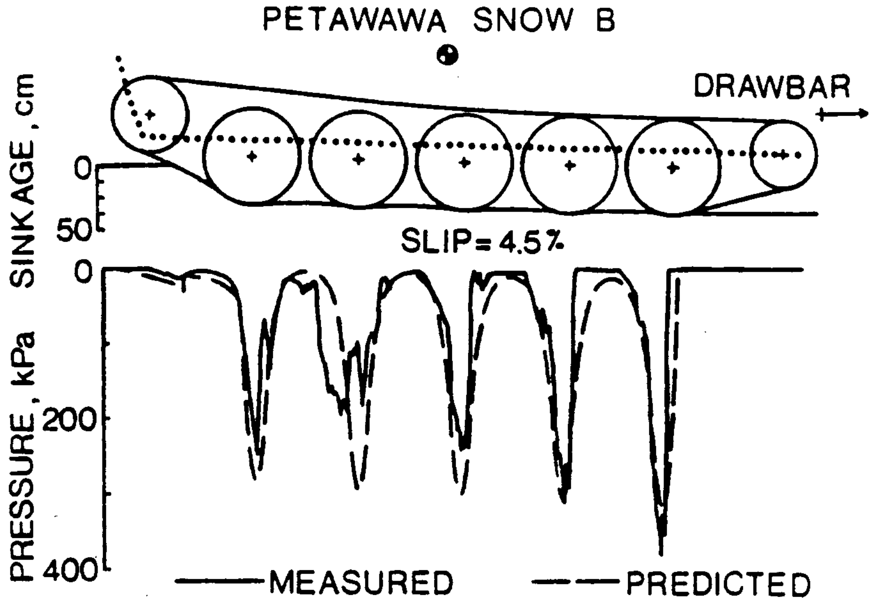

(a).

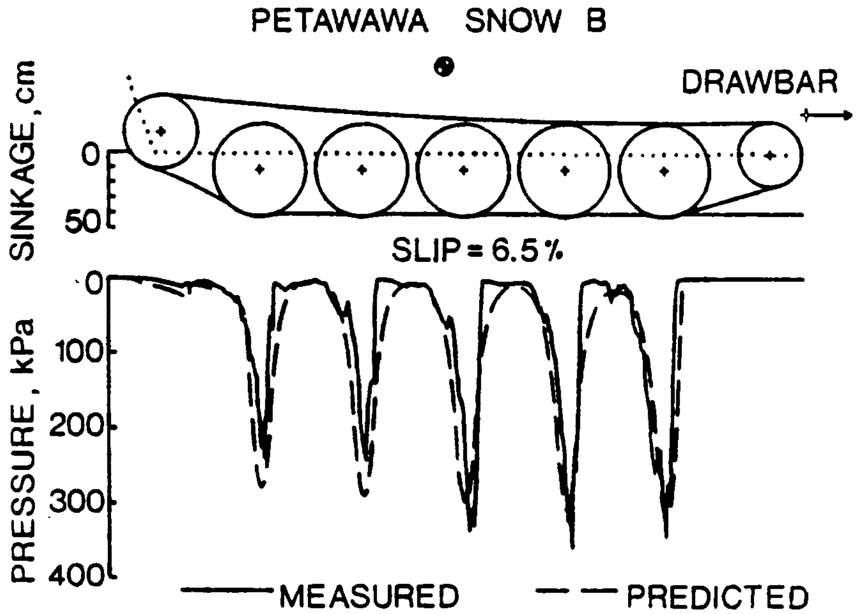

(b).

Fig. 3.7 Predicted and measured normal pressure under the track pad over Petawawa snow B at (a) 4.5% and (b) 6.5% slip.

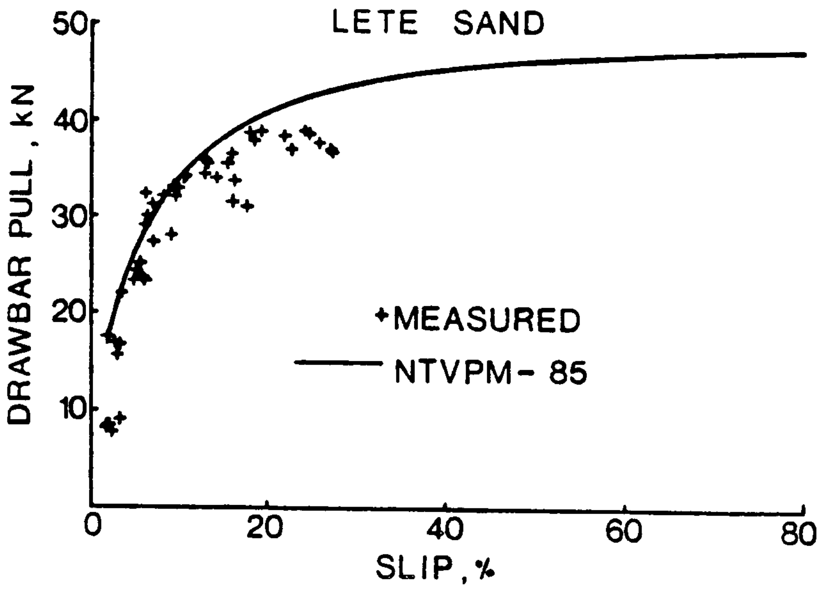

Fig. 3.8 Predicted and measured drawbar performance over LETE sand.

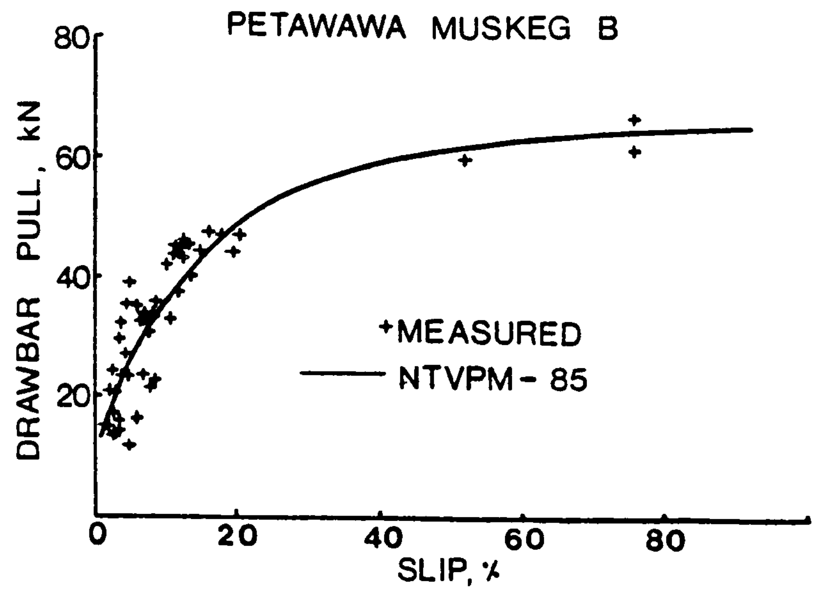

Fig. 3.9 Predicted and measured drawbar performance over Petawawa muskeg B.

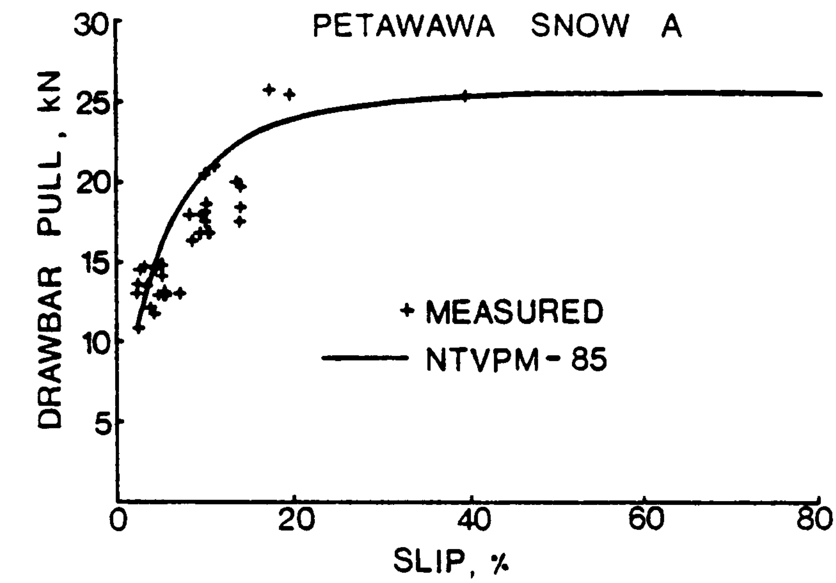

Fig. 3.10 Predicted and measured drawbar performance over Petawawa snow A.

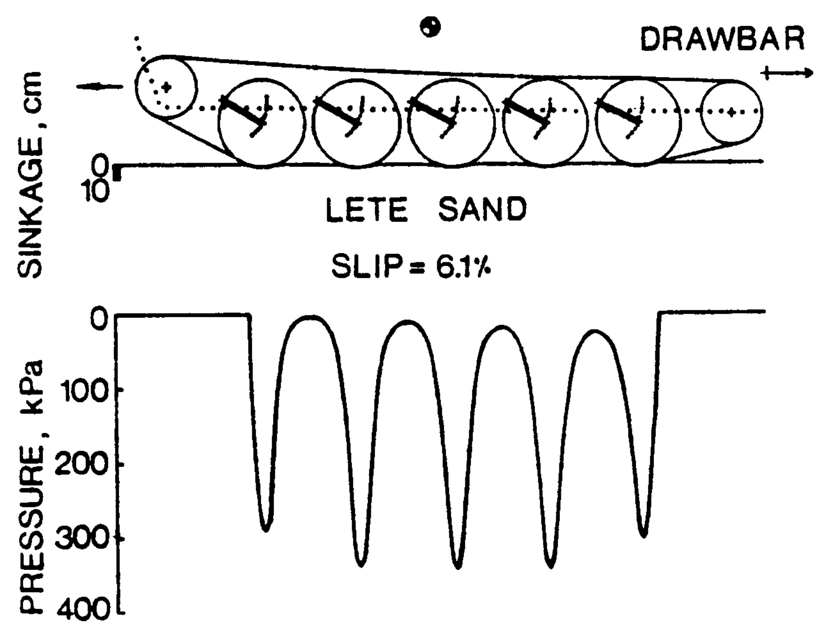

Fig. 3.11 Normal pressure under the track pad over LETE sand predicted using NTVPM-86.

over various types of terrain are shown in Figs. 3.4-3.7. Over a sandy terrain (LETE Sand), the normal pressure distributions predicted using NTVPM-85 are very close to those measured, as shown in Fig. 3.4. The maximum normal pressure measured under the track pad over this sandy terrain is about 430 kPa, which is approximately ten times the nominal ground pressure of 43.7 kPa. The nominal ground pressure is obtained by dividing the vehicle weight by the track contact area. Over a muskeg (Petawawa Muskeg A), a good agreement exists between the predicted normal pressure distribution and the measured one as shown in Fig. 3.5. The measured maximum normal pressure under the track pad over this muskeg is approximately 130 kPa, in contrast with the nominal ground pressure of 43.7 kPa. This means that the nominal ground pressure is only about 34% of the measured maximum pressure. Over two types of snow-covered terrain (Petawawa Snow A and B), good-to-excellent agreement again exists between the measured and predicted normal pressure distributions, as shown in Figs. 3.6 and 3.7. The nominal ground pressure of 43.7 kPa is only about 12% of the measured maximum normal pressure.

The generally good agreement between the measured and predicted normal pressure distributions using NTVPM-85 is due primarily to the inclusion of the response of the terrain to repetitive normal load and to the detailed analysis of the track-terrain interaction. As mentioned previously, an element of the terrain under the track is subject to the repetitive loading of consecutive roadwheels. The terrain, after being compacted by the first (or preceding) roadwheel, becomes much stiffer than in its virgin state. Consequently this promotes the concentration of normal pressure under the roadwheels, and significant pressure peaks are always observed, even on a terrain like muskeg which is relatively soft in its virgin state.

Furthermore, the behaviour of the terrain during the unloading-reloading cycle also explains why it is possible that the pressure at a point on the track segment between two adjacent roadwheels can be as low as zero, while the sinkage at that point, measured from the original terrain surface, is not zero.

The good agreement between the measured and the predicted normal pressure distributions also indicates that the assumption that the track may be modelled as a flexible belt is reasonable for the type of track system examined.

As mentioned previously, in the simulation model NTVPM-86, the characteristics of the independent suspension have been fully taken into consideration. Figure 3.11 shows the normal pressure distribution under the track pad of an M113A1 armoured personnel carrier over LETE sand predicted using NTVPM-86. It shows that the peak pressures under the front and rear roadwheels are lower than those under the middle roadwheels. This is due to the effects of independent suspension of the roadwheels. The vertical component of the tension in the track segment in front of the front roadwheel and that in the segment behind the rear roadwheel tend to relieve the loads exerted on the terrain by the front and rear roadwheels, respectively. The effects of the independent suspension of the roadwheels are correctly predicted by NTVPM-86, as can be seen in Fig. 3.12.

2. Comparisons between the measured drawbar pulls and the predicted ones using NTVPM-85 at various slips over different terrains are shown in Figs. 3.8-3.10. As can be seen from the figures, there is a good-to-excellent agreement between the measured drawbar pulls and the predicted ones using the simulation model NTVPM-85.

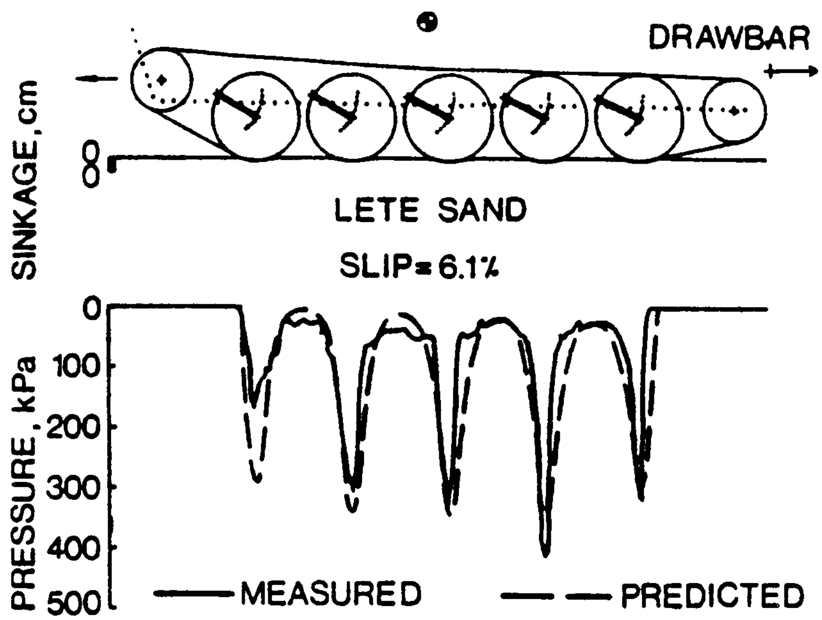

Fig. 3.12 A comparison of the measured and predicted normal pressure under the track pad using NTVPM-86 over LETE sand.

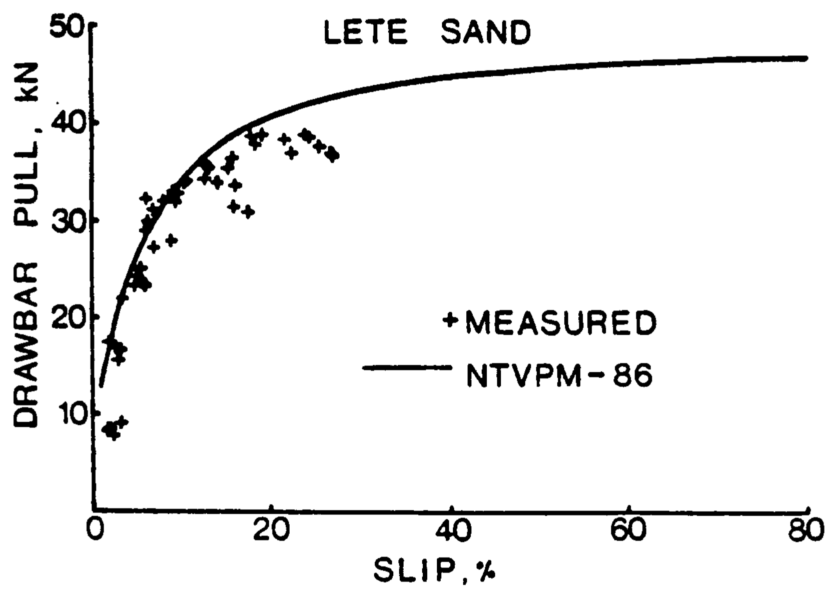

Fig. 3.13 Measured and predicted drawbar performance using NTVPM-86 over LETE sand.

The good agreement between the measured and predicted drawbar pulls is primarily due to the inclusion of the terrain response to repetitive shear loading and the shearing characteristics of terrain under varying pressure in the prediction of shear stress distribution under the track. The behaviour of the terrain under repetitive shearing has a significant effect of the development of tractive effort, particularly at low track slips. Furthermore NTVPM-85 gives a reasonable prediction of sinkage and motion resistance. This results in a fairly accurate prediction of drawbar pull. Figures 3.13 and 3.14 show that there is also a good-to-excellent agreement between the measured drawbar pull and the predicted one using NTVPM-86. Results of a detailed study have shown that over soft marginal terrain, NTVPM-86 gives more accurate prediction of ground pressure distribution and drawbar performance of a tracked vehicle with independent suspension than NTVPM-85. NTVPM-86 represents the latest computer simulation model for parametric analysis of tracked vehicle performance and design.

The close agreement between the predicted and measured normal pressure distribution and drawbar performance shows that the basic features of the computer simulation model have been substantiated. Thus, the model can be an extremely useful tool for the development and design engineer, as well as the procurement manager.

Since the model takes into account all major design parameters of the vehicle as well as terrain characteristics, it is particularly suited for the evaluation of competing designs and for the examination of the effects on performance of design modifications and changing operational environment. This provides a rational basis for the selection of the most promising design

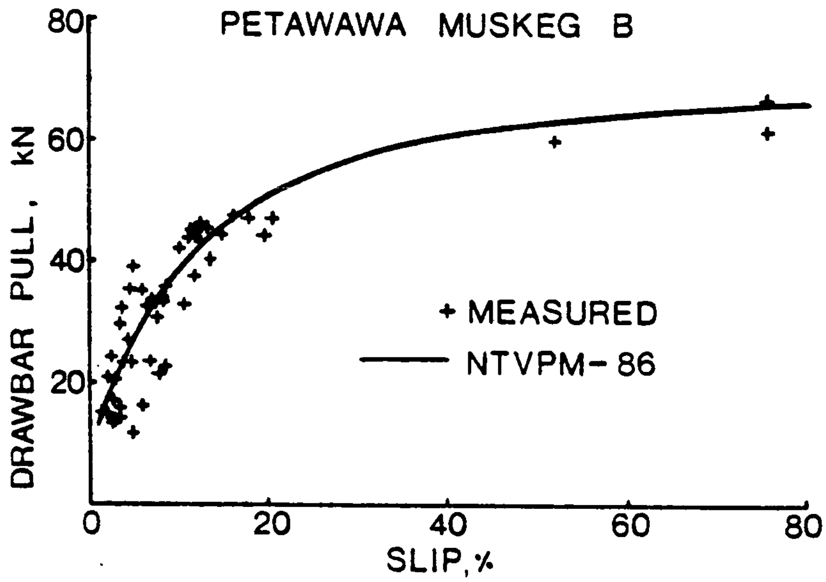

Fig. 3.14 Measured and predicted drawbar performance using NTVPM-86 over Petawawa muskeg B.

for a given mission and environment, prior to expensive hardware construction.

4. CORRELATION STUDY OF THE MEASURED AND PREDICTED VEHICLE PERFORMANCE USING NTVPM-85

As shown in the preceding chapter, the basic features of the computer simulation model NTVPM-85 have been validated over a variety of terrains, including snow-covered terrain. However, originally the simulation model requires terrain data obtained using the bevameter as input. To examine the feasibility of using terrain data obtained with the Rammsonde as input to NTVPM-85 for predicting tracked vehicle performance, it is necessary to carry out a detailed correlation study. The field performance of an all-terrain vehicle BV 206 over two types of snow, undisturbed and preconditioned, in Fernie, British Columbia was measured. The measured performance was then correlated with the predicted one using NTVPM-85 with terrain data obtained by the Rammsonde as input, and compared with that obtained by the bevameter as well as by the Rammsonde cone mounted on the bevameter assembly. It should be noted that the Rammsonde is an instrument originally designed for use in the Swiss Alps and later adapted by the U.S. Army to characterize snow behaviour. It is to provide a measure of resistance to penetration of snow at various depths, based on the penetration of a cone under impact of known energy input. The resistance to penetration of the cone can be converted to pressure by dividing it by the projected contact area of the cone. As a result, a pressure-sinkage relationship for snow can be derived from the Rammsonde data (Wong, 1990a). It should be pointed out that following the standard procedure to calculate the Rammsonde resistance, the energy loss during impact is completely ignored. It has been reported that this may lead to an overestimate of the actual resistance under certain circumstances. To examine this problem, the pressure-sinkage data with the Rammsonde cone mounted on the shaft of the bevameter, in place of the sinkage plate, at a constant penetration speed were obtained. The data were also used as input to NTVPM-85 for predicting vehicle performance over snow (Wong, 1990a).

4.1 Measured Drawbar Performance of the Test Vehicle on Undisturbed and Preconditioned Snow

The test vehicle was a BV 206, which is a two-unit tracked vehicle with articulated steering. Its general layout is shown in Fig. 4.1.1. The weight of the front unit of the test vehicle was 28.06 kN, and that of the rear unit was 17.95 kN. The initial track tension for the front unit was estimated to be 3.53 kN and that for the rear unit was estimated to be 4.69 kN, based on the measured sags of the upper runs of the tracks in the test vehicle.

The drawbar performance of the test vehicle over undisturbed and preconditioned snow in Fernie, British Columbia was measured by Mining Resource Engineering Limited (MREL). The preconditioned snow referred to herein was a snow cover which was compacted by the passage of the tracks of a BV 206 prior to testing. It should be mentioned that the preconditioned snow for February 15, 1990 was allowed to age for 21 hours before measurements were taken. The test results are described in a report entitled "Validation of a model for track performance in a variety of snow conditions as a module to NATO Reference Mobility Model" by MREL (1990). It should be noted that Vehicle Systems Development Corporation did not participate in the field measurement of the performance of the test vehicle and in the processing of the vehicle test data.

Figures 4.1.2 - 4.1.7 show the measured relationships between drawbar pull and slip of the test vehicle over undisturbed snow obtained on February 8, 12, 13, 16, 20 and 21, 1990, respectively. The measured drawbar performance of the test vehicle over preconditioned snow obtained on February 14, 15 and 19, 1990 was shown in Figs. 4.1.8 - 4.1.10, respectively. It can be seen that the measured data scatter in a wide range.

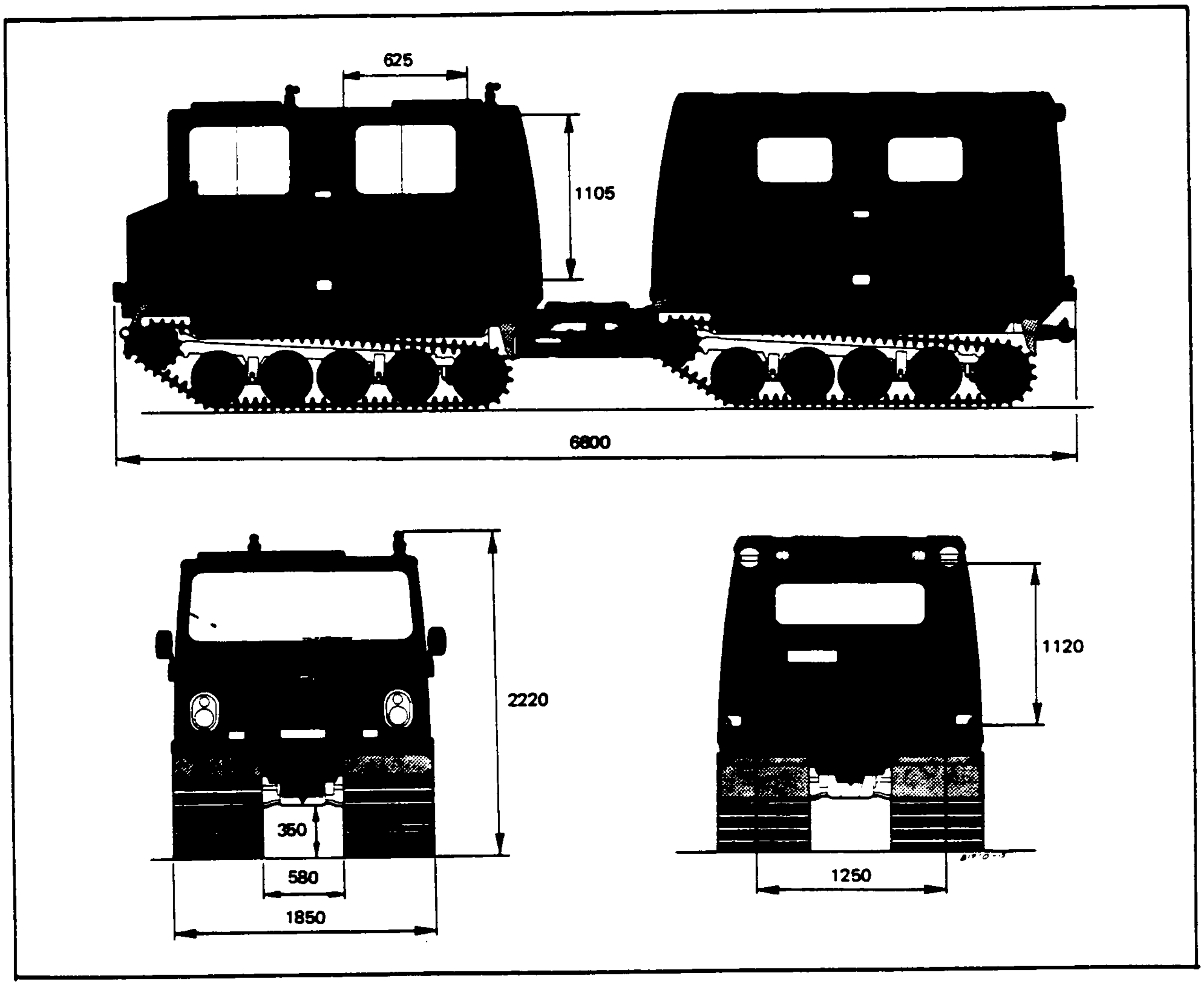

Fig. 4.1.1 General layout of the test vehicle (BV 206)

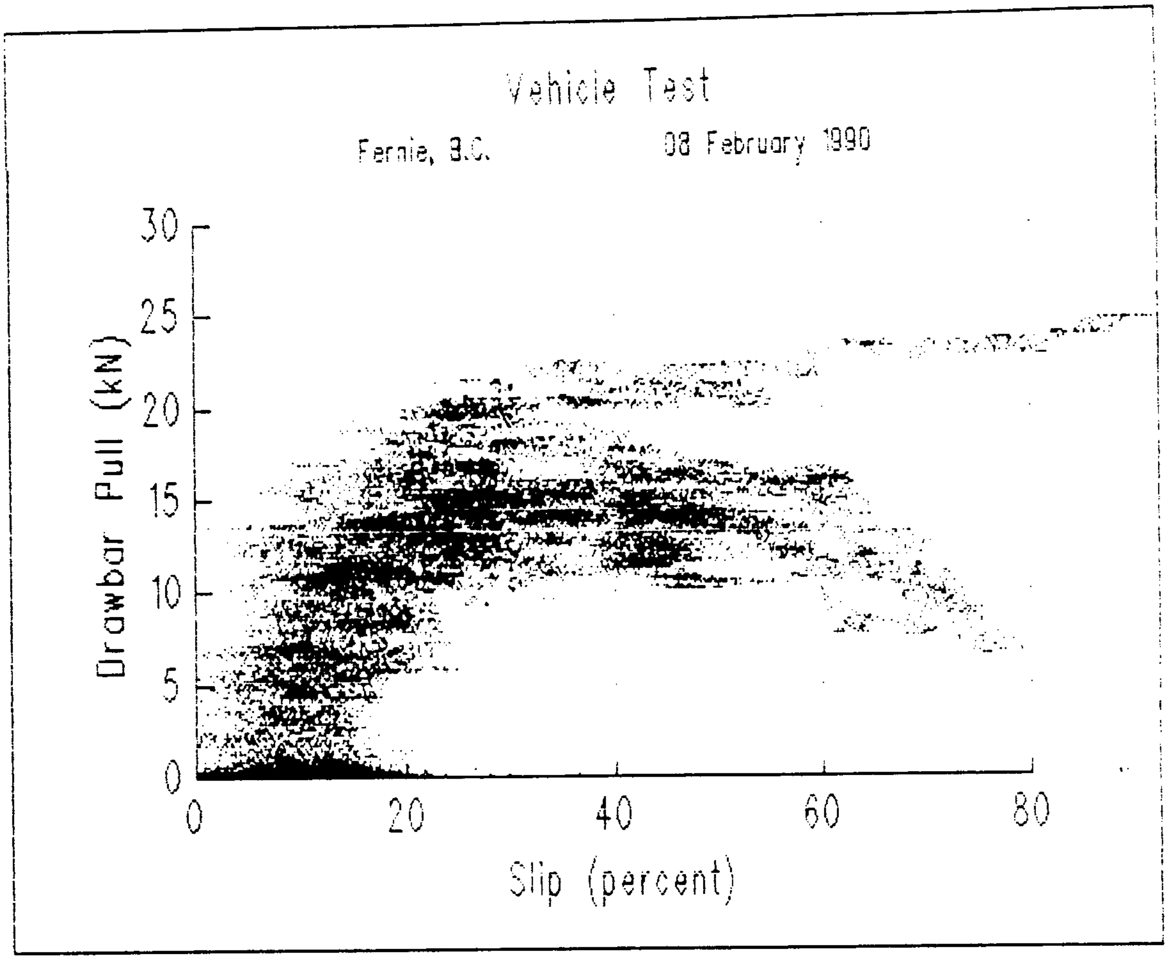

Fig. 4.1.2 Measured vehicle performance on undisturbed snow

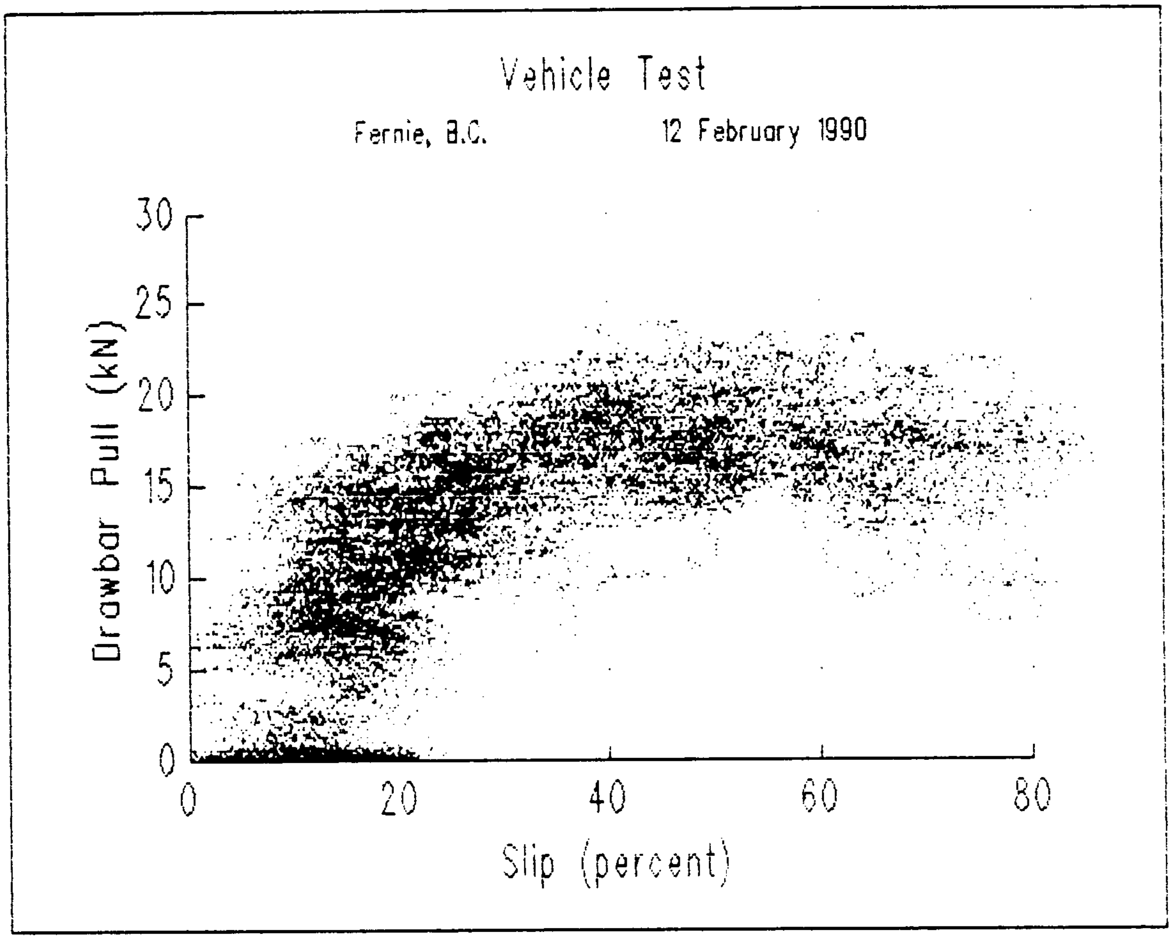

Fig. 4.1.3 Measured vehicle performance on undisturbed snow

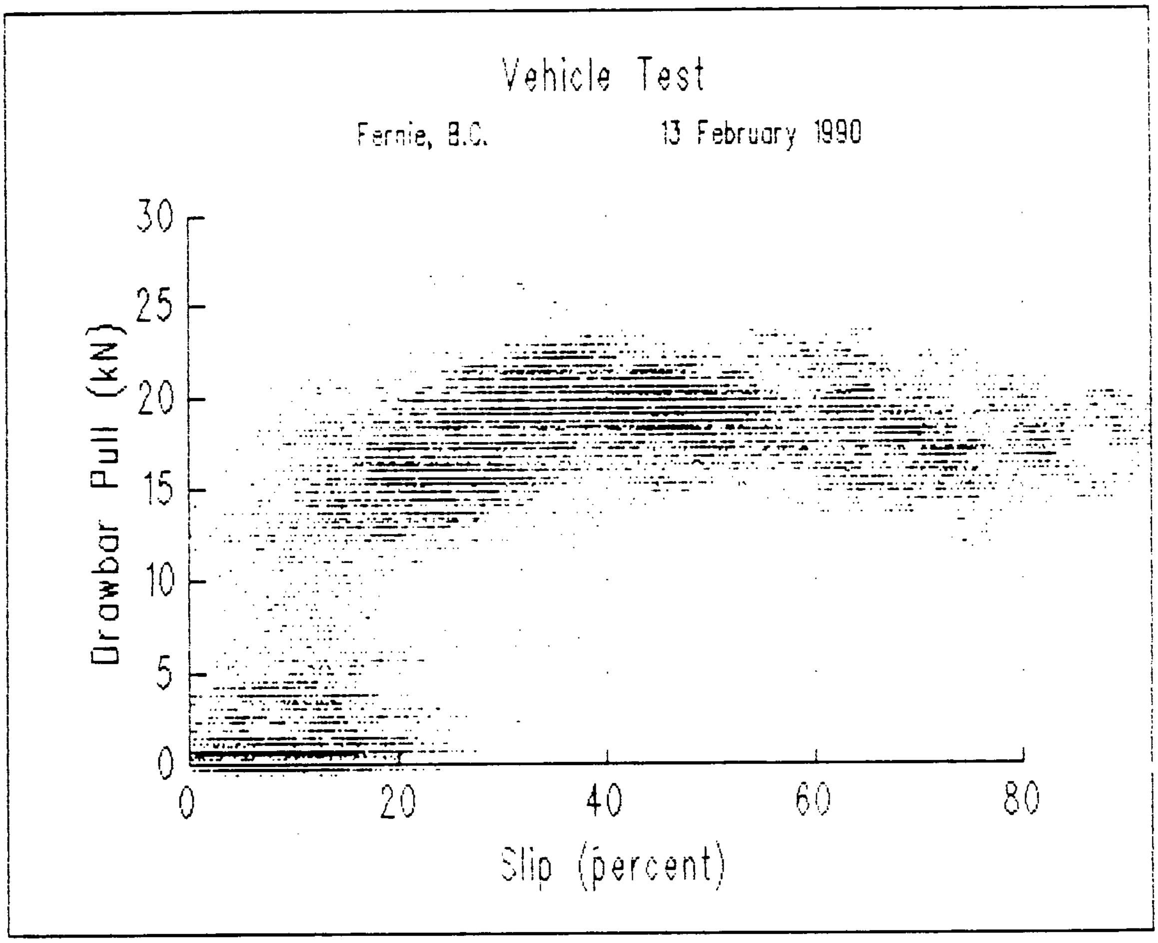

Fig. 4.1.4 Measured vehicle performance on undisturbed snow

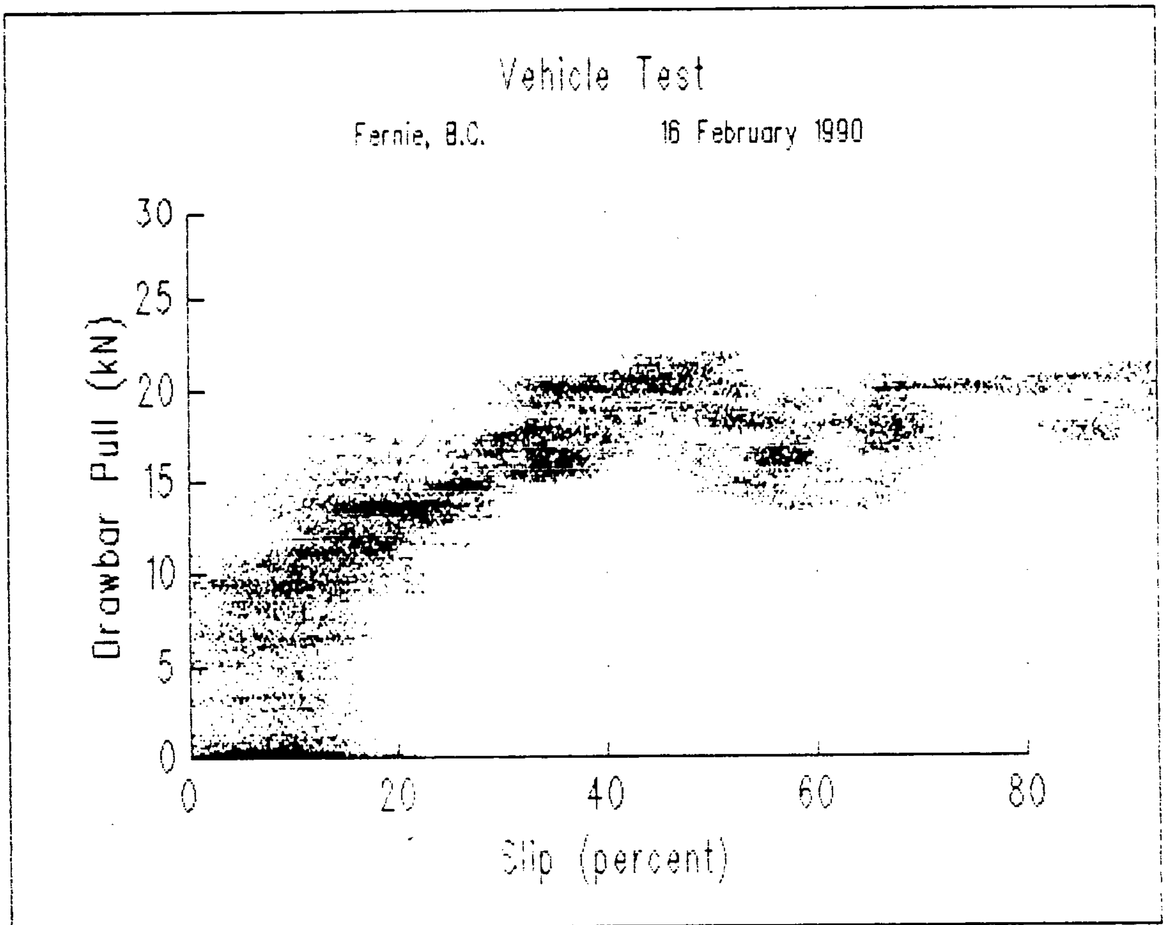

Fig. 4.1.5 Measured vehicle performance on undisturbed snow

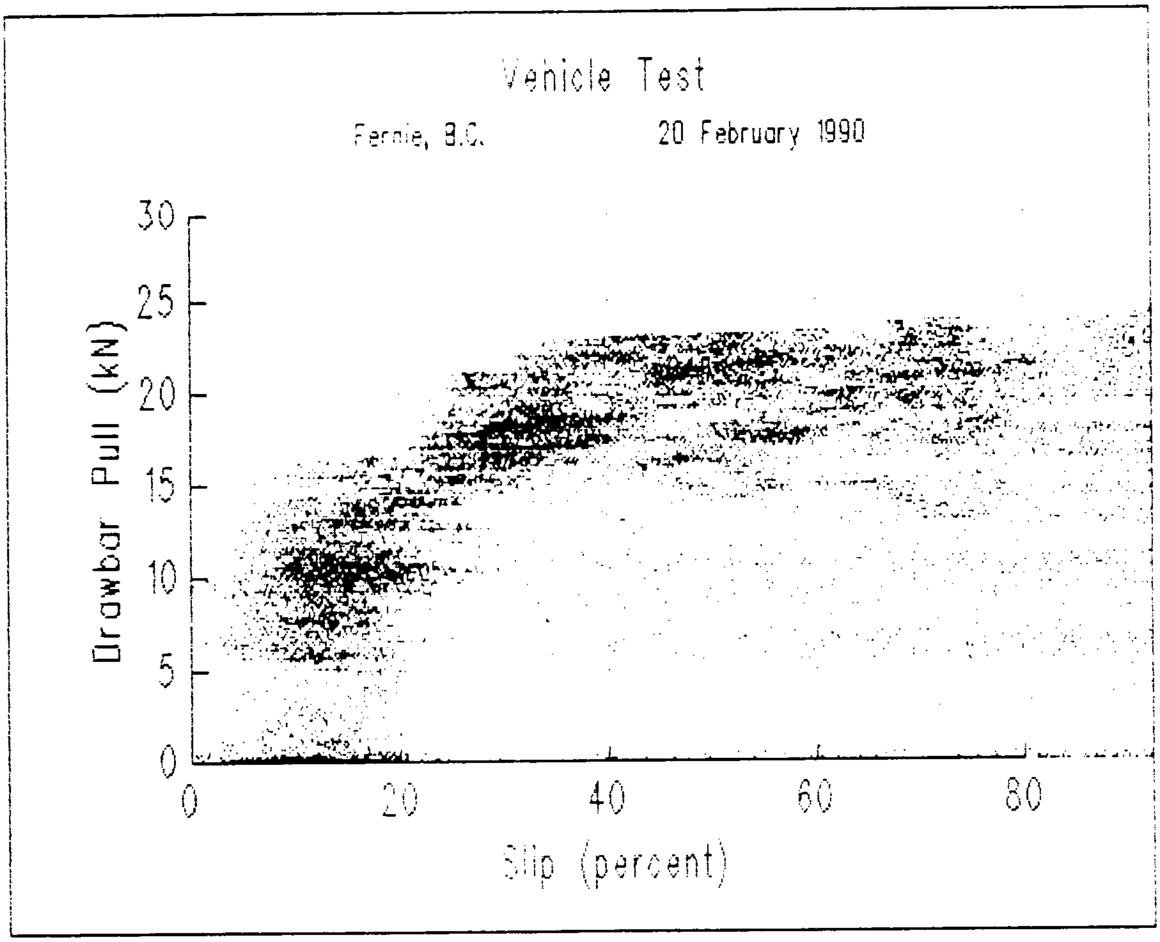

Fig. 4.1.6 Measured vehicle performance on undisturbed snow

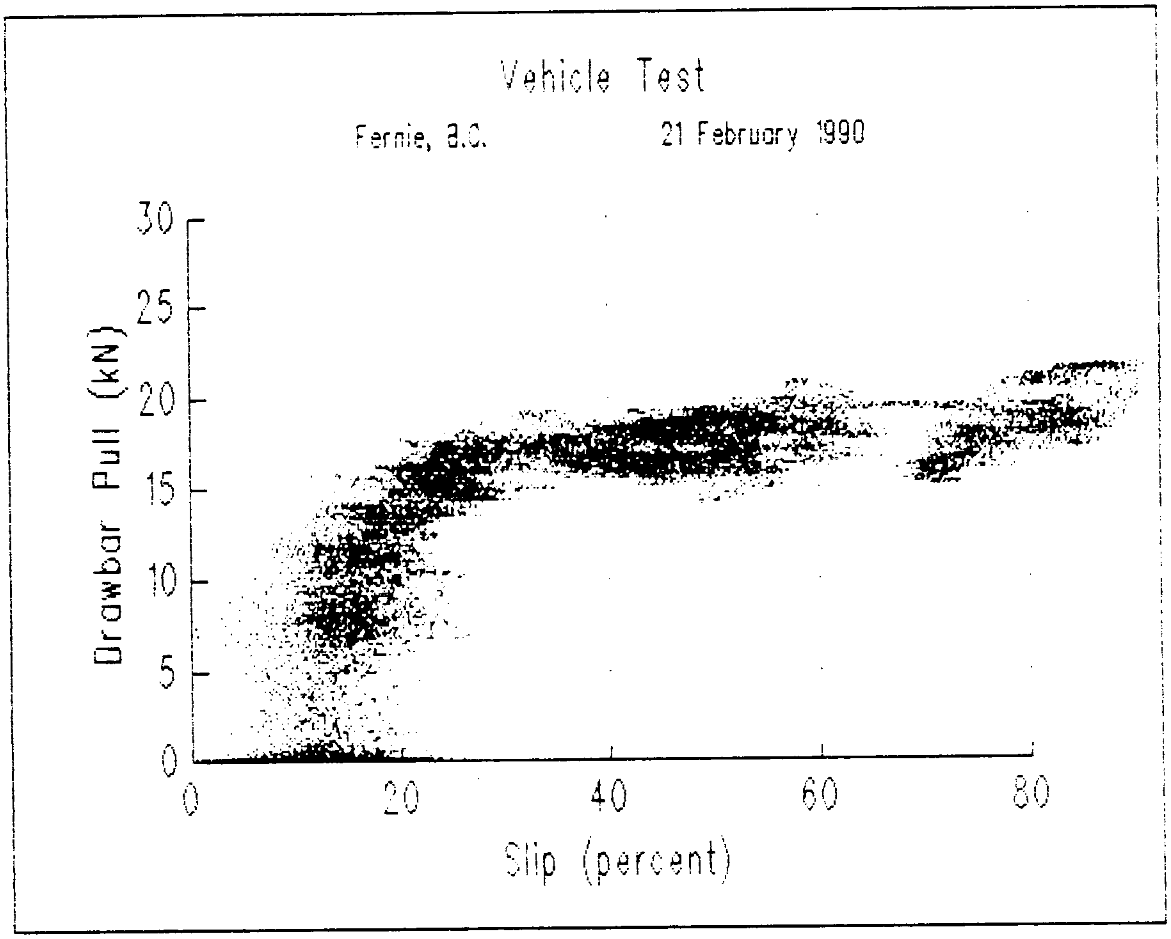

Fig. 4.1.7 Measured vehicle performance on undisturbed snow

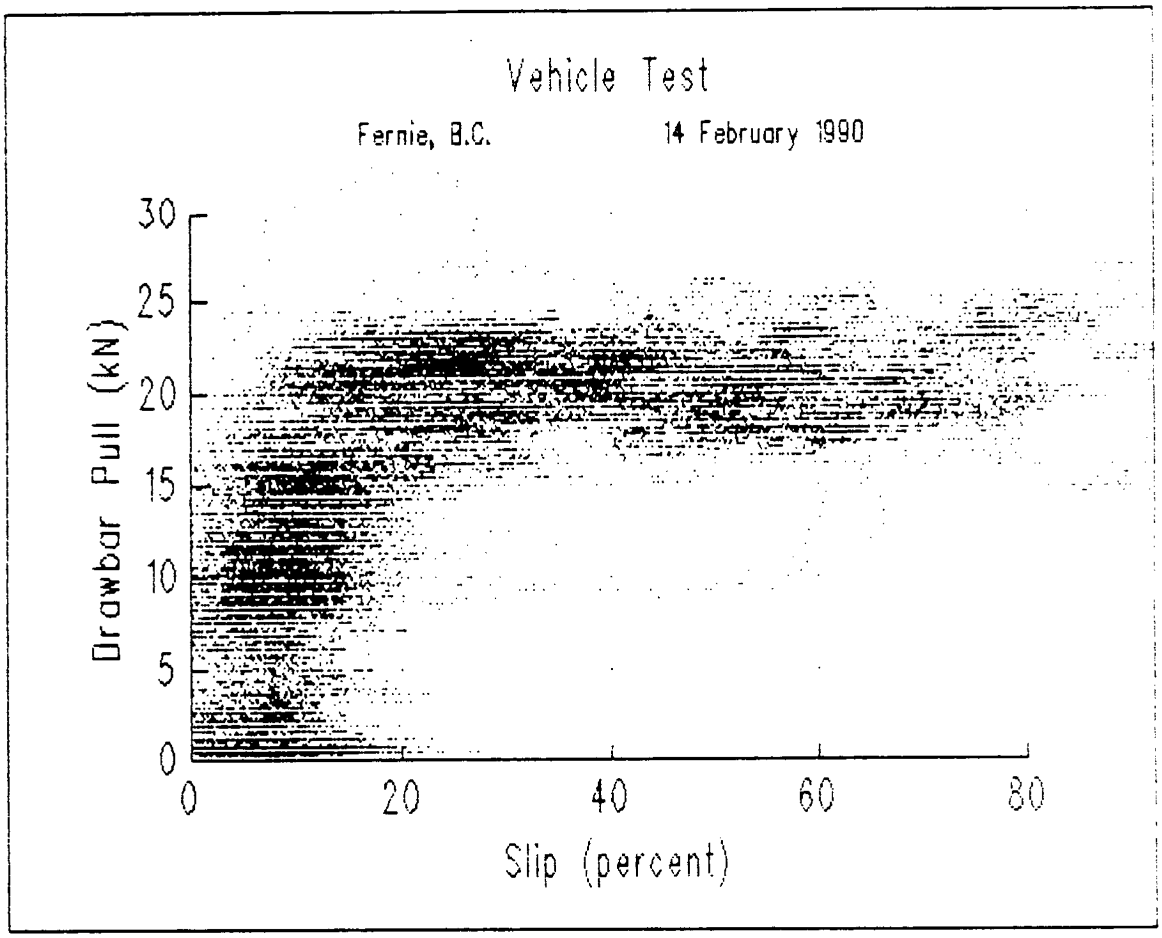

Fig. 4.1.8 Measured vehicle performance on preconditioned snow

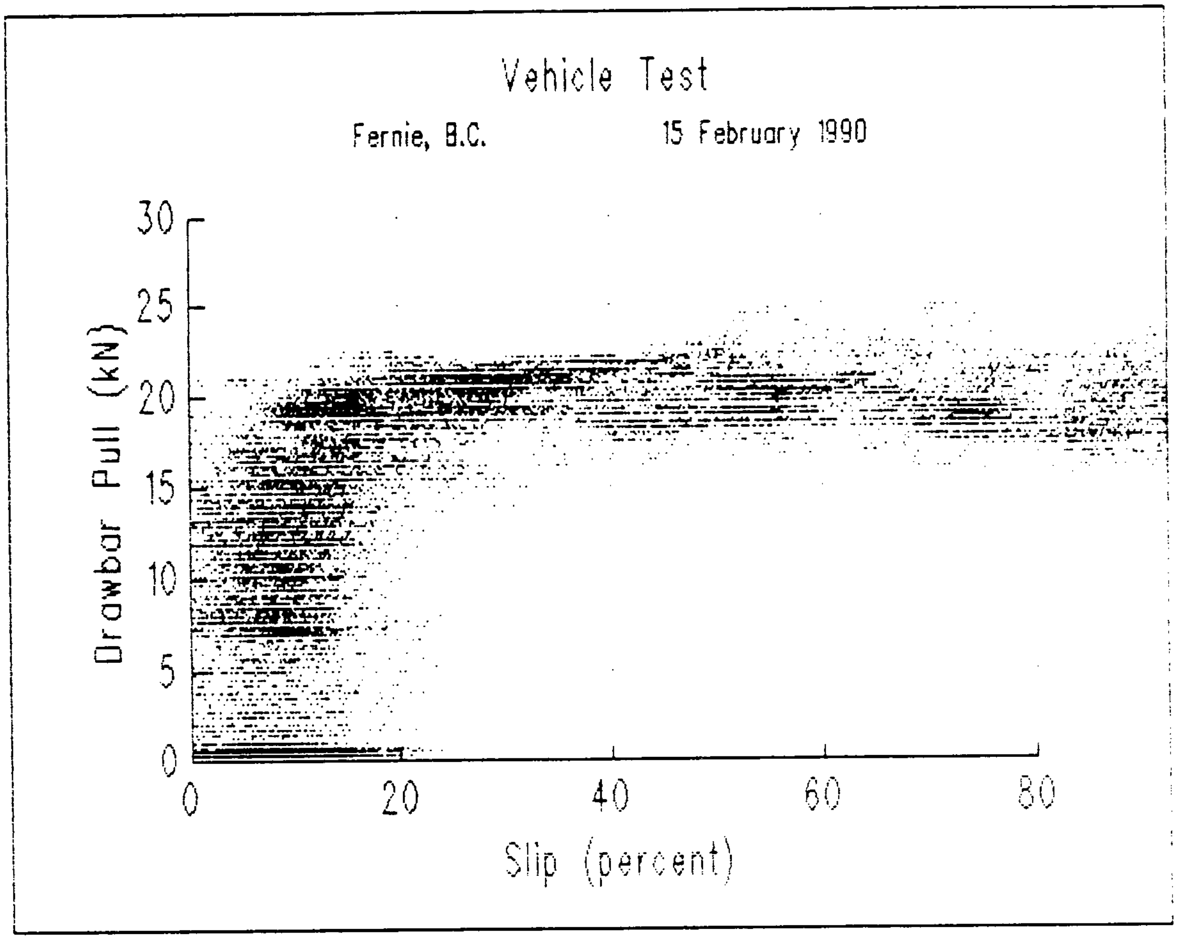

Fig. 4.1.9 Measured vehicle performance on preconditioned snow

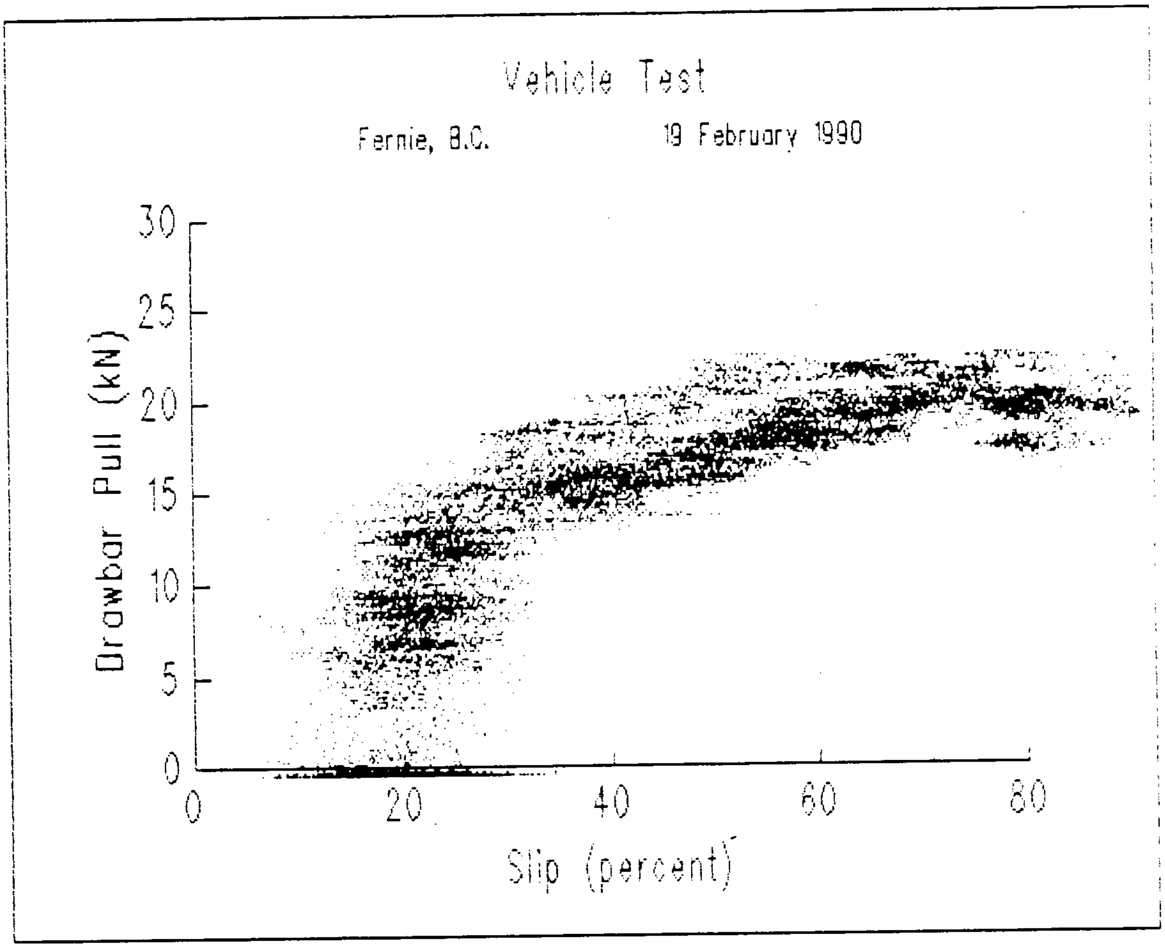

Fig. 4.1.10 Measured vehicle performance on preconditioned snow

4.2 Correlation of the Measured and Predicted Vehicle Performance on Undisturbed Snow

The measurement and characterization of the properties of the snow covers, including both undisturbed and preconditioned snow, in Fernie, British Columbia, over which the performance of the test vehicle was measured, are described in detail in two previous reports, "Measurement and characterization of the pressure-sinkage relationships for snow obtained using a Rammsonde and a bevameter" and "Measurement of the shear strength of snow using a bevameter and a hand-held shear device" (Wong, 1990a and b).

Owing to the limited scope of the field test program and limitations of the equipment and manpower available, the amount of terrain and vehicle test data collected is rather limited. For instance, for pressure-sinkage tests, the Rammsonde was used on February 7, 12, 16, 20 and 21, 1990, as shown in Table 4.2.1 (Wong, 1990a); the bevameter was employed on February 8, 12, 13, 20 and 21; and the Rammsonde cone mounted on the bevameter assembly was used on February 9, 12, 13, 20 and 21. On the other hand, the shear strength data were only collected on February 9, 12, 13, 19, 20, as shown in Table 4.2.2 (Wong, 1990b), while, as mentioned in the previous section, the performance of the test vehicle over undisturbed snow was measured on February 8, 12, 13, 16, 20 and 21, 1990. Because of these, not all the relevant terrain data and the corresponding vehicle test results are available for a particular date over the test period. Also, on a given date, the measurements of terrain parameters and vehicle performance were not necessarily carried out at the same time. Therefore, the terrain conditions under which the vehicle performance was measured may differ from those when the pressure-sinkage and shear strength data were taken, because of possible changes in atmospheric conditions during the day. As a result, it appears more meaningful and appropriate to conduct the basic correlation study based on the average conditions for the undisturbed snow and the average measured vehicle performance over the test period. However, as

Table 4.2.1 Pressure-Sinkage Parameters for Undisturbed Snow (Using Equation $p = (k_c/b + k_\phi)\, z^n$)

Date		Bevameter	Rammsonde Cone	Rammsonde Cone on Bevameter
Date	Diameter, cm	4 10	4 10	4 10
Feb. 7	Fitting Range, cm		0 - 80	
	n		1.10	
	k_c , $kN/m^{(n+1)}$		-1.38	
	k_ϕ , $kN/m^{(n+2)}$		116.00	
Feb. 8	Fitting Range, cm	0 - 50		
	n ,	1.25		
	k_c , $kN/m^{(n+1)}$	-2.77		
	k_ϕ , $kN/m^{(n+2)}$	224.22		
Feb. 9	Fitting Range, cm			0 - 50
	n ,			1.28
	k_c , $kN/m^{(n+1)}$			-1.03
	k_ϕ , $kN/m^{(n+2)}$			96.04
Feb. 12	Fitting Range, cm	0 - 30	0 - 17	0 - 30
	n ,	.84	1.00	.901
	k_c , $kN/m^{(n+1)}$	2.53	8.95	-.78
	k_ϕ , $kN/m^{(n+2)}$	149.47	194.48	222.22

Table 4.2.1 (Continued)

Date		Bevameter		Rammsonde Cone		Rammsonde Cone on Bevameter	
	Diameter, cm	4	10	4	10	4	10
Feb. 13	Fitting Range, cm	0 - 15				0 - 15	
	n	.41				.41	
	k_c , $kN/m^{(n+1)}$	-.37				.24	
	k_ϕ , $kN/m^{(n+2)}$	162.29				128.68	
Feb. 16	Fitting Range, cm			0 - 35			
	n ,			1.08			
	k_c , $kN/m^{(n+1)}$			12.27			
	k_ϕ , $kN/m^{(n+2)}$			349.85			
Feb. 20	Fitting Range, cm	0 - 50		0 - 57.5		0 - 50	
	n ,	1.51		1.44		1.45	
	k_c , $kN/m^{(n+1)}$	-.21		8.68		-7.44	
	k_ϕ , $kN/m^{(n+2)}$	518.03		722.67		582.35	
Feb. 21	Fitting Range, cm	0 - 50		0 - 59.5		0 - 45	
	n ,	1.45		1.52		1.75	
	k_c , $kN/m^{(n+1)}$	-4.90		7.67		.78	
	k_ϕ , $kN/m^{(n+2)}$	659.00		534.64		480.72	

Table 4.2.2 Shear Strength Parameters for Undisturbed Snow Obtained Using a Bevameter

Date		Internal Shearing	Rubber-Snow Shearing
Feb. 9	c, kPa		0
	ϕ, deg.		10.04
Feb. 12	c, kPa	0	0
	ϕ, deg.	23.86	10.31
Feb. 13	c, kPa	0	0.82
	ϕ, deg.	28.62	11.52
Feb. 19	c, kPa	7.86	
	ϕ, deg.	17.8	
Feb. 20	c, kPa	0	0
	ϕ, deg.	29.63	13.65

a supplement to the basic correlation study, comparative study of the measured and predicted performance of the test vehicle on specific dates has also been carried out, with a view to further substantiating the findings of the basic correlation study.

To determine the average conditions for the undisturbed snow over the test period, all the pressure-sinkage data obtained using the same device were combined and the Bekker pressure-sinkage equation shown below was fitted to the combined data:

$$p = (k_c/b + k_\phi)z^n$$

where p is pressure, b is the smaller dimension of a rectangular contact area or the radius of a circular contact area, z is sinkage, and n, k_c and k_ϕ are pressure-sinkage parameters.

The average values of the pressure-sinkage parameters, n, k_c and k_ϕ, derived from the combined data obtained using the Rammsonde, the bevameter and the Rammsonde cone mounted on the bevameter assembly, with 4 and 10 cm diameter sensing elements (cones or plates), in undisturbed snow are shown in Table 4.2.3.

Table 4.2.3 Average Pressure-Sinkage Parameters, n, k_c and k_ϕ, for Undisturbed Snow

Pressure-Sinkage Parameters	Measuring Device		
	Rammsonde	Bevameter	Rammsonde Cone on Bevameter
n	1.006	0.588	0.712
k_c (kN/m^{n+1})	12.13	-0.57	-0.12
k_ϕ (kN/m^{n+2})	45.62	178.14	145.01

As pointed out in a previous report "Measurement and characterization of the pressure-sinkage relationships for snow obtained using a Rammsonde and a bevameter" (Wong, 1990a), over undisturbed snow, the small size sensing element (cone or plate) with diameter of 4 cm could not provide consistent pressure-sinkage data, particularly with the Rammsonde. This is because the resistance to penetration of the small sensing element is very low in the upper layer of the fresh snow cover, and as a result it cannot provide meaningful data for a considerable depth. The pressure-sinkage data obtained using the sensing element with diameter of 10 cm were found to be more consistent and reliable. However, to characterize the pressure-sinkage relationship based on data obtained using a single size sensing element, the following simplified Bekker pressure-sinkage equation containing only two parameters, n and k, has to be used:

$$p = k\, z^n$$

where p is pressure, z is sinkage, and n and k are pressure-sinkage parameters.

Table 4.2.4 shows the pressure-sinkage parameters, n and k, derived from data obtained using various devices on different dates during the test period. To determine the average snow conditions, a procedure similar to that described previously was followed. All the pressure-sinkage data obtained using the same device were combined, and the average values of the pressure-sinkage parameters, n and k, derived from the combined data obtained using 10 cm diameter sensing element (cone or plate) are shown in Table 4.2.5.

Table 4.2.5 Average Pressure-Sinkage Parameters, n and k, for Undisturbed Snow

Pressure-Sinkage Parameters	Measuring Device		
	Rammsonde	Bevameter	Rammsonde Cone on Bevameter
n	0.721	0.710	0.717
k (kPa/m^n)	221.12	192.89	143.59

Similar approach was followed to derive the average values of the shear strength parameters from the combined shear data for the undisturbed snow over the test period.

Table 4.2.4 Pressure-Sinkage Parameters for Undisturbed Snow (Using Equation $p = k z^n$)

Date		Bevameter		Rammsonde Cone		Rammsonde Cone on Bevameter	
	Diameter	4	10	4	10	4	10
Feb. 7	Fitting Range, cm			0 - 90	0 - 78		
	n ,			1.04	1.02		
	k , kPa/m^n			43.94	87.50		
Feb. 8	Fitting Range, cm	0 - 44.5	0 - 50				
	n ,	1.26	1.10				
	k , kPa/m^n	81.41	138.33				
Feb. 9	Fitting Range, cm					0 - 50	0 - 77
	n ,					1.11	1.18
	k , kPa/m^n					37.14	73.97
Feb. 12	Fitting Range, cm	0 - 30	0 - 33	0 - 18	0 - 16	0 - 36	0 - 27
	n ,	.94	.74	1.47	1.47	.96	.96
	k , kPa/m^n	279.74	172.35	1497.7	1101.1	283.02	204.33
Feb. 13	Fitting Range, cm	0 - 22	0 - 35		0 - 27	0 - 15	0 - 15
	n ,	.47	.48		.42	.40	.43
	k , kPa/m^n	191.78	227.23		309.38	136.24	137.96

Table 4.2.4 (Continued)

		Bevameter		Rammsonde Cone		Rammsonde Cone on Bevameter	
Date	Diameter	4	10	4	10	4	10
Feb. 16	Fitting Range, cm			0 - 35	0 - 36		
	n ,			1.28	1.27		
	k , kPa/m^n			1248.7	803.98		
Feb. 20	Fitting Range, cm	0 - 26	0-29.7	0 - 55	0 - 62	0 - 44	0 - 55
	n ,	1.46	1.45	1.21	1.44	1.24	1.43
	k , kPa/m^n	257.28	169.18	1041.9	895.25	159.44	419.81
Feb. 21	Fitting Range, cm	0 - 45	0 - 54	0-65.5	0-58.5	0-55.5	0 - 50
	n ,	1.49	1.49	1.48	1.44	1.46	1.43
	k , kPa/m^n	452.41	533.90	876.83	649.64	396.10	330.15

The average values of the shear strength parameters, c and ϕ, derived from the combined shear data obtained using the bevameter shear device are shown in Table 4.2.6 (Wong, 1990b). It should be pointed out that a hand-held shear device provided by the Defence Research Establishment Suffield was also used to collect shear data. However, it was found that this device could not provide consistent and reliable data (Wong, 1990b). The data obtained by the hand-held shear device, therefore, were not used in the correlation study.

Table 4.2.6 Average Shear Strength Parameters c, ϕ and K, for Undisturbed Snow

Shear Strength Parameters	Internal Shearing	Rubber-Snow Shearing
c (kPa)	1.96	0.21
ϕ (degrees)	24.98	11.38
K (m)	5.50	0.39

It should be noted that data on the response of the undisturbed snow to repetitive normal load and on the shear deformation modulus were also required as input to the simulation model. The response of terrain to repetitive normal load may be characterized by the average slope of the unloading-reloading line in a repetitive loading cycle, which can be assumed to be proportional to the unloading sinkage with a constant coefficient of A_u (Wong, 1989a). The value of A_u for the undisturbed snow was not available and an estimate value of 33,333 kPa/m^2, based on data for similar terrain stored in our data bank, was used in the simulation. The shear deformation module K for internal and rubber-terrain shearing for the undisturbed snow were also unavailable. Estimated values, as shown in Table 4.2.6, based on data for similar terrain, were used in the simulations.

Using the terrain parameters described above as input, the tractive performance of the test vehicle, BV206, over undisturbed snow was predicted using NTMPV-85. The vehicle parameters used as input to NTVPM-85 are given in Table 4.2.7 and sample output from the simulation model is given in Appendix A. Figures 4.2.1 - 4.2.3 show the relationships between the drawbar pull and slip for the test vehicle over undisturbed snow predicted using NTVPM-85 with the pressure-sinkage data shown in Table 4.2.4 as input, obtained by the Rammsonde, the bevameter and the Rammsonde cone mounted on the bevameter assembly, respectively. The pressure-sinkage parameters were derived from data obtained using sensing elements with diameters of 4 and 10 cm. The shear strength parameters used in the predictions were those shown in Table 4.2.6. In the figures, the measured drawbar pull at various slips of the test vehicle, expressed in terms of the mean value ± standard deviation derived from the experimental data shown in Figs. 4.1.2 -4.1.7, is also presented. Using the mean value and standard deviation of the measured drawbar pull to represent the experimental data gives a more meaningful statistical description of the measured vehicle performance than the scatter plots shown in Figs. 4.1.2 - 4.1.7. It can be seen that in general the predicted performance, based on pressure-sinkage data obtained using the three devices, all lies within the limits defined by the mean value ± standard deviation of the measured performance. Table 4.2.8 shows a comparison of the measured and predicted drawbar pull at slips of 20, 30 and 40%.

Figures 4.2.4 - 4.2.6 show the relationships between the drawbar pull and slip for the test vehicle over undisturbed snow predicted using NTVPM-85 with the pressure-sinkage data shown in Table 4.2.5 as input, obtained using the three devices. The pressure-sinkage parameters were derived from data obtained with sensing elements with diameter of 10 cm. The shear strength parameters used in the predictions are the same as those shown in Table 4.2.6. In the figures, the measured drawbar pull at various slips of the test vehicle, expressed in terms of the mean value ± standard deviation derived from the experimental data shown in Figs. 4.1.2 - 4.1.7, is also presented. It can be seen that again there is a reasonable correlation between the measured performance and the predicted one using NTVPM-85. Table 4.2.9 shows a comparison between the measured and predicted drawbar pull at slips of 20, 30 and 40%. Figures 4.2.7 - 4.2.9 show a

Table 4.2.7 Vehicle input parameters for NTVPM-85

PREDICTION OF TRACKED VEHICLE PERFORMANCE
(MODEL: NTVPM-85)
VEHICLE SYSTEMS DEVELOPMENT CORPORATION
NEPEAN, ONTARIO, CANADA

SEPTEMBER 11, 1990

VEHICLE TYPE (Expt.)

VEHICLE PARAMETERS FOR THE FRONT UNIT:

Parameter	Value
WEIGHT	28.06 KN
CENTRE OF GRAVITY X-COORDINATE	131.50 CM
CENTRE OF GRAVITY Y-COORDINATE	-14.40 CM
SPROCKET RADIUS	19.00 CM
SPROCKET CENTRE X-COORDINATE	.00 CM
SPROCKET CENTRE Y-COORDINATE	.00 CM
TENSIONING WHEEL RADIUS	19.00 CM
TENSIONING WHEEL CENTRE X-COORDINATE	233.13 CM
TENSIONING WHEEL CENTRE Y-COORDINATE	30.50 CM
ROADWHEEL RADIUS	19.00 CM
INITIAL TRACK TENSION	3.53 KN
DOUBLE PIVOT JOINT X-COORDINATE (AT THE REAR OF THE UNIT)	273.00 CM
DOUBLE PIVOT JOINT Y-COORDINATE (AT THE REAR OF THE UNIT)	3.00 CM
LENGTH OF THE INTERCONNECTING LINK	76.00 CM
SUSPENSION HEAVE STIFFNESS	.69 KN/CM

FRONT UNIT -- ROADWHEEL GEOMETRY

X-COORDINATE OF WHEEL CENTRE (CM)	Y-COORDINATE OF WHEEL CENTRE (CM)
34.04	30.50
86.28	30.50
129.28	30.50
173.28	30.50

BELLY SHAPE		SUPPORTING ROLLERS		TRACK LINK CONTACT AREA			
WIDTH: 61.0 CM		RADIUS: 10.0 CM		SINKAGE (CM)		INCREMENTAL AREA	PERCENTAGE CAUSING RUBBER SHEARING
COORDINATES (CM) X	Y	COORDINATES (CM) X	Y	FROM	TO	(CM**2)	
-20.0	-3.0	128.0	2.0	.00	.00	76.00	100.0
-6.0	11.0			.00	1.40	64.00	.0
260.0	11.0			1.40	2.70	71.00	.0
				2.70	5.50	351.00	.0

NOTE: COORDINATE ORIGIN IS AT THE CENTRE OF THE SPROCKET. POSITIVE X- AND Y-COORDINATES ARE TO THE REAR AND DOWN, RESPECTIVELY.

Table 4.2.7 (continued)

(Expt.) SEPTEMBER 11, 1990 Fernie Snow(RSF-12D)

TRACK PARAMETERS FOR THE FRONT UNIT:

WEIGHT PER UNIT LENGTH	.330 KN/M
WIDTH	62.0 CM
PITCH	9.1 CM
HEIGHT OF THE GROUSERS	5.5 CM
PERCENT RUBBER FOR COHESIVE SHEARING	13.5 %
LONGITUDINAL ELASTICITY CONSTANT TE (FROM T=TE*E)	10910. KN

VEHICLE PARAMETERS FOR THE REAR UNIT:

WEIGHT	17.95 KN
CENTRE OF GRAVITY X-COORDINATE	96.50 CM
CENTRE OF GRAVITY Y-COORDINATE	-.40 CM
SPROCKET RADIUS	19.00 CM
SPROCKET CENTRE X-COORDINATE	.00 CM
SPROCKET CENTRE Y-COORDINATE	.00 CM
TENSIONING WHEEL RADIUS	19.00 CM
TENSIONING WHEEL CENTRE X-COORDINATE	233.13 CM
TENSIONING WHEEL CENTRE Y-COORDINATE	30.50 CM
ROADWHEEL RADIUS	19.00 CM
INITIAL TRACK TENSION	4.69 KN
DOUBLE PIVOT JOINT X-COORDINATE (AT THE FRONT OF THE UNIT)	-29.00 CM
DOUBLE PIVOT JOINT Y-COORDINATE (AT THE FRONT OF THE UNIT)	3.00 CM
DRAWBAR HITCH X-COORDINATE	265.00 CM
DRAWBAR HITCH Y-COORDINATE	-2.00 CM
SUSPENSION HEAVE STIFFNESS	.67 KN/CM

REAR UNIT -- ROADWHEEL GEOMETRY

X-COORDINATE OF WHEEL CENTRE (CM)	Y-COORDINATE OF WHEEL CENTRE (CM)
34.04	30.50
86.28	30.50
131.97	30.50
177.84	30.50

NOTE: COORDINATE ORIGIN IS AT THE CENTRE OF THE SPROCKET. POSITIVE X- AND Y-COORDINATES ARE TO THE REAR AND DOWN, RESPECTIVELY.

Table 4.2.7 (continued)

(Expt.) SEPTEMBER 11, 1990 Fernie Snow(RSF-12D)

BELLY SHAPE		SUPPORTING ROLLERS		TRACK LINK CONTACT AREA			
WIDTH: 61.0 CM		RADIUS: 10.0 CM				INCRE-	PERCENTAGE
				SINKAGE		MENTAL	CAUSING
COORDINATES (CM)		COORDINATES (CM)		(CM)		AREA	RUBBER
X	Y	X	Y	FROM	TO	(CM**2)	SHEARING
*****	*****	*****	*****	******	******	*******	********
-20.0	-3.0	128.0	2.0	.00	.00	76.00	100.0
-6.0	11.0			.00	1.40	64.00	.0
260.0	11.0			1.40	2.70	71.00	.0
				2.70	5.50	351.00	.0

TRACK PARAMETERS FOR THE REAR UNIT:

WEIGHT PER UNIT LENGTH		.330 KN/M
WIDTH		62.0 CM
PITCH		9.1 CM
HEIGHT OF THE GROUSERS		5.5 CM
PERCENT RUBBER FOR COHESIVE SHEARING		13.5 %
LONGITUDINAL ELASTICITY CONSTANT TE	(FROM T=TE*E)	10910. KN

NOTE: COORDINATE ORIGIN IS AT THE CENTRE OF THE SPROCKET. POSITIVE X- AND Y-COORDINATES ARE TO THE REAR AND DOWN, RESPECTIVELY.

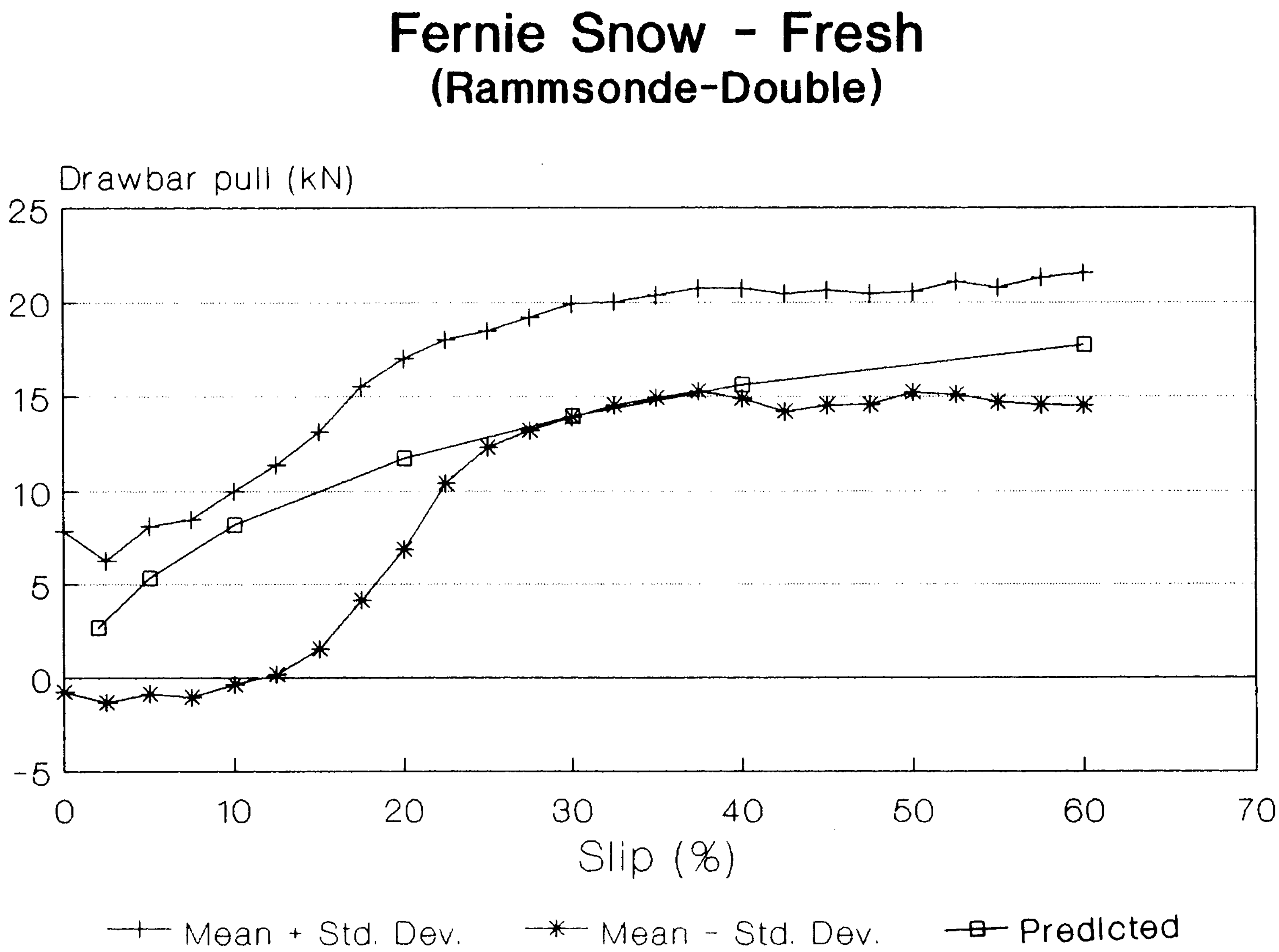

Fig. 4.2.1 Measured and predicted vehicle performance using NTVPM-85 on undisturbed snow

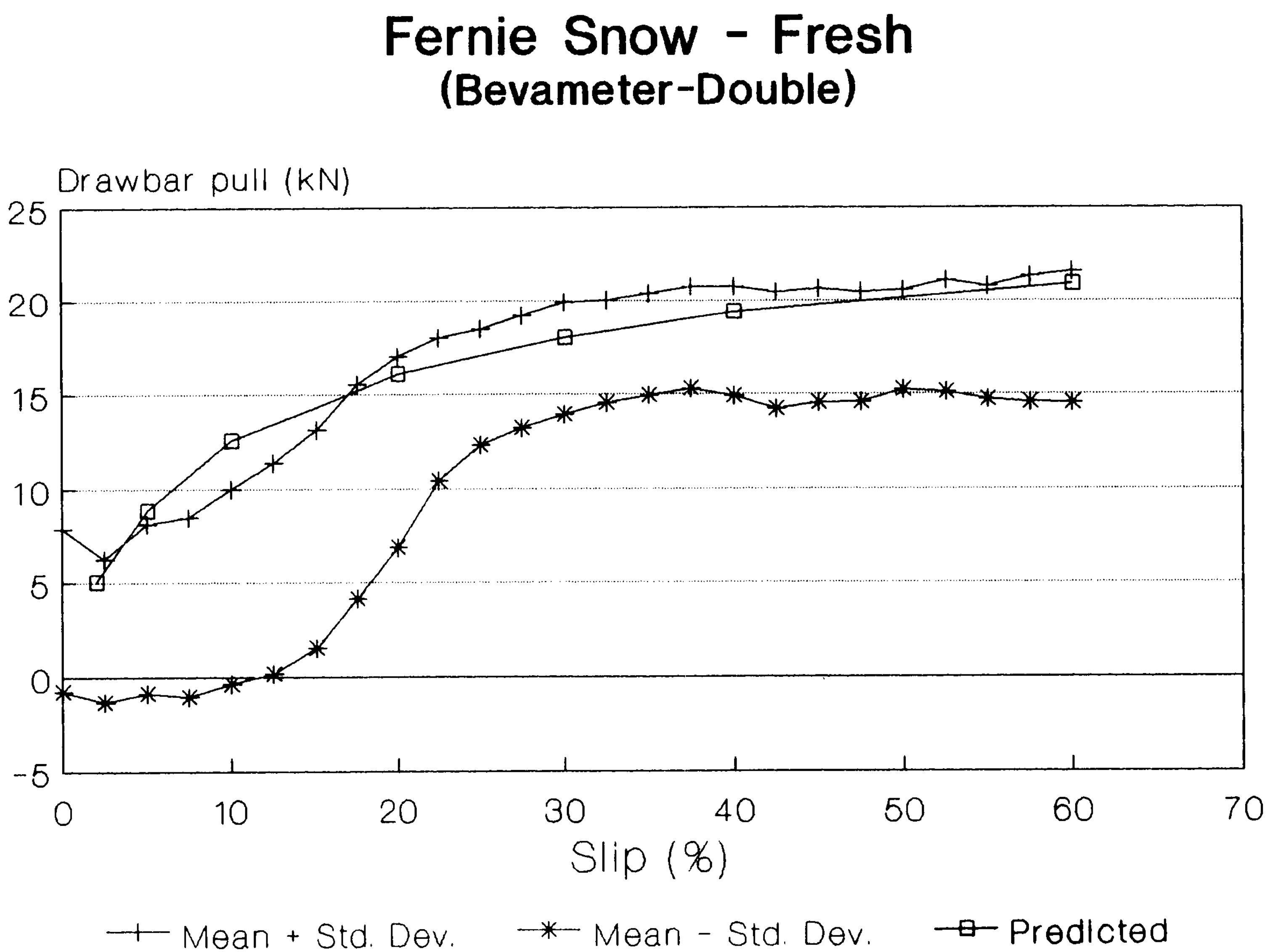

Fig. 4.2.2 Measured and predicted vehicle performance using NTVPM-85 on undisturbed snow

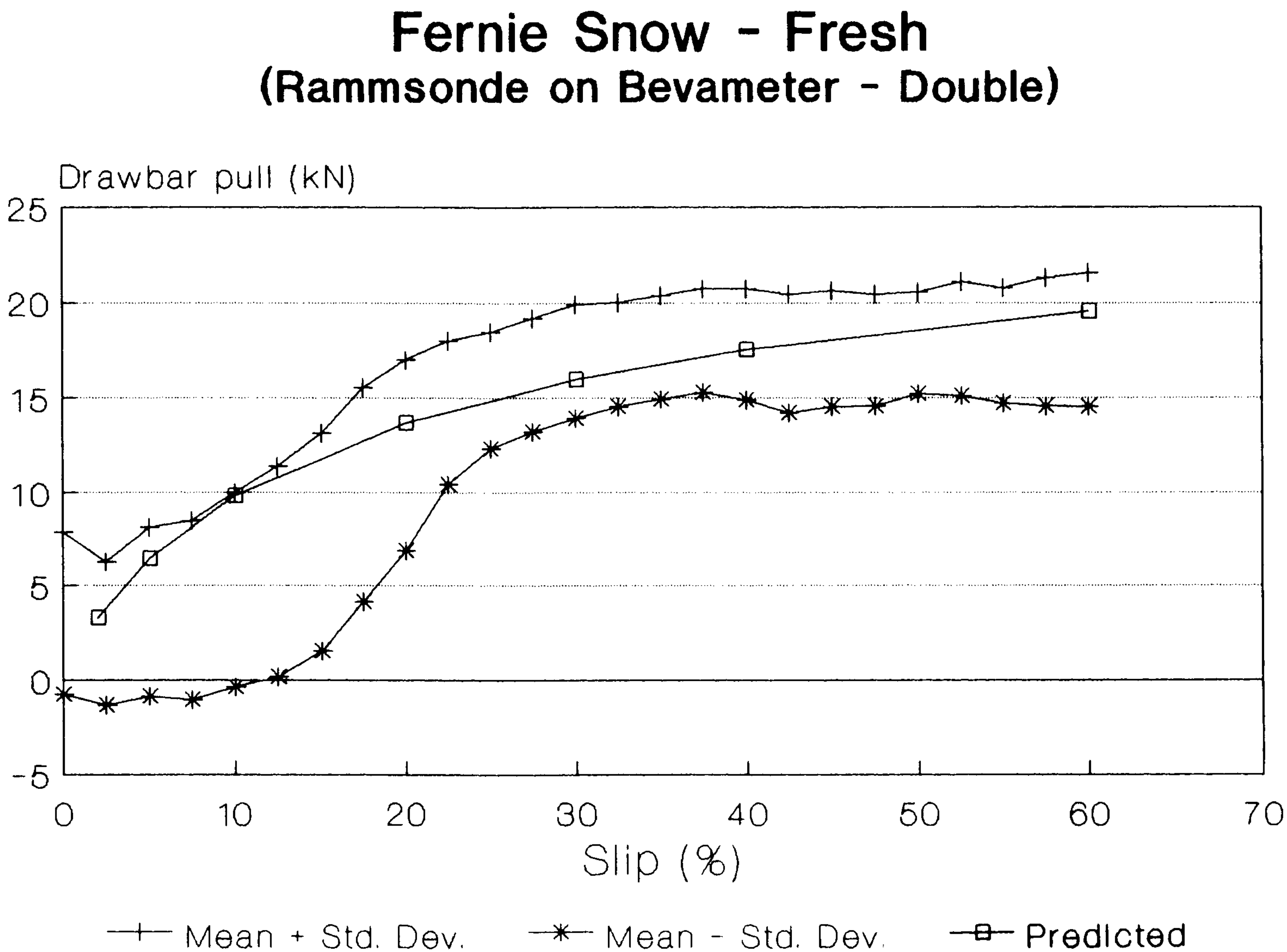

Fig. 4.2.3 Measured and predicted vehicle performance using NTVPM-85 on undisturbed snow

Table 4.2.8 Comparison of the Measured Vehicle Drawbar Pull with the Predicted Ones for Undisturbed Snow (Using Equation: $p = (k_c/b + k_\phi) z^n$)

Slip (%)	Drawbar Pull (kN)				
	Measured		Predicted		
	Mean	Standard Deviation	Using Rammsonde	Using Bevameter	Using Rammsonde on Bevameter
20	11.93	5.06	11.74	16.09	13.68
30	16.92	2.99	13.96	18.01	15.96
40	17.82	2.92	15.62	19.39	17.54

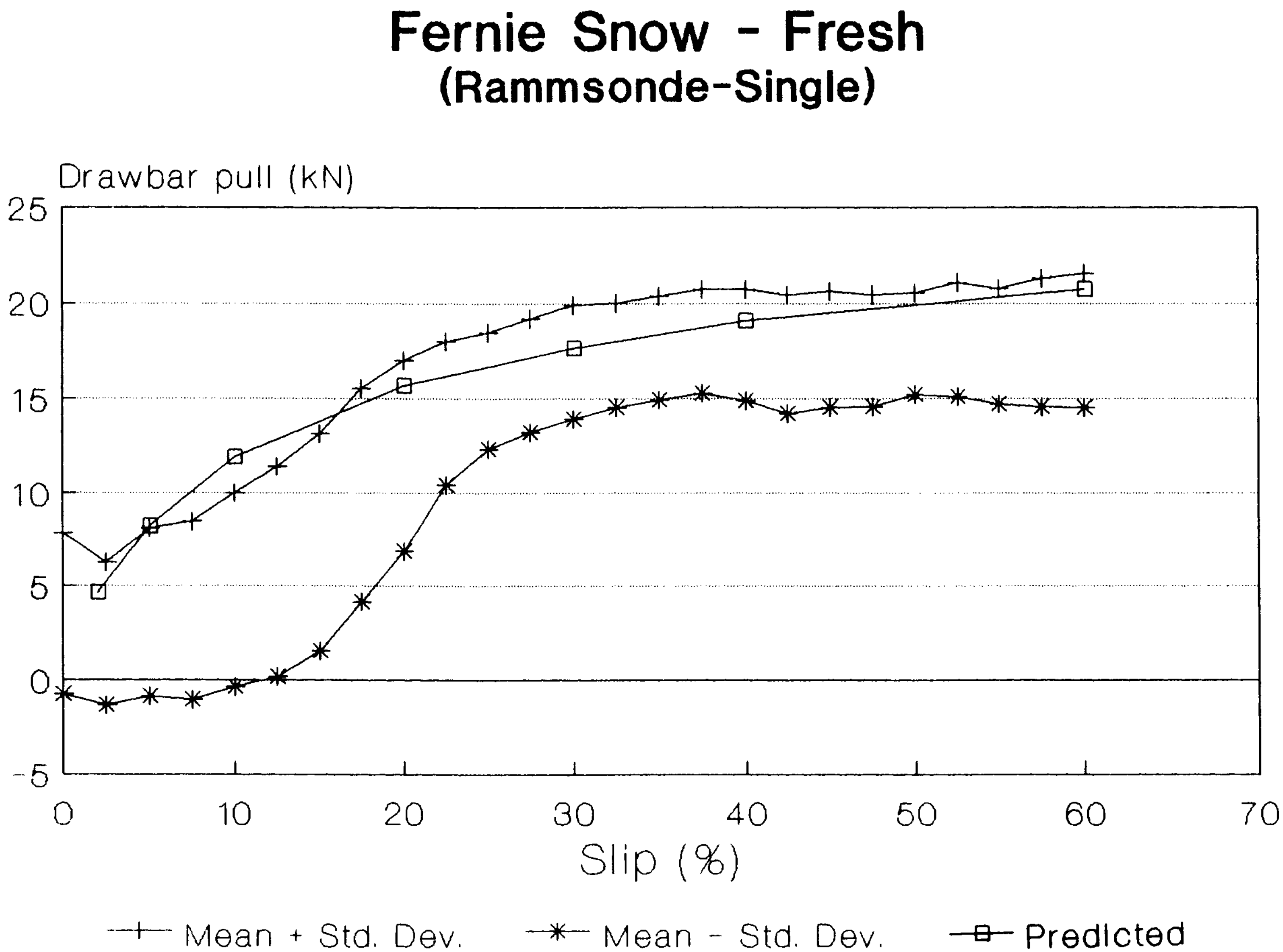

Fig. 4.2.4 Measured and predicted vehicle performance using NTVPM-85 on undisturbed snow

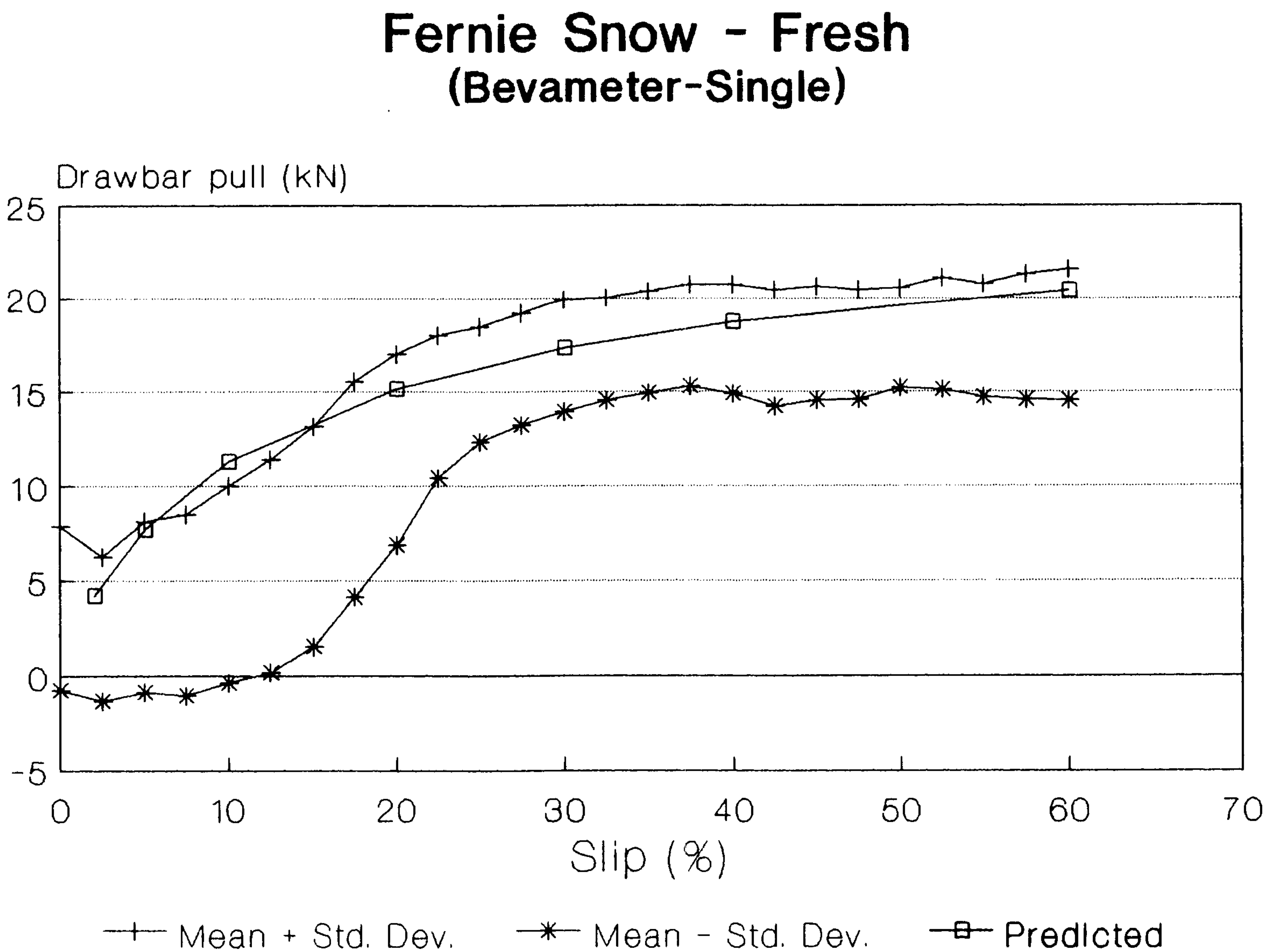

Fig. 4.2.5 Measured and predicted vehicle performance using NTVPM-85 on undisturbed snow

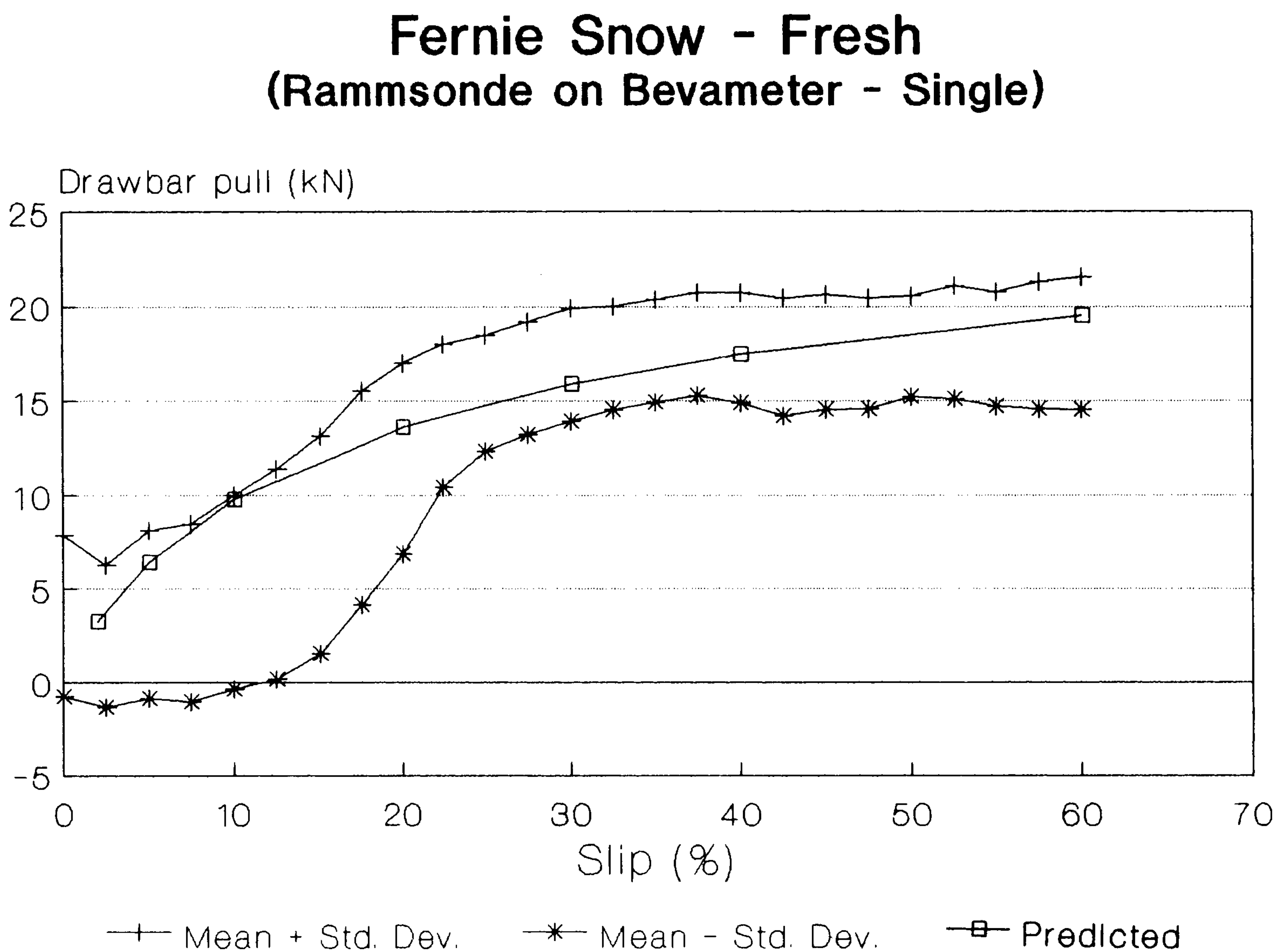

Fig. 4.2.6 Measured and predicted vehicle performance using NTVPM-85 on undisturbed snow

Table 4.2.9 **Comparison of the Measured Vehicle Drawbar Pull with the Predicted Ones for Undisturbed Snow (Using Equation: $p = k z^n$)**

Slip (%)	Drawbar Pull (kN)				
	Measured		Predicted		
	Mean	Standard Deviation	Using Rammsonde	Using Bevameter	Using Rammsonde on Bevameter
20	11.93	5.06	15.68	15.16	13.62
30	16.92	2.99	17.67	17.32	15.90
40	17.82	2.92	19.08	18.72	17.48

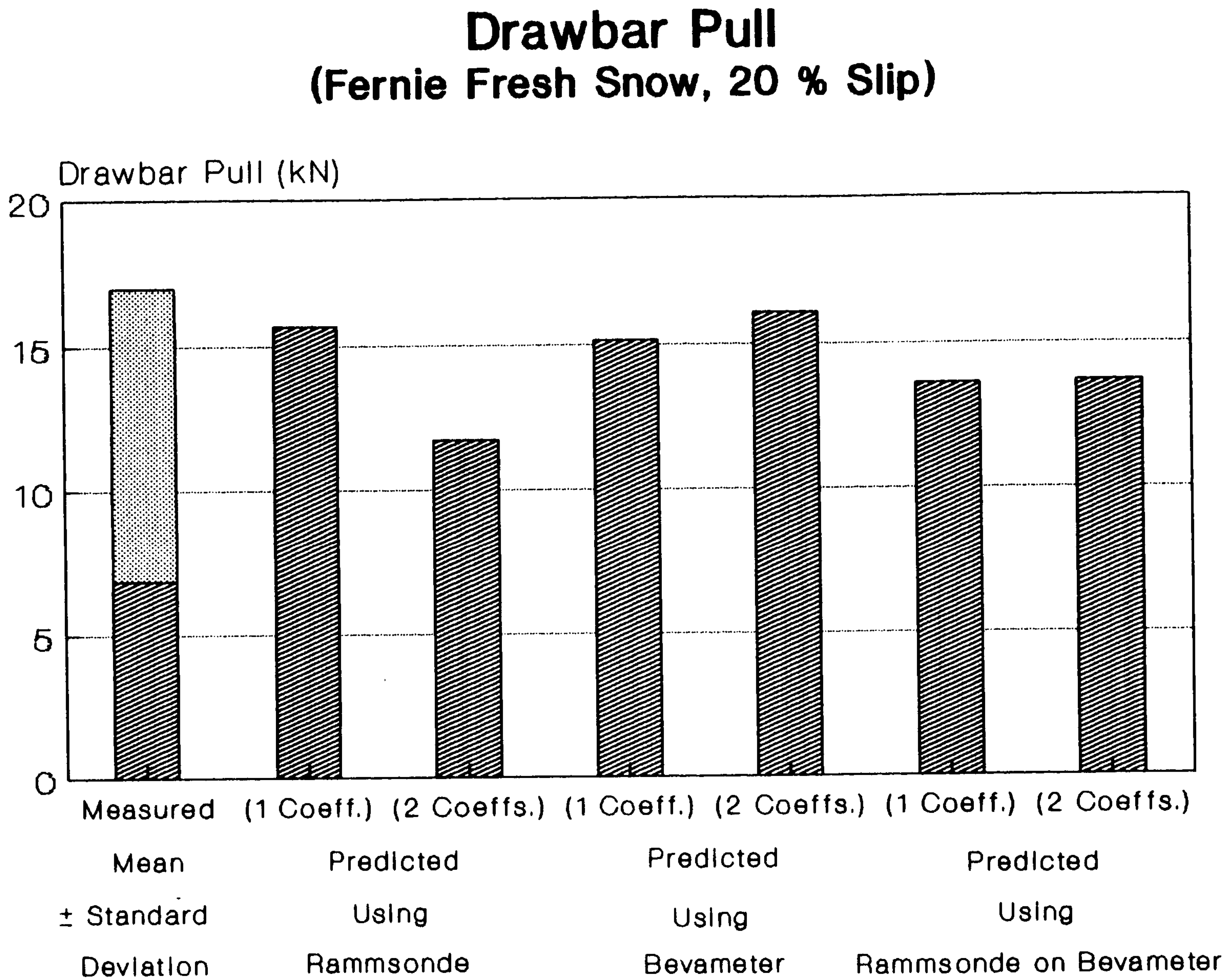

Fig. 4.2.7 Measured and predicted vehicle performance at 20% slip on undisturbed snow

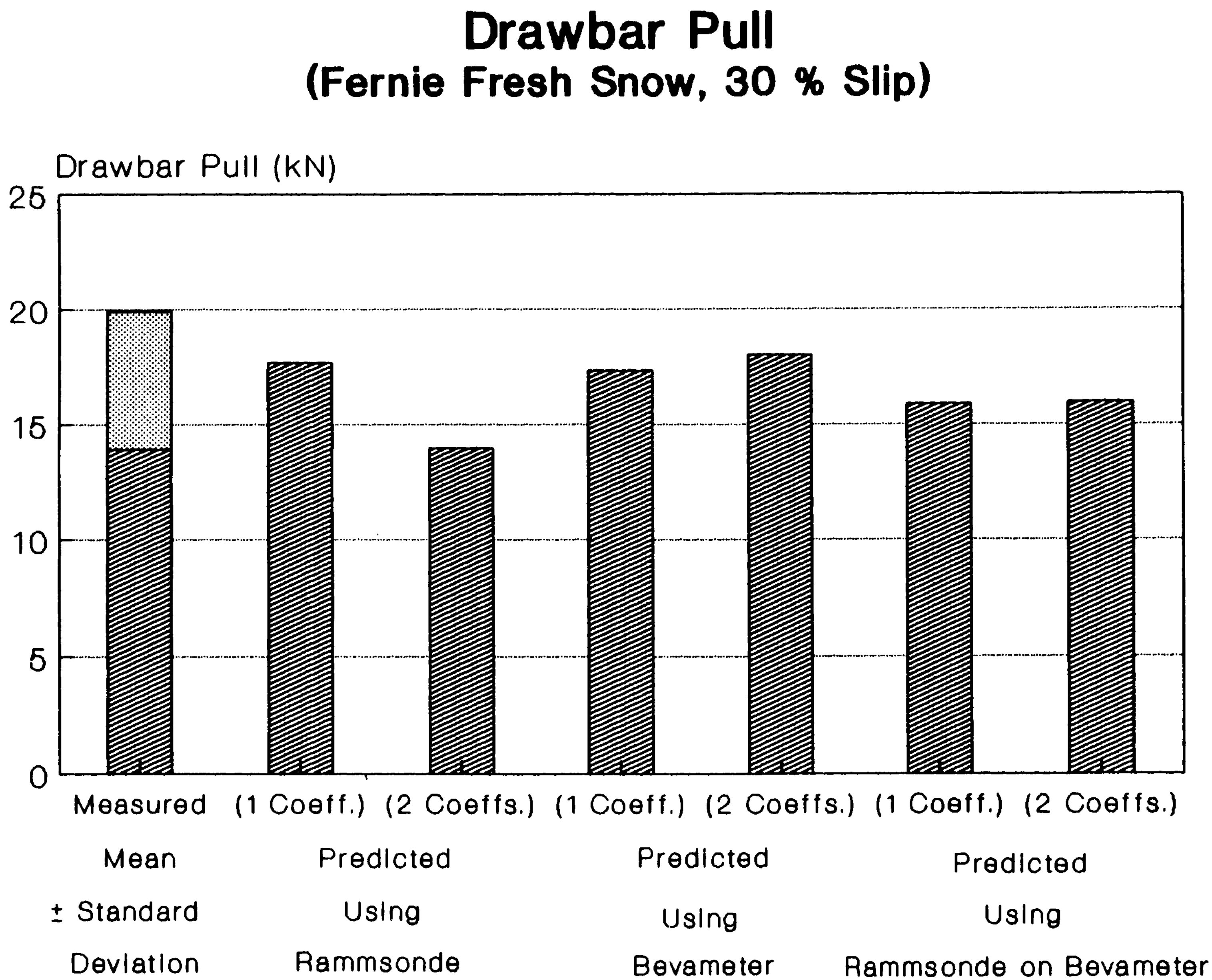

Fig. 4.2.8 Measured and predicted vehicle performance at 30% slip on undisturbed snow

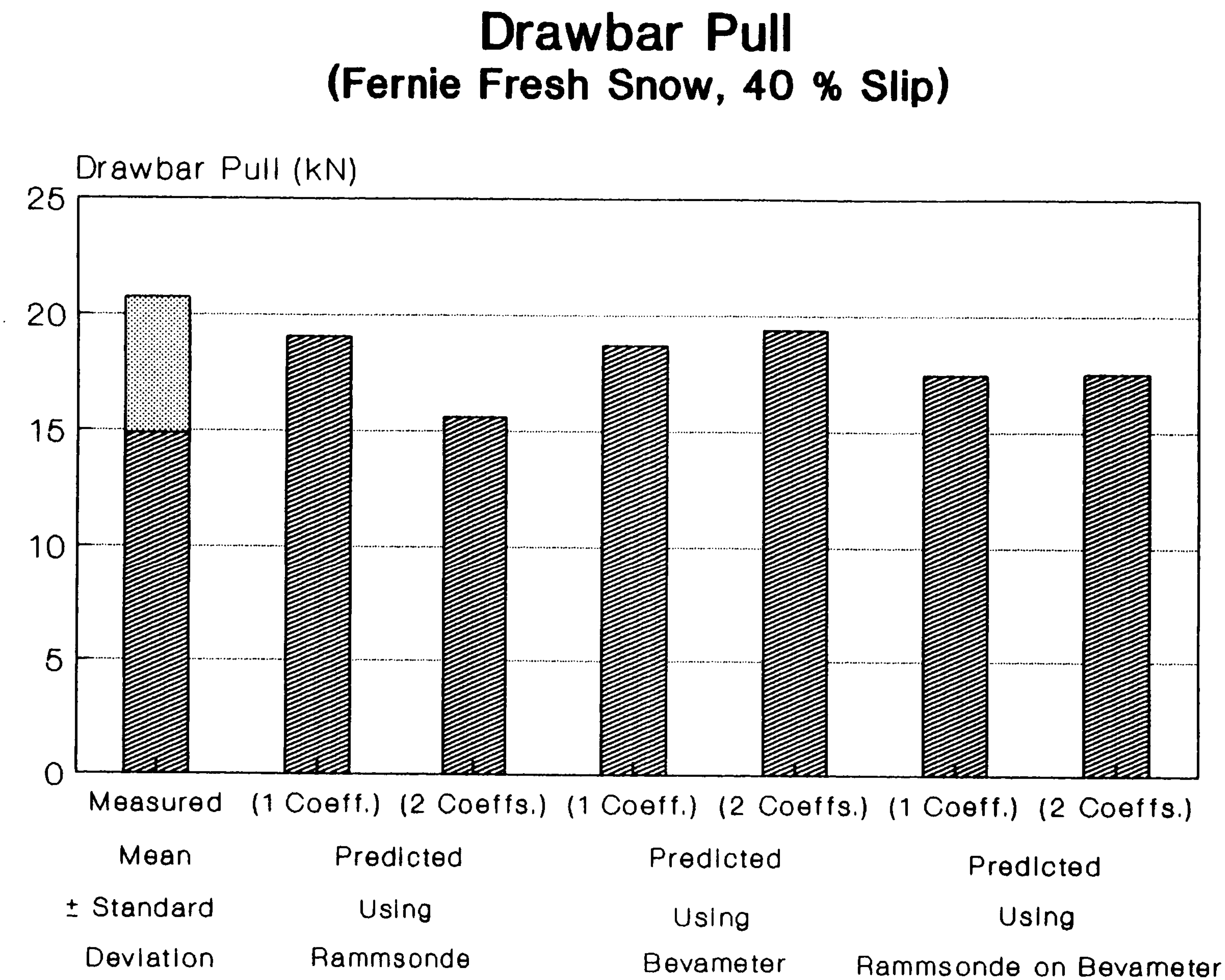

Fig, 4.2.9 Measured and predicted vehicle performance at 40% slip on undisturbed snow

comparison between the measured drawbar pull and the predicted ones, using pressure-sinkage data obtained with the three devices, at slips of 20, 30 and 40%, respectively. The terms (1 Coeff.) and 2 (Coeffs.) shown in the figures represent predictions obtained using pressure-sinkage parameters n and k (Table 4.2.5) and n, k_c and k_ϕ (Table 4.2.3), respectively.

It can be seen from the figures and tables that on undisturbed snow there is, in general, a reasonable agreement between the measured tractive performance and predicted ones using NTVPM-85 with pressure-sinkage data obtained using the three devices. It appears, however, that predictions based on pressure-sinkage data obtained using a single sensing element with diameter of 10 cm and characterized by parameters n and k are less sensitive to the type of device used (Rammsonde, bevameter or Rammsonde cone mounted on bevameter assembly) than those obtained using two sensing elements with diameters of 4 and 10 cm and characterized by parameters n, k_c and k_ϕ.

To further substantiate the findings described above, additional comparative study was performed. The comparative study was to examine the correlation of the predicted vehicle performance based on the pressure-sinkage data obtained on a specific date with the corresponding measured vehicle performance.

As shown in Figs. 4.1.2 - 4.1.7, measured data on vehicle performance over undisturbed snow were available for February 8, 12, 13, 16, 20 and 21, 1990. Therefore, the performance of the test vehicle was predicted using NTVPM-85 based on the pressure-sinkage data obtained on these dates as shown in Table 4.2.1. The average values of the shear strength parameters shown in Table 4.2.6 were used in the predictions.

Figures 4.2.10 - 4.2.22 show the correlations between the measured vehicle performance, expressed in terms of the mean value ± standard deviation of the drawbar pull, and the predicted one using pressure-sinkage parameters, n, k_c and k_ϕ, obtained with

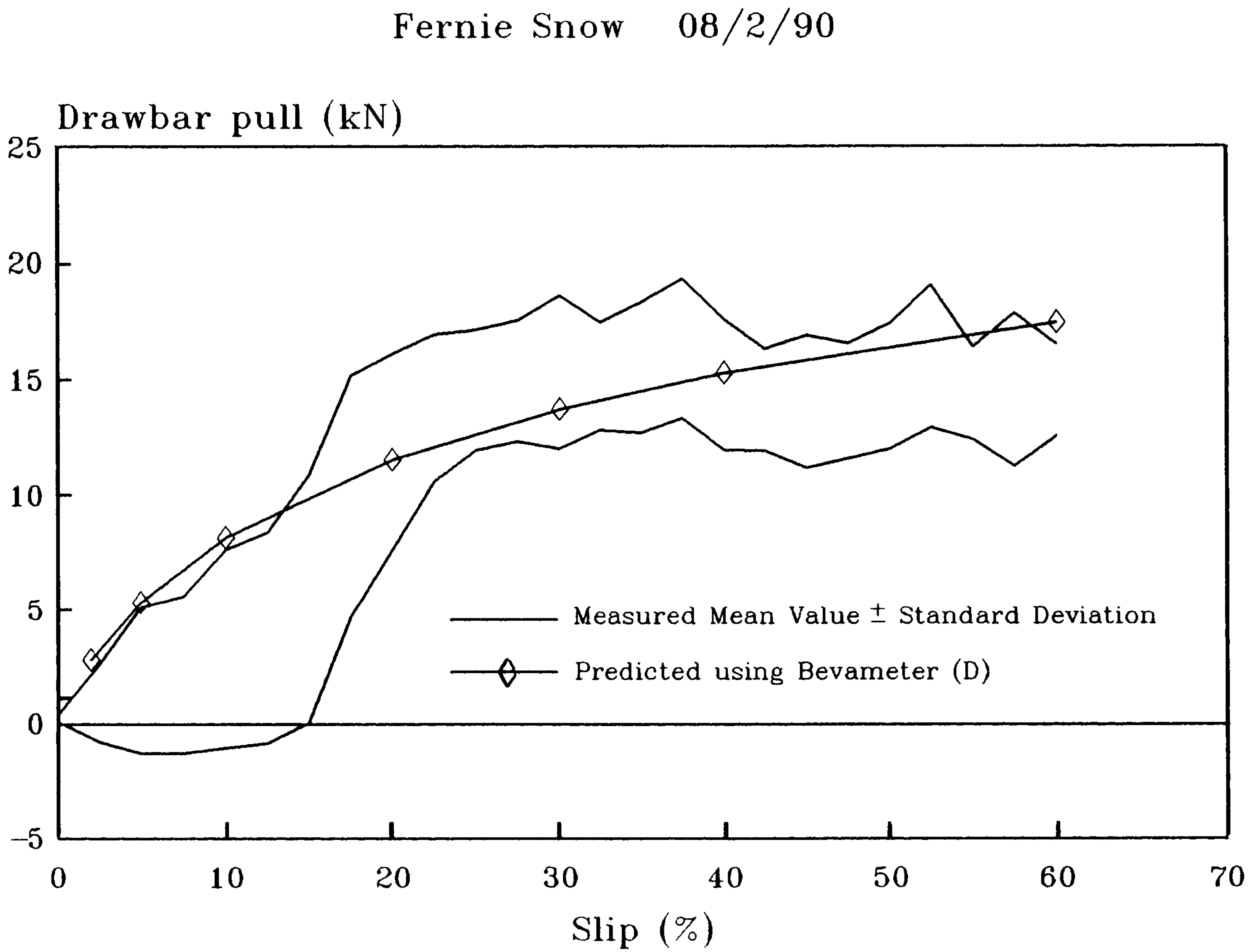

Fig. 4.2.10 Measured and predicted vehicle performance using NTVPM-85 on undisturbed snow

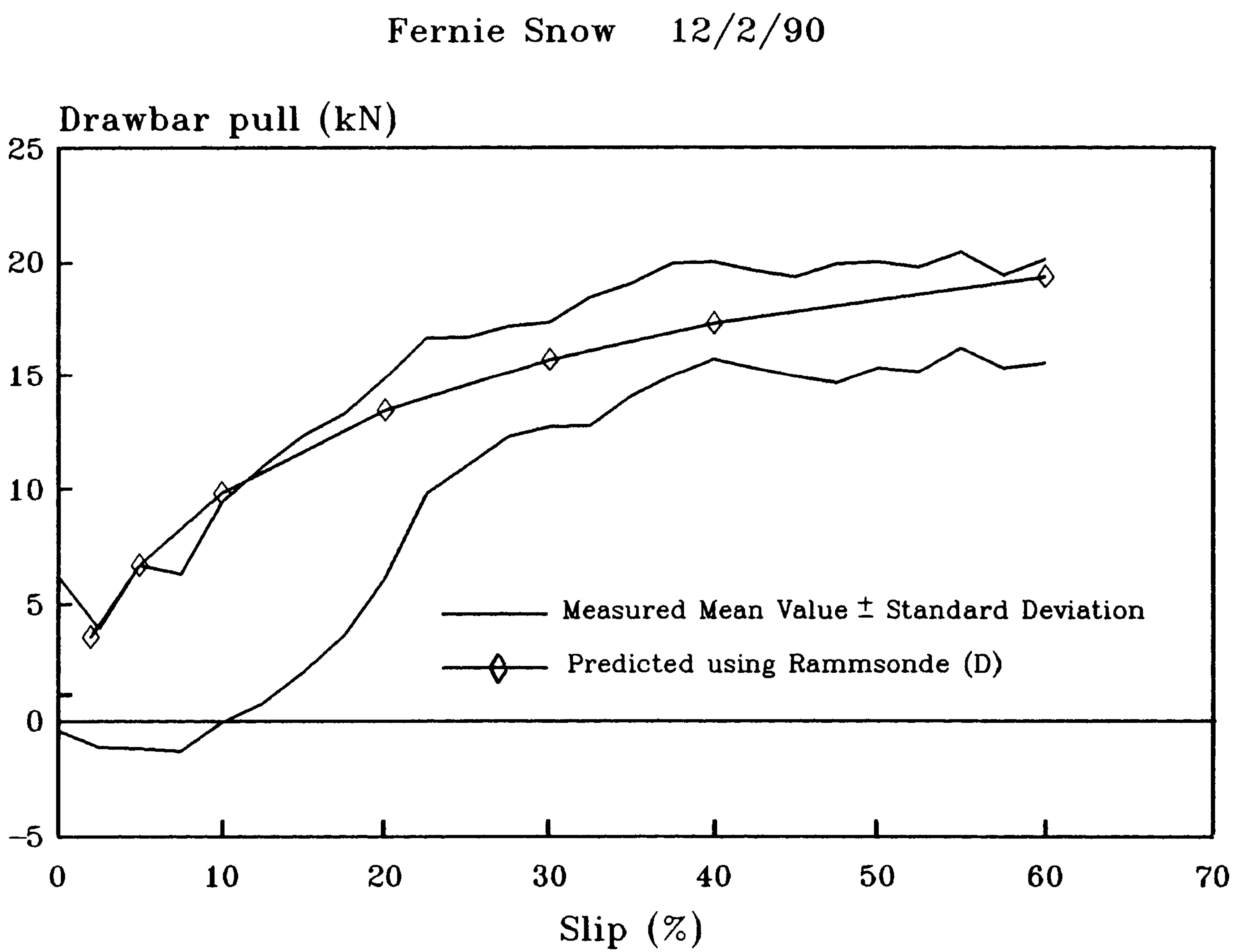

Fig. 4.2.11 Measured and predicted vehicle performance using NTVPM-85 on undisturbed snow

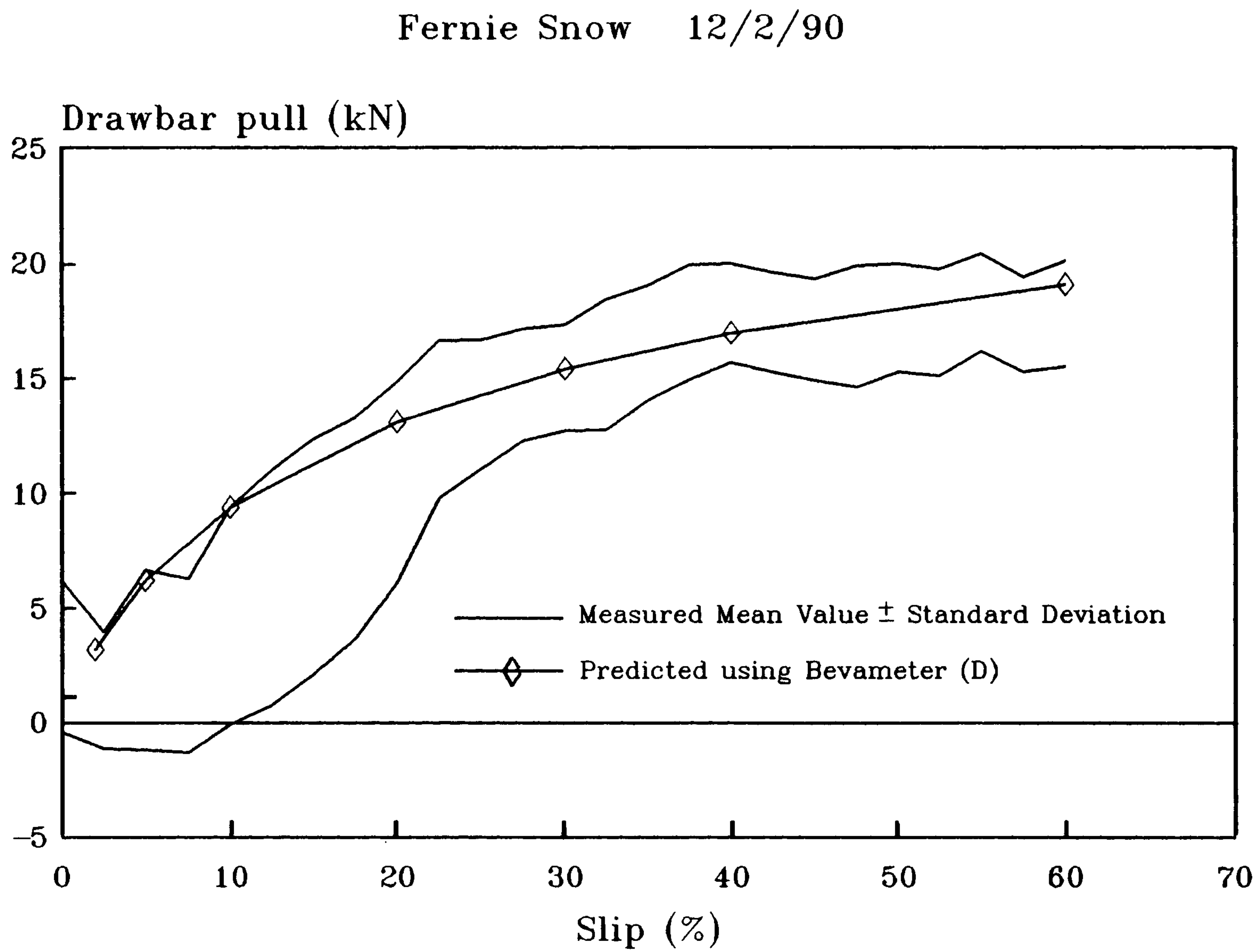

Fig. 4.2.12 Measured and predicted vehicle performance using NTVPM-85 on undisturbed snow

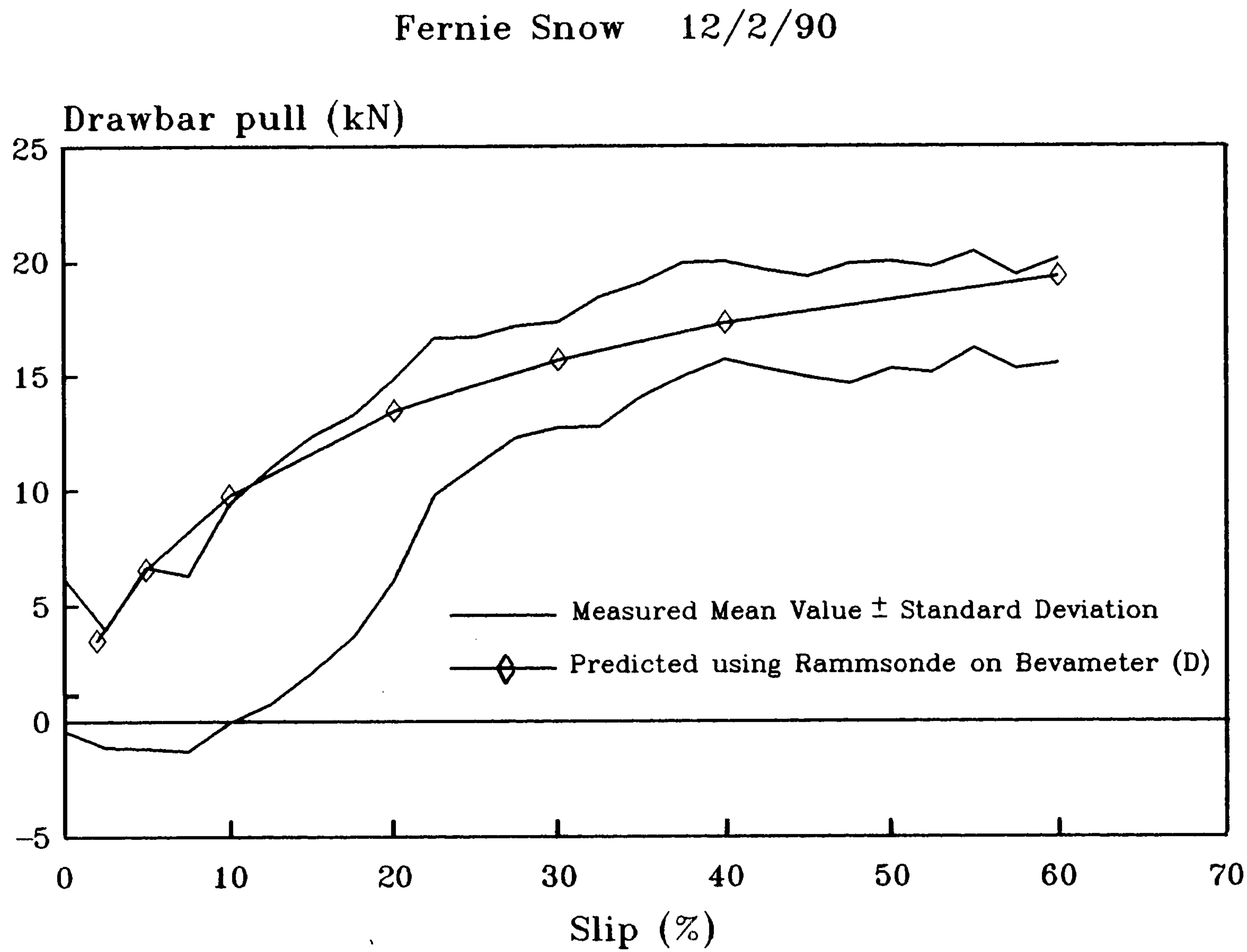

Fig. 4.2.13 Measured and predicted vehicle performance using NTVPM-85 on undisturbed snow

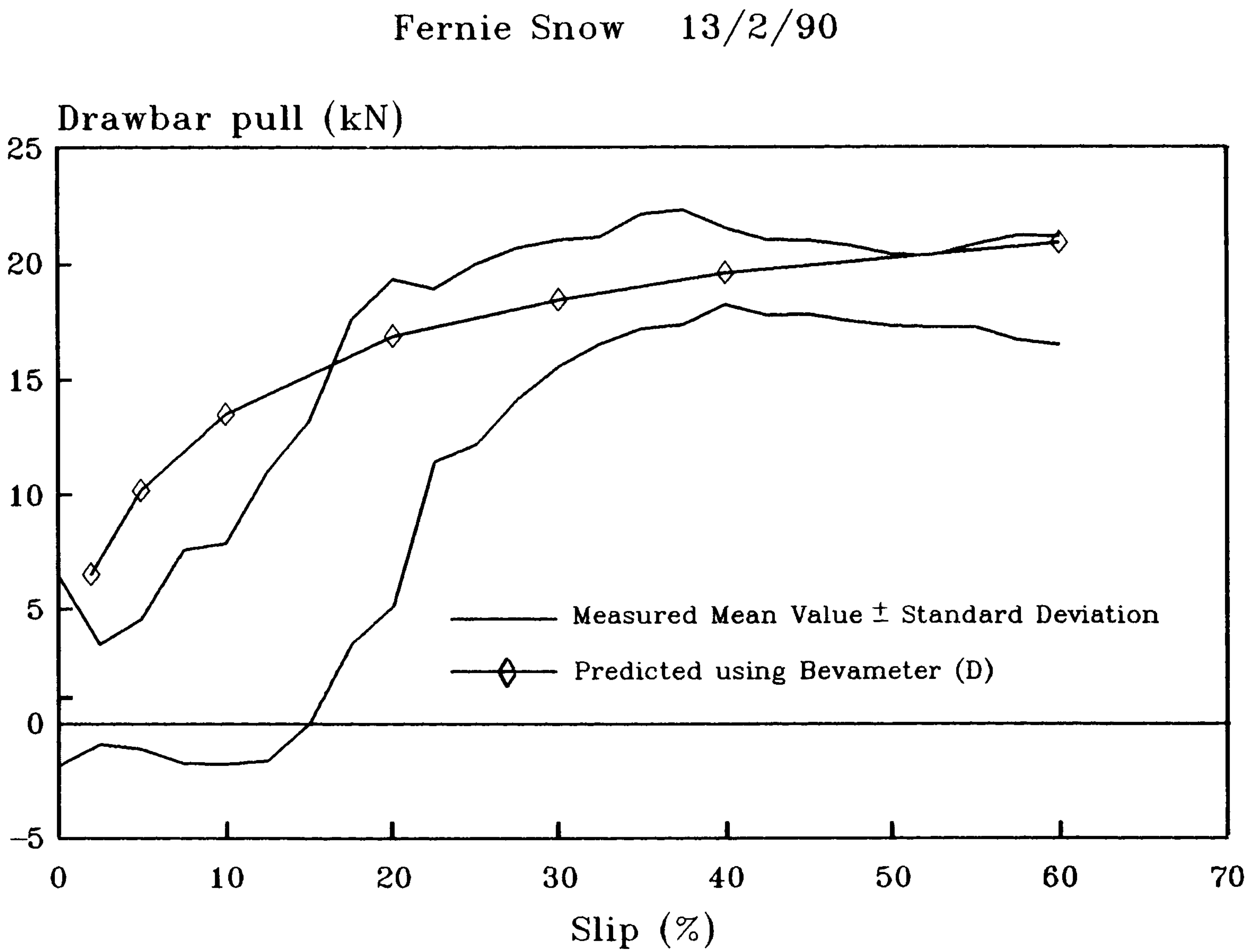

Fig. 4.2.14 Measured and predicted vehicle performance using NTVPM-85 on undisturbed snow

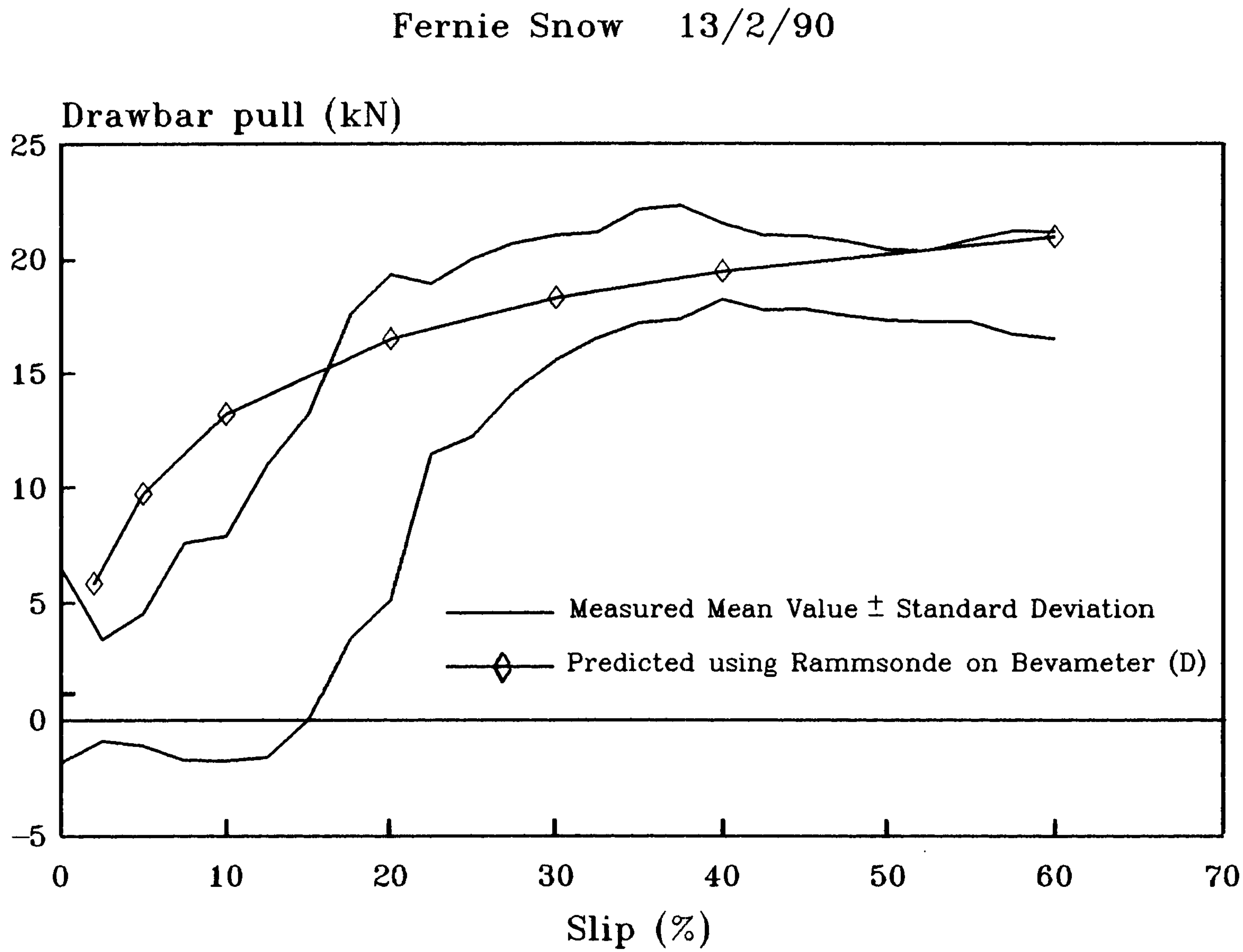

Fig, 4.2.15 Measured and predicted vehicle performance using NTVPM-85 on undisturbed snow

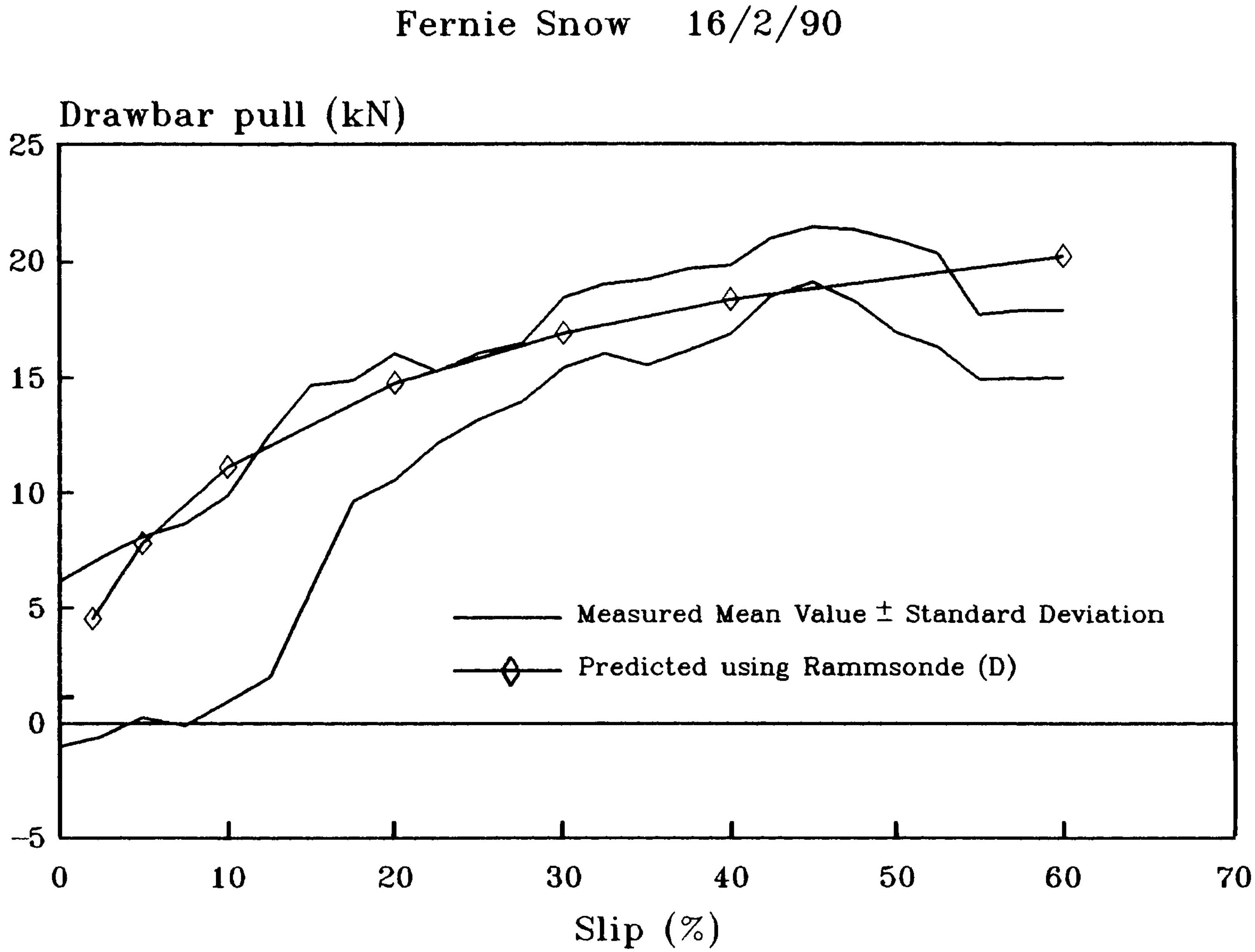

Fig. 4.2.16 Measured and predicted vehicle performance using NTVPM-85 on undisturbed snow

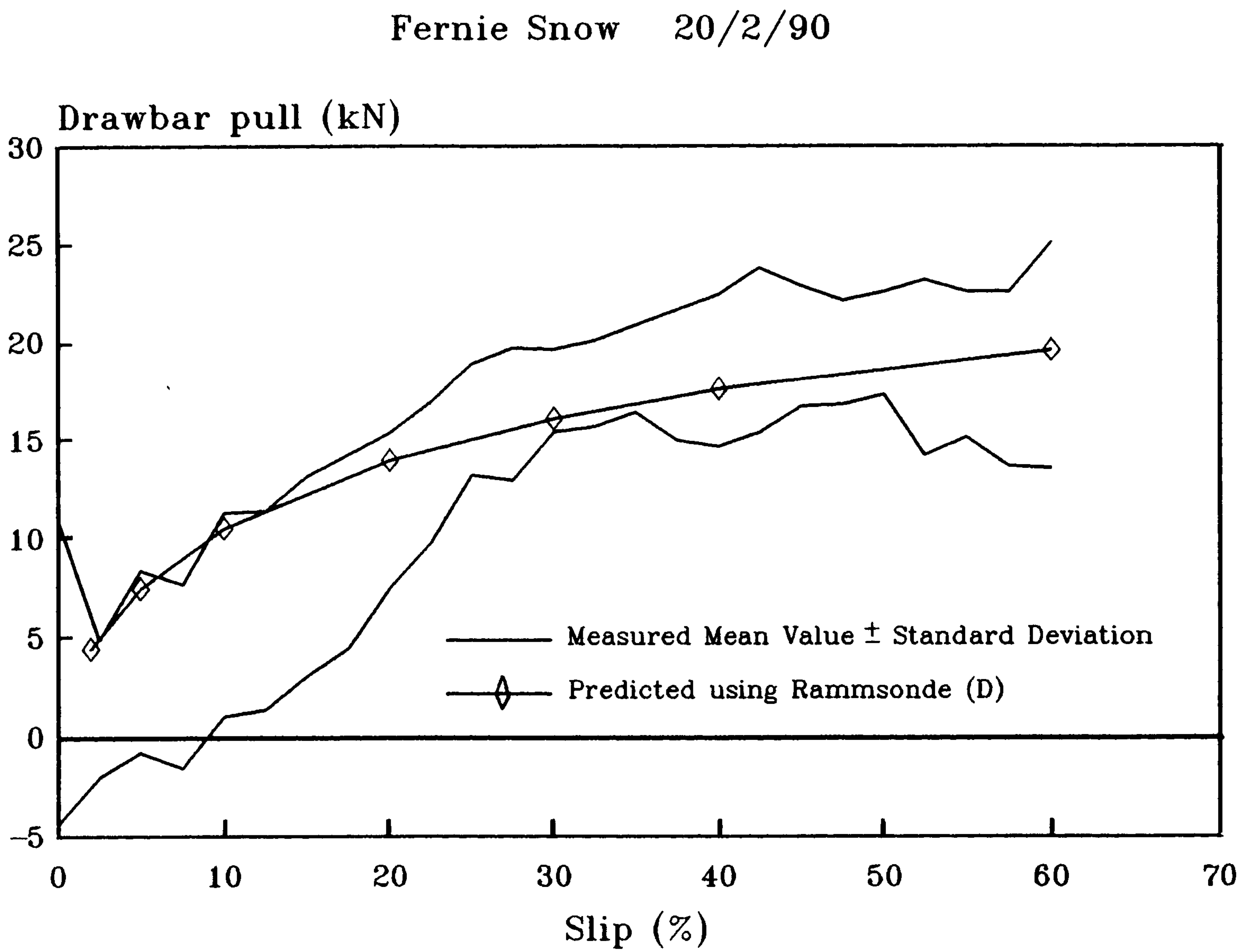

Fig. 4.2.17 Measured and predicted vehicle performance using NTVPM-85 on undisturbed snow

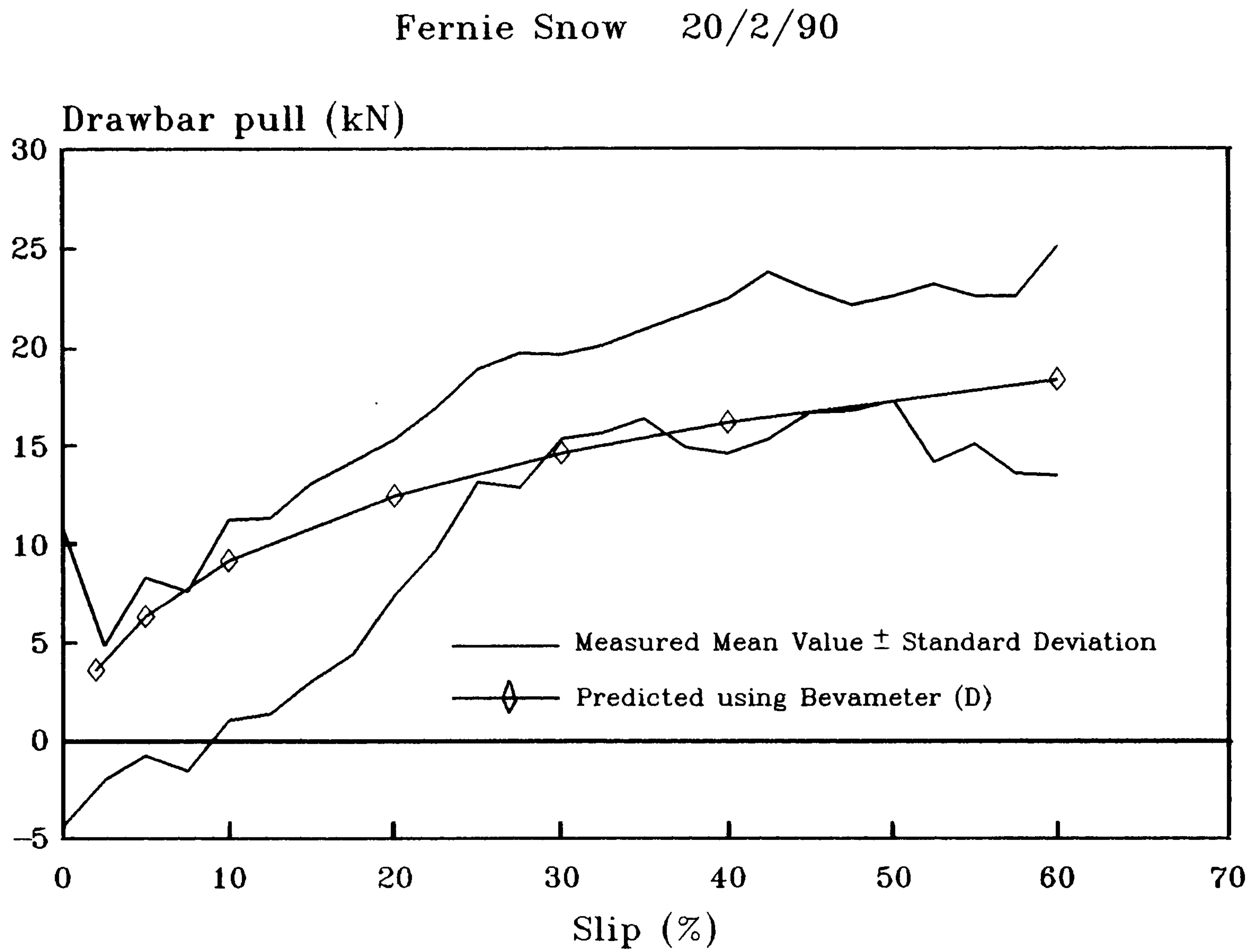

Fig. 4.2.18 Measured and predicted vehicle performance using NTVPM-85 on undisturbed snow

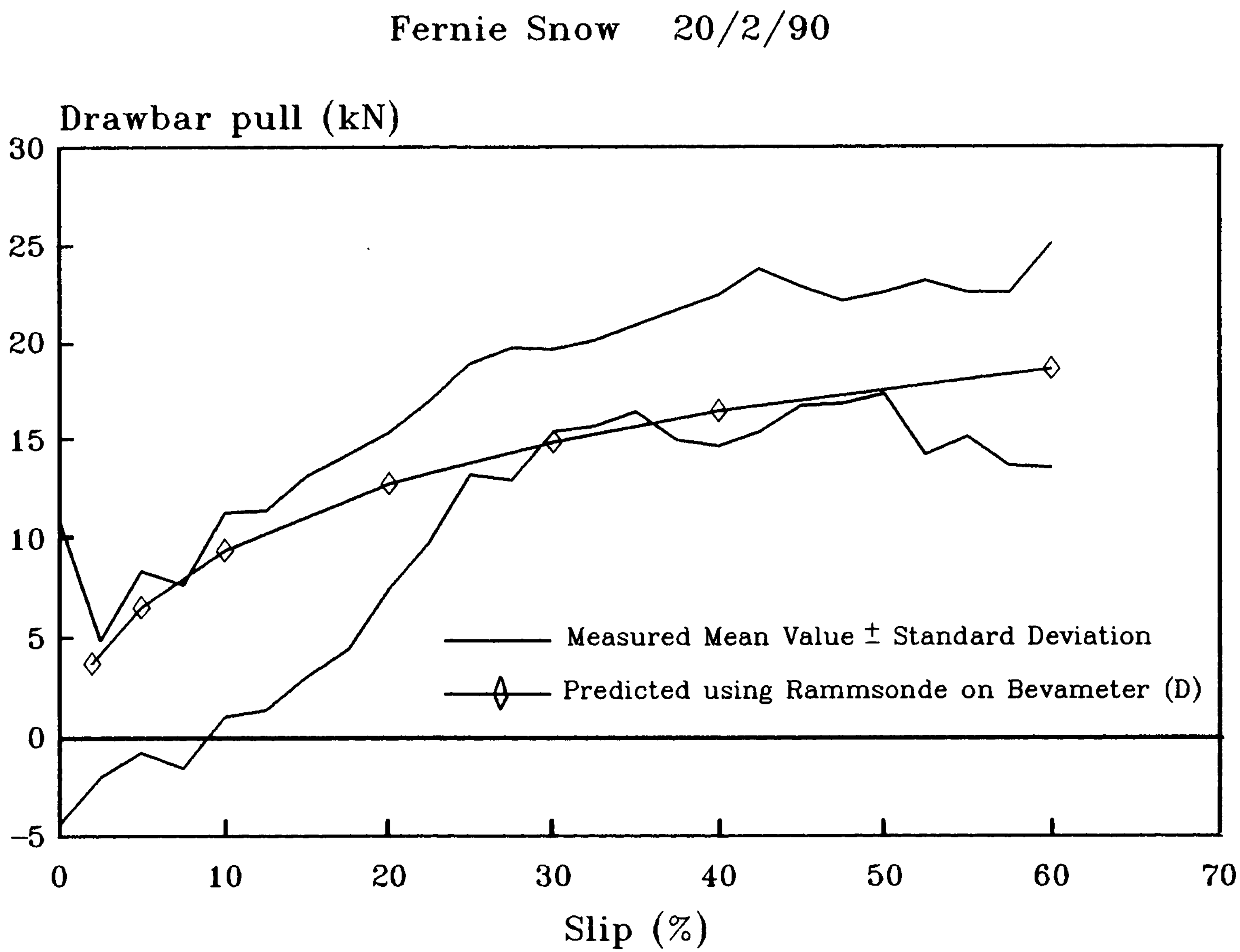

Fig. 4.2.19 Measured and predicted vehicle performance using NTVPM-85 on undisturbed snow

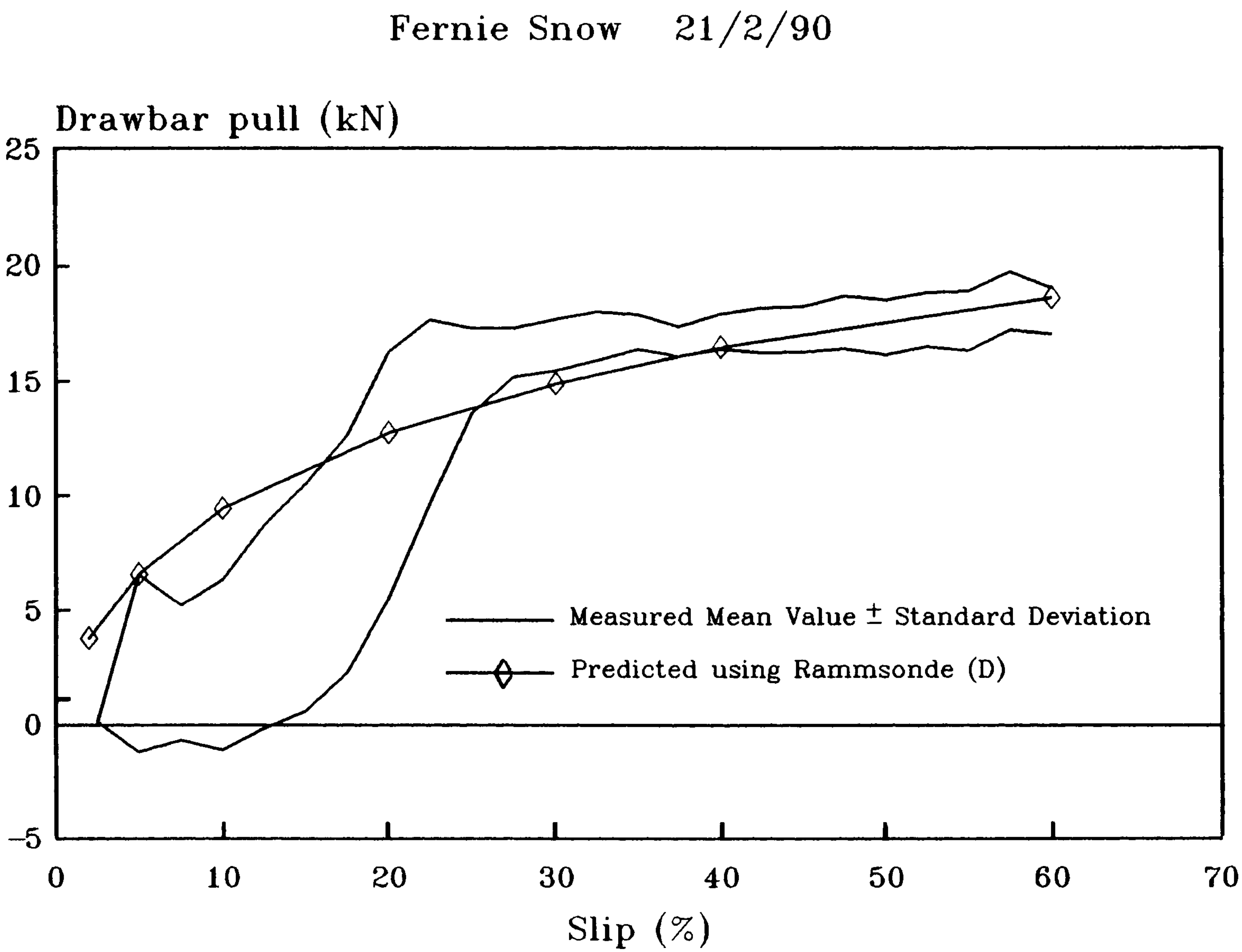

Fig. 4.2.20 Measured and predicted vehicle performance using NTVPM-85 on undisturbed snow

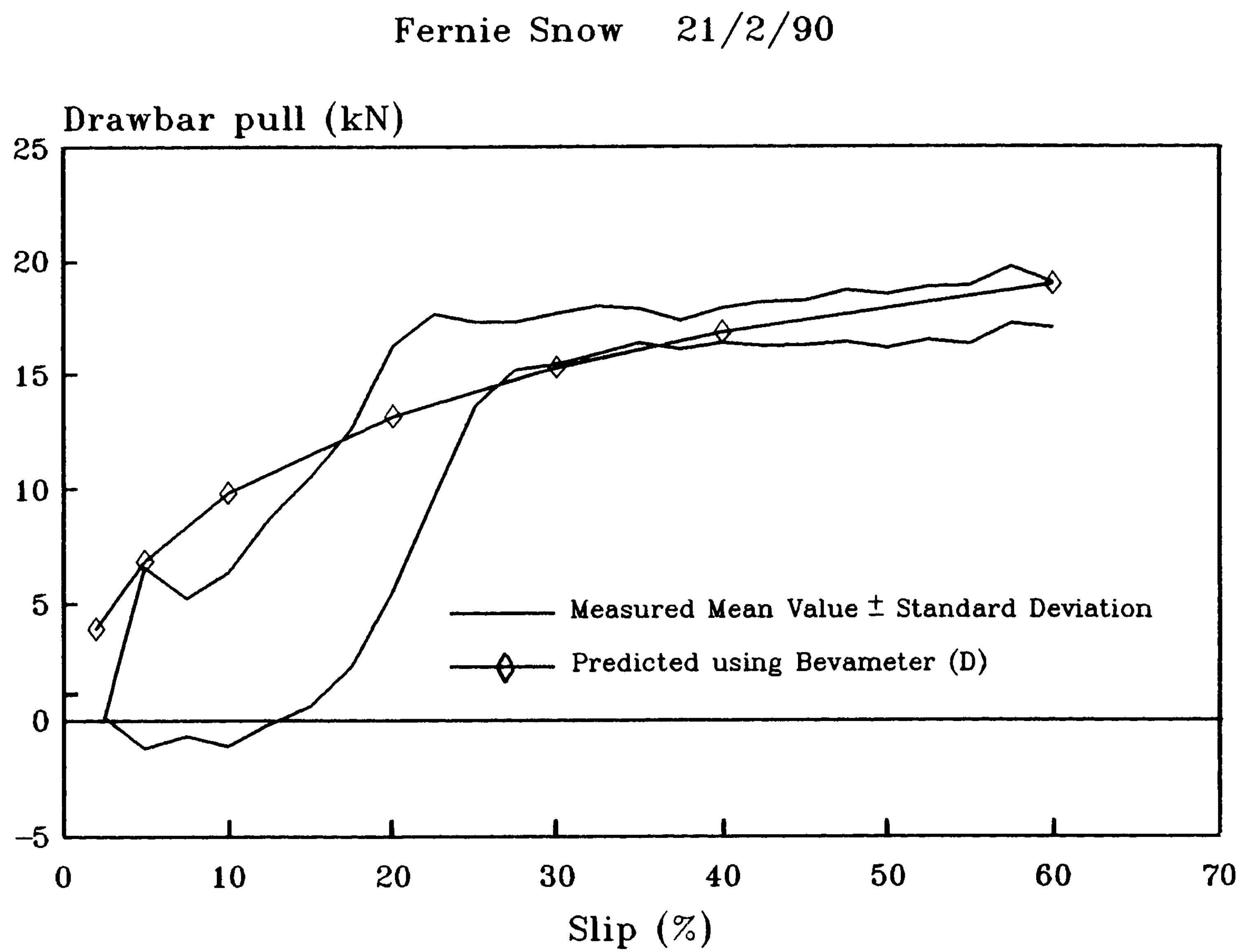

Fig. 4.2.21 Measured and predicted vehicle performance using NTVPM-85 on undisturbed snow

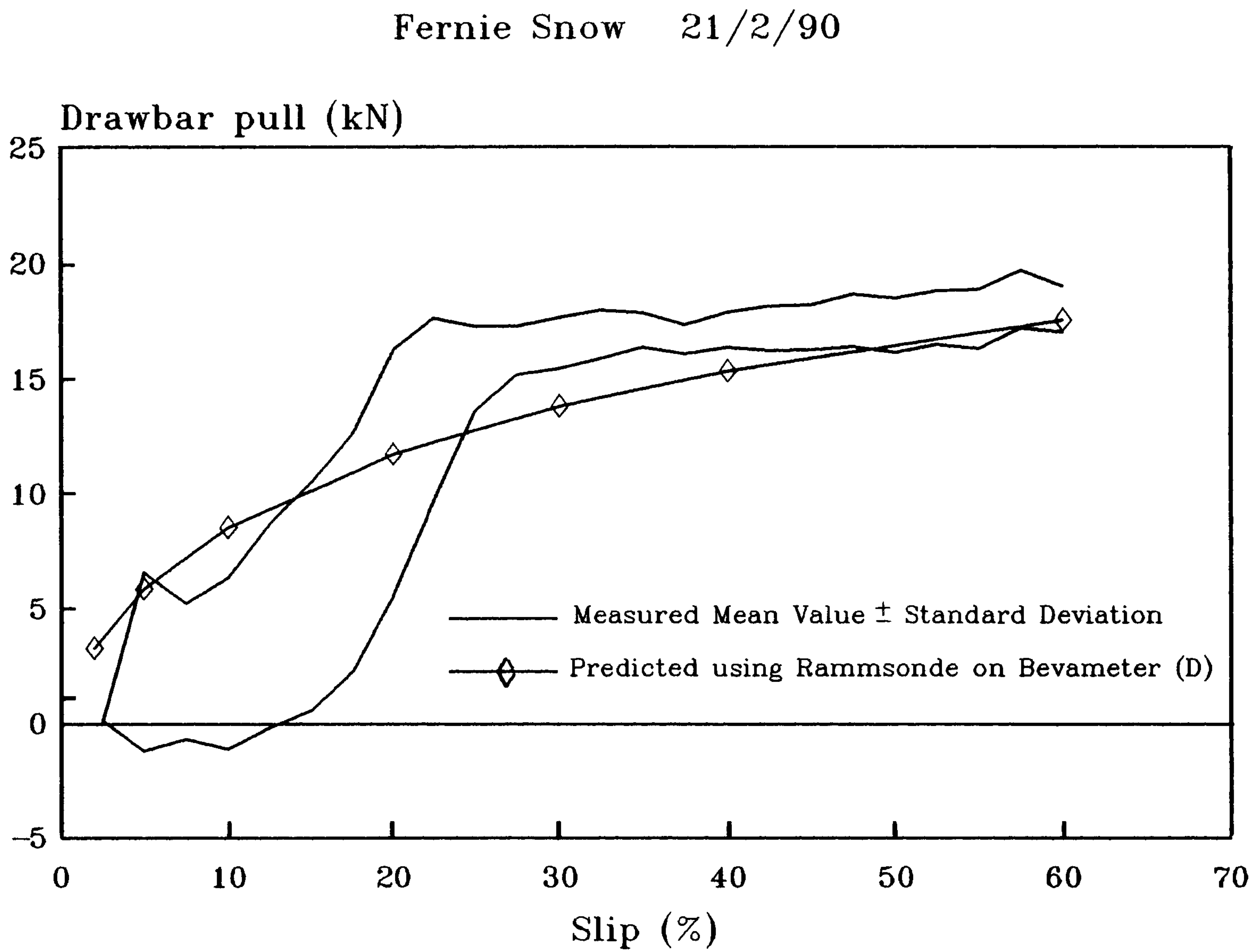

Fig. 4.2.22 Measured and predicted vehicle performance using NTVPM-85 on undisturbed snow

various devices and shown in Table 4.2.1, for February 8, 12, 13, 16, 20 and 21, 1990. Tables 4.2.10, 4.2.11 and 4.2.12 show comparisons between the measured and predicted drawbar pulls for various dates at slips of 20, 30 and 40%, respectively. Figures 4.2.23 - 4.2.40 show comparisons between the measured drawbar pulls and predicted ones, using pressure-sinkage parameters, n, k_c and k_ϕ, obtained with various devices and shown in Table 4.2.1, at slips of 20, 30 and 40% for February 8, 12, 13, 16, 20 and 21, 1990.

Figures 4.2.41 - 4.2.53 show the correlations between the measured vehicle performance and the predicted one using pressure-sinkage parameters, n and k, obtained with various devices and shown in Table 4.2.4, for February 8, 12, 13, 16, 20 and 21, 1990. Tables 4.2.13, 4.2.14 and 4.2.15 show comparisons between the measured and predicted drawbar pulls for various dates at slips of 20, 30 and 40%, respectively. Figures 4.2.54 - 4.2.71 show comparisons between the measured drawbar pull and predicted one, using pressure-sinkage parameters, n and k, obtained with various devices and shown in Table 4.2.4, for February 8, 12, 13, 16, 20 and 21, 1990.

It can be seen from the figures and tables that in most cases, the predicted performance lies within the range of the mean value ± standard deviation of the measured performance. Thus, the results of the comparative study further substantiate the findings that on undisturbed snow, there is a reasonable correlation between the measured vehicle performance and predicted one using NTVPM-85, with pressure-sinkage data obtained by the Rammsonde, the bevameter and the Rammsonde cone mounted on the bevameter assembly.

Table 4.2.10 Comparison of Measured and Predicted Drawbar Pull at 20% Slip on Undisturbed Snow (Using Equation: $p = (k_c/b + k_\phi) z^n$)

Date	Measured Mean Value ± Standard Deviation (kN)	Predicted Using Bevameter Data (kN)	Predicted Using Rammsonde Data (kN)	Predicted Using Rammsonde on Bevameter Data (kN)
Feb. 8	16.10 ± 7.63	11.54		
Feb. 12	14.86 ± 6.14	13.09	13.45	13.44
Feb. 13	19.31 ± 5.12	16.87		16.50
Feb. 16	16.05 ± 10.56		14.77	
Feb. 20	15.34 ± 7.43	12.49	13.92	12.73
Feb. 21	16.26 ± 5.58	13.17	12.77	11.71

Table 4.2.11 **Comparison of Measured and Predicted Drawbar Pull at 30% Slip on Undisturbed Snow (Using Equation: $p = (k_c/b + k_\phi)\, z^n$)**

Date	Measured Mean Value ± Standard Deviation (kN)	Predicted Using Bevameter Data (kN)	Predicted Using Rammsonde Data (kN)	Predicted Using Rammsonde on Bevameter Data (kN)
Feb. 8	18.60 ± 12.04	13.73		
Feb. 12	17.33 ± 12.71	15.40	15.66	15.67
Feb. 13	21.00 ± 15.58	18.43		18.29
Feb. 16	18.43 ± 15.42		16.91	
Feb. 20	19.61 ± 15.38	14.64	16.06	14.96
Feb. 21	17.67 ± 15.45	15.30	14.90	13.82

Table 4.2.12 **Comparison of Measured and Predicted Drawbar Pull at 40% Slip on Undisturbed Snow (Using Equation: $p = (k_c/b + k_\phi)\, z^n$)**

Date	Measured Mean Value ± Standard Deviation (kN)	Predicted Using Bevameter Data (kN)	Predicted Using Rammsonde Data (kN)	Predicted Using Rammsonde on Bevameter Data (kN)
Feb. 8	17.58 ± 11.97	15.29		
Feb. 12	19.99 ± 15.68	16.96	17.27	17.28
Feb. 13	21.52 ± 18.23	19.57		19.44
Feb. 16	19.82 ± 16.87		18.33	
Feb. 20	22.40 ± 14.47	16.19	17.56	16.43
Feb. 21	17.91 ± 16.38	16.85	16.46	15.34

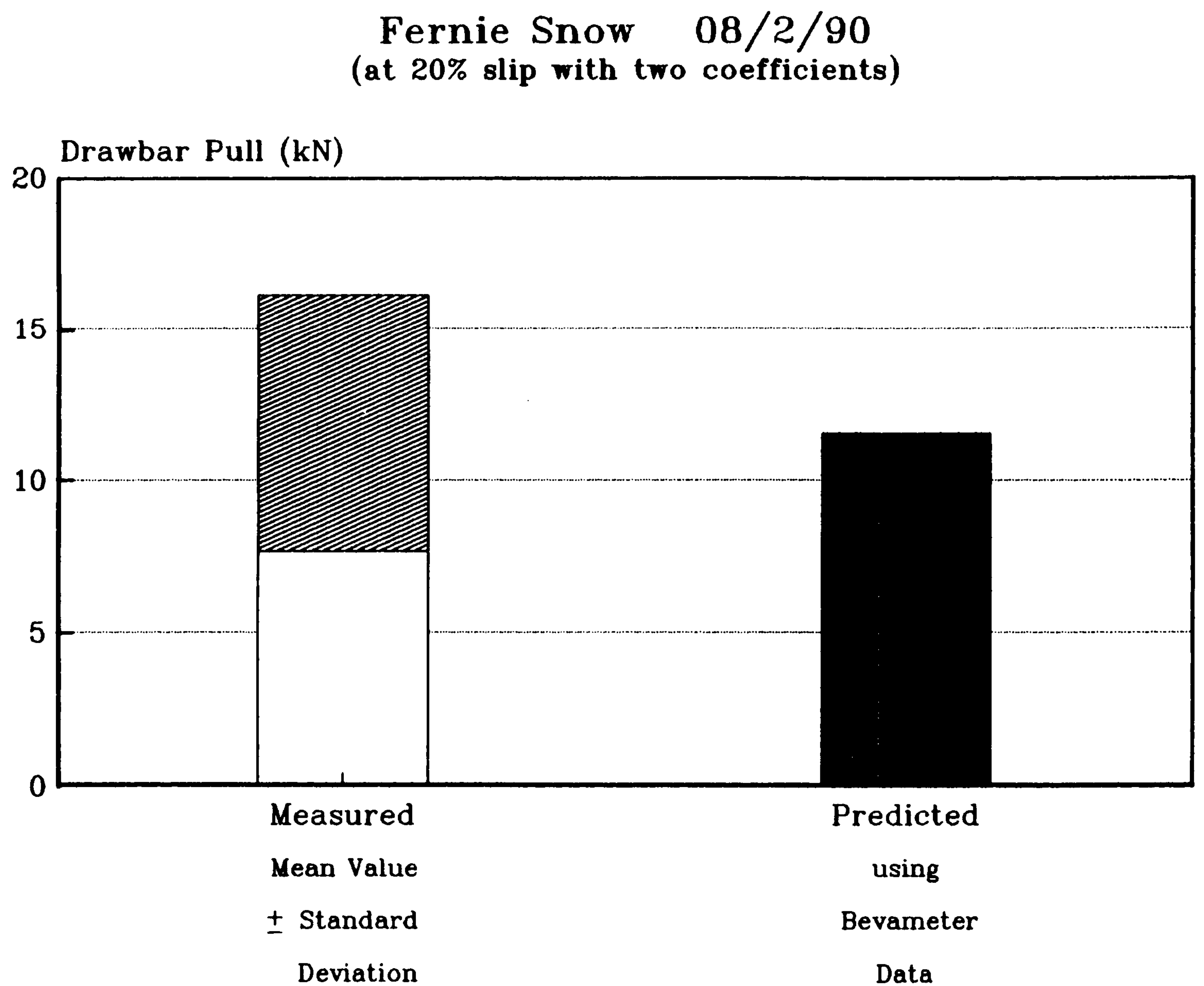

Fig. 4.2.23 Measured and predicted vehicle performance at 20% slip on undisturbed snow

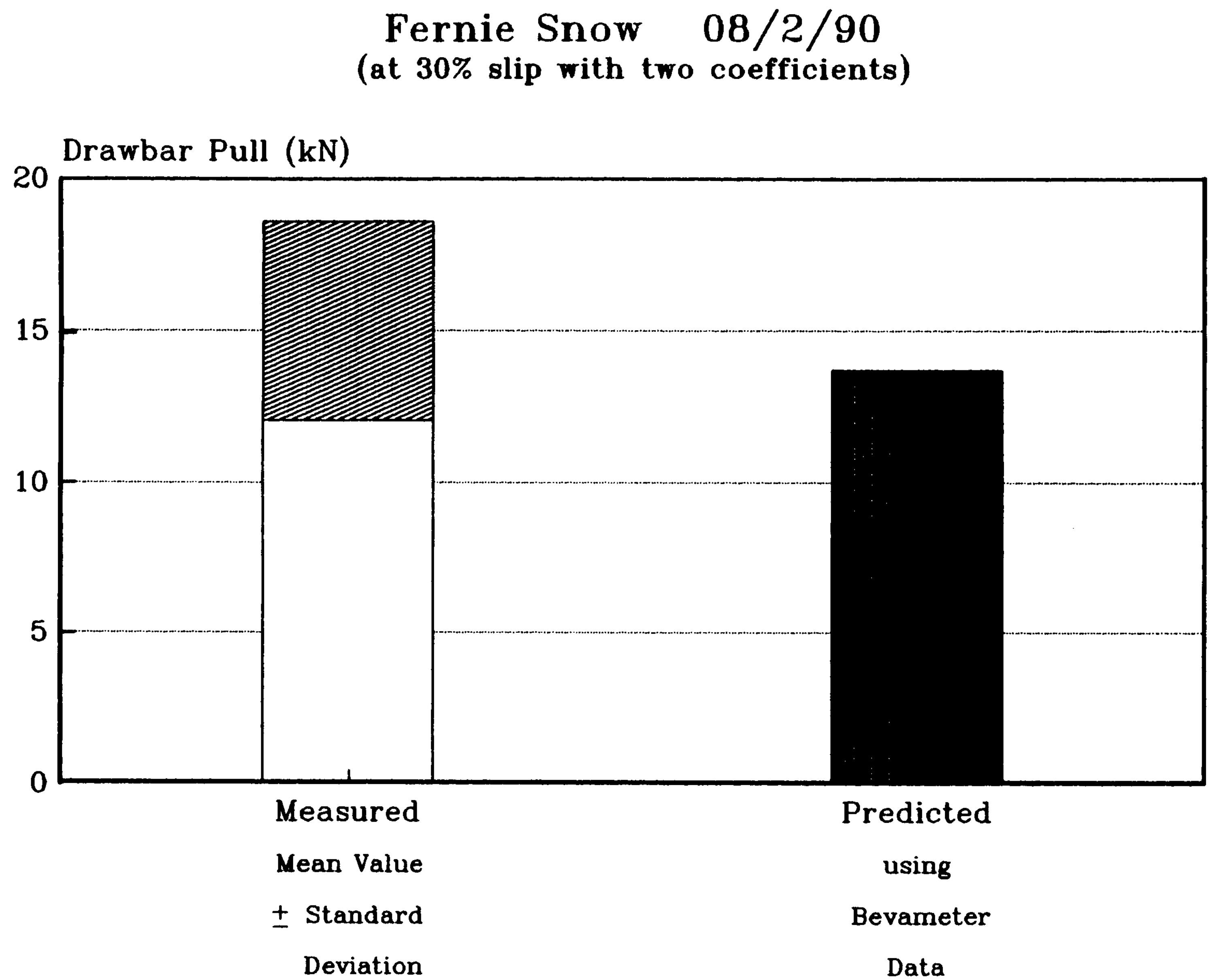

Fig. 4.2.24 Measured and predicted vehicle performance at 30% slip on undisturbed snow

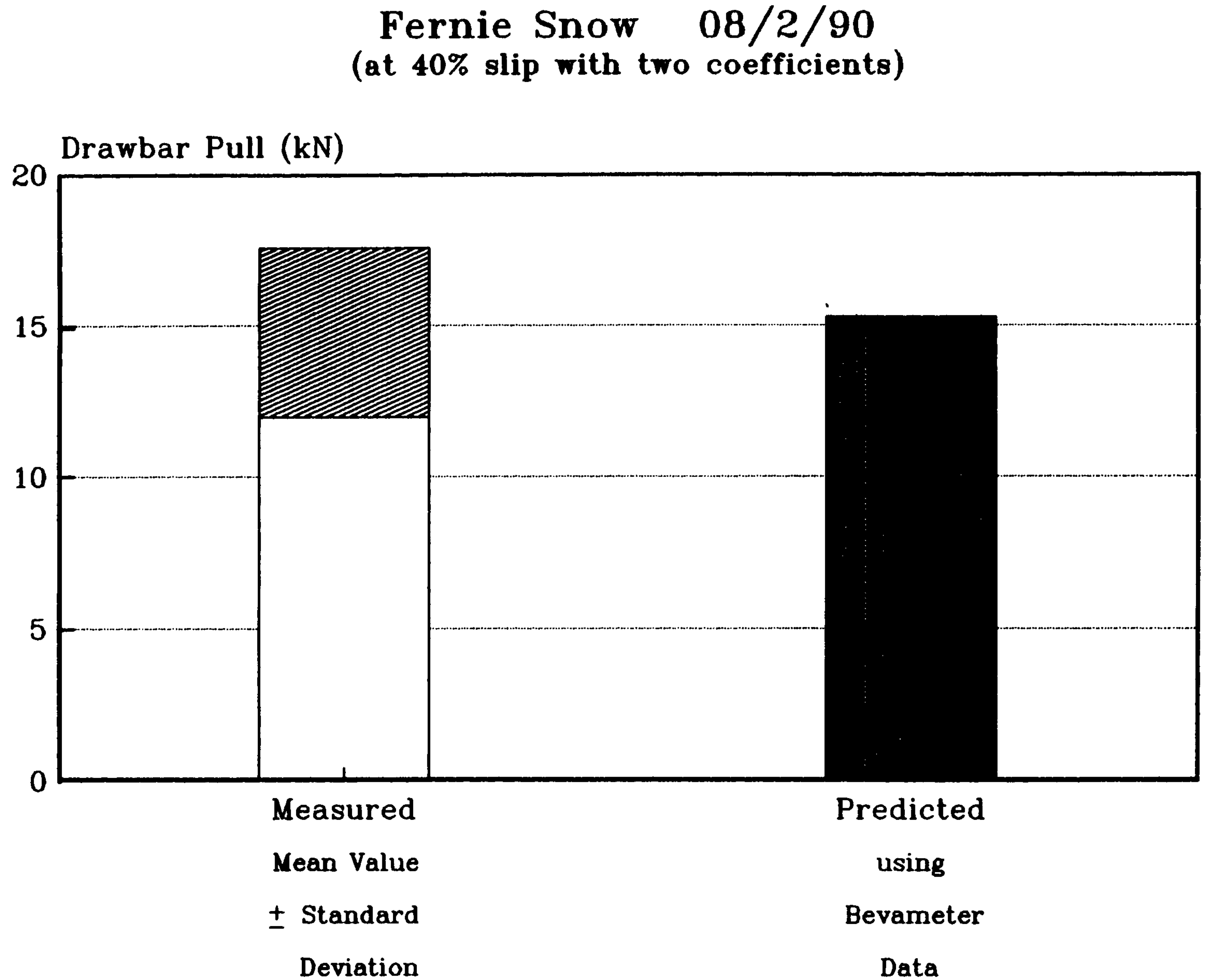

Fig. 4.2.25 Measured and predicted vehicle performance at 40% slip on undisturbed snow

Fernie Snow 12/2/90
(at 20% slip with two coefficients)

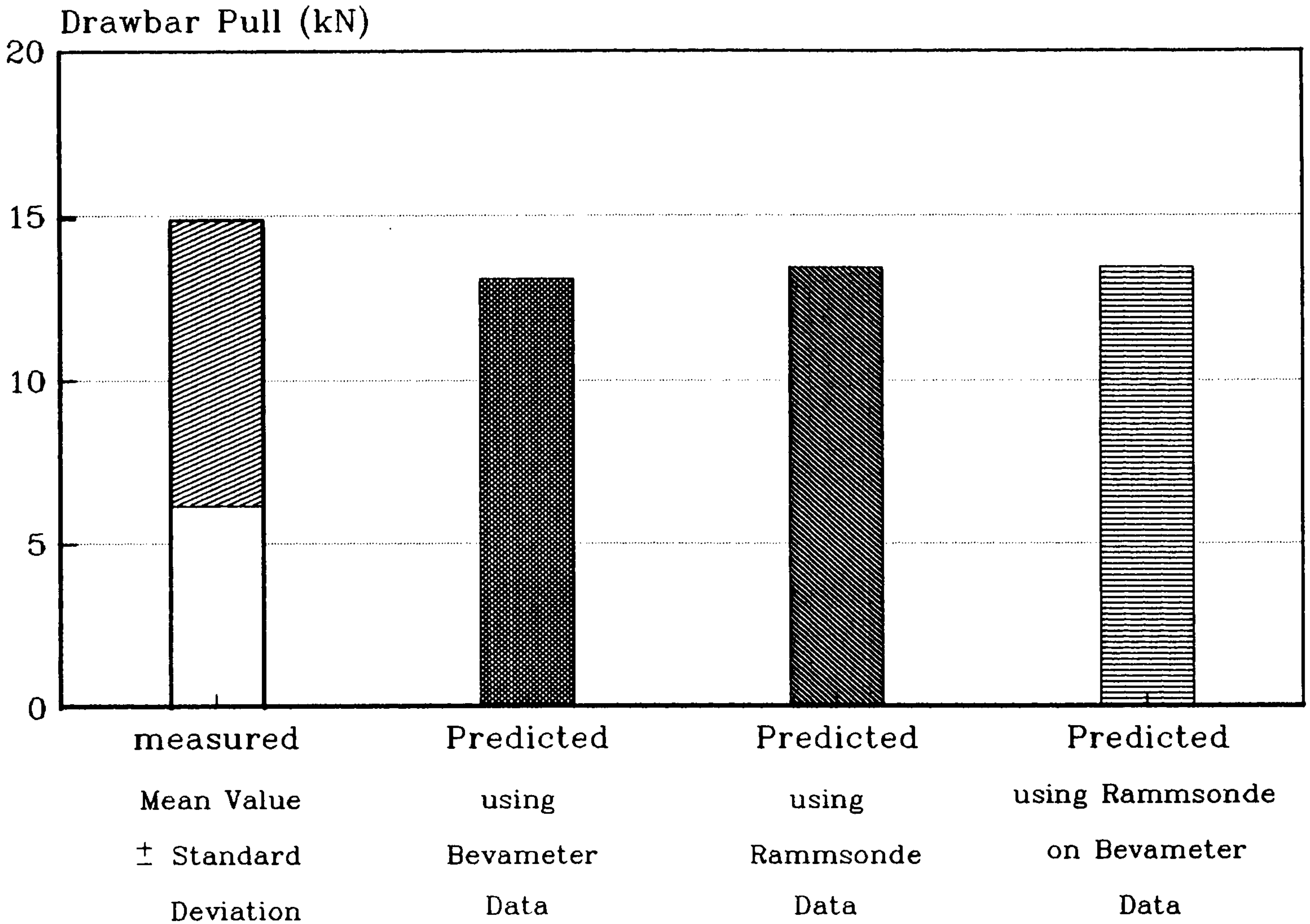

Fig. 4.2.26 Measured and predicted vehicle performance at 20% slip on undisturbed snow

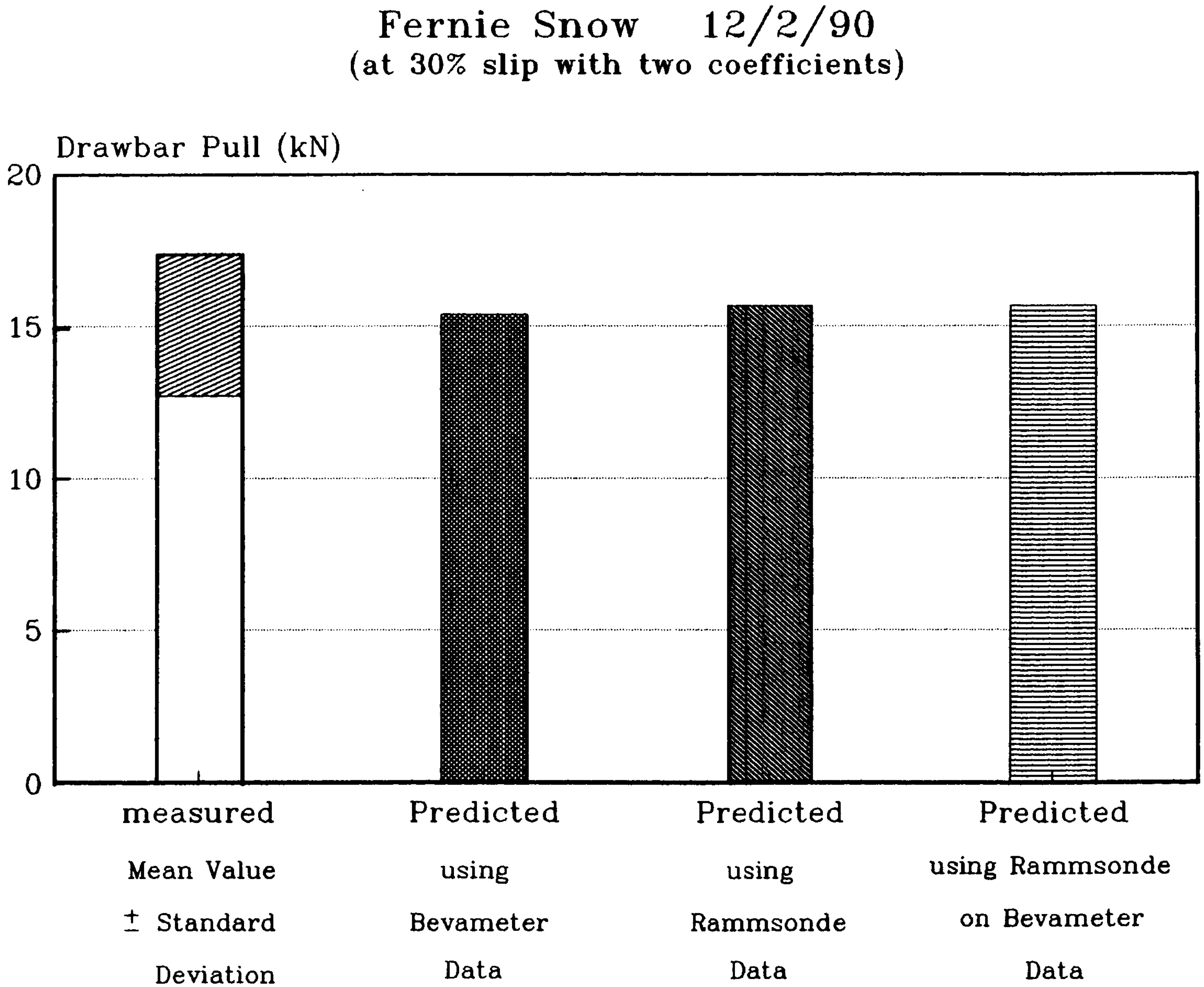

Fig. 4.2.27 Measured and predicted vehicle performance at 30% slip on undisturbed snow

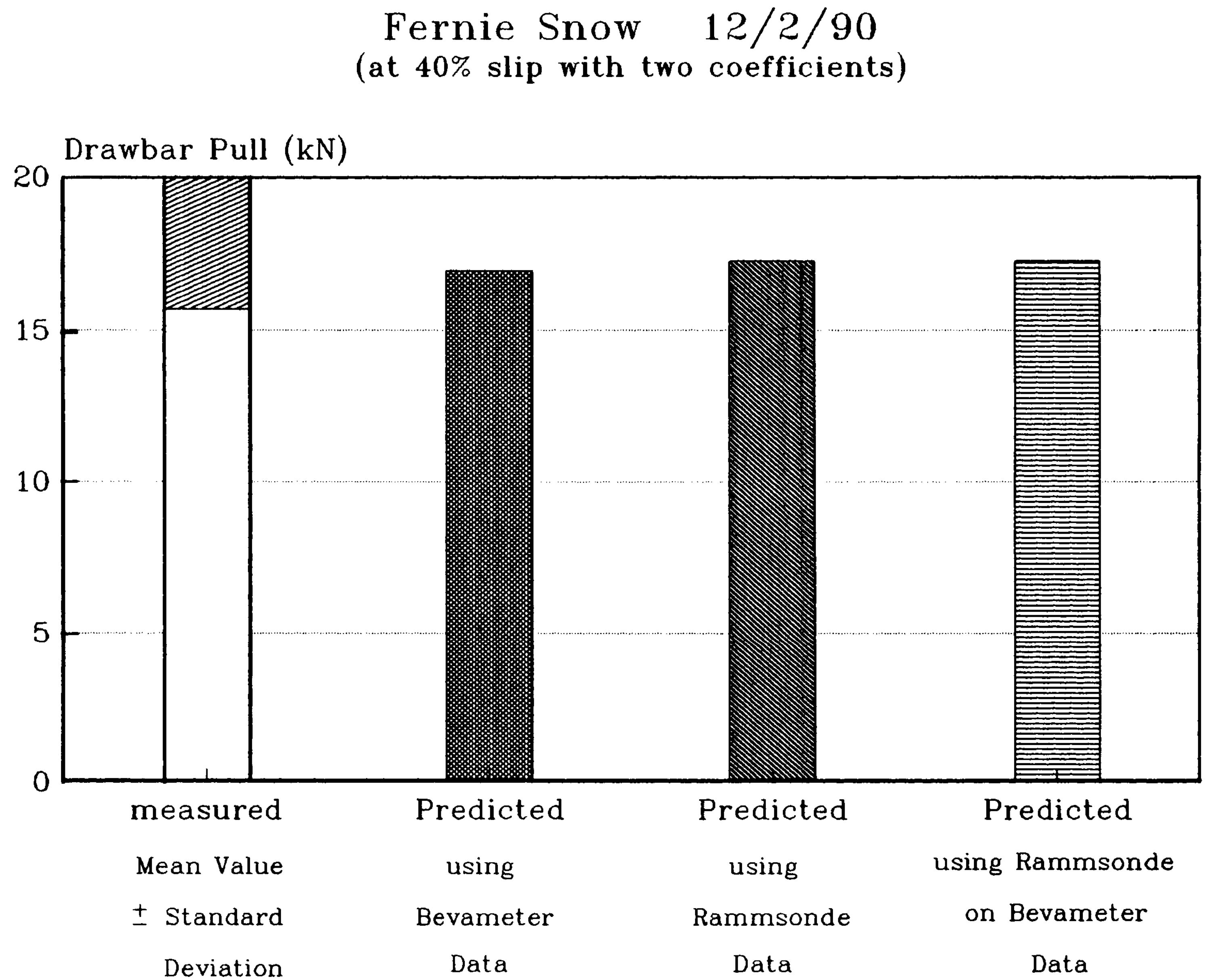

Fig. 4.2.28 Measured and predicted vehicle performance at 40% slip on undisturbed snow

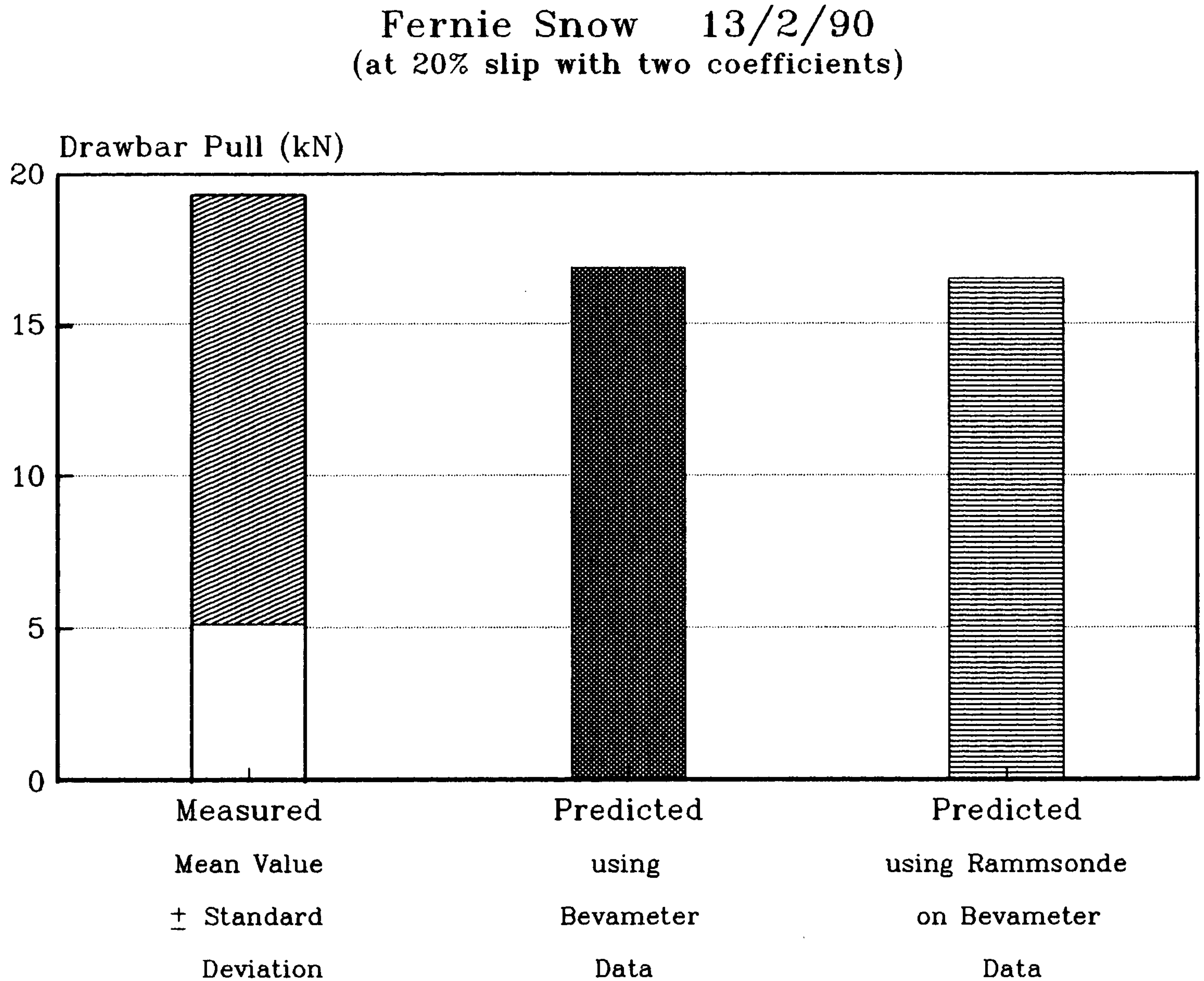

Fig. 4.2.29 Measured and predicted vehicle performance at 20% slip on undisturbed snow

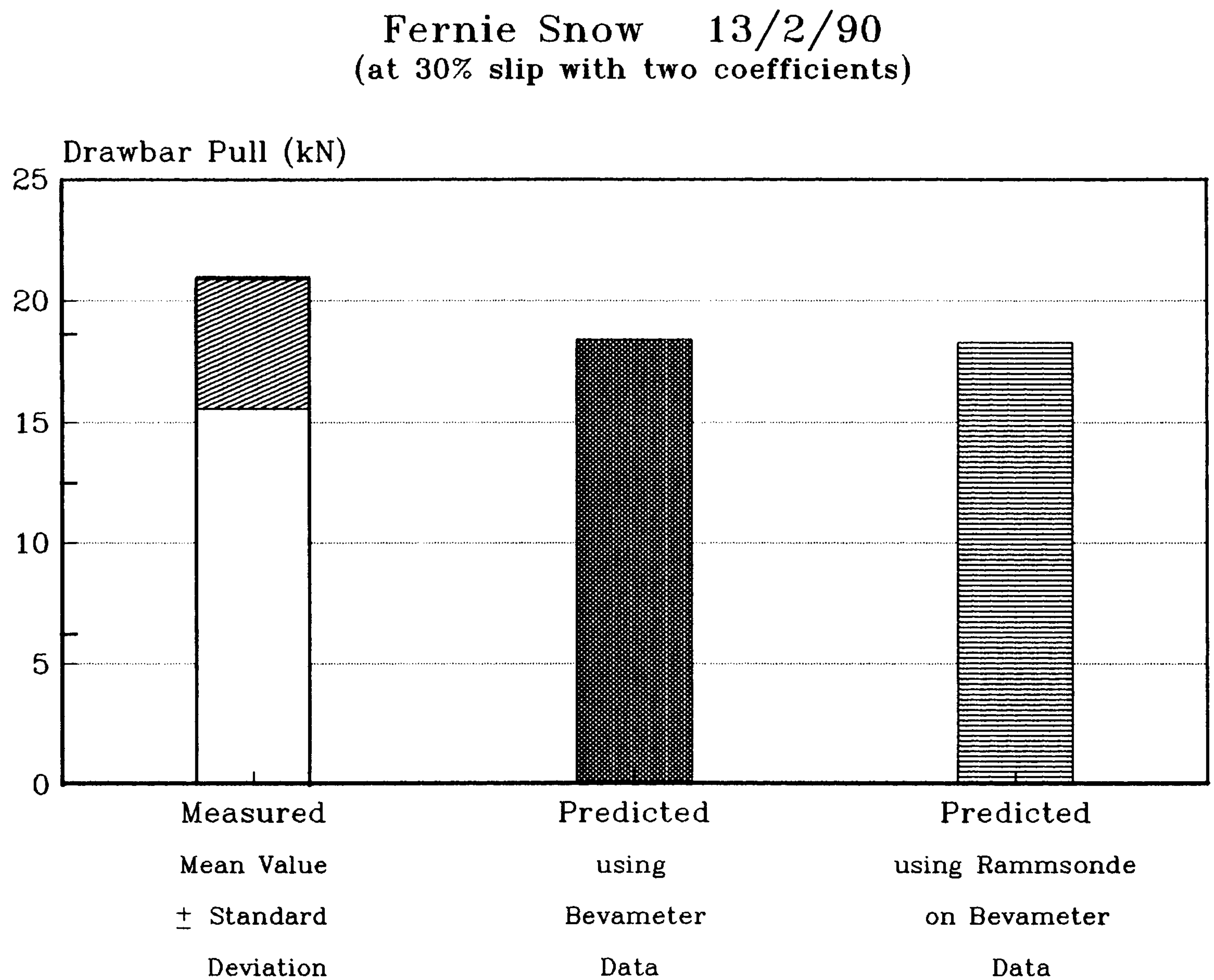

Fig. 4.2.30 Measured and predicted vehicle performance at 30% slip on undisturbed snow

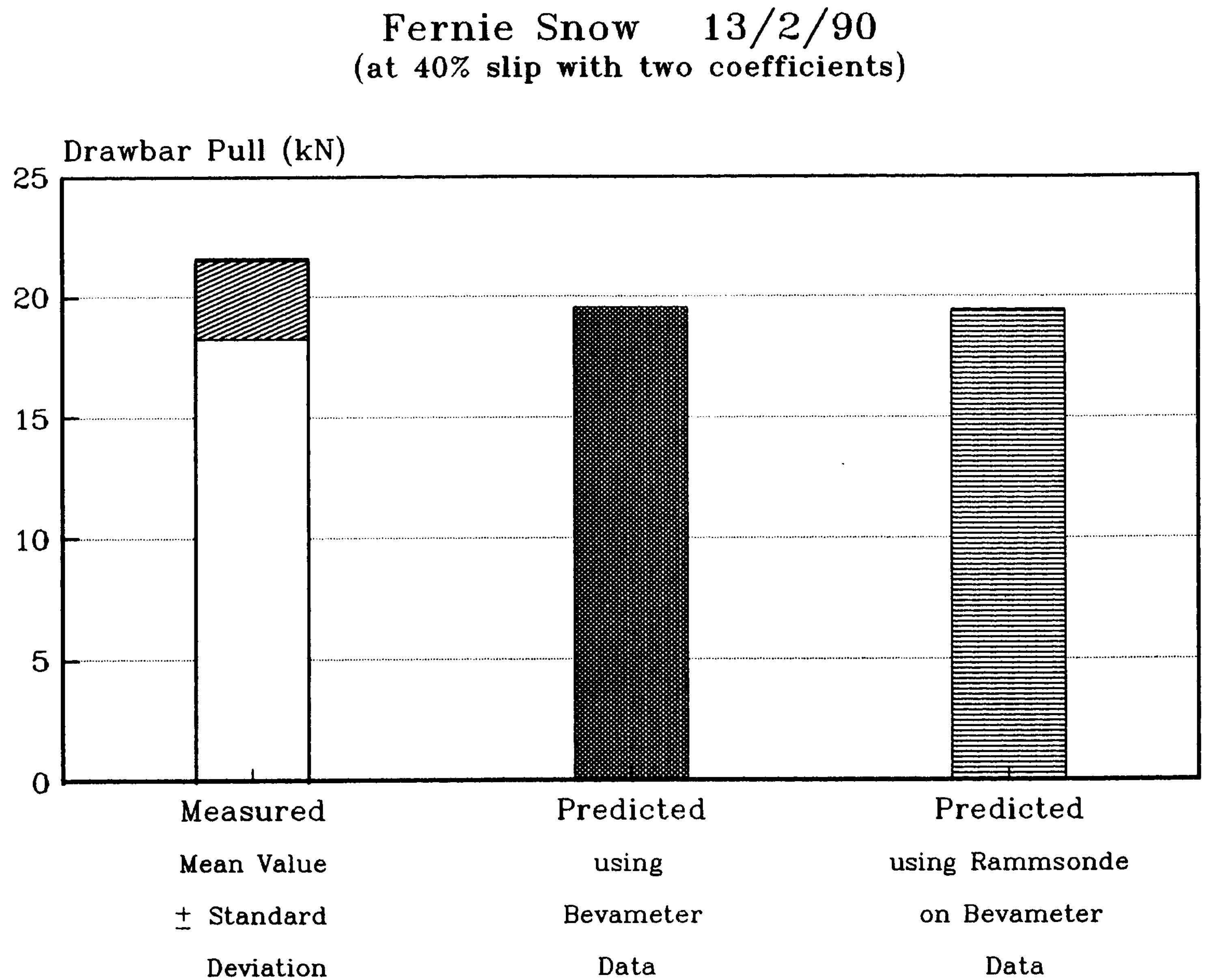

Fig. 4.2.31 Measured and predicted vehicle performance at 40% slip on undisturbed snow

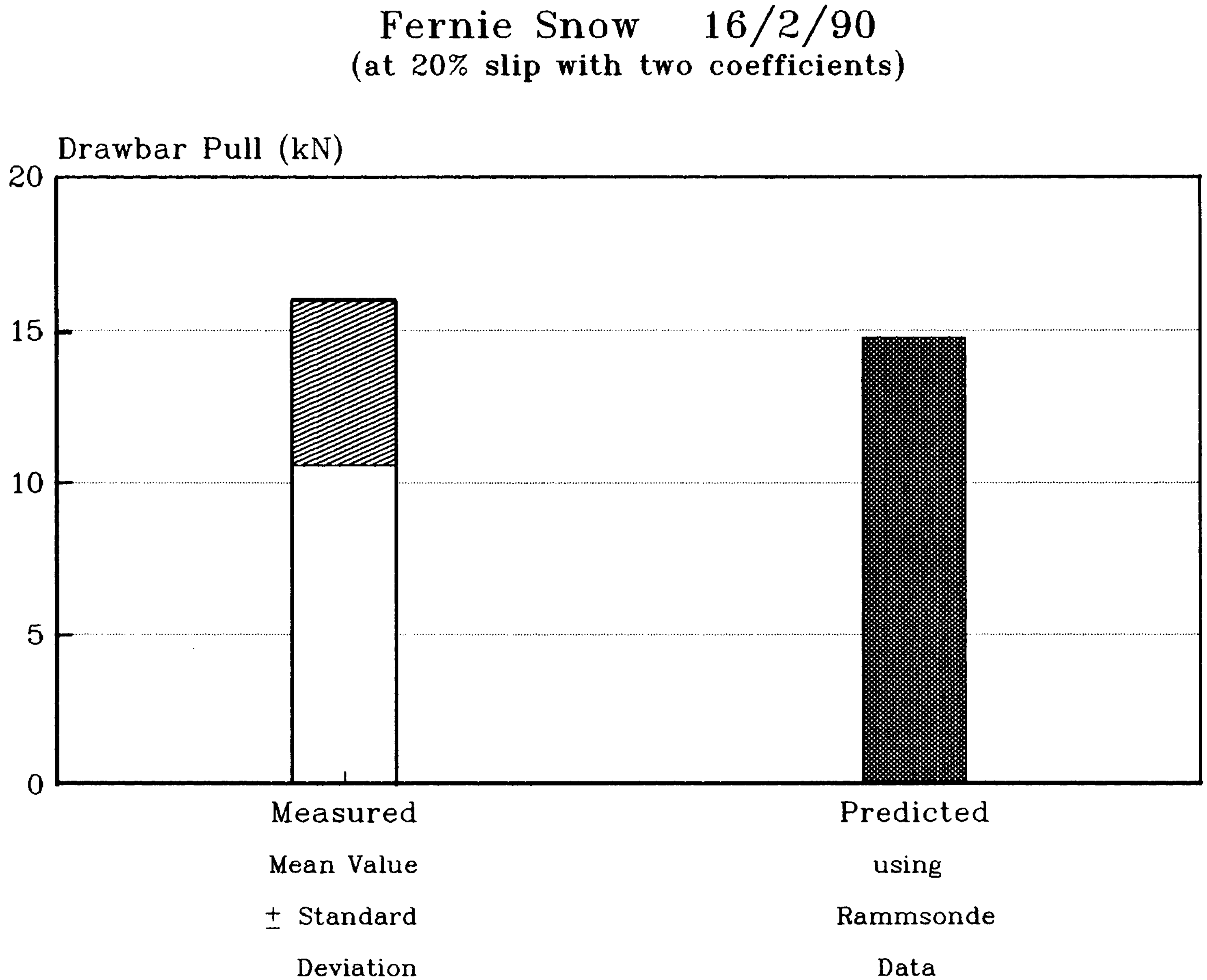

Fig. 4.2.32 Measured and predicted vehicle performance at 20% slip on undisturbed snow

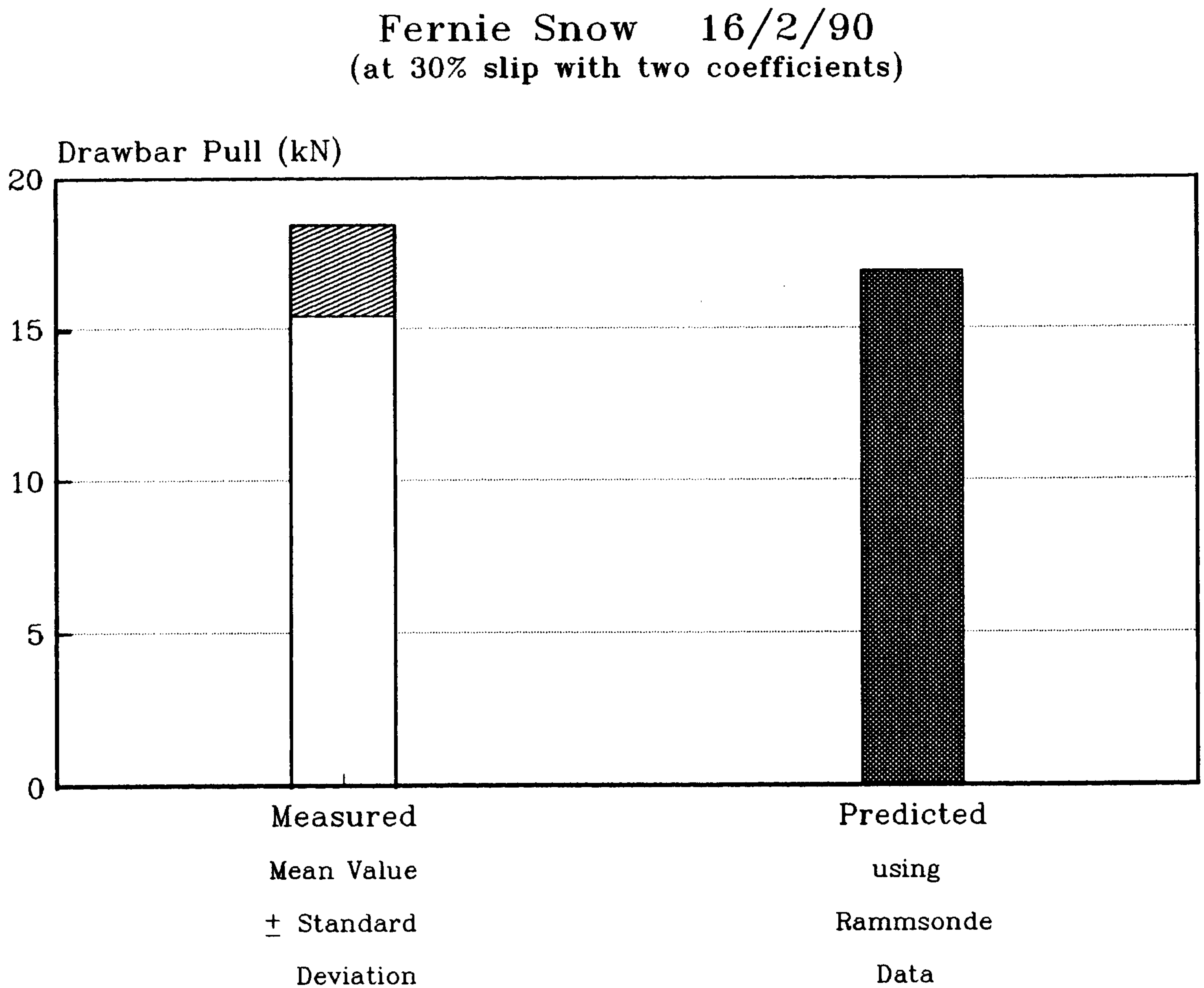

Fig. 4.2.33 Measured and predicted vehicle performance at 30% slip on undisturbed snow

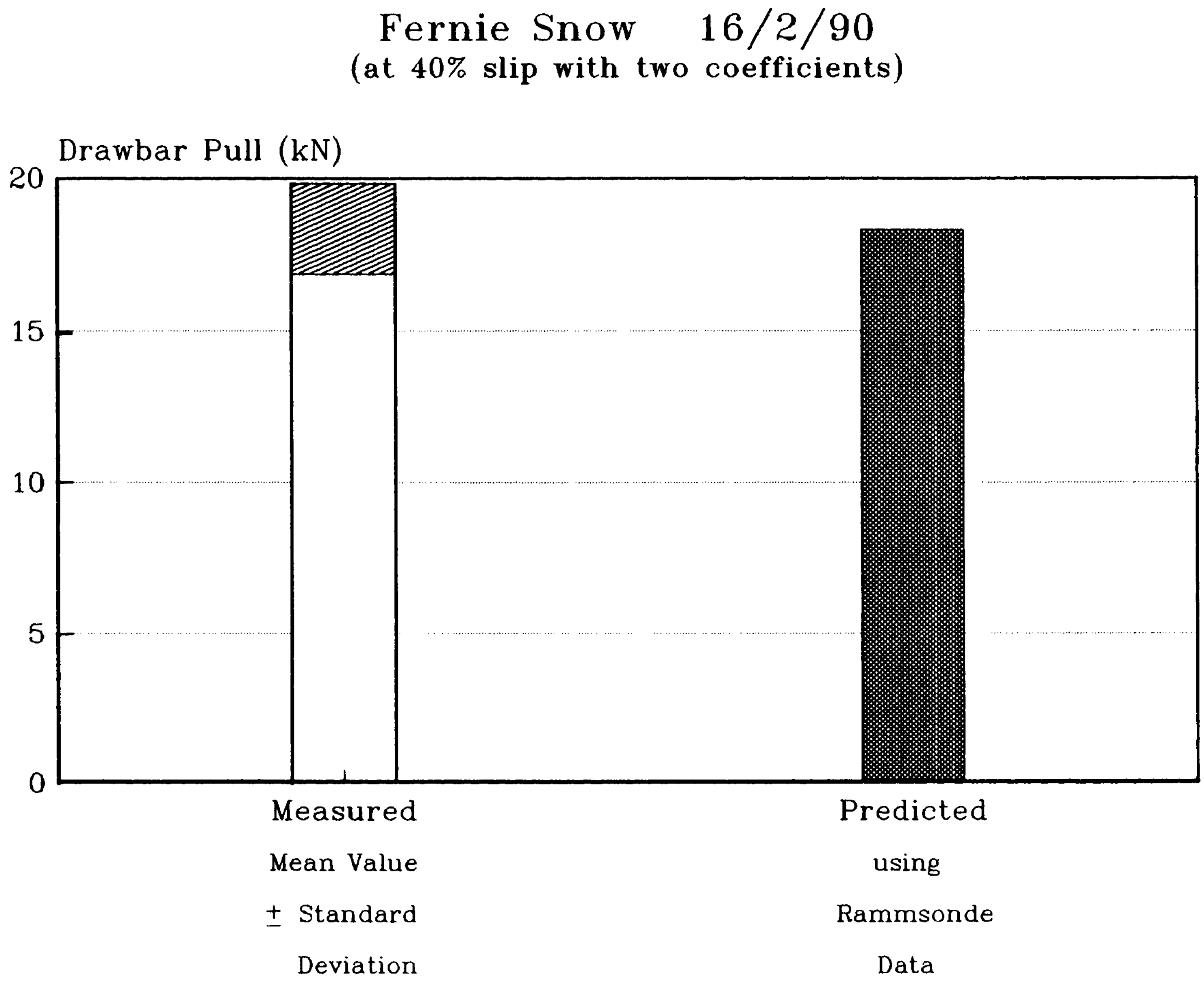

Fig. 4.2.34 Measured and predicted vehicle performance at 40% slip on undisturbed snow

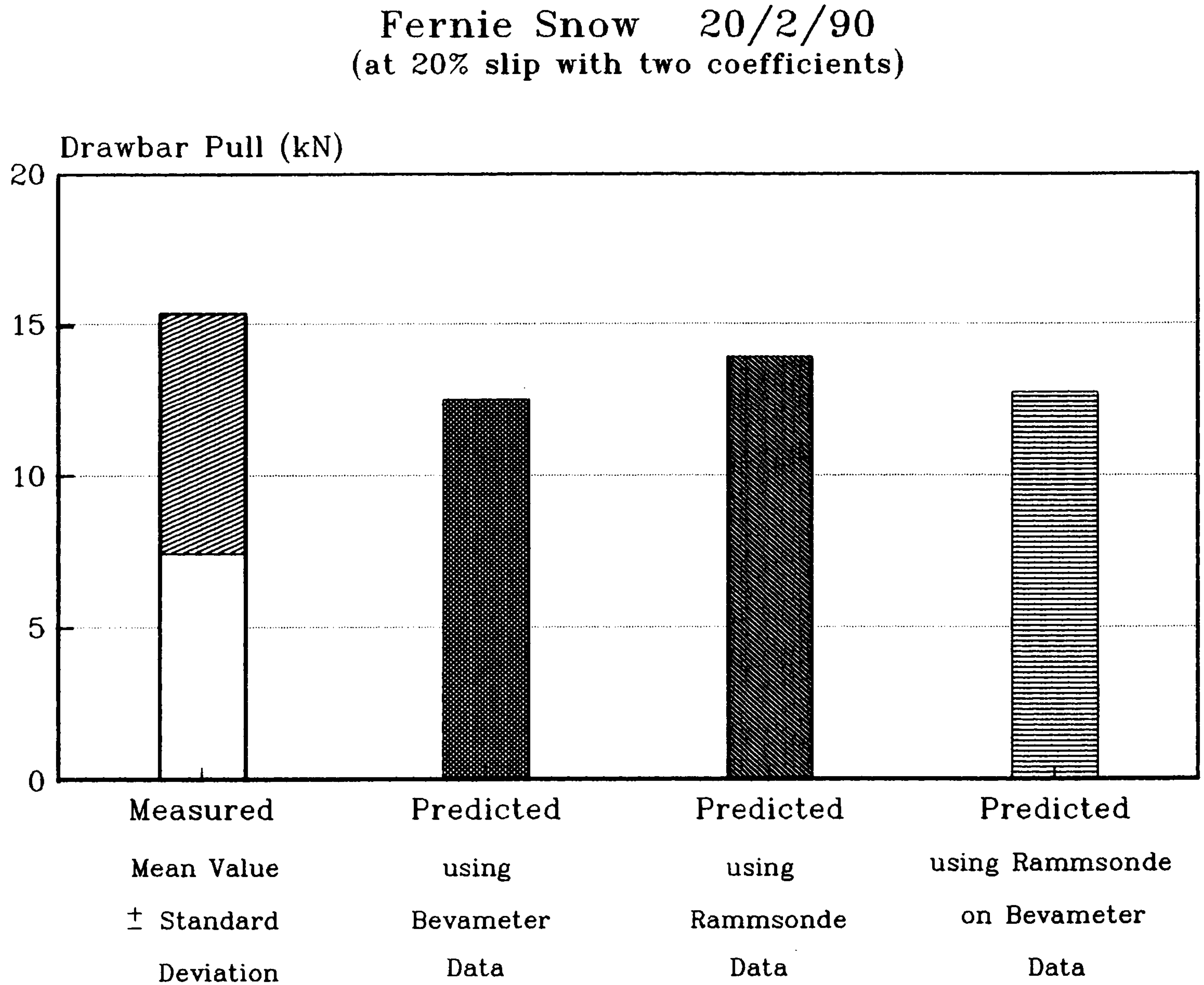

Fig. 4.2.35 Measured and predicted vehicle performance at 20% slip on undisturbed snow

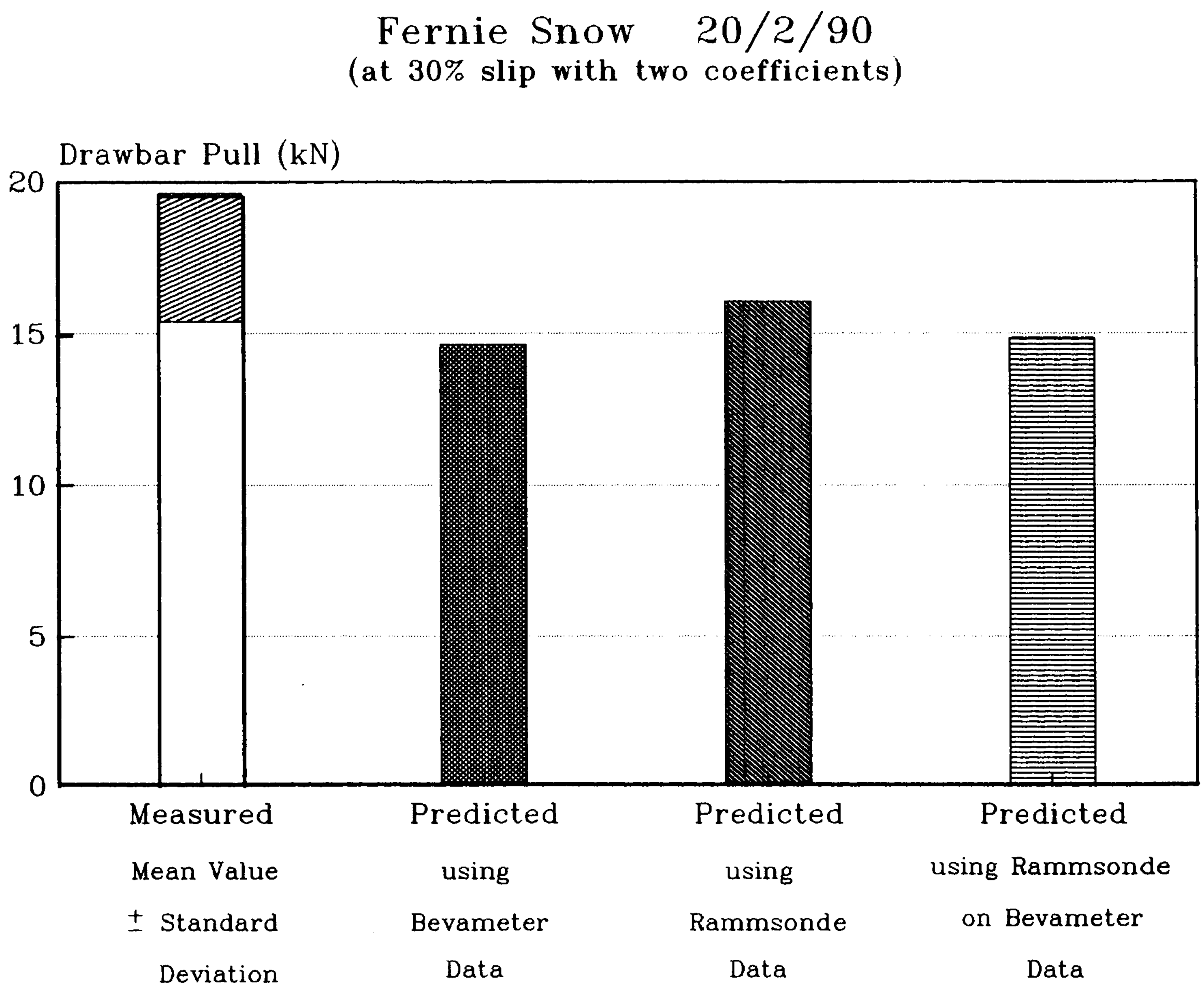

Fig. 4.2.36 Measured and predicted vehicle performance at 30% slip on undisturbed snow

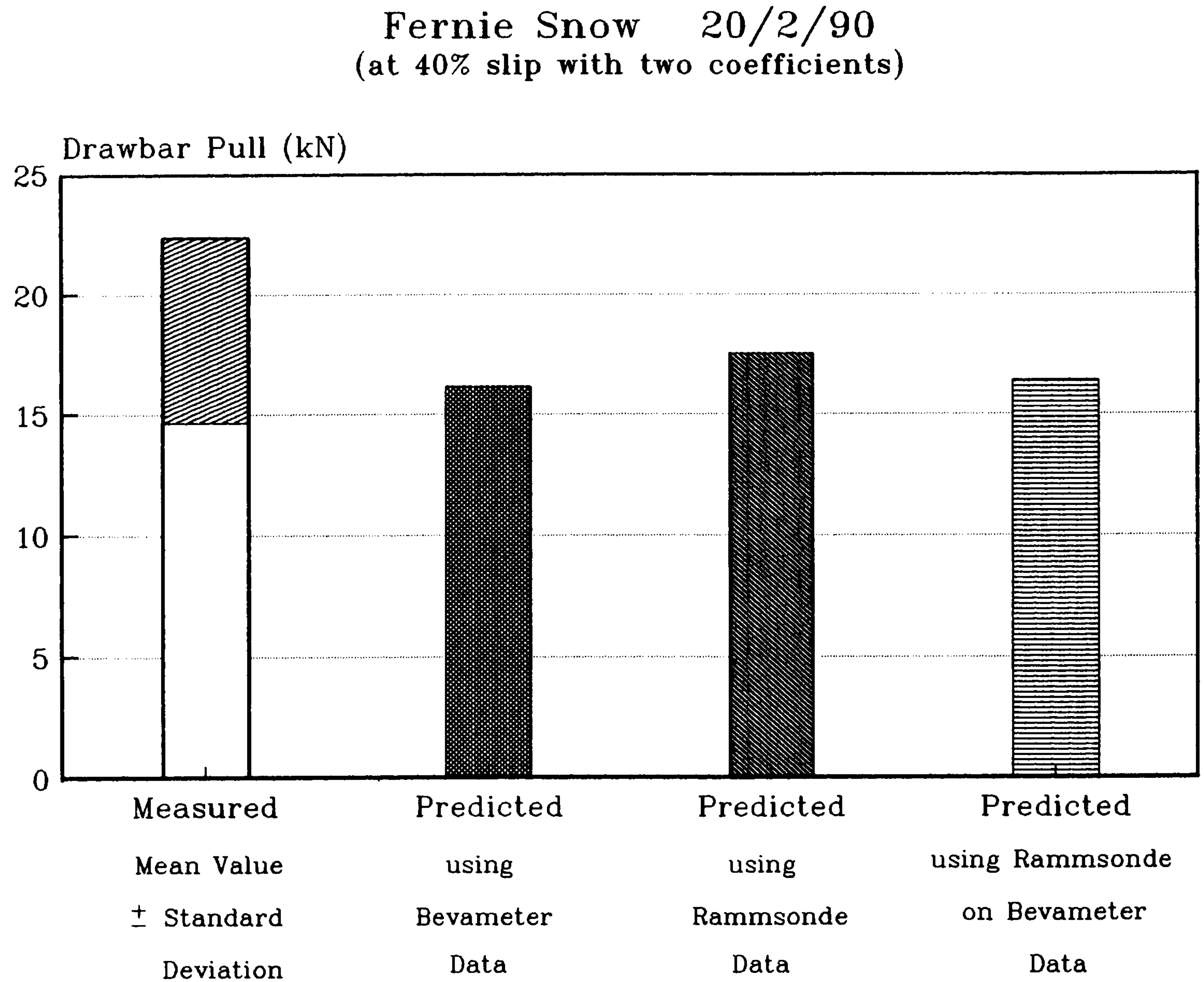

Fig. 4.2.37 Measured and predicted vehicle performance at 40% slip on undisturbed snow

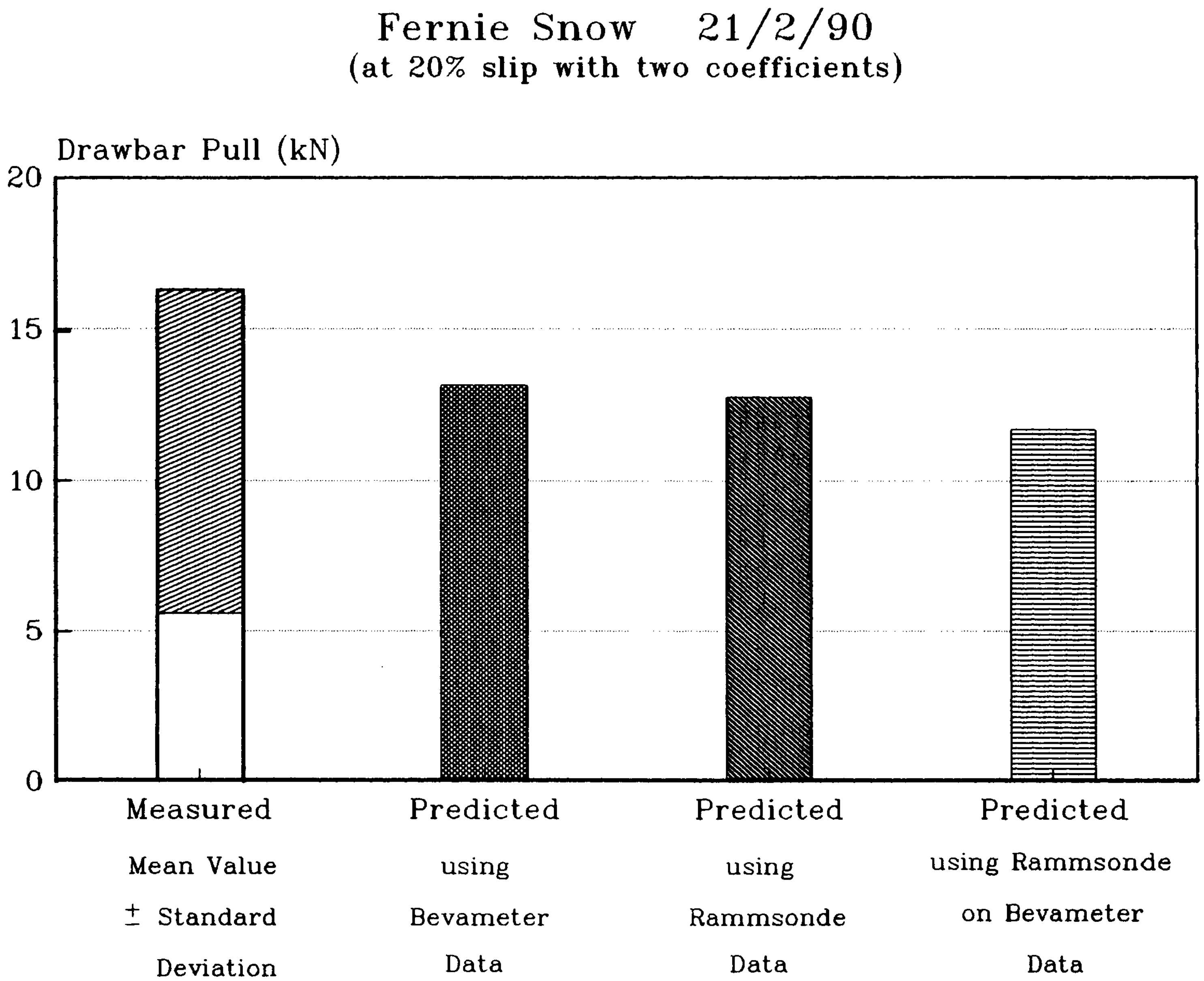

Fig. 4.2.38 Measured and predicted vehicle performance at 20% slip on undisturbed snow

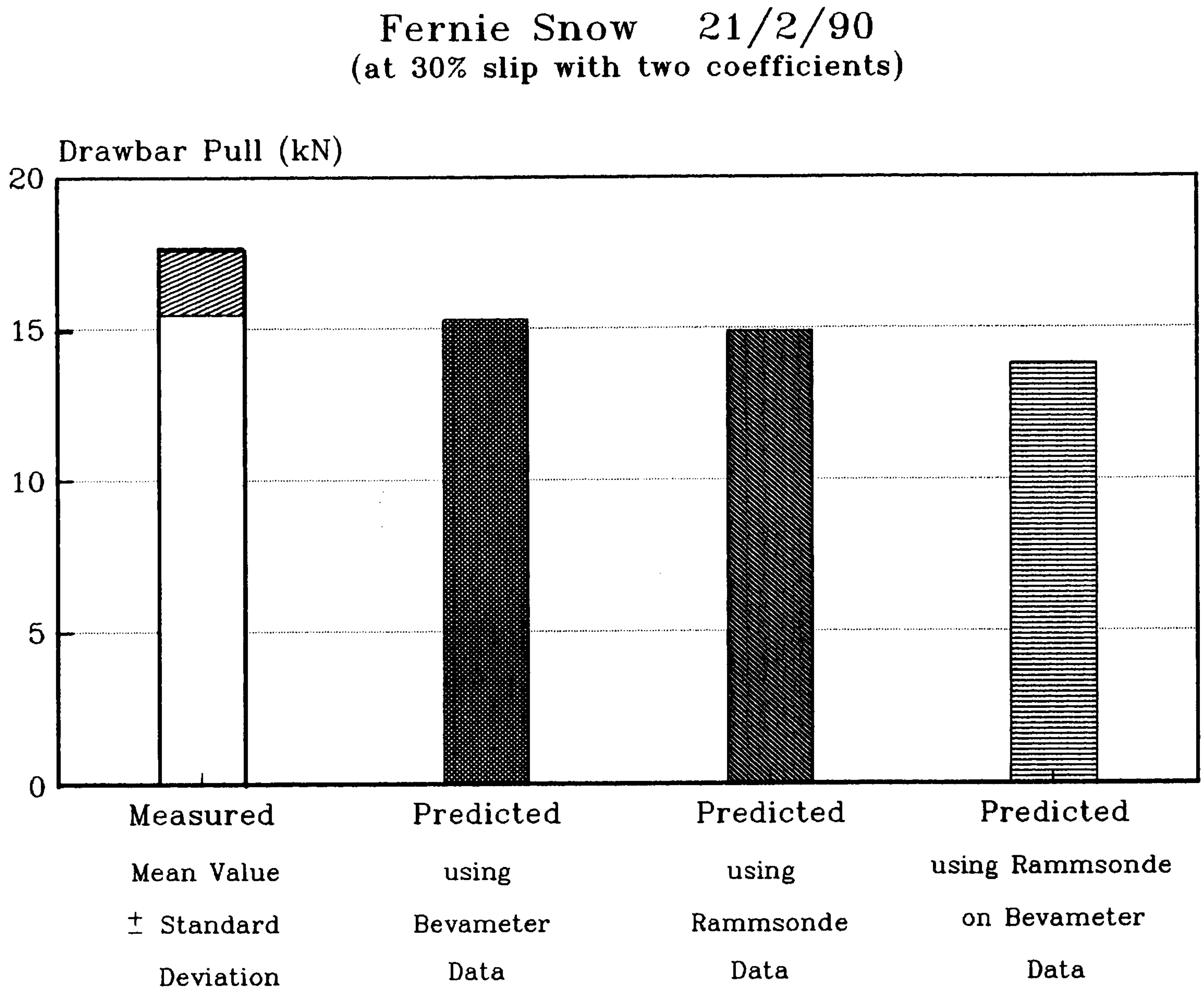

Fig. 4.2.39 Measured and predicted vehicle performance at 30% slip on undisturbed snow

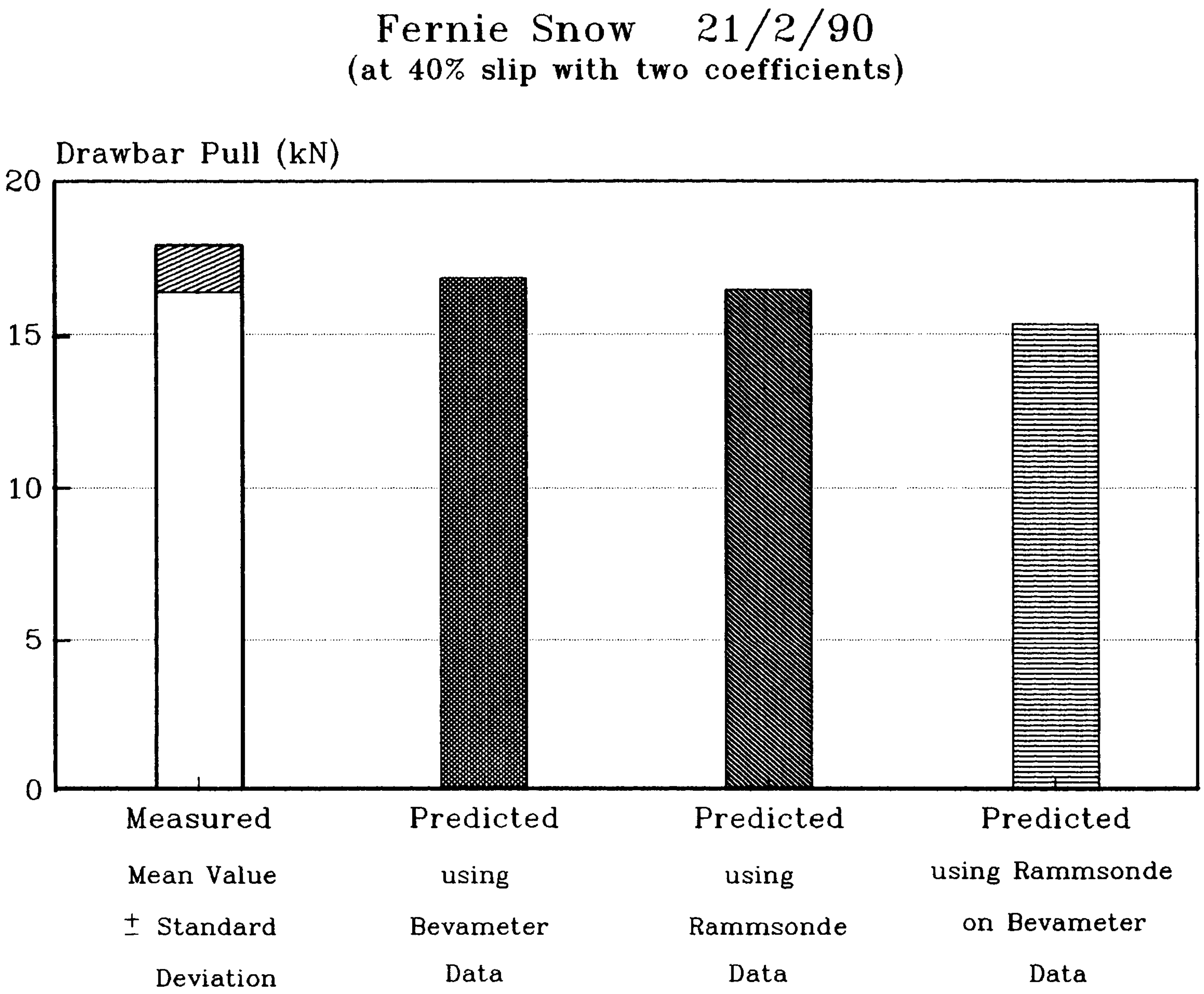

Fig. 4.2.40 Measured and predicted vehicle performance at 40% slip on undisturbed snow

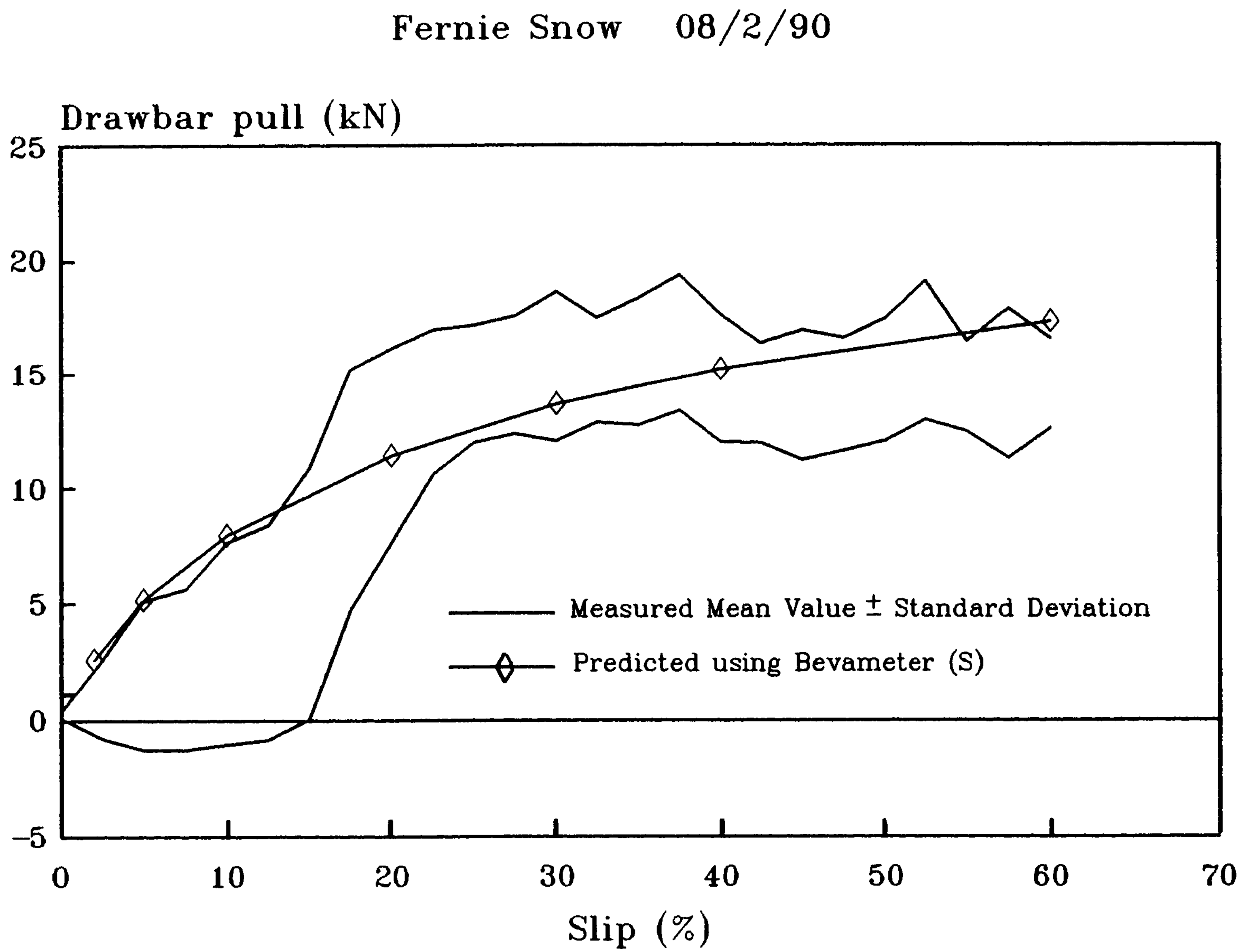

Fig. 4.2.41 Measured and predicted vehicle performance using NTVPM-85 on undisturbed snow

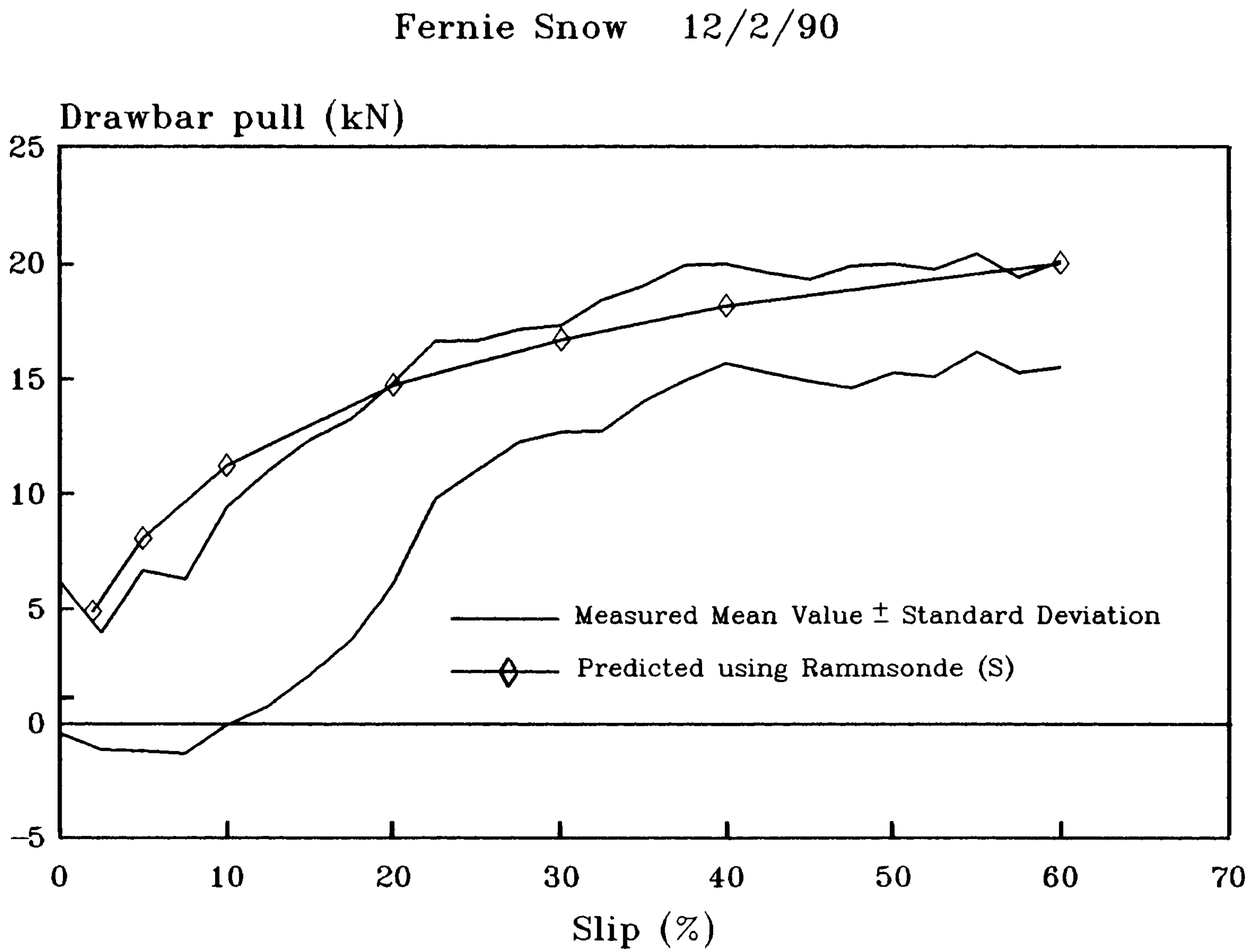

Fig. 4.2.42 Measured and predicted vehicle performance using NTVPM-85 on undisturbed snow

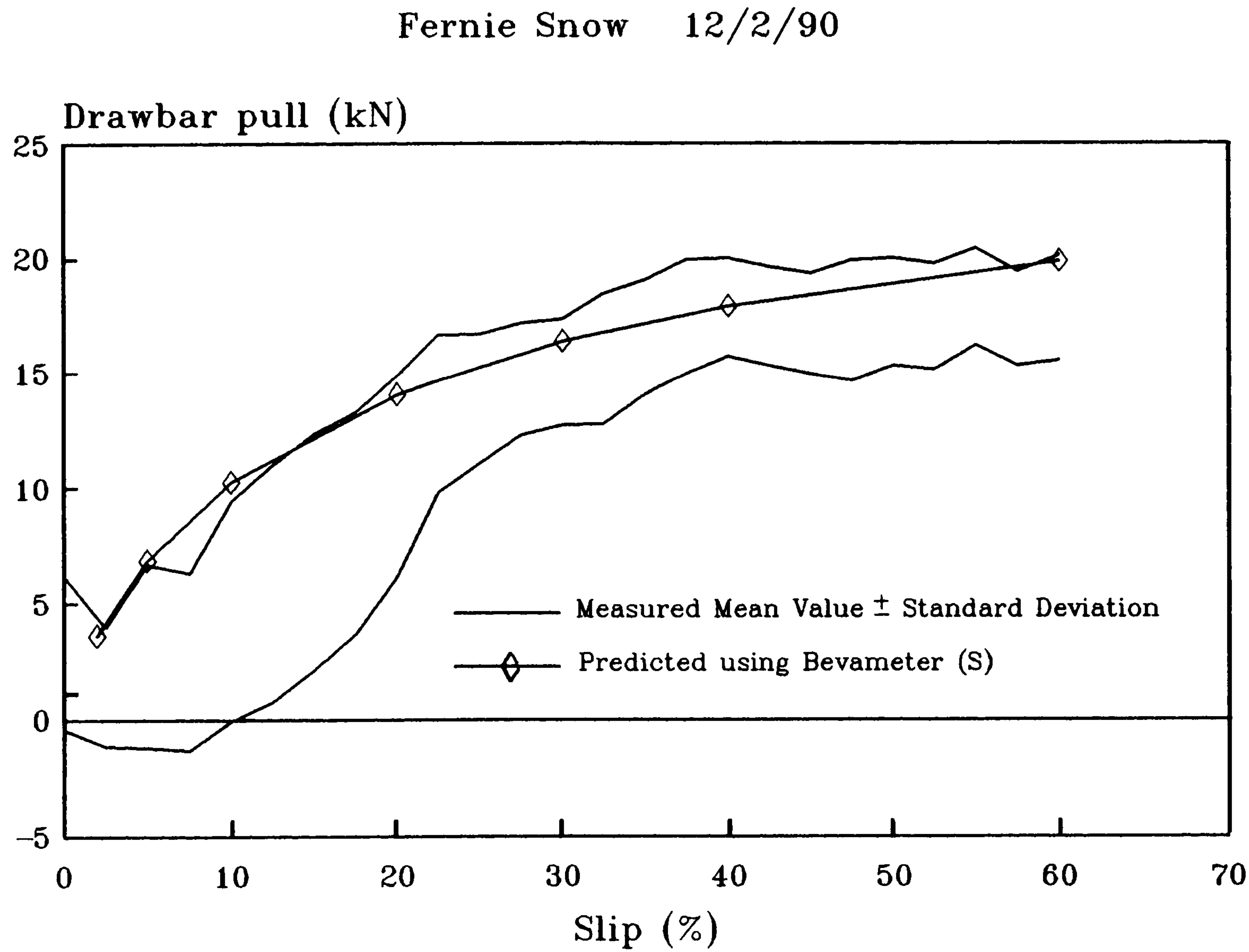

Fig. 4.2.43 Measured and predicted vehicle performance using NTVPM-85 on undisturbed snow

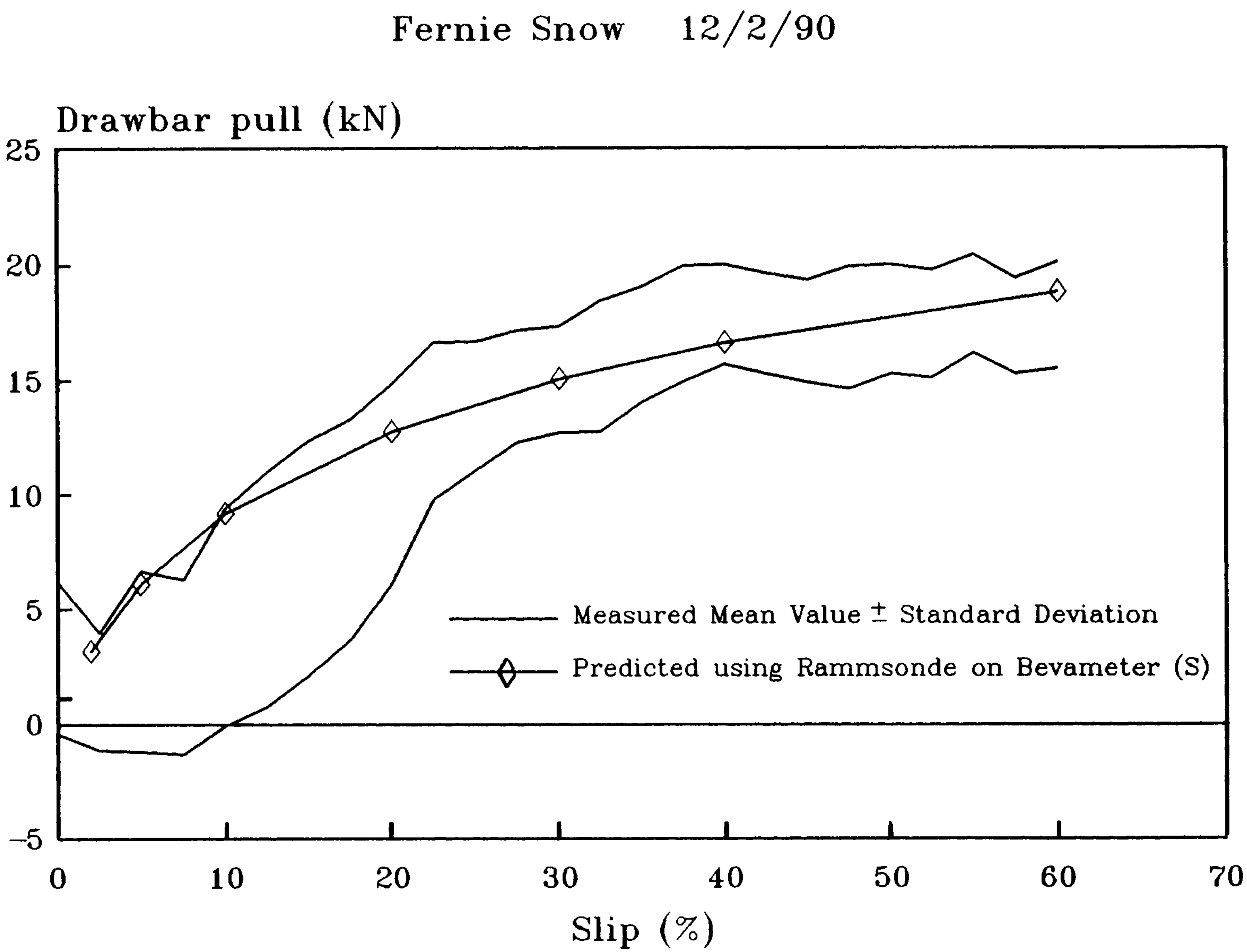

Fig. 4.2.44 Measured and predicted vehicle performance using NTVPM-85 on undisturbed snow

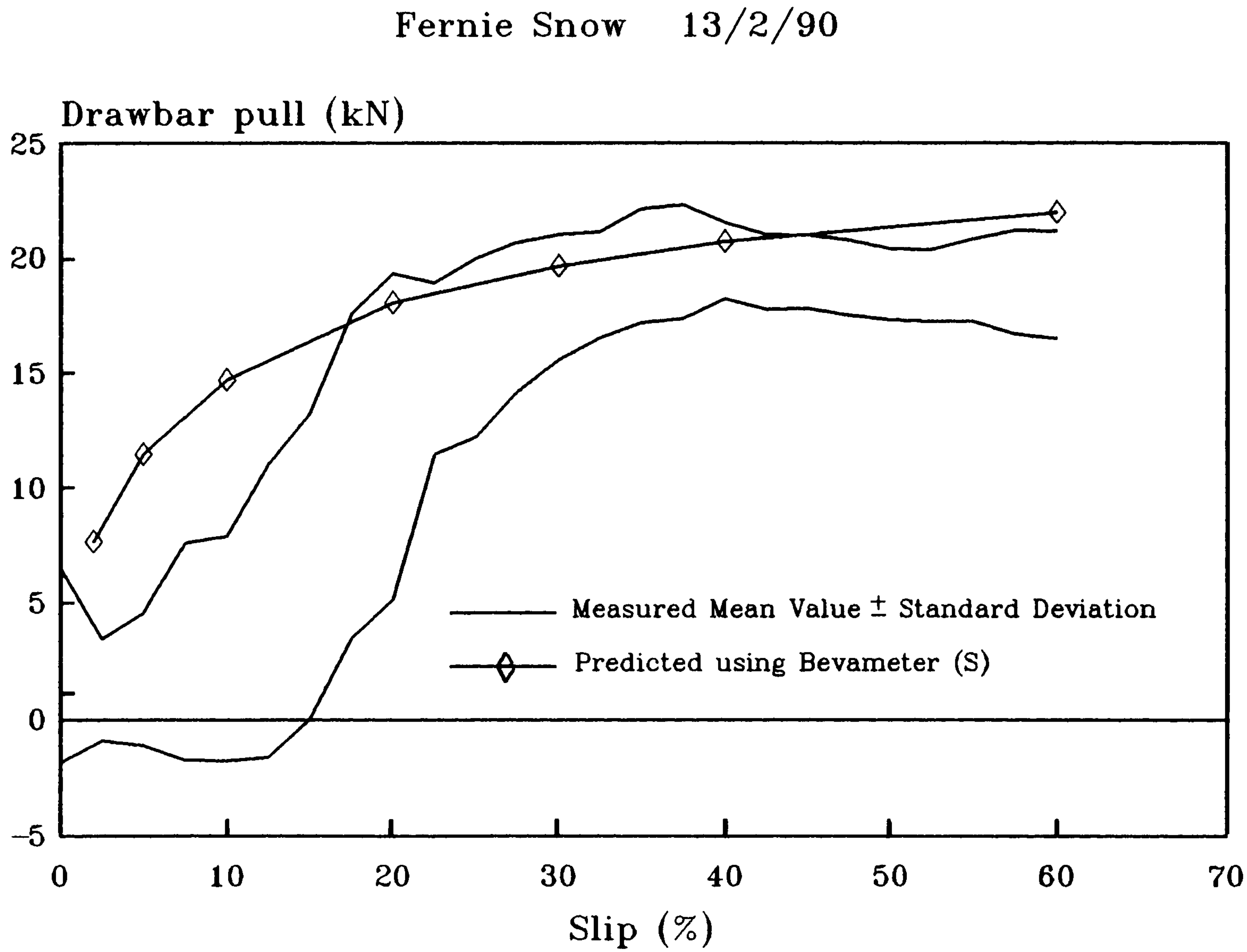

Fig. 4.2.45 Measured and predicted vehicle performance using NTVPM-85 on undisturbed snow

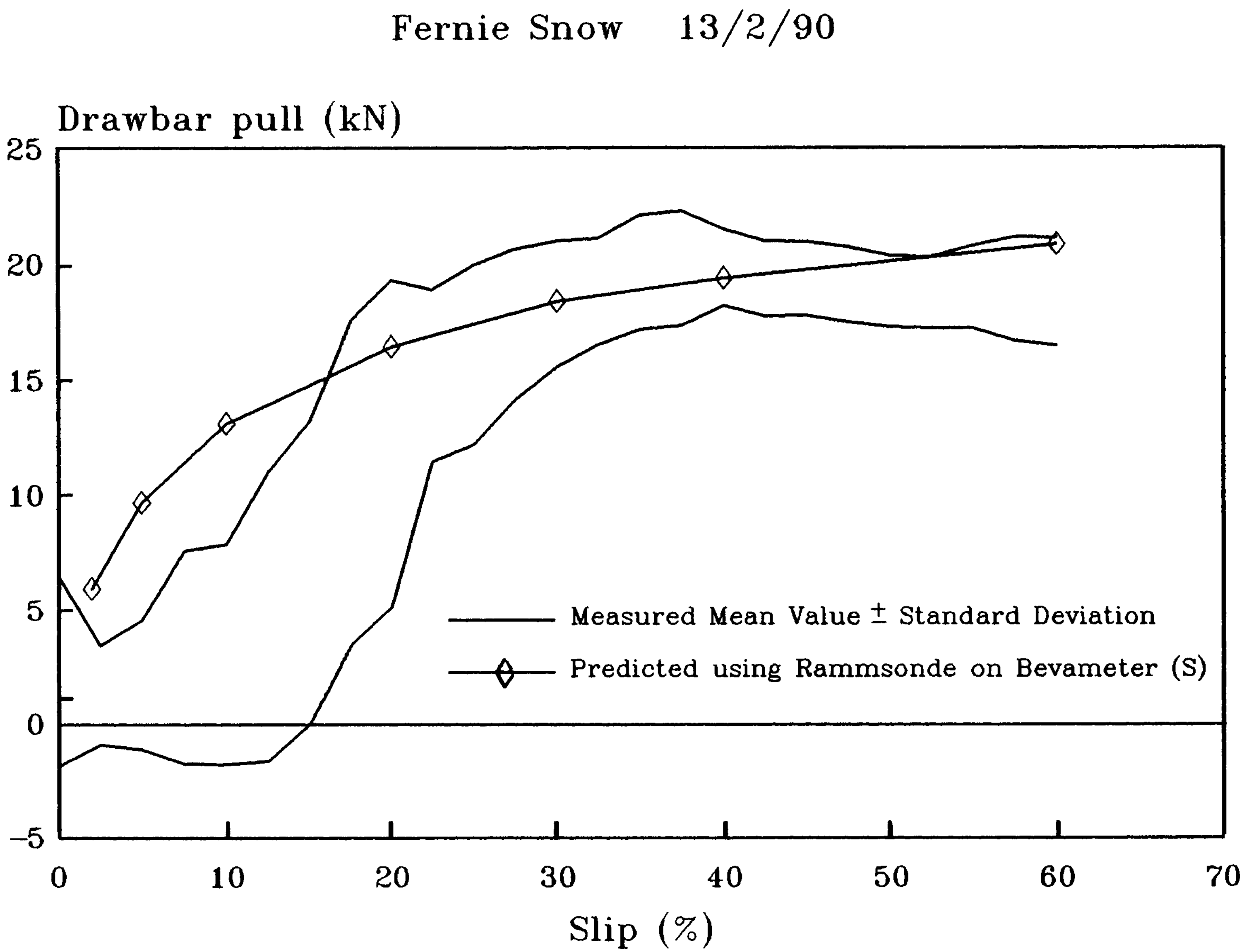

Fig. 4.2.46 Measured and predicted vehicle performance using NTVPM-85 on undisturbed snow

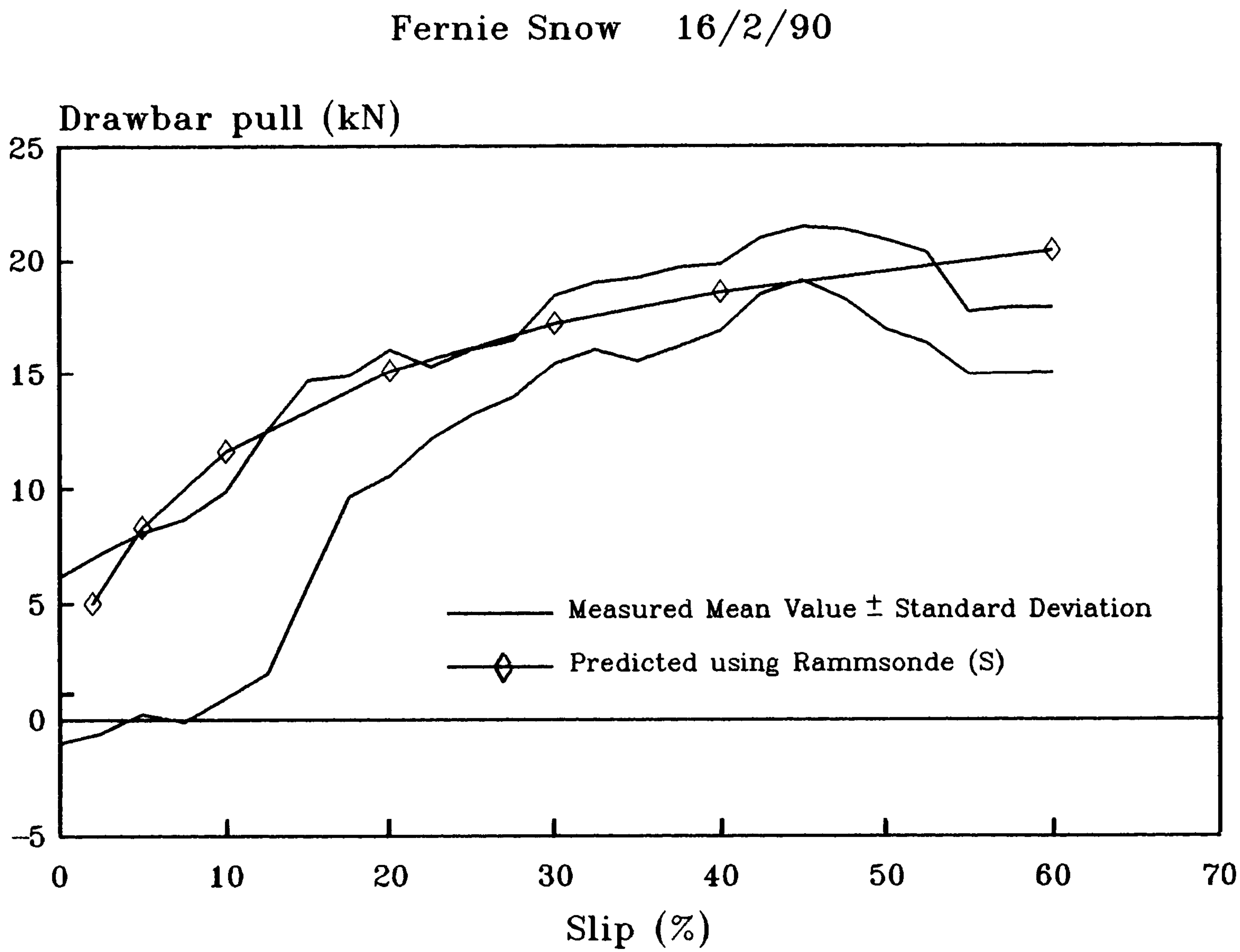

Fig. 4.2.47 Measured and predicted vehicle performance using NTVPM-85 on undisturbed snow

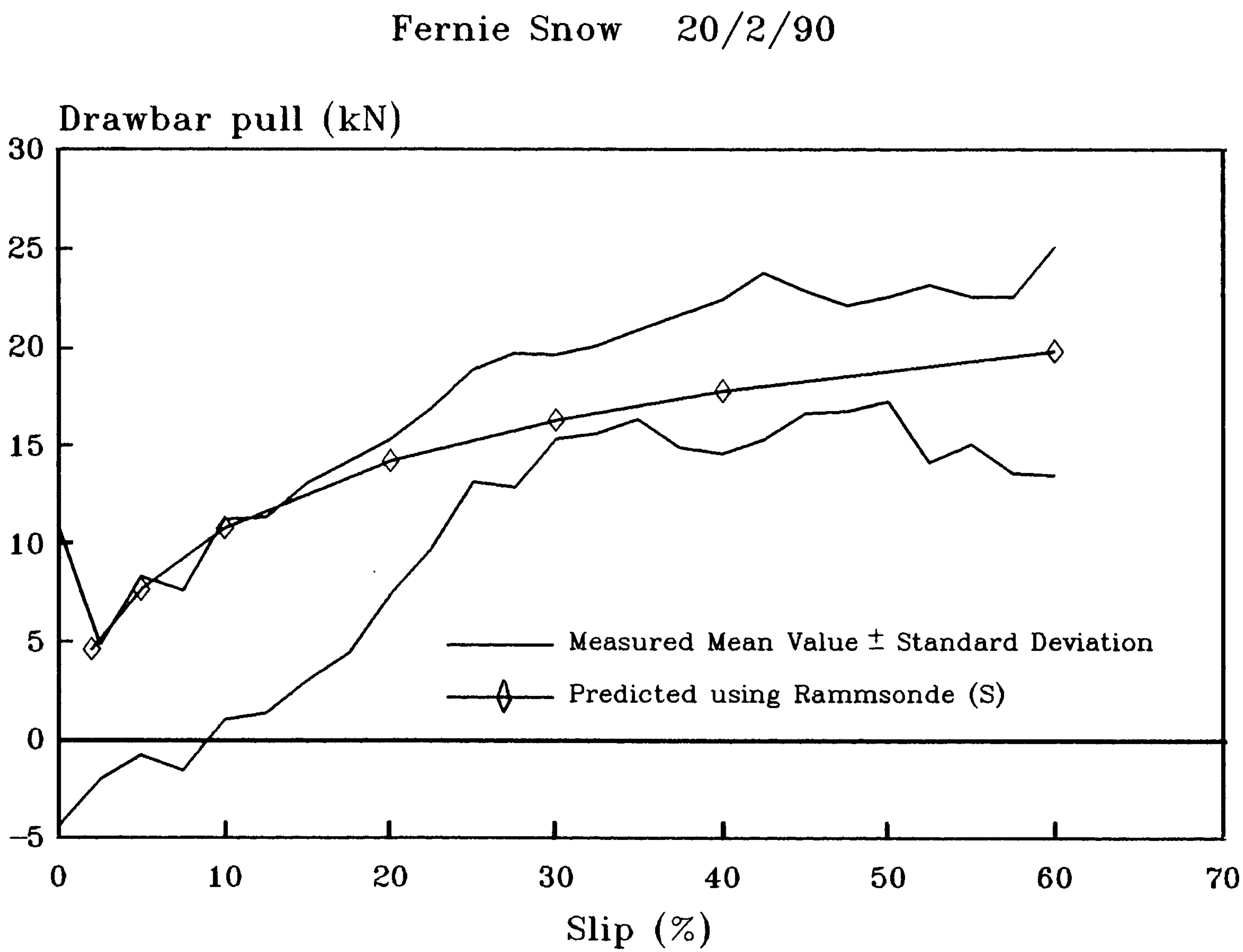

Fig. 4.2.48 Measured and predicted vehicle performance using NTVPM-85 on undisturbed snow

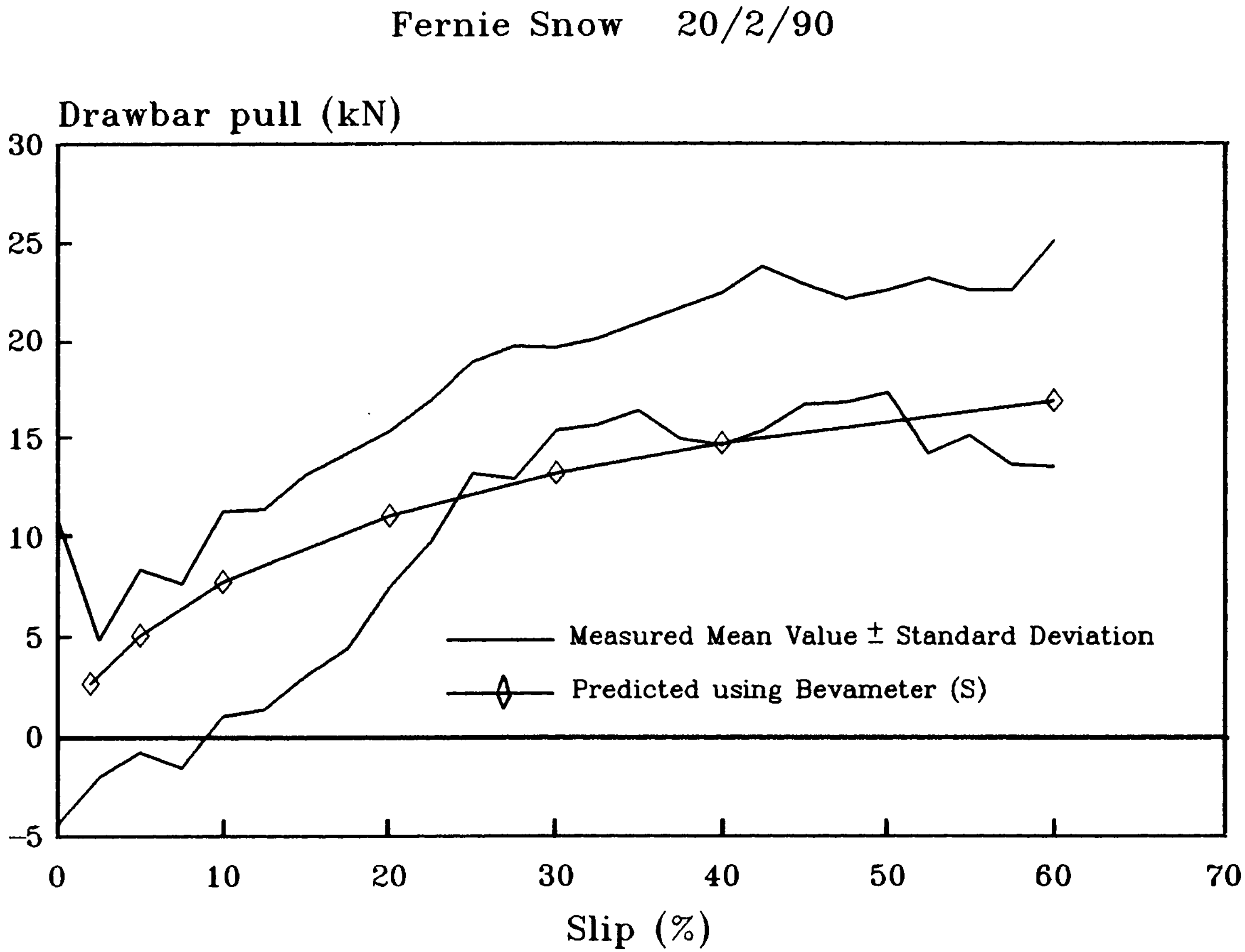

Fig. 4.2.49 Measured and predicted vehicle performance using NTVPM-85 on undisturbed snow

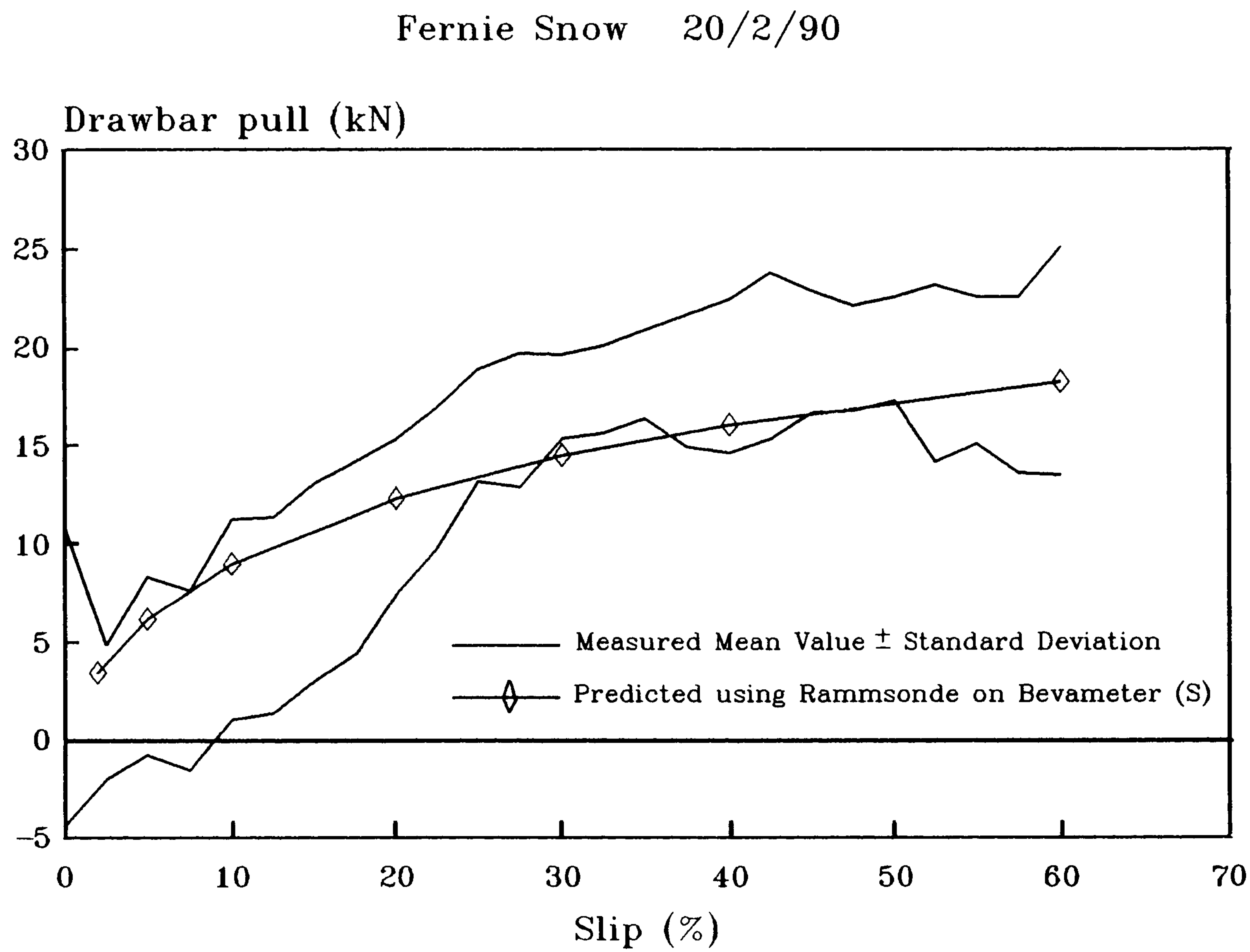

Fig. 4.2.50 Measured and predicted vehicle performance using NTVPM-85 on undisturbed snow

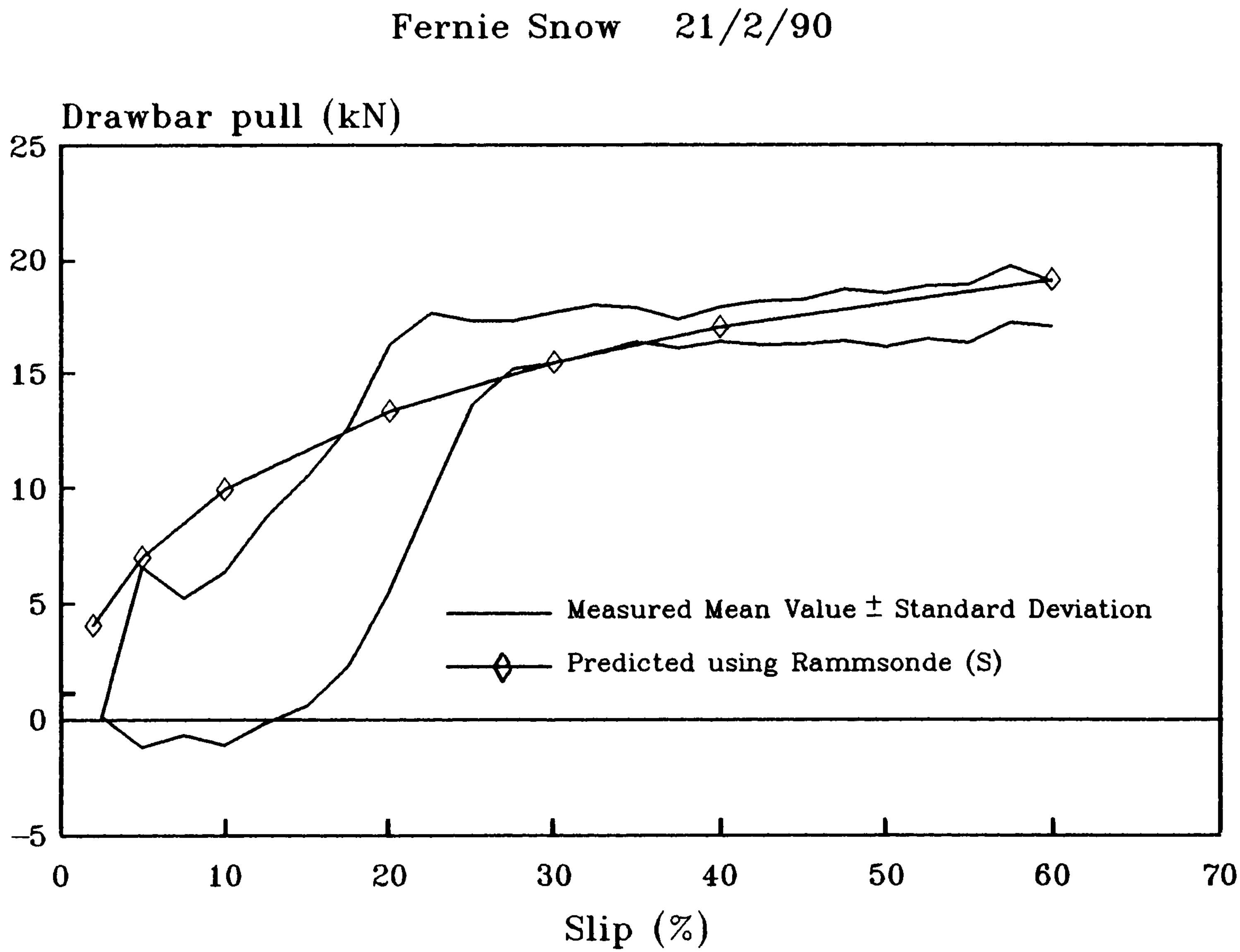

Fig. 4.2.51 Measured and predicted vehicle performance using NTVPM-85 on undisturbed snow

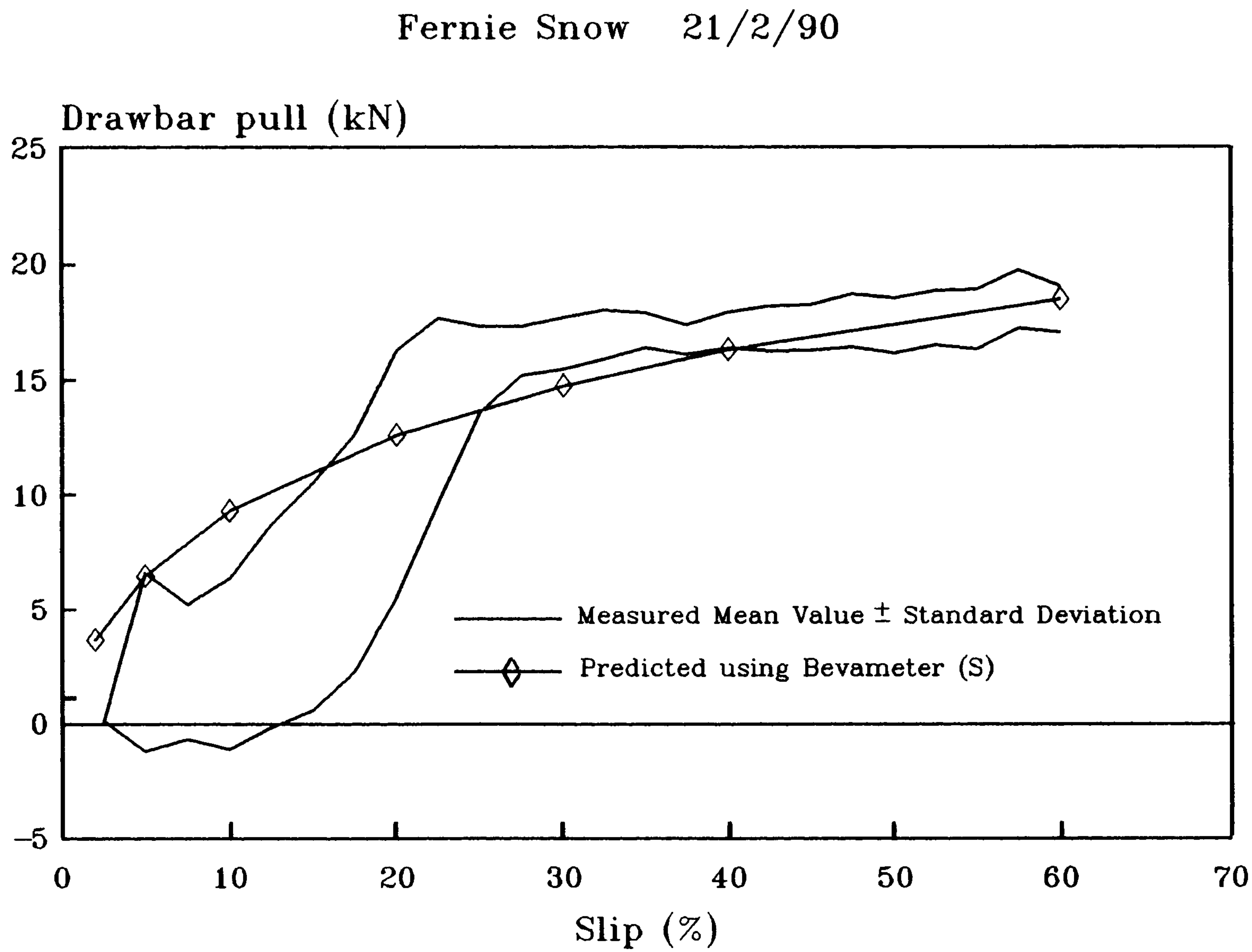

Fig. 4.2.52 Measured and predicted vehicle performance using NTVPM-85 on undisturbed snow

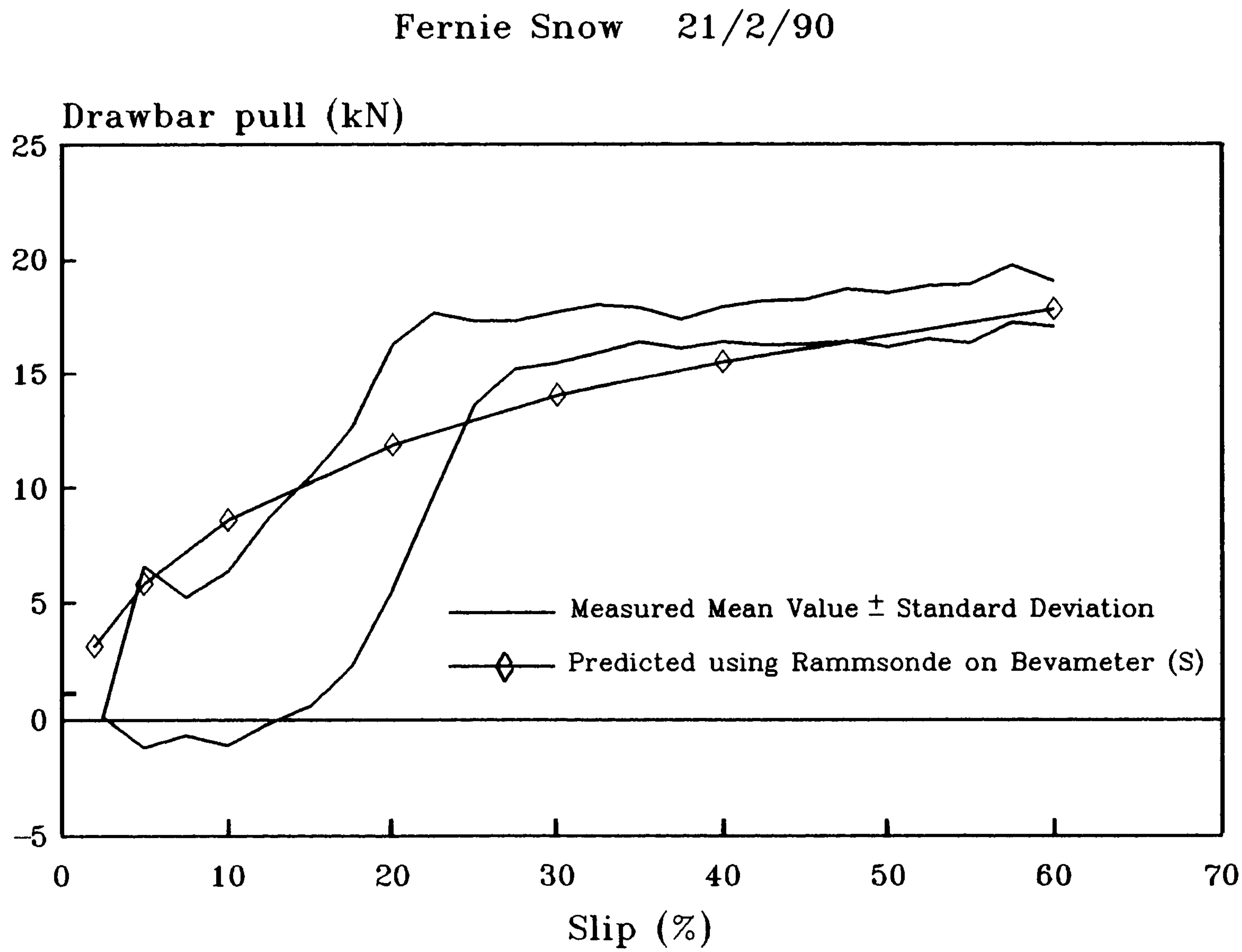

Fig. 4.2.53 Measured and predicted vehicle performance using NTVPM-85 on undisturbed snow

Table 4.2.13 **Comparison of Measured and Predicted Drawbar Pull at 20% Slip on Undisturbed Snow (Using Equation: $p = k z^n$)**

Date	Measured Mean Value ± Standard Deviation (kN)	Predicted Using Bevameter Data (kN)	Predicted Using Rammsonde Data (kN)	Predicted Using Rammsonde on Bevameter Data (kN)
Feb. 8	16.10 ± 7.63	11.39		
Feb. 12	14.86 ± 6.14	14.06	14.73	12.77
Feb. 13	19.31 ± 5.12	18.06	18.4	16.43
Feb. 16	16.05 ± 10.56		15.09	
Feb. 20	15.34 ± 7.43	11.06	14.23	12.32
Feb. 21	16.26 ± 5.58	12.61	13.34	11.86

Table 4.2.14 Comparison of Measured and Predicted Drawbar Pull at 30% Slip on Undisturbed Snow (Using Equation: $p = k z^n$)

Date	Measured Mean Value ± Standard Deviation (kN)	Predicted Using Bevameter Data (kN)	Predicted Using Rammsonde Data (kN)	Predicted Using Rammsonde on Bevameter Data (kN)
Feb. 8	18.60 ± 12.04	13.66		
Feb. 12	17.33 ± 12.71	16.35	16.69	15.05
Feb. 13	21.00 ± 15.58	19.65	19.95	18.39
Feb. 16	18.43 ± 15.42		17.20	
Feb. 20	19.61 ± 15.38	13.19	16.32	14.50
Feb. 21	17.67 ± 15.45	14.75	15.47	14.03

Table 4.2.15 Comparison of Measured and Predicted Drawbar Pull at 40% Slip on Undisturbed Snow (Using Equation: $p = k z^n$)

Date	Measured Mean Value ± Standard Deviation (kN)	Predicted Using Bevameter Data (kN)	Predicted Using Rammsonde Data (kN)	Predicted Using Rammsonde on Bevameter Data (kN)
Feb. 8	17.58 ± 11.97	15.19		
Feb. 12	19.99 ± 15.68	17.87	18.17	16.62
Feb. 13	21.52 ± 18.23	20.69	20.77	19.41
Feb. 16	19.82 ± 16.87		18.57	
Feb. 20	22.40 ± 14.47	14.71	17.81	16.07
Feb. 21	17.91 ± 16.38	16.31	17.02	15.58

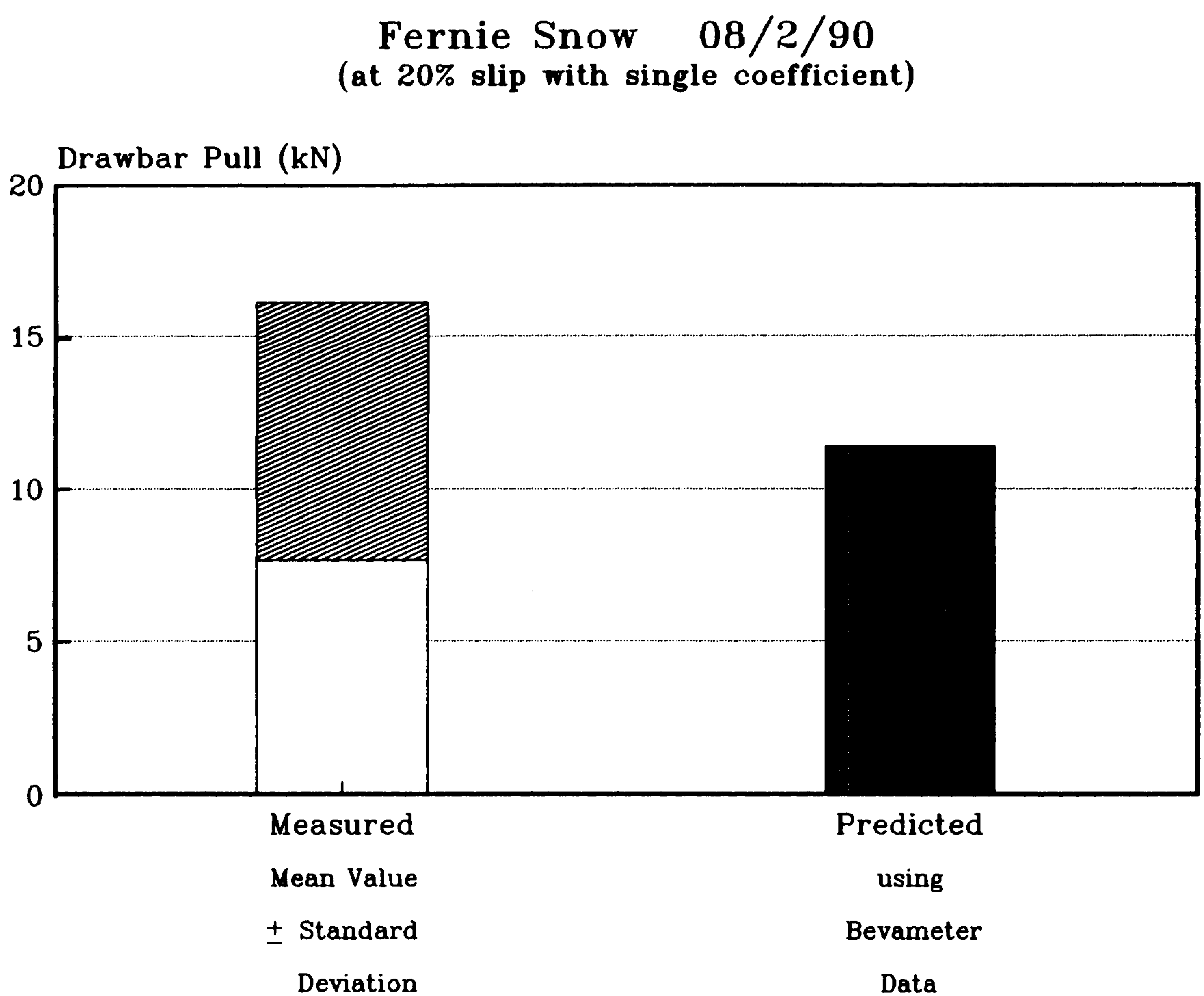

Fig. 4.2.54 Measured and predicted vehicle performance at 20% slip on undisturbed snow

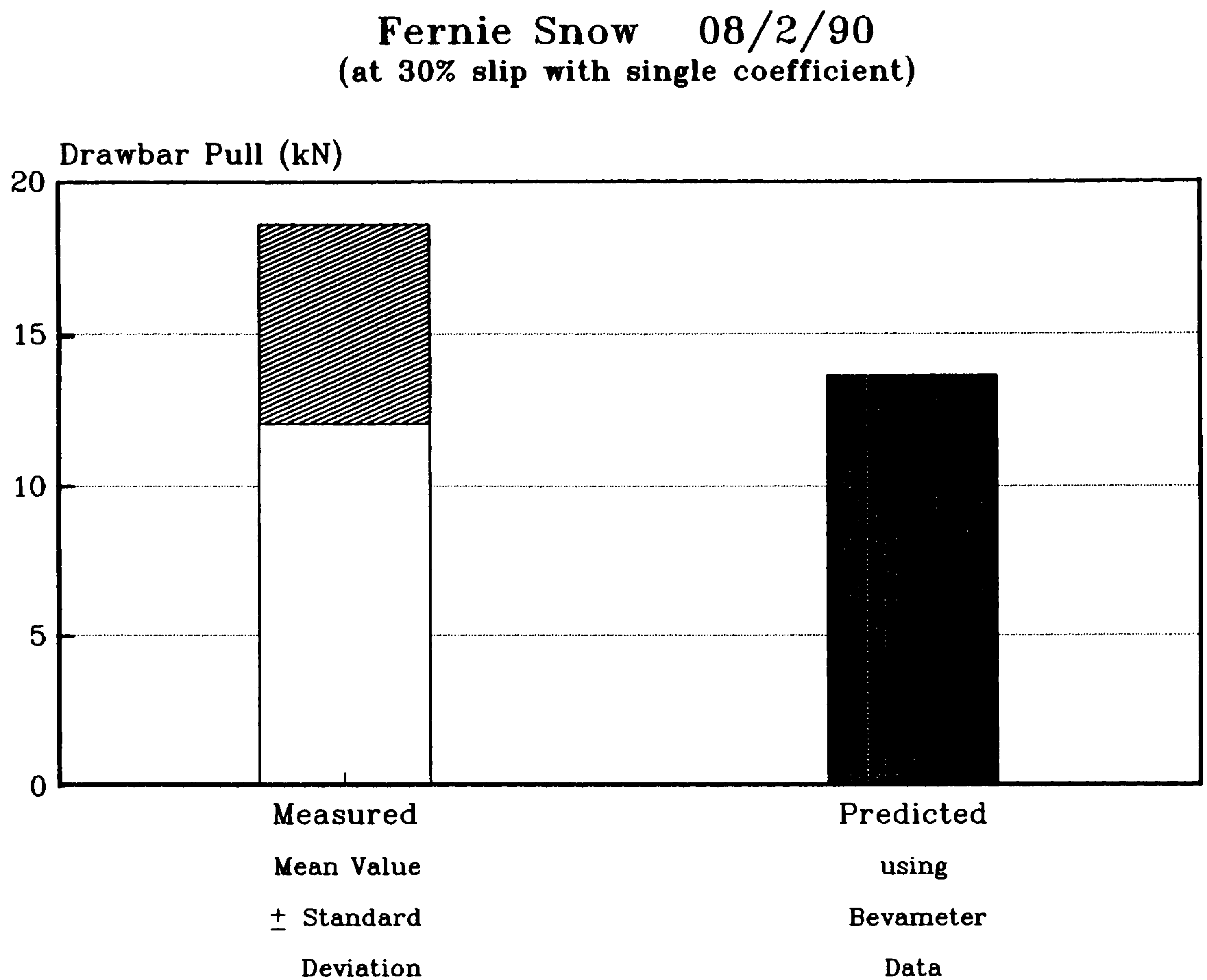

Fig. 4.2.55 Measured and predicted vehicle performance at 30% slip on undisturbed snow

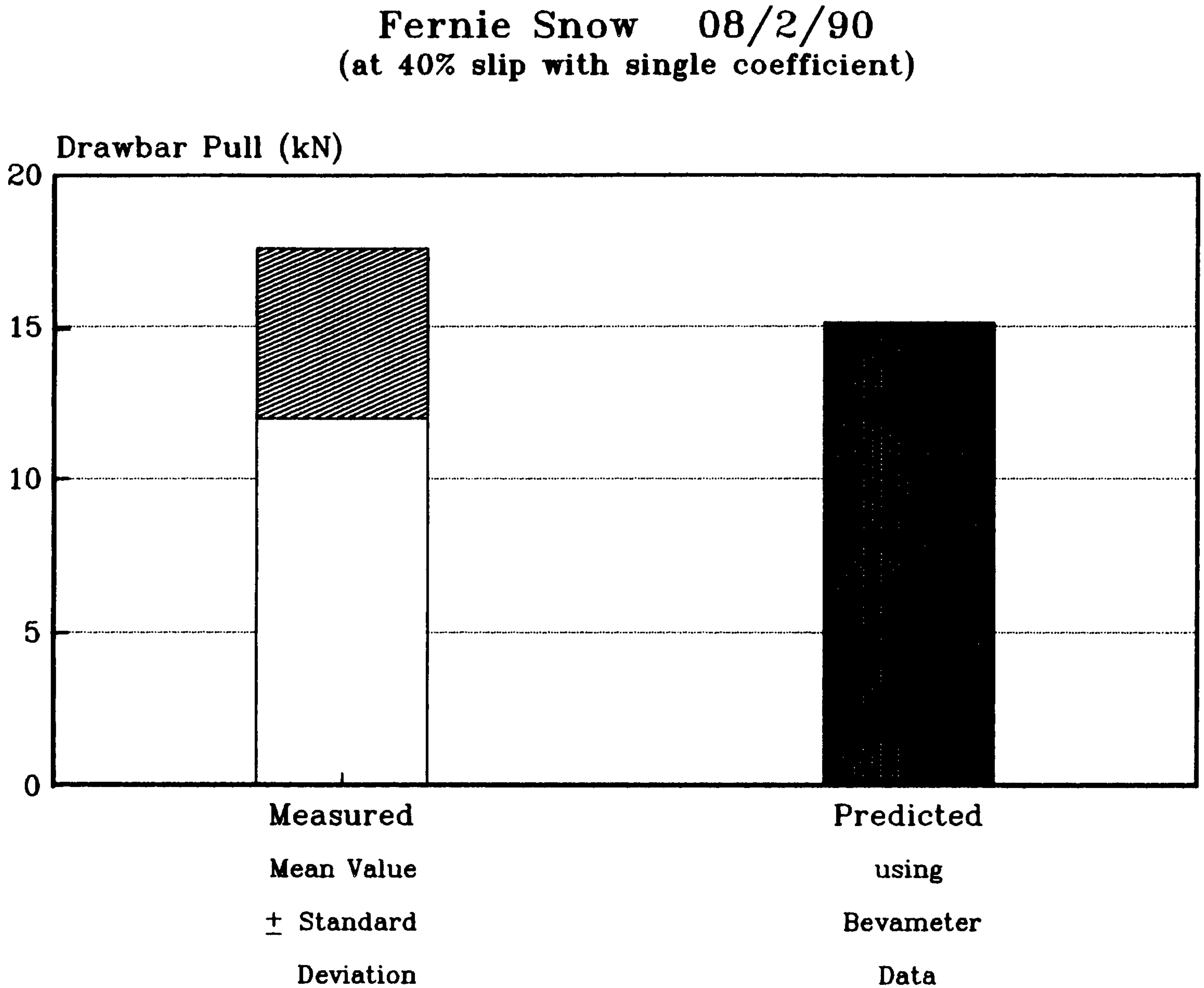

Fig. 4.2.56 Measured and predicted vehicle performance at 40% slip on undisturbed snow

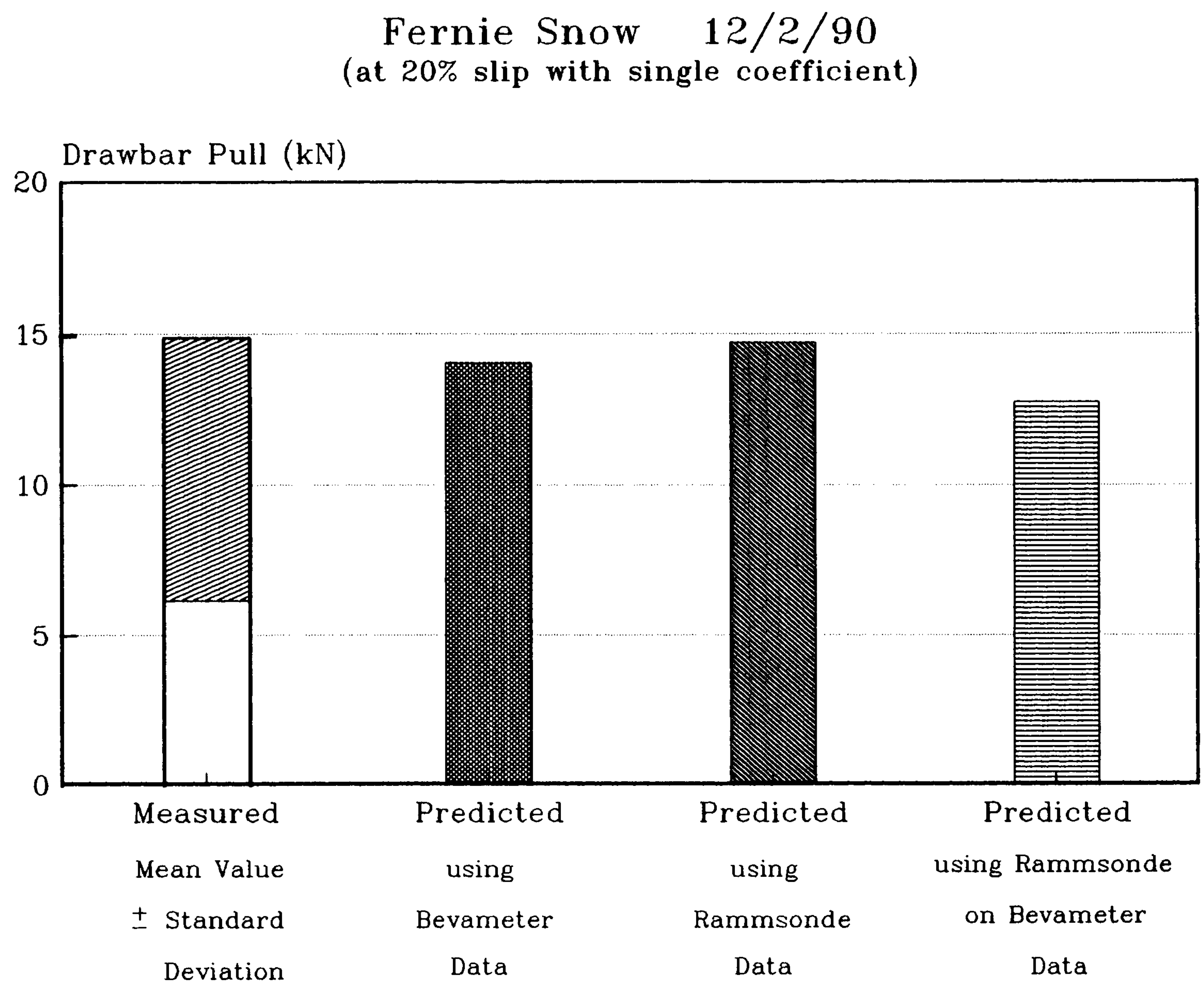

Fig. 4.2.57 Measured and predicted vehicle performance at 20% slip on undisturbed snow

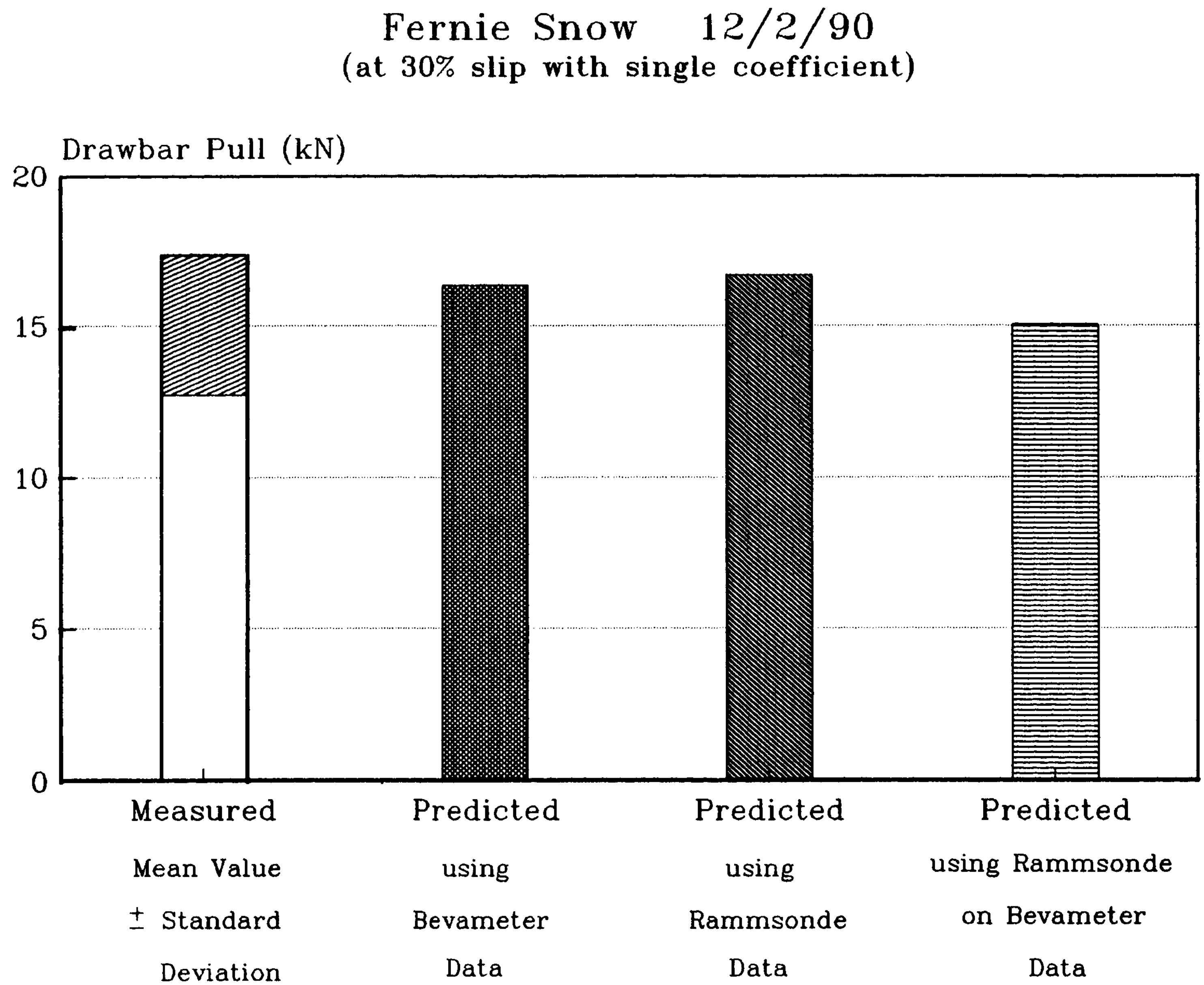

Fig. 4.2.58 Measured and predicted vehicle performance at 30% slip on undisturbed snow

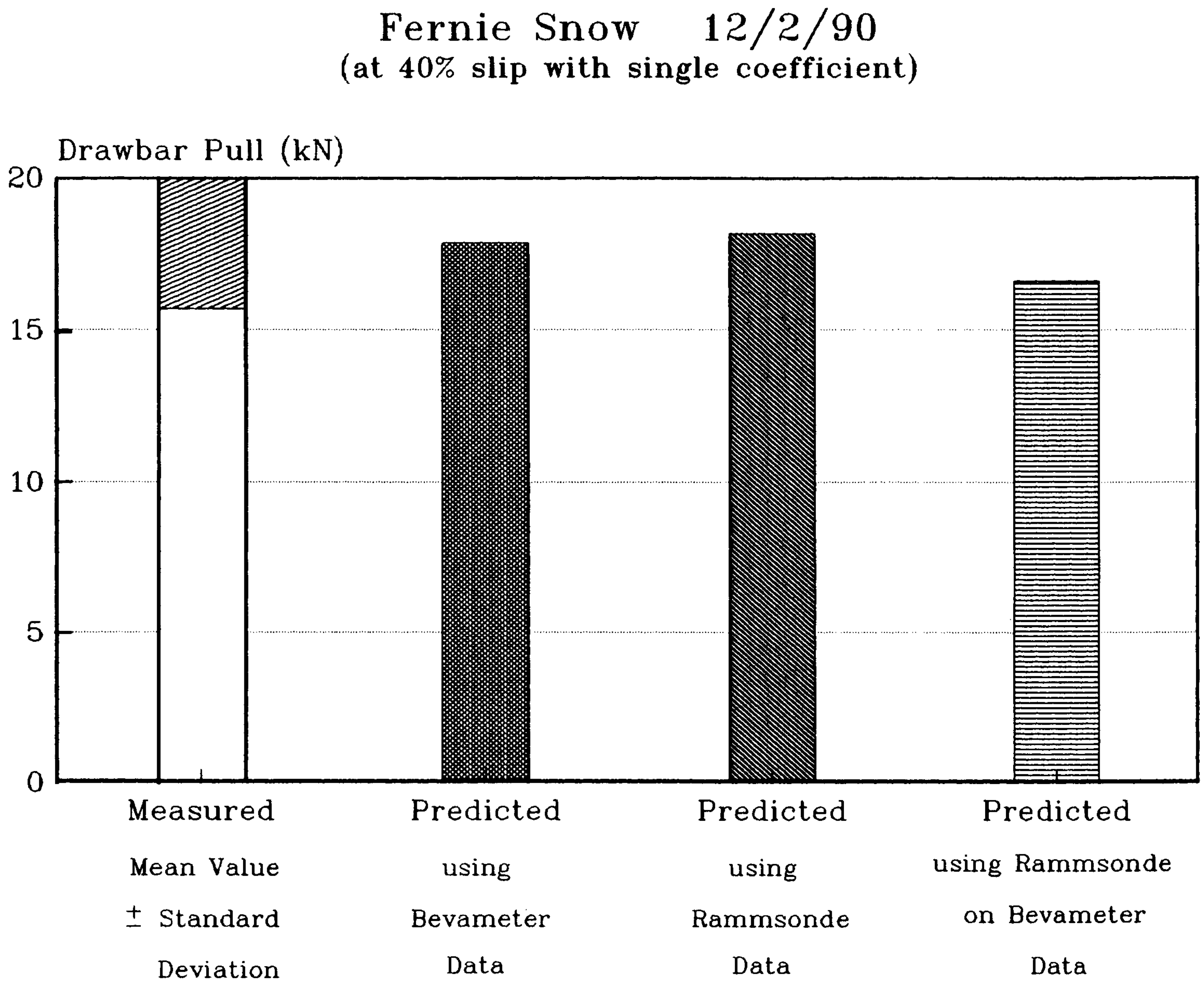

Fig. 4.2.59 Measured and predicted vehicle performance at 40% slip on undisturbed snow

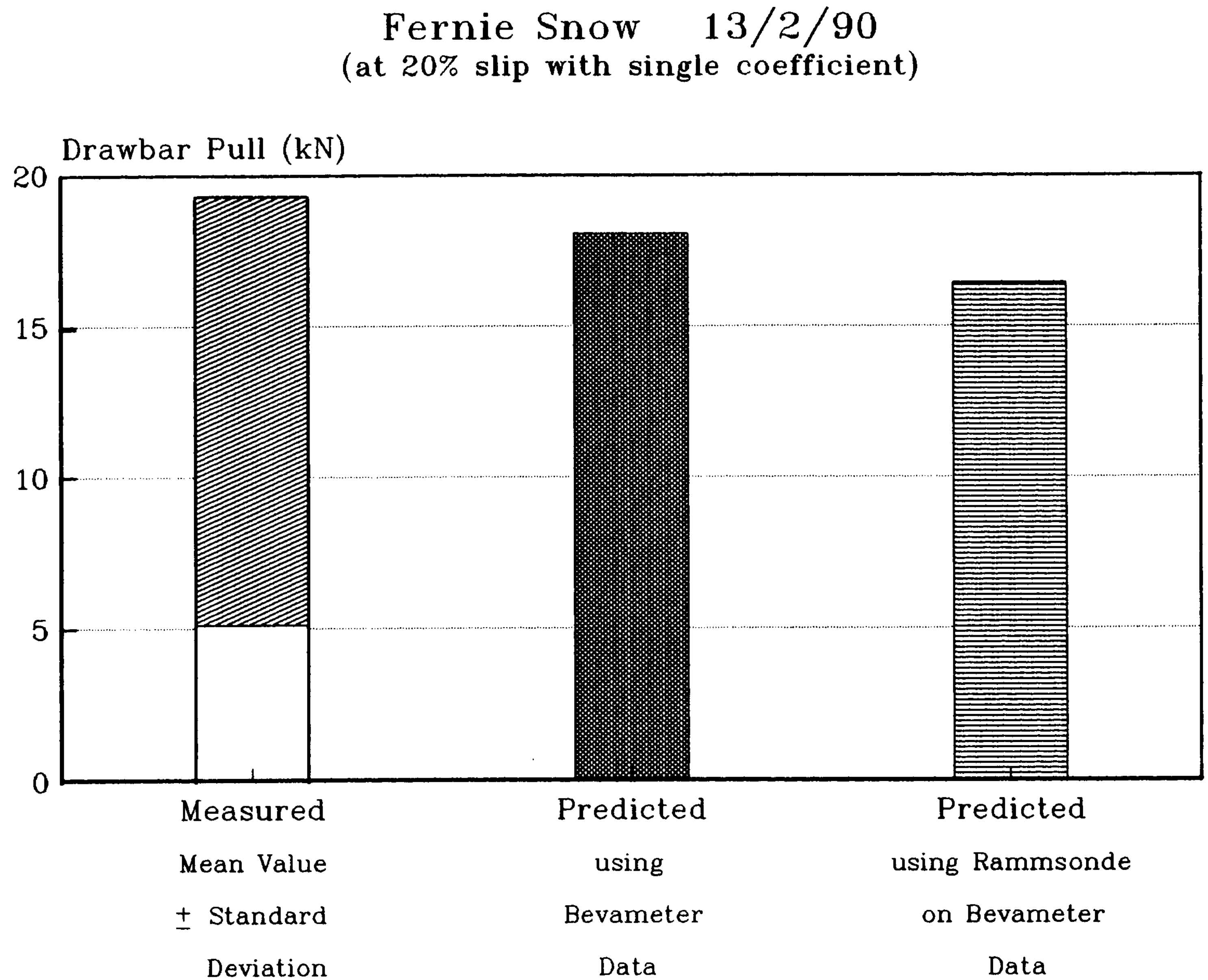

Fig. 4.2.60 Measured and predicted vehicle performance at 20% slip on undisturbed snow

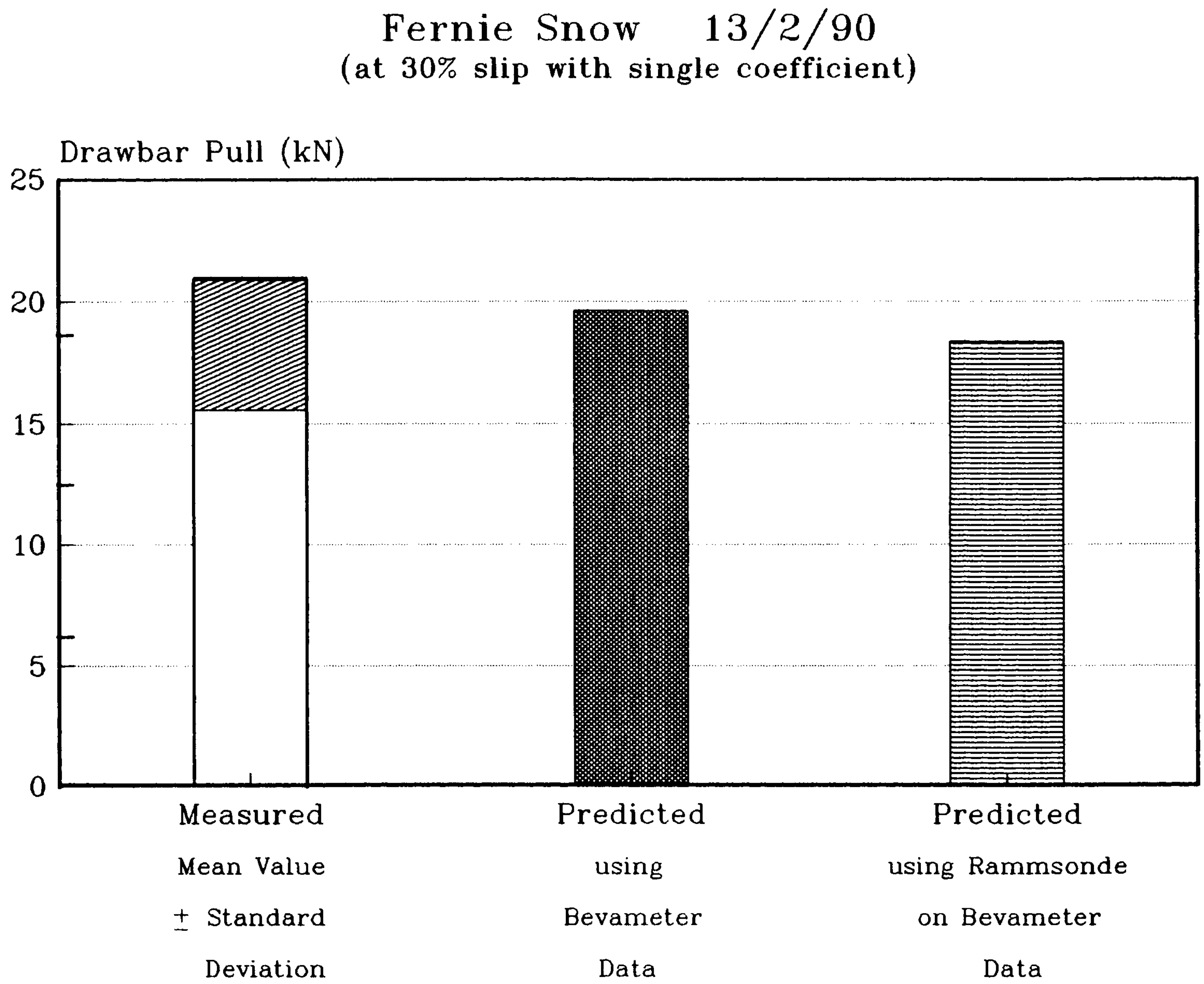

Fig. 4.2.61 Measured and predicted vehicle performance at 30% slip on undisturbed snow

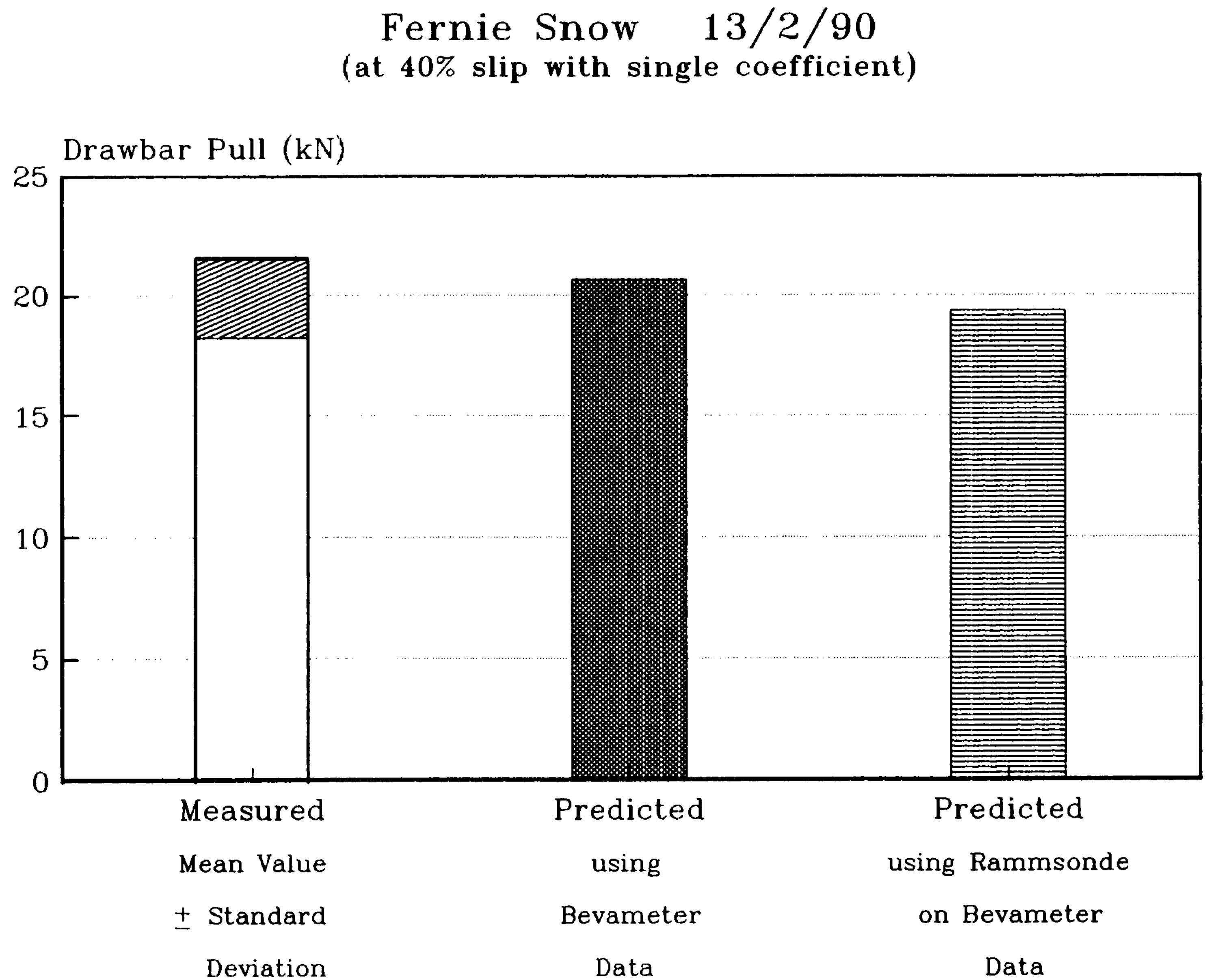

Fig. 4.2.62 Measured and predicted vehicle performance at 40% slip on undisturbed snow

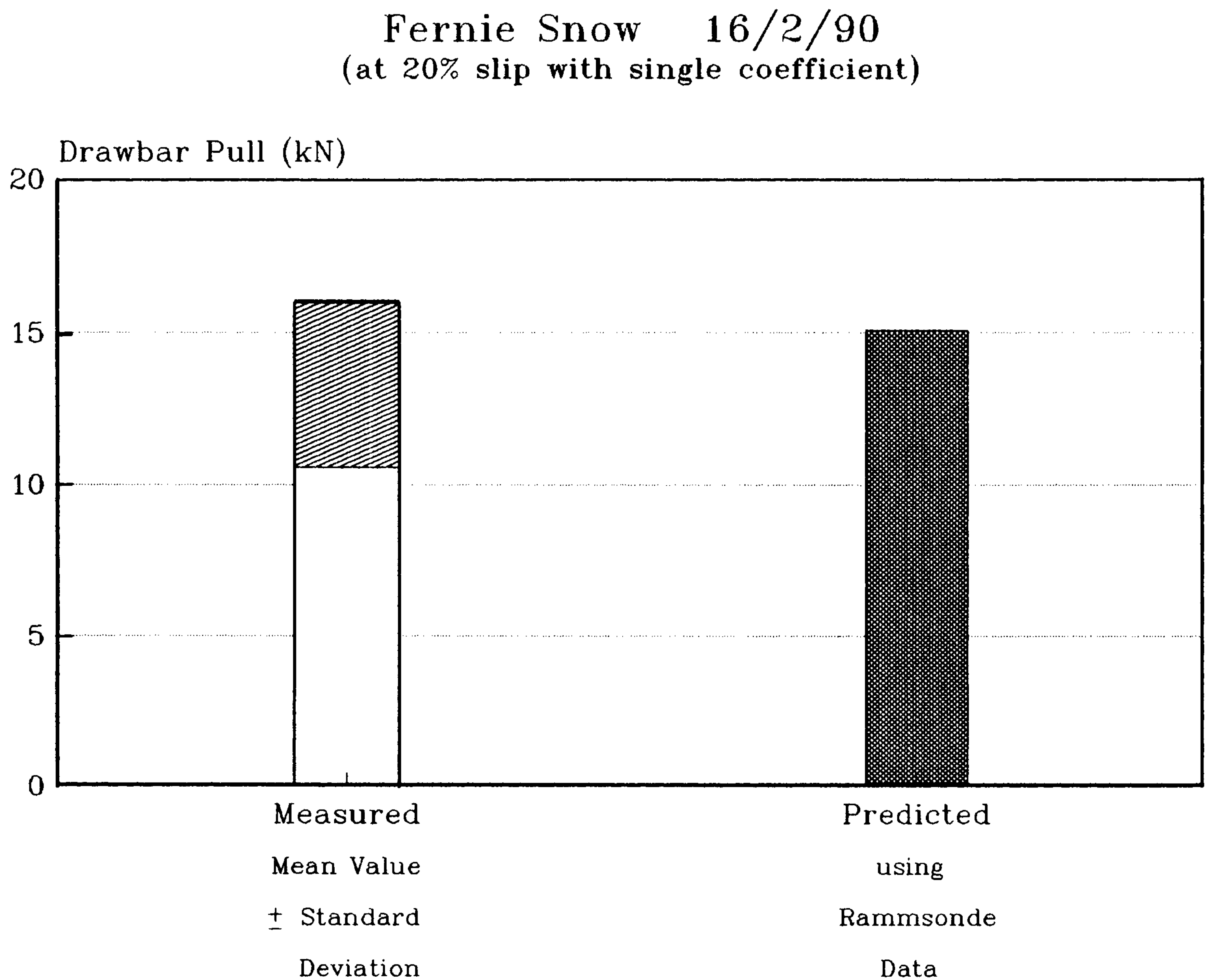

Fig. 4.2.63 Measured and predicted vehicle performance at 20% slip on undisturbed snow

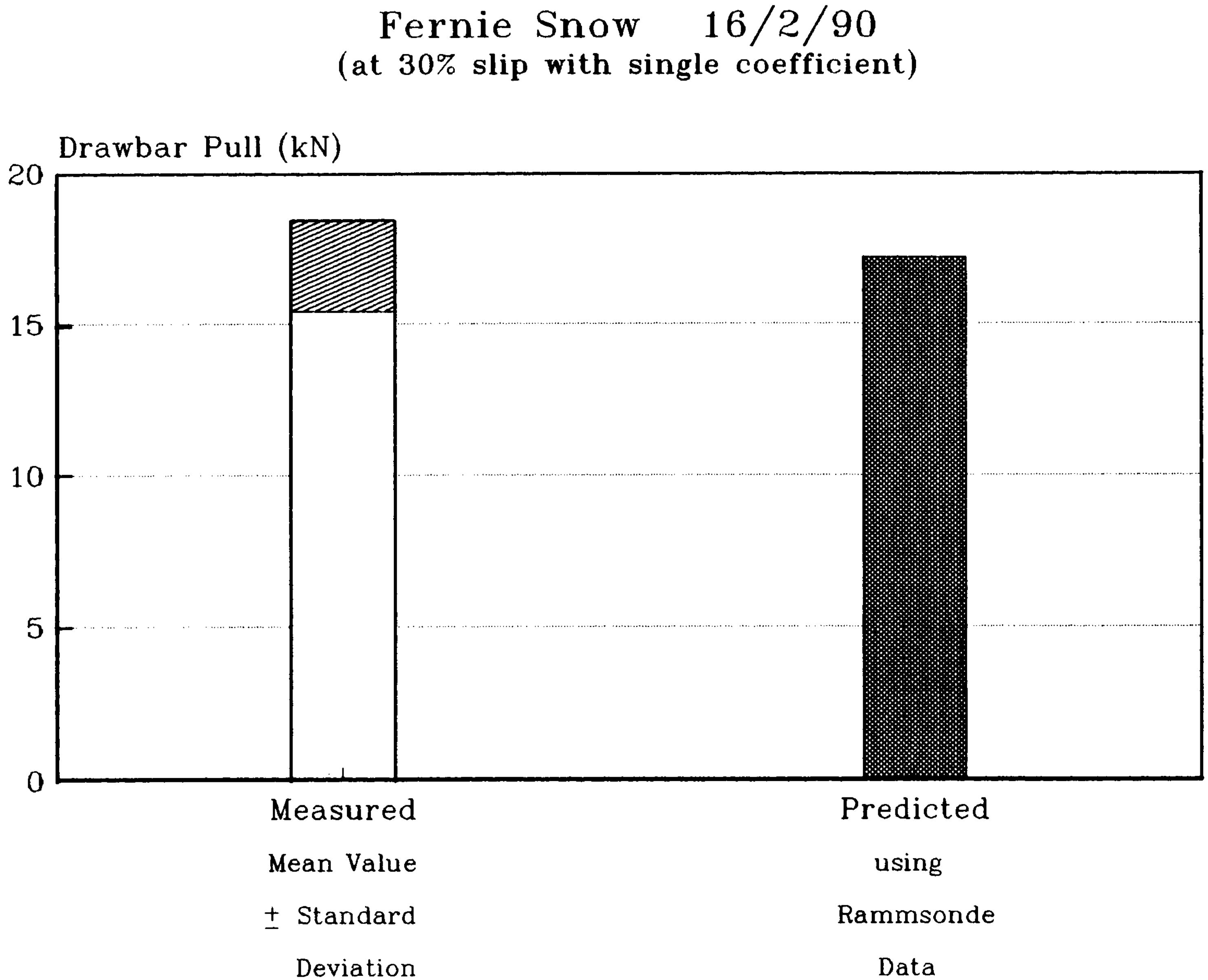

Fig. 4.2.64 Measured and predicted vehicle performance at 30% slip on undisturbed snow

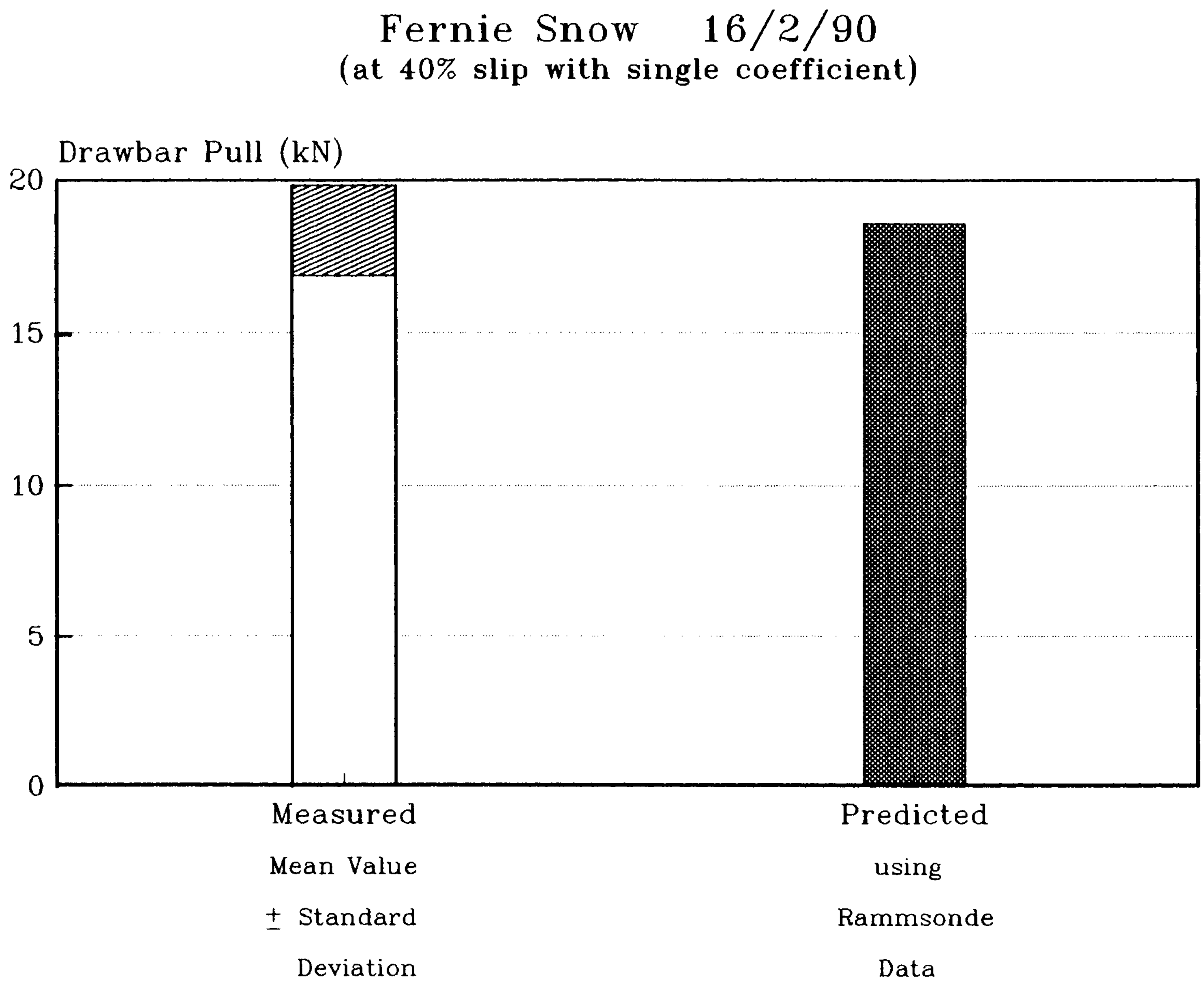

Fig. 4.2.65 Measured and predicted vehicle performance at 40% slip on undisturbed snow

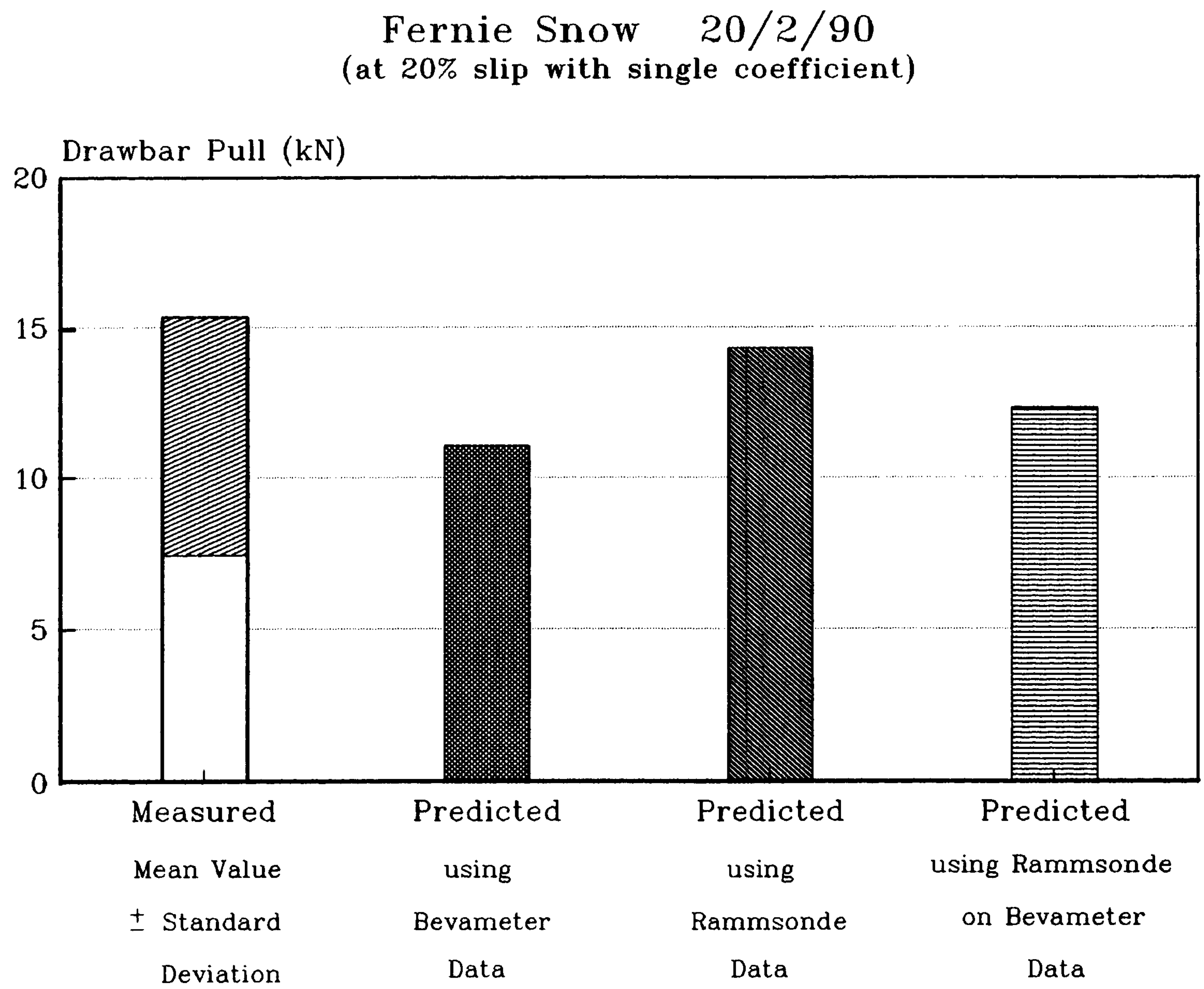

Fig. 4.2.66 Measured and predicted vehicle performance at 20% slip on undisturbed snow

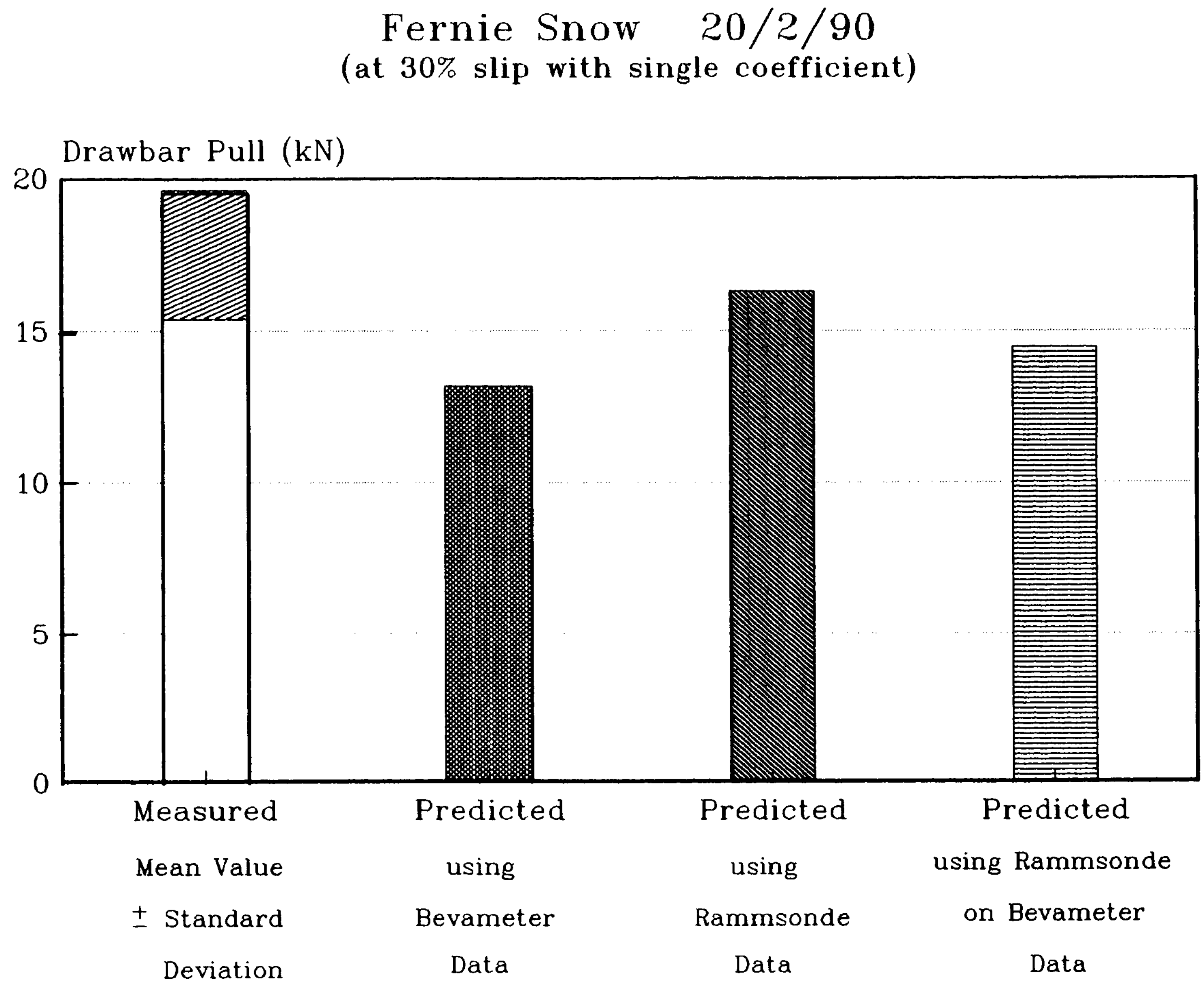

Fig. 4.2.67 Measured and predicted vehicle performance at 30% slip on undisturbed snow

Fernie Snow 20/2/90
(at 40% slip with single coefficient)

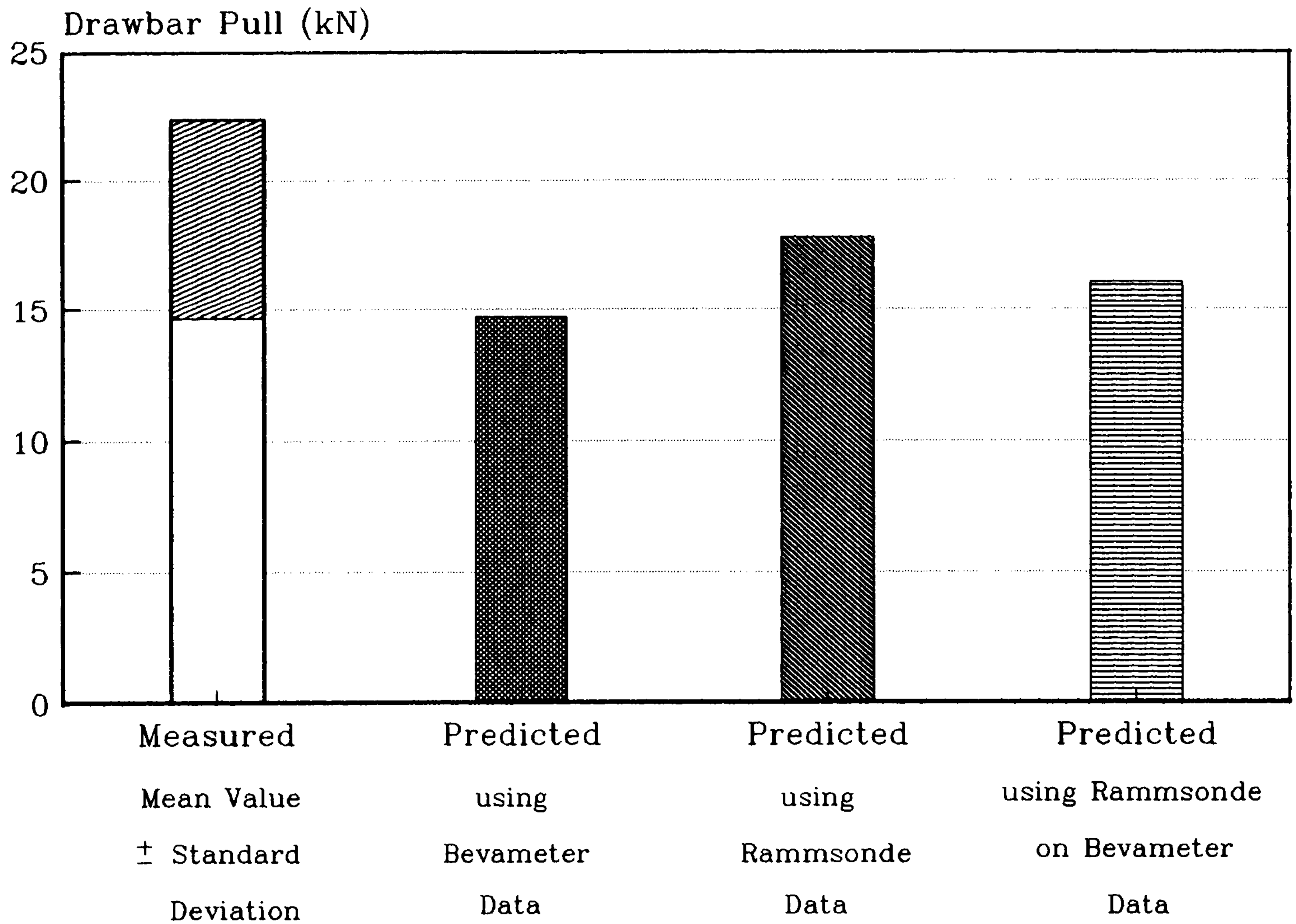

Fig. 4.2.68 Measured and predicted vehicle performance at 40% slip on undisturbed snow

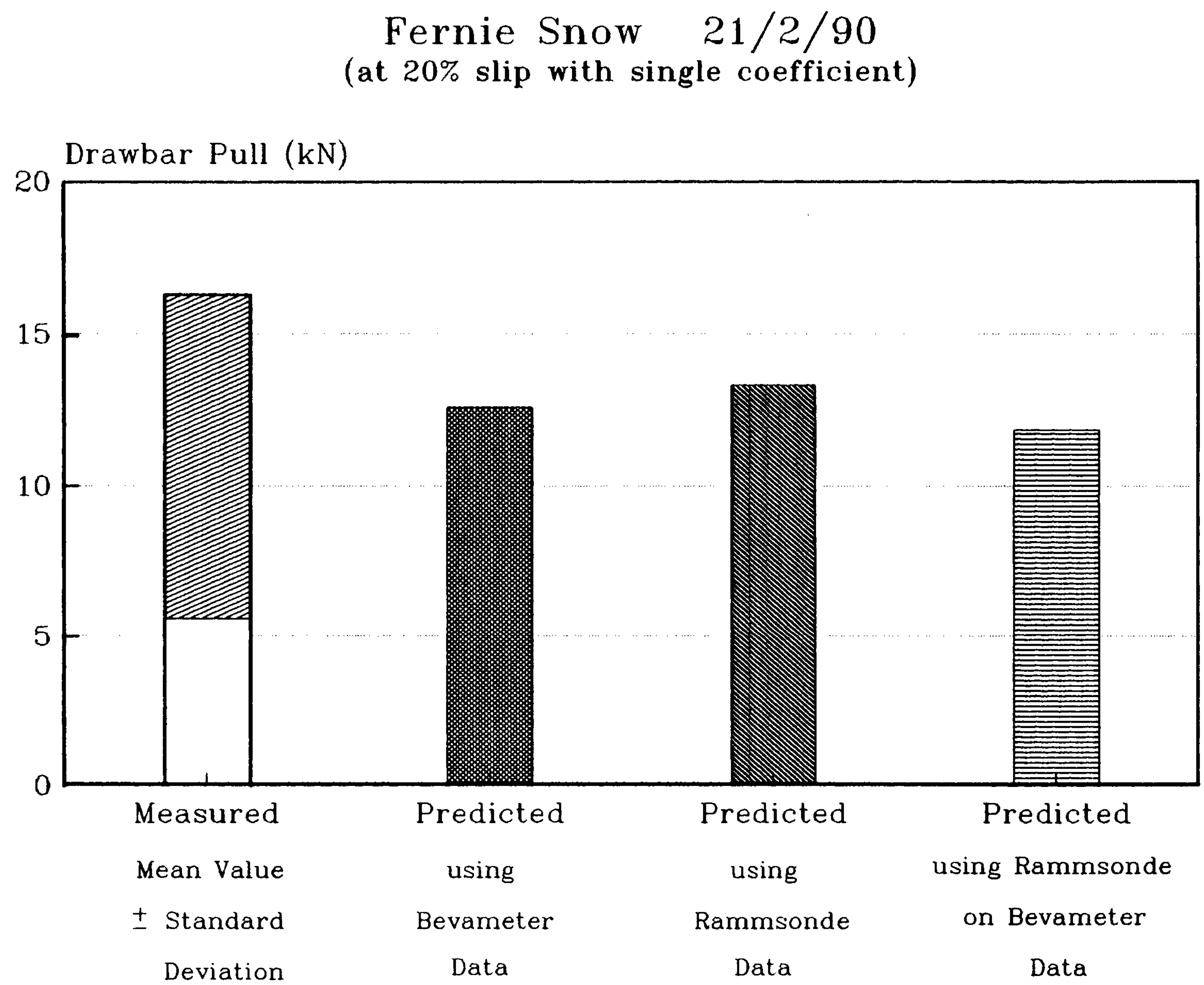

Fig. 4.2.69 Measured and predicted vehicle performance at 20% slip on undisturbed snow

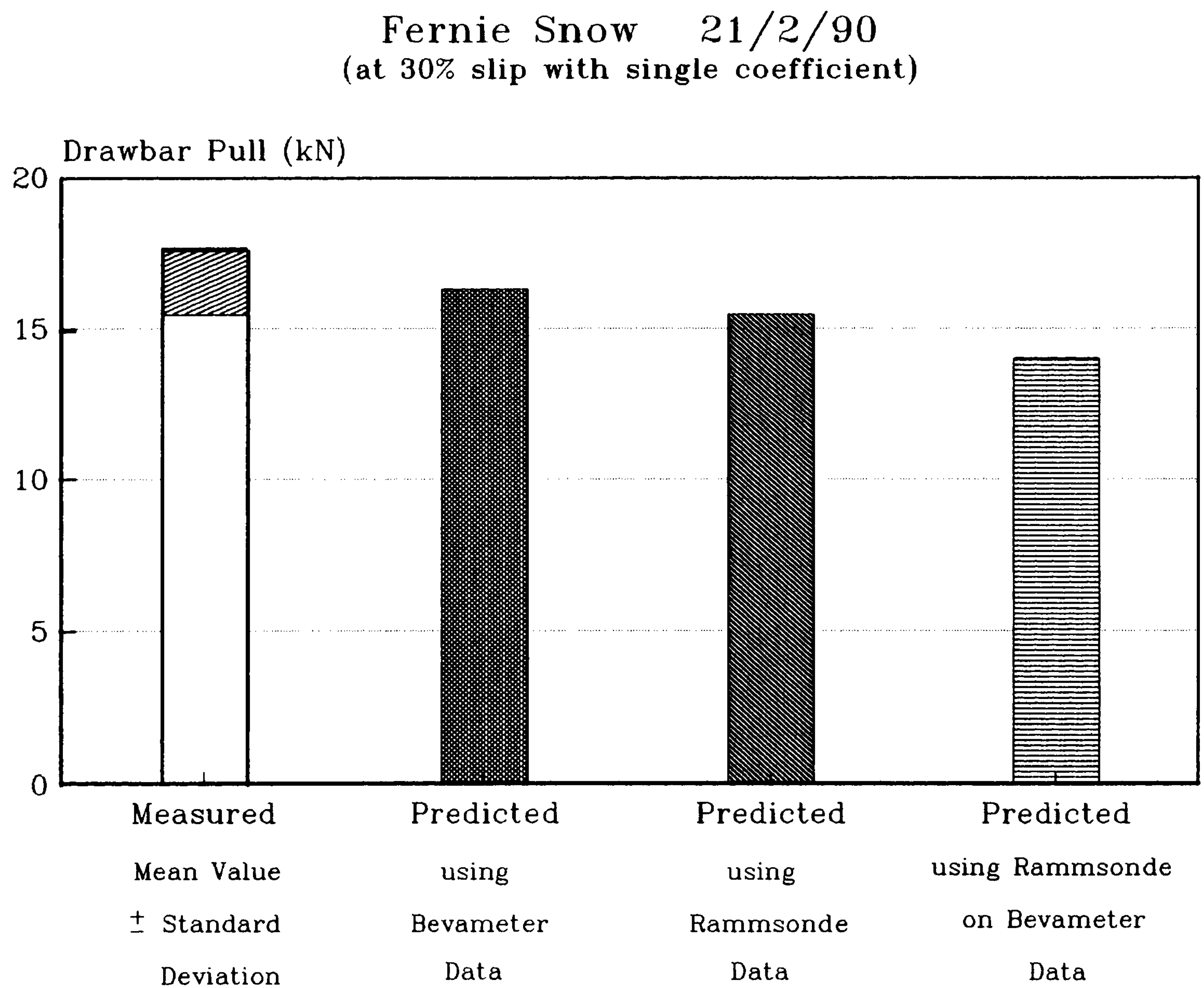

Fig. 4.2.70 Measured and predicted vehicle performance at 30% slip on undisturbed snow

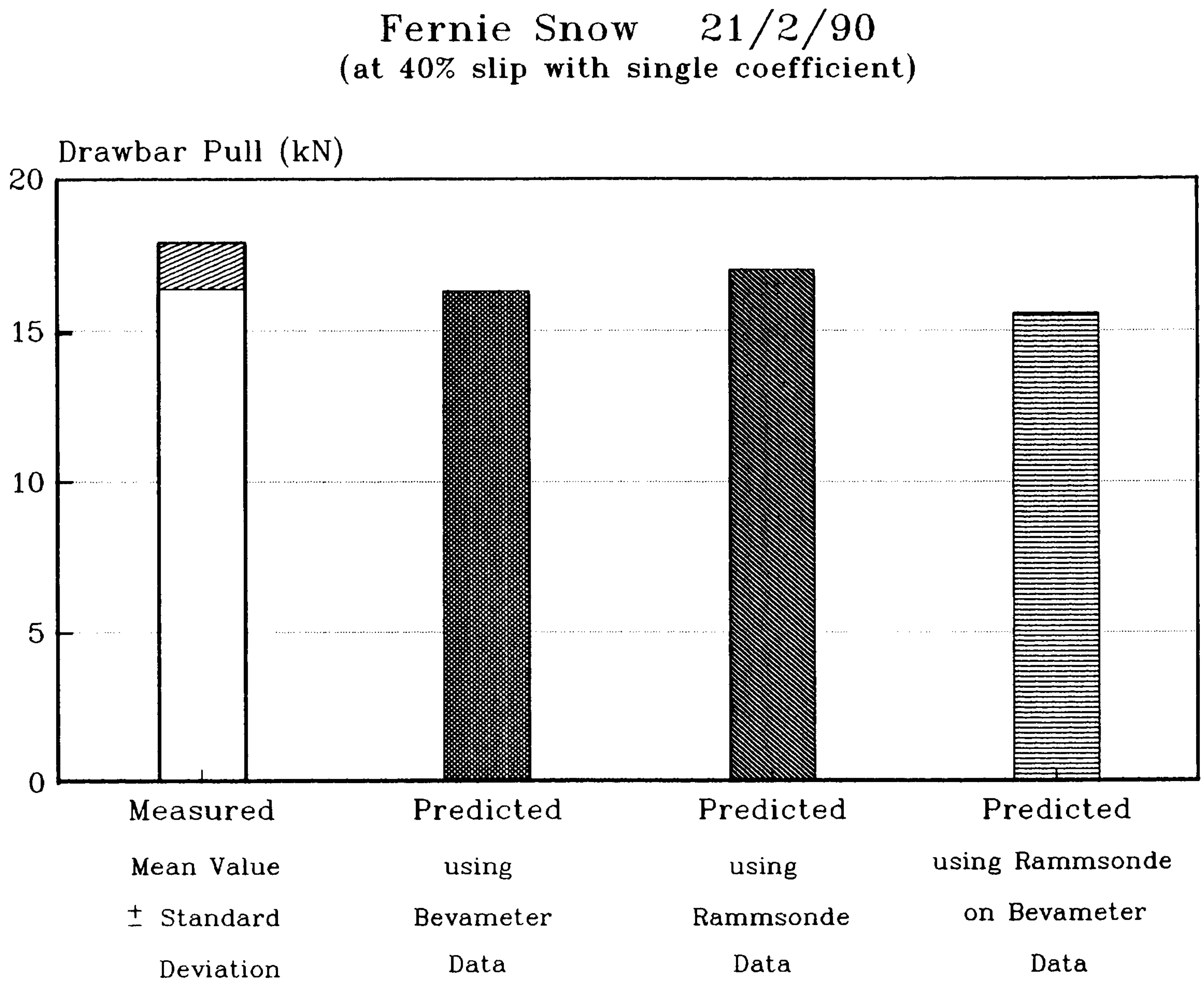

Fig. 4.2.71 Measured and predicted vehicle performance at 40% slip on undisturbed snow

4.3 Correlation of the Measured and Predicted Vehicle Performance on Preconditioned Snow

The preconditioned snow covers were those that had been compacted by a single passage of the test vehicle prior to measurements. The measurement and characterization of the properties of the preconditioned snow were described in detail in two previous reports (Wong, 1990a and b).

Similar to the situation for undisturbed snow, the basic correlation study of the measured and predicted performance of the test vehicle over preconditioned snow was performed based on the average snow conditions and the average measured vehicle performance over the test period. As mentioned previously, this is because the amount of terrain and vehicle test data collected is rather limited. Not all the relevant terrain data and the corresponding vehicle test results are available for a particular date. Furthermore, on a given date, the measurements of terrain properties and vehicle performance were not carried out at the same time. For instance, owing to the limitations of equipment and manpower available, on February 15, 1990 vehicle performance testing was carried out in the morning between 9:09 to 10:04 a.m., while the measurement of the shear strength of the preconditioned snow cover was taken in the afternoon between 4:13 to 4:49 p.m. The terrain conditions under which the vehicle performance was measured may, therefore, differ noticeably from those when the pressure-sinkage and shear strength data were taken, because of the possible aging effect on the properties of the preconditioned snow and changing atmospheric conditions during the day. As a result, it would not be meaningful to examine the correlation between the measured and predicted performance of the test vehicle for individual cases on specific dates.

Table 4.3.1 shows the pressure-sinkage parameters, n, k_c and k_ϕ, for preconditioned snow derived from data obtained using various devices with sensing elements of diameters

Table 4.3.1 **Pressure-Sinkage Parameters for Preconditioned Snow (Using Equation $p = (k_c/b + k_\phi) z^n$**

		Bevameter		Rammsonde Cone		Rammsonde Cone on Bevameter	
Date	Diameter, cm	4	10	4	10	4	10
Feb. 14	Fitting Range, cm	0 - 4.5 & 0 - 5		0 - 12			
	n	.93		.98			
	k_c , $kN/m^{(n+1)}$	70.66		-19.06			
	k_ϕ , $kN/m^{(n+2)}$	1927.7		2546.2			
Feb. 15	Fitting Range, cm	0 - 4		0 - 10		0 - 6	
	n ,	1.00		.93		.90	
	k_c , $kN/m^{(n+1)}$	86.14		11.42		-23.61	
	k_ϕ , $kN/m^{(n+2)}$	1632.2		2330.3		2297.5	
Feb. 16	Fitting Range, cm	0 - 4 & 0 - 3.5		0 - 10		0 - 14	
	n ,	.94		.99		.98	
	k_c , $kN/m^{(n+1)}$	4.05		56.73		13.76	
	k_ϕ , $kN/m^{(n+2)}$	3555.0		1445.5		1198.9	
Feb. 19	Fitting Range, cm	0 - 6		0 - 8.5		0 - 6	
	n ,	.98		.79		1.01	
	k_c , $kN/m^{(n+1)}$	29.70		-3.10		-1.87	
	k_ϕ , $kN/m^{(n+2)}$	1585.2		1383.1		1889.4	

of 4 and 10 cm on different dates (Wong, 1990a). To determine the average conditions for the preconditioned snow over the test period, all the pressure-sinkage data obtained using the same device were combined and the Bekker pressure-sinkage equation (Wong, 1990a) was fitted to the combined data. The average values of the pressure-sinkage parameters, n, k_c and k_ϕ, derived from the combined data obtained using the three devices, with 4 and 10 cm diameter sensing elements (cones of plates), in preconditioned snow are shown in Table 4.3.2.

Table 4.3.2 Average Pressure-Sinkage Parameters, n, k_c and k_ϕ, for Preconditioned Snow

Pressure-Sinkage Parameters	Measuring Device		
	Rammsonde	Bevameter	Rammsonde Cone on Bevameter
n	0.772	0.708	1.020
k_c (kN/m^{n+1})	3.74	17.98	14.27
k_ϕ (kN/m^{n+2})	1371.70	927.80	1401.10

Table 4.3.3 shows the pressure-sinkage parameters, n and k, for preconditioned snow derived from data obtained using the three devices with sensing element of 10 cm in diameter on different dates (Wong 1990a). Similar to the situation for undisturbed snow described previously, the simplified Bekker equation containing only two parameters, n and k, was also fitted to the combined pressure-sinkage data obtained using the three devices with 10 cm diameter sensing element (cone or plate). The average values of n and k derived from the combined data for preconditioned snow over the test period are given in Table 4.3.4.

Table 4.3.3 Pressure-Sinkage Parameters for Preconditioned Snow (Using Equation: $p = k\ z^n$)

		Bevameter		Rammsonde Cone		Rammsonde Cone on Bevameter	
Date	Diameter	4	10	4	10	4	10
Feb. 14	Fitting Range, cm	0 - 5.3	0 - 3	0 - 12	0 - 12		
	n ,	.98	.98	.99	0.97		
	k , kPa/m^n	6592.9	5241.5	1645.2	2103.8		
Feb. 15	Fitting Range, cm	0 - 6.4	0 - 9.9	0 - 10.5	0 - 9	0 - 12.7	0 - 7.5
	n ,	.97	.66	.89	.97	.97	.93
	k , kPa/m^n	5644.6	1164.0	2364.5	2976.5	1927.7	1787.1
Feb. 16	Fitting Range, cm	0 - 5.8	0 - 3.9	0 - 10	0 - 10	0 - 14.8	0 - 11.5
	n ,	.82	1.01	1.06	.93	.97	.86
	k , kPa/m^n	2907.5	4463.2	5084.7	2168.5	1673.8	1118.2
Feb. 19	Fitting Range, cm	0 - 6	0 - 6	0 - 8.5	0 - 8.5	0 - 7.4	0 - 10
	n ,	.92	1.04	.60	.98	.99	1.01
	k , kPa/m^n	2548.9	2622.9	719.22	2313.3	1633.1	1724.3

Table 4.3.4 Average Pressure-Sinkage Parameters, n and k, for Preconditioned Snow

Pressure-Sinkage Parameters	Measuring Device		
	Rammsonde	Bevameter	Rammsonde Cone on Bevameter
n	0.609	0.311	0.663
k (kPa/m^n)	927.18	319.66	647.39

The shear strength data on preconditioned snow obtained on February 14, 15, 16 and 19, 1990 are given in Table 4.3.5. The average values of the shear strength parameters c and ϕ for preconditioned snow, derived from the combined shear data obtained using the bevameter shear device, over the test period are shown in Table 4.3.6.

Table 4.3.6 Average Shear Strength Parameters c, ϕ and K, for Preconditioned Snow

Shear Strength Parameters	Internal Shearing	Rubber-Snow Shearing
c (kPa)	0.32	0.02
ϕ (degrees)	29.4	12.0
K (m)	2.50	0.39

Using the average terrain parameters shown in Tables 4.3.2 and 4.3.6, the tractive performance of the test vehicle, BV 206, over preconditioned snow was predicted using NTVPM-85. It should be noted that data on the response of the preconditioned snow to repetitive normal load and on the shear deformation modulus were also required as input. However, these data were not available. Similar to the situation for undisturbed snow described in Sections 4.2, estimated values were used in the simulations. The estimated value of 33,333 kPa/m^2 for coefficient A_u characterizing the response of preconditioned

Table 4.3.5 Shear Strength Parameters for Preconditioned Snow Obtained Using a Bevameter

Date		Internal Shearing	Rubber-Snow Shearing
Feb. 14	c, kPa	1.16	0
	φ, deg.	28.00	10.73
Feb. 15	c, kPa	0	0
	φ, deg.	30.68	9.30
Feb. 16	c, kPa	0.10	0.07
	φ, deg.	27.67	11.24
Feb. 19	c, kPa	0	0
	φ, deg.	31.28	16.62

snow to repetitive normal load was used. The estimated values of the shear deformation module K shown in Table 4.3.6, based on data for similar terrain stored in our data bank, were used as input to the simulation model. Sample output from the simulation model NTVPM-85 is given in Appendix B.

Figures 4.3.1 - 4.3.3 show the relationships between drawbar pull and slip for the test vehicle over preconditioned snow predicted using NTVPM-85, with pressure-sinkage data shown in Table 4.3.2 obtained by the Rammsonde, the bevameter and the Rammsonde cone mounted on the bevameter assembly, respectively. The pressure-sinkage parameters were derived from data obtained using sensing elements with diameters of 4 and 10 cm. The shear strength parameters used in the predictions were those shown in Table 4.3.6. In the figures, the measured drawbar pull at various slips of the test vehicle, expressed in terms of the mean value ± standard deviation derived from the experimental data shown in Figs. 4.1.8 -4.1.10, is also presented. It can be seen that in general the predicted performance, based on pressure-sinkage data obtained using the three devices, lies within the limits defined by the mean value ± standard deviation of the measured performance, with the exception when the slip is higher than about 50% in some cases. Table 4.3.7 shows a comparison of the measured and predicted drawbar pull at slips of 20, 30 and 40%.

Figures 4.3.4 - 4.3.6 show the relationships between drawbar pull and slip for the test vehicle over preconditions snow predicted using NTVPM-85, with pressure-sinkage data shown in Table 4.3.4 obtained by the three devices. The pressure-sinkage parameters were derived from data obtained using sensing elements with diameter of 10 cm. The shear strength parameters used in the predictions were the same as those shown in Table 4.3.6. In the figures, the measured drawbar pull at various slips of the test vehicle, expressed in terms of the mean value ± standard deviation derived from the experimental data shown in Figs. 4.1.8 - 4.1.10, is also presented. It can be seen that again there is a reasonable correlation between the measured performance and the predicted one using

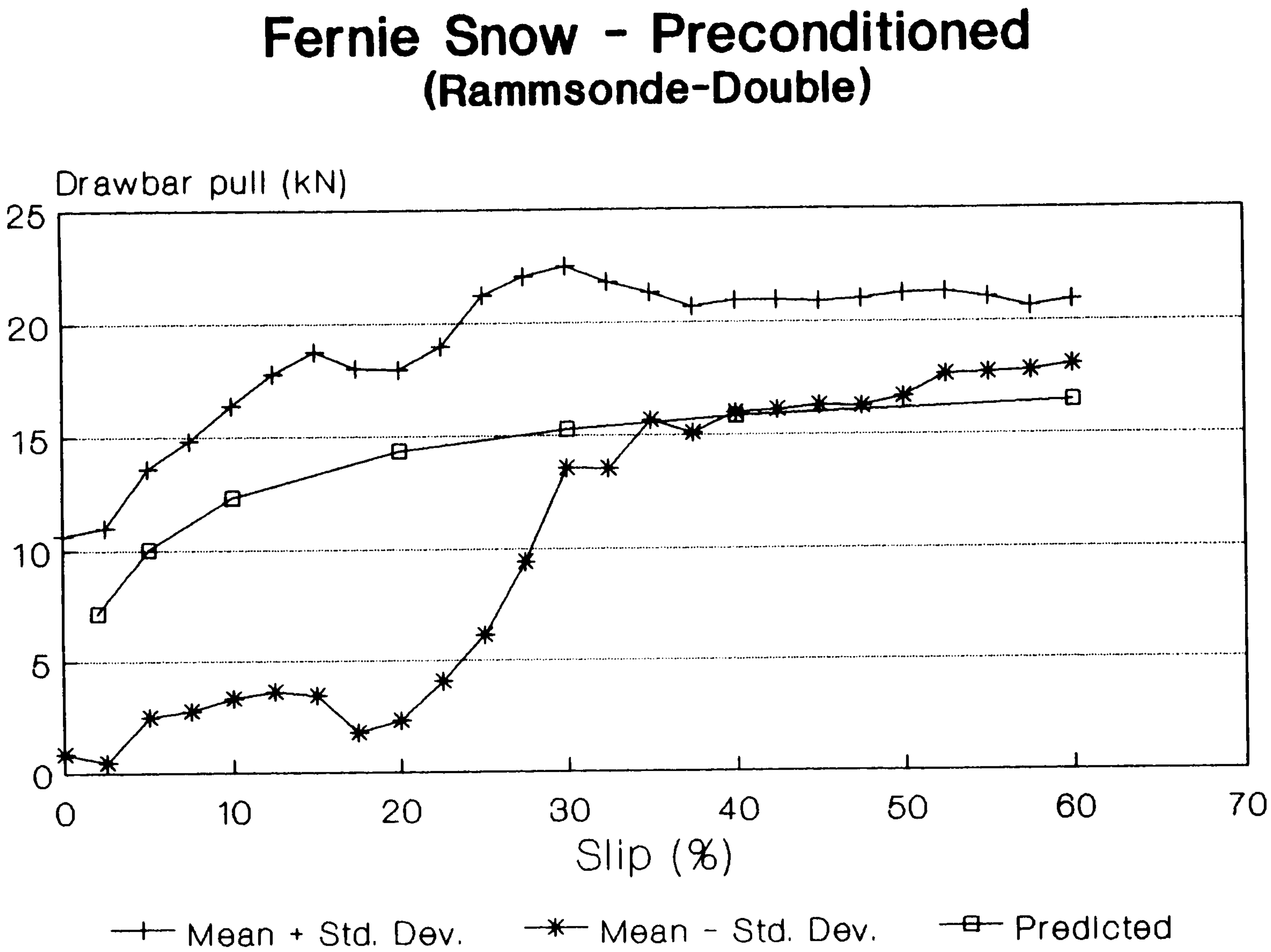

Fig. 4.3.1 Measured and predicted vehicle performance using NTVPM-85 on preconditioned snow

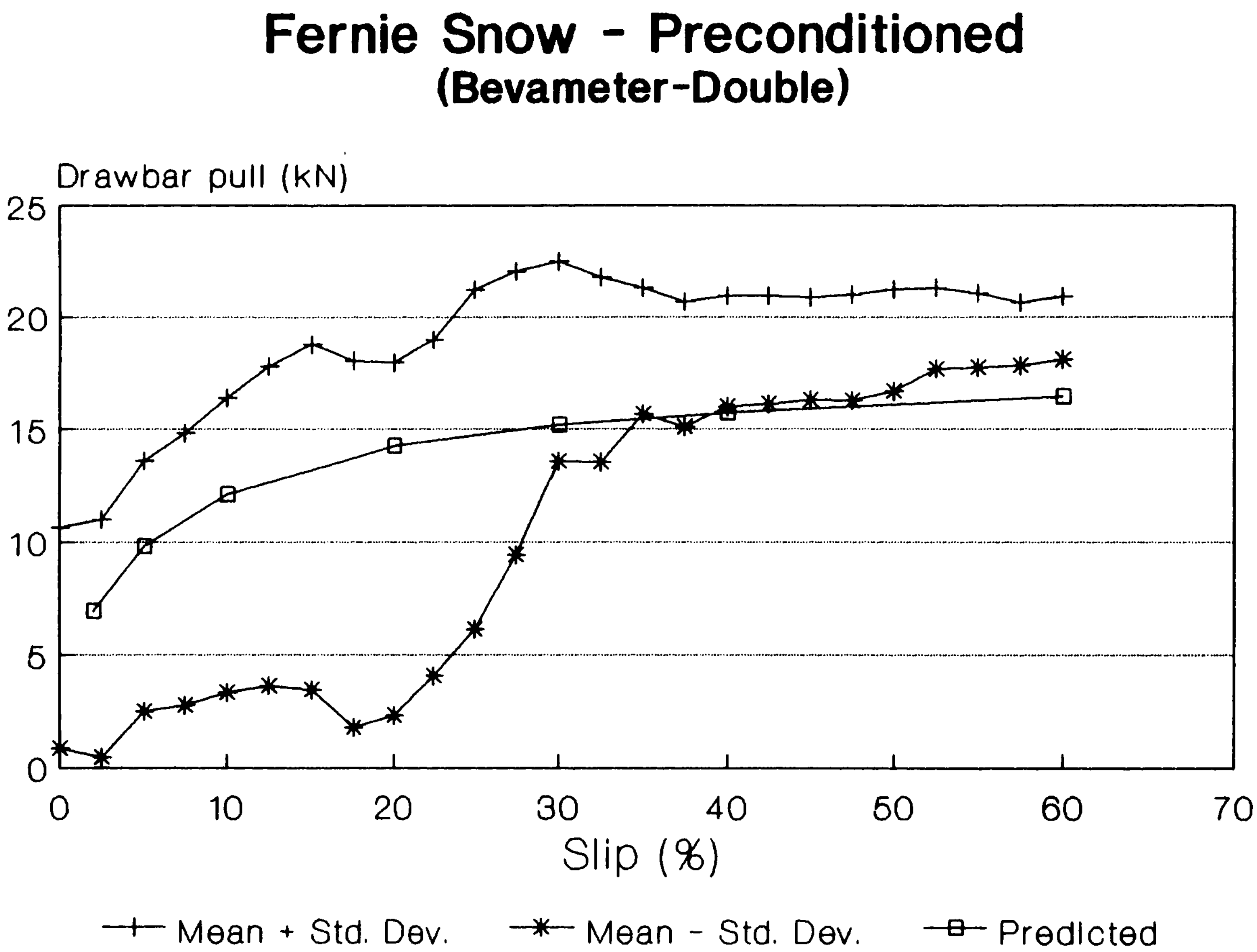

Fig. 4.3.2 Measured and predicted vehicle performance using NTVPM-85 on preconditioned snow

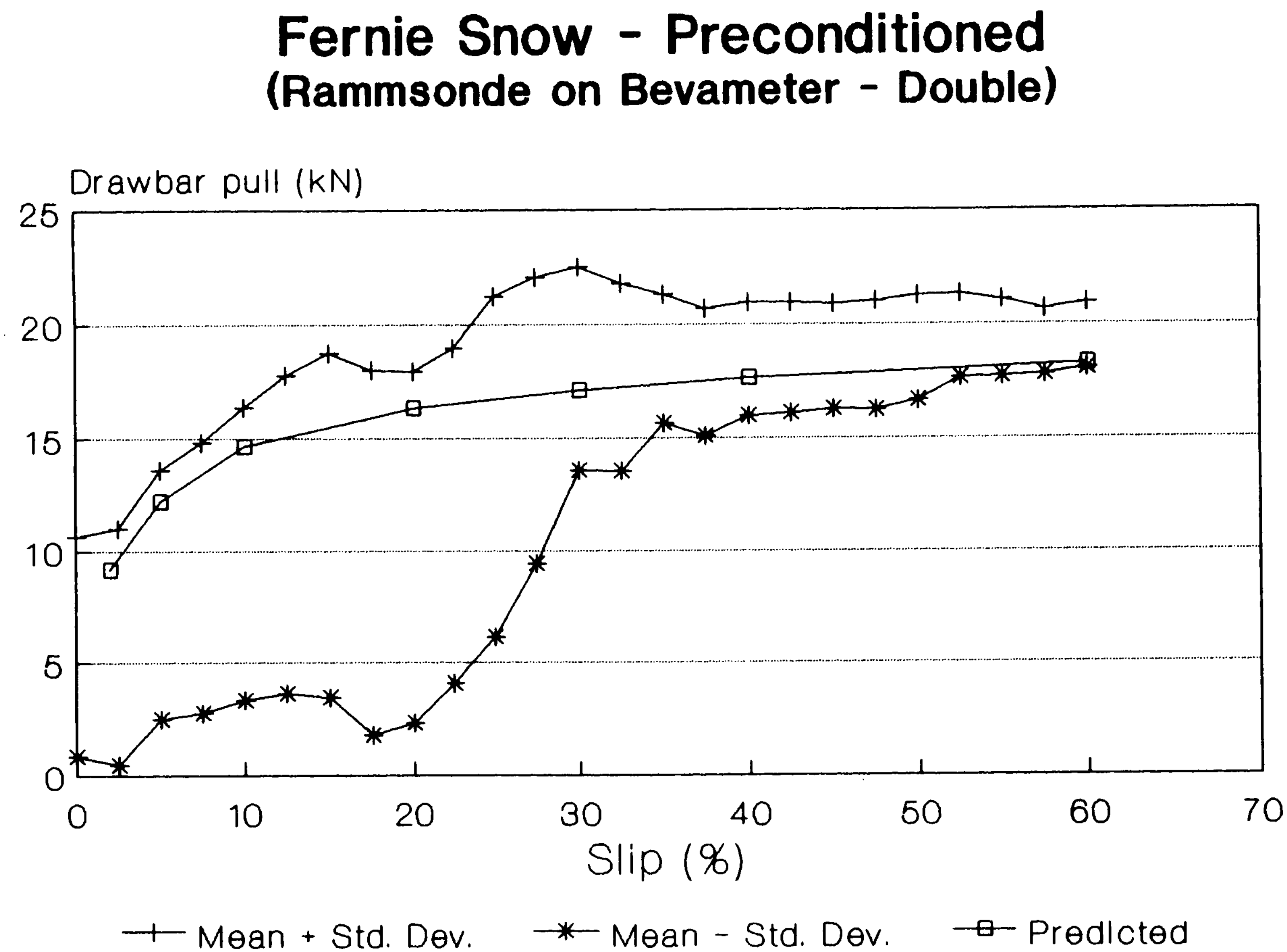

Fig. 4.3.3 Measured and predicted vehicle performance using NTVPM-85 on preconditioned snow

Table 4.3.7 Comparison of the Measured Vehicle Drawbar Pull with the Predicted Ones for Preconditioned Snow (Using Equation: $p = (k_c/b + k_\phi)\, z^n$)

Slip (%)	Drawbar Pull (kN)				
	Measured		Predicted		
	Mean	Standard Deviation	Using Rammsonde	Using Bevameter	Using Rammsonde on Bevameter
20	10.13	7.83	14.34	14.26	16.34
30	18.03	2.46	15.27	15.17	17.11
40	18.46	2.48	15.84	15.72	17.67

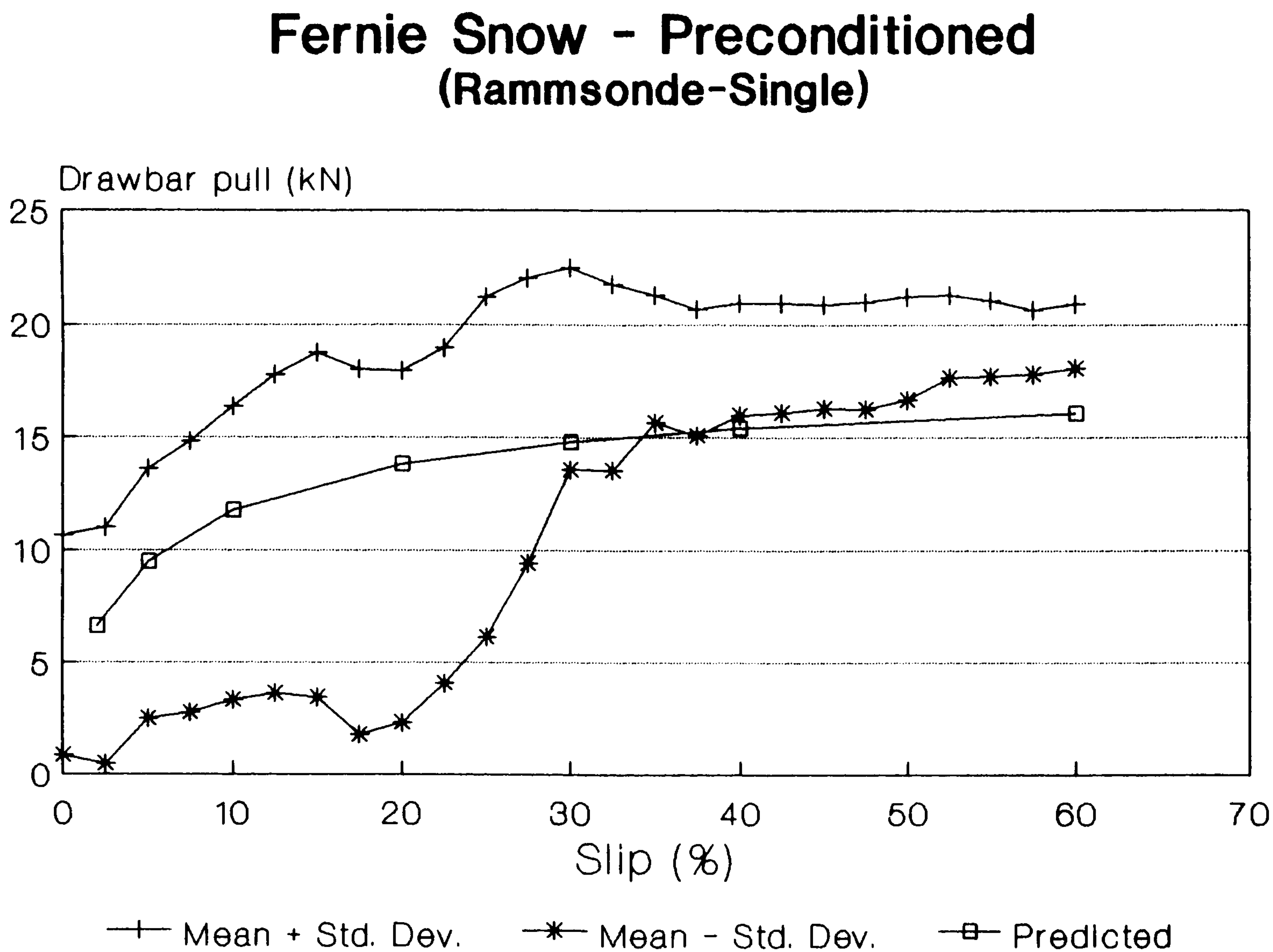

Fig. 4.3.4 Measured and predicted vehicle performance using NTVPM-85 on preconditioned snow

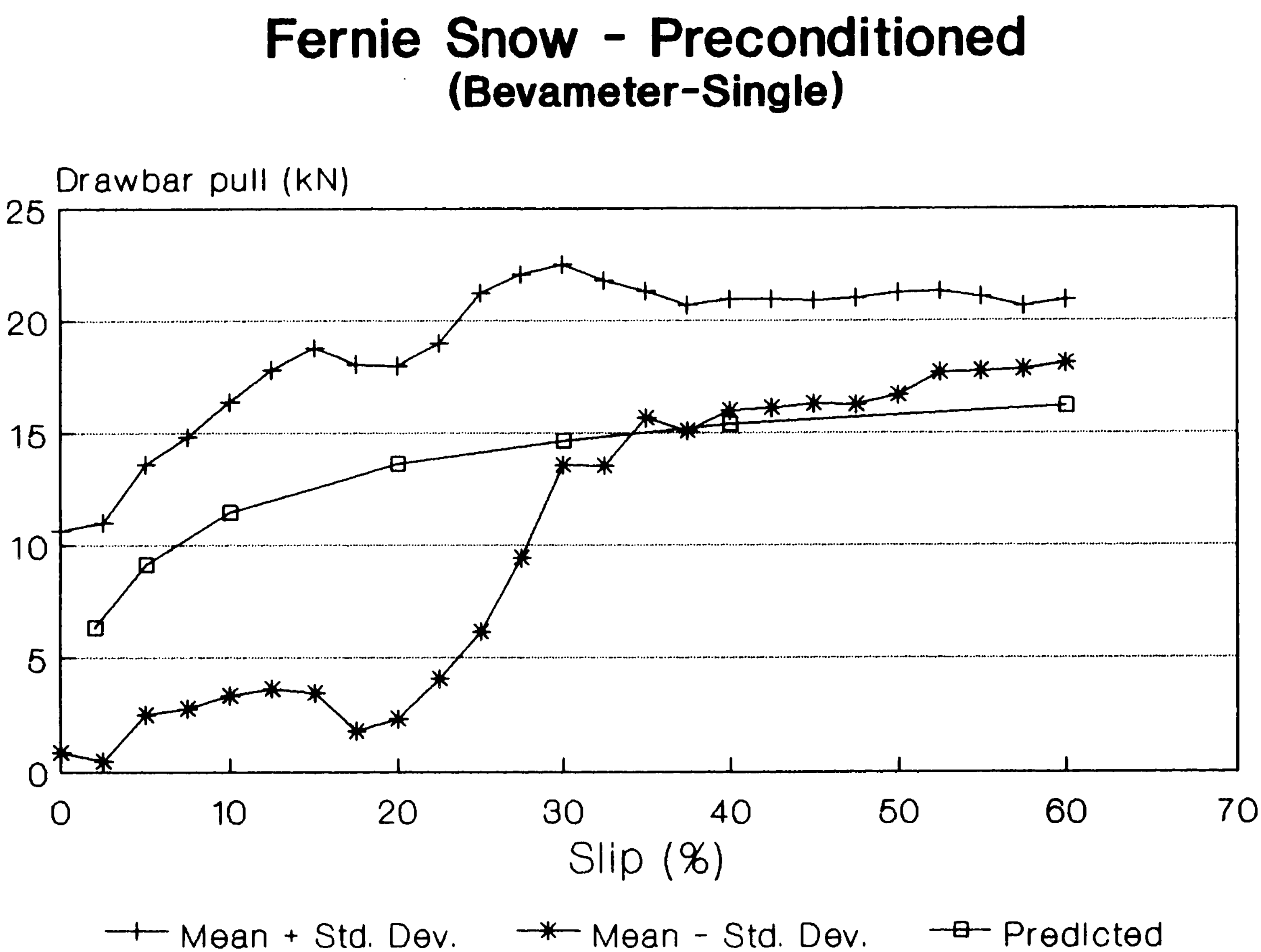

Fig. 4.3.5 Measured and predicted vehicle performance using NTVPM-85 on preconditioned snow

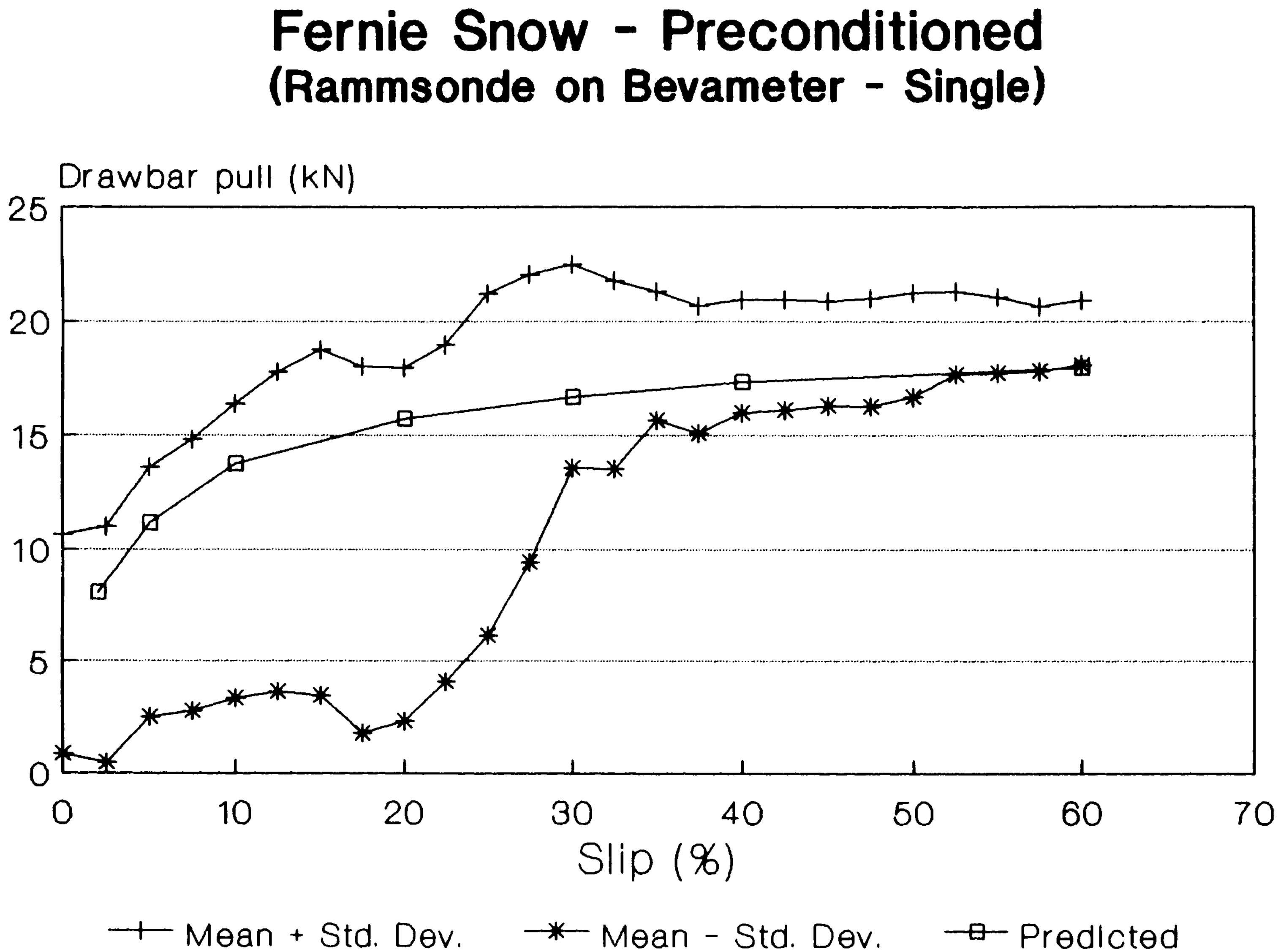

Fig. 4.3.6 Measured and predicted vehicle performance using NTVPM-85 on preconditioned snow

NTVPM-85. Table 4.3.8 shows a comparison between the measured and predicted drawbar pull at slips of 20, 30 and 40%.

Figures 4.3.7 - 4.3.9 show a comparison between the measured drawbar pull and the predicted one, using pressure-sinkage data obtained with the three devices at slips of 20, 30 and 40%. It can be seen from the figures and tables that over preconditioned snow there is a reasonable agreement between the measured tractive performance and predicted one using NTVPM-85, with pressure-sinkage data obtained with the three devices. In contrast with the situation on undisturbed snow described in the previous section, it appears that predictions based on pressure-sinkage parameters, n, k_c and k_ϕ, derived from data obtained using sensing elements with diameters of 4 and 10 cm do not differ significantly from those based on pressure-sinkage parameters, n and k, derived from data obtained using a single sensing element with diameter of 10 cm for the same type of device. This indicates that for practical purposes, it would be adequate to use a single sensing element (cone or plate) with diameter of 10 cm to obtain pressure-sinkage data as input to NTVPM-85 for predicting tracked vehicle performance over preconditioned snow.

Table 4.3.8 Comparison of the Measured Vehicle Drawbar Pull with the Predicted Ones for Preconditioned Snow (Using Equation: $p = k z^n$)

Slip (%)	Drawbar Pull (kN)				
	Measured		Predicted		
	Mean	Standard Deviation	Using Rammsonde	Using Bevameter	Using Rammsonde on Bevameter
20	10.13	7.83	13.82	13.62	15.73
30	18.03	4.46	14.78	14.65	16.67
40	18.46	2.48	15.41	15.40	17.33

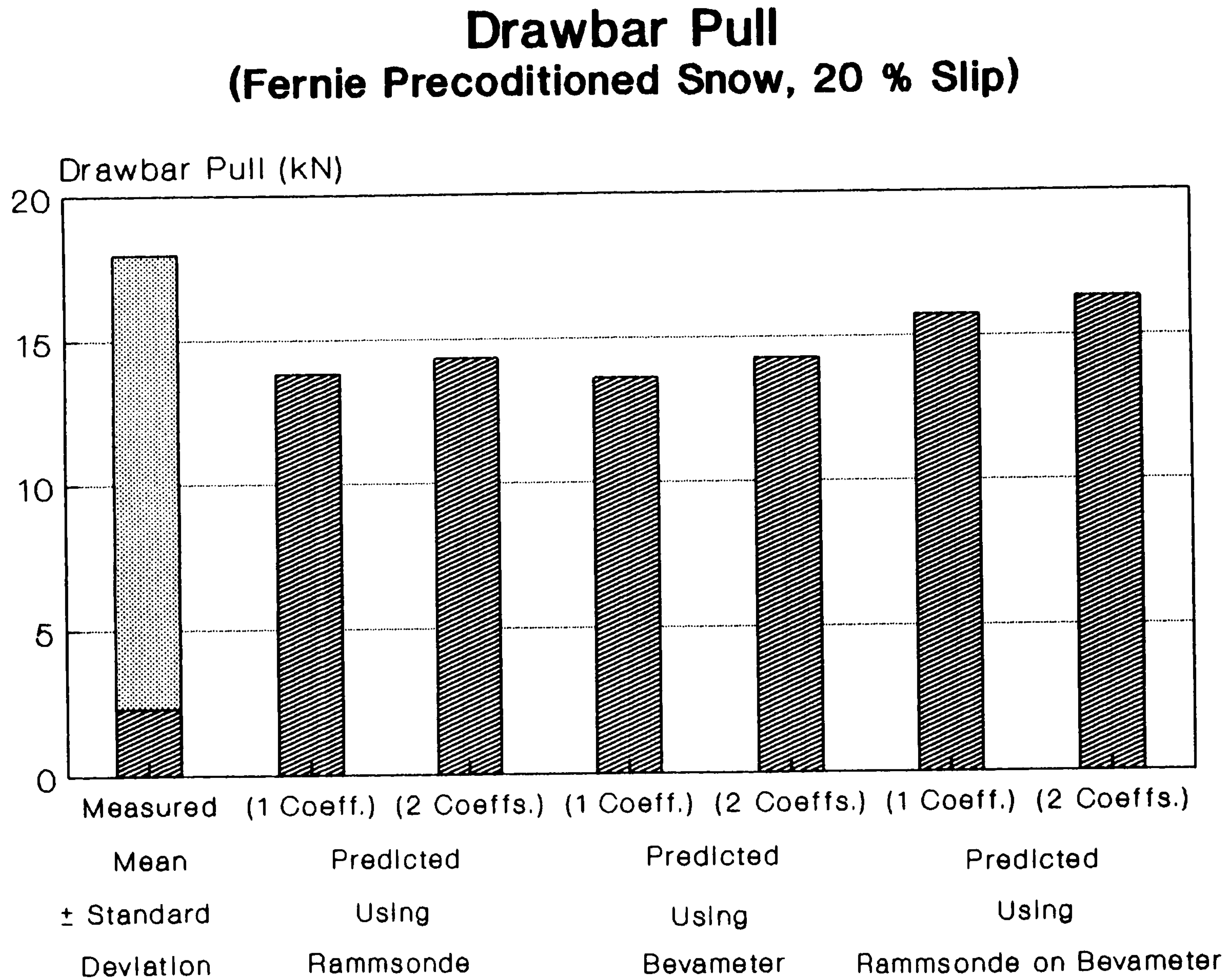

Fig. 4.3.7 Measured and predicted vehicle performance at 20% slip on preconditioned snow

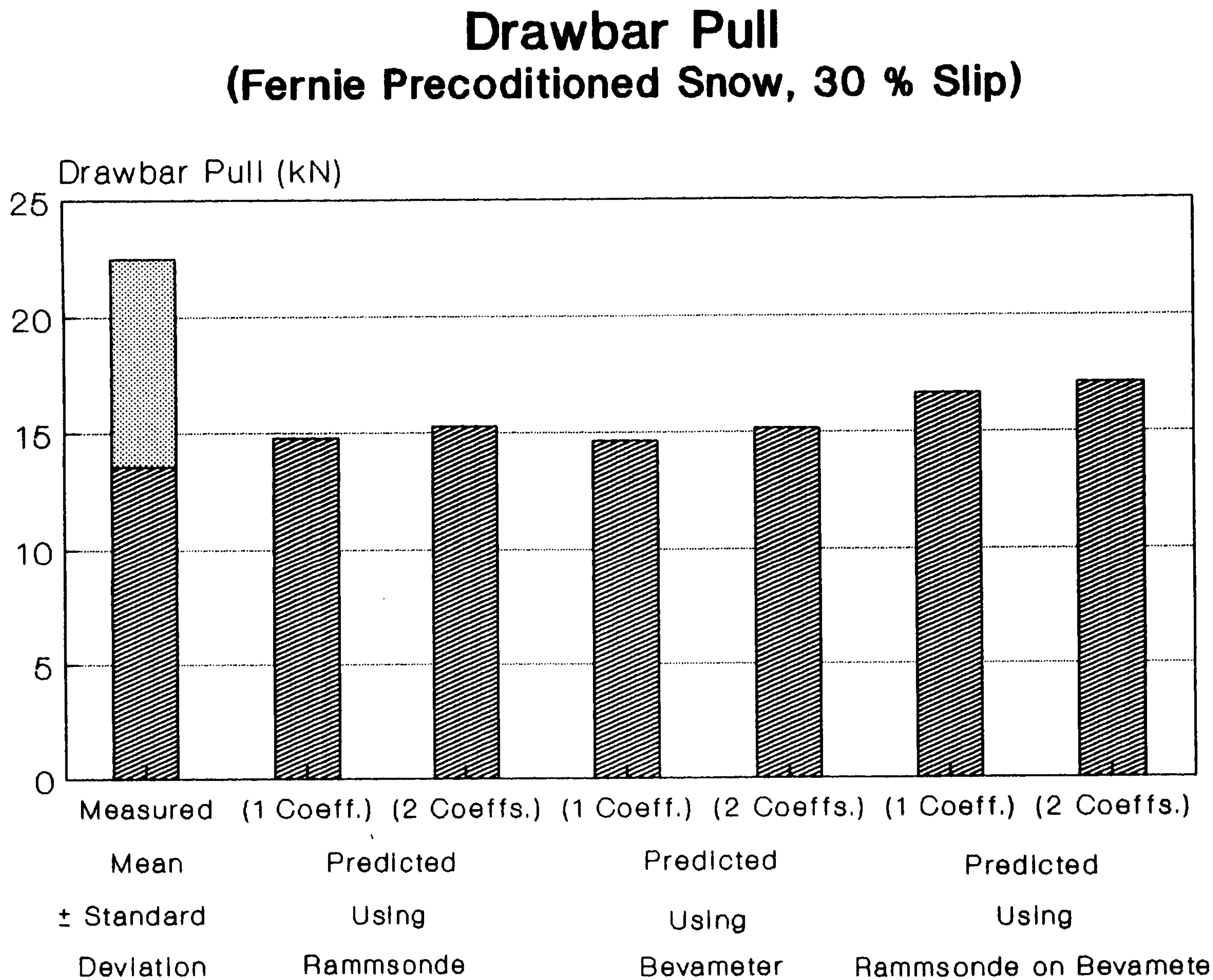

Fig. 4.3.8 Measured and predicted vehicle performance at 30% slip on preconditioned snow

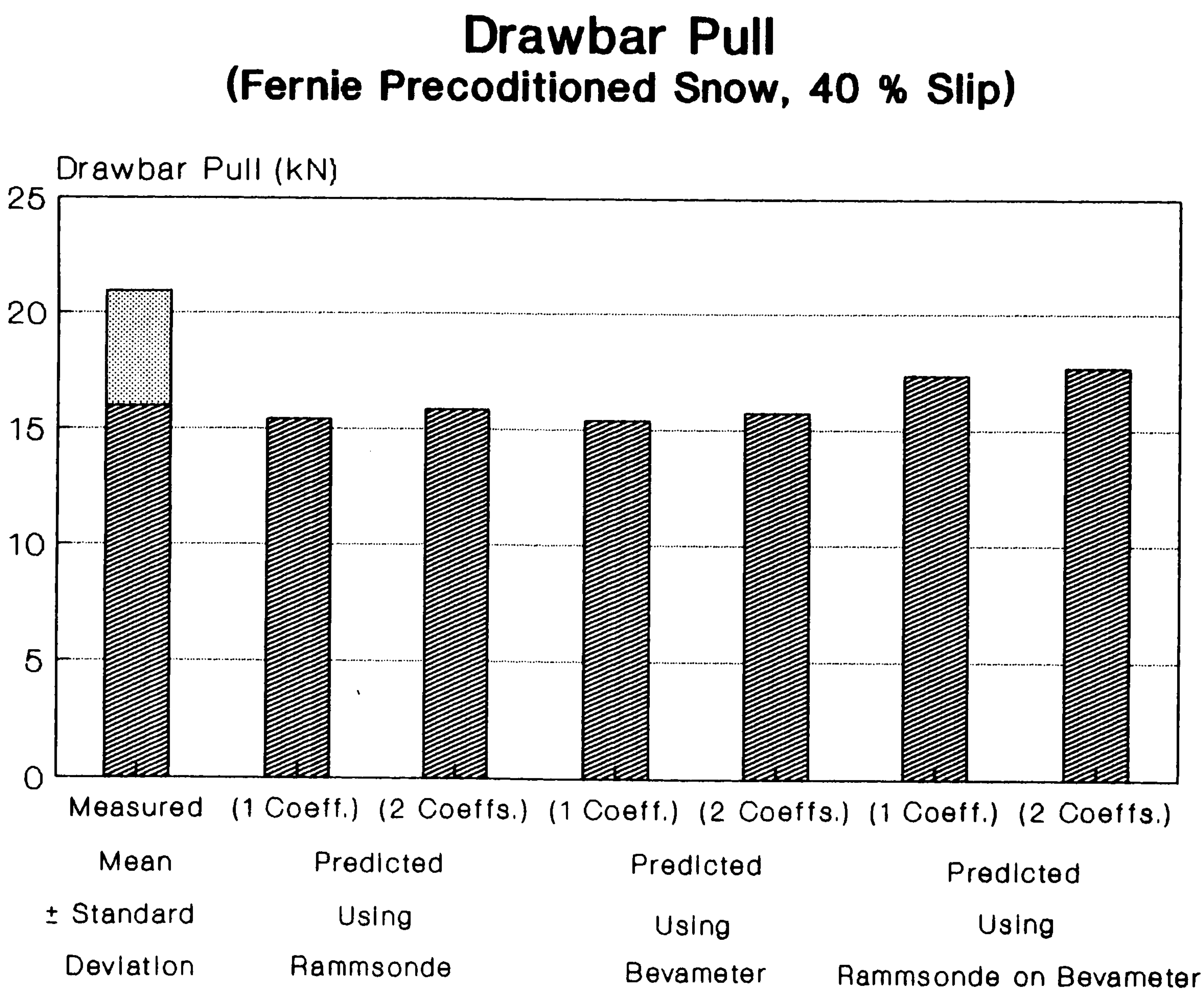

Fig. 4.3.9 Measured and predicted vehicle performance at 40% slip on preconditioned snow

5. CORRELATION STUDY OF THE MEASURED AND PREDICTED VEHICLE PERFORMANCE USING NTVPM-86

As mentioned in Chapter 3, the Nepean Tracked Vehicle Performance Model NTVPM currently has two versions, NTVPM-85 and NTVPM-86. In comparison with NTVPM-85, NTVPM-86 has a number of additional features. For instance, the characteristics of the independent suspension of the roadwheels are fully taken into account. The non-linear tension-elongation characteristics of the track link can also be accommodated. Furthermore, the algorithms of NTVPM-86 have been greatly improved.

To compare the predictive capabilities of the two versions of NTVPM, the performance of the test vehicle, BV 206, over the undisturbed and preconditioned snow in Fernie, British Columbia was predicted using NTVPM-86. In the predictions, the average values of the pressure-sinkage and shear strength parameters for the two types of snow were used.

5.1 Correlation of the Measured and Predicted Vehicle Performance on Undisturbed Snow

Using the average values of the pressure-sinkage parameters of n, k_c and k_ϕ shown in Table 4.2.3 and the average shear strength parameters, c, ϕ and K shown in Table 4.2.6, the performance of the test vehicle over undisturbed snow was predicted using NTVPM-86. The parameters of the test vehicle used as input to NTVPM-86 are given in Table 5.1.1.

Figures 5.1.1 - 5.1.3 show the relationships between the drawbar pull and slip for the test vehicle over undisturbed snow predicted using NTVPM-86 with the pressure-

Table 5.1.1 Vehicle input parameters for NTVPM-86

PREDICTION OF TRACKED VEHICLE PERFORMANCE
(MODEL: NTVPM-86)
VEHICLE SYSTEMS DEVELOPMENT CORPORATION
NEPEAN, ONTARIO, CANADA

January 9, 1991

VEHICLE TYPE	(Expt.)
VEHICLE PARAMETERS FOR THE FRONT UNIT:	
SPRUNG WEIGHT	23.56 KN
UNSPRUNG WEIGHT	4.50 KN
SPRUNG WEIGHT CENTRE OF GRAVITY X-COORDINATE	134.00 CM
SPRUNG WEIGHT CENTRE OF GRAVITY Y-COORDINATE	-20.97 CM
INITIAL TRACK TENSION	3.53 KN
DOUBLE PIVOT JOINT X-COORDINATE (AT THE REAR OF THE UNIT)	273.00 CM
DOUBLE PIVOT JOINT Y-COORDINATE (AT THE REAR OF THE UNIT)	3.00 CM
LENGTH OF THE INTERCONNECTING LINK	76.00 CM
LEADING PIVOT IS UNRESTRICTED	
TRAILING PIVOT IS UNRESTRICTED	

FIXED WHEELS

WHEEL RADIUS (CM)	X-COORDINATE OF WHEEL CENTRE (CM)	Y-COORDINATE OF WHEEL CENTRE (CM)	NOTES
19.00	.00	.00	SPROCKET

TORSION BAR SUSPENSION WHEELS

WHEEL RADIUS (CM)	TORSION ARM PIVOTS X-COORD. (+ IS TO THE REAR) (CM)	TORSION ARM PIVOTS Y-COORD. (+ IS DOWN) (CM)	TORSION BAR STIFFNESS (KN-M/DEG)	TORSION ARM ANGLES (+ IS CW FROM HORIZONTAL) REBOUND LIMIT (DEG)	FREE POSITION (DEG)	JOUNCE LIMIT (DEG)	TORSION ARM LENGTH (CM)	NOTES
19.00	28.00	7.00	.0530	89.00	76.00	15.00	25.00	T
19.00	68.00	20.00	.0530	89.00	43.00	-15.00	25.00	T
19.00	111.00	20.00	.0530	89.00	43.00	-15.00	25.00	T
19.00	155.00	20.00	.0530	89.00	43.00	-15.00	25.00	T
19.00	214.00	20.00	.0530	17.00	17.00	-20.00	20.00	T

NOTE: T = TRAILING ARM

NOTE: COORDINATE ORIGIN IS AT THE CENTRE OF THE SPROCKET. POSITIVE X- AND Y-COORDINATES ARE TO THE REAR AND DOWN, RESPECTIVELY.

Table 5.1.1 (continued)

(Expt.) January 9, 1991 Fernie Snow (RSC-2)

BELLY SHAPE	
WIDTH: 61.0 CM	
COORDINATES (CM)	
X	Y
-20.0	-3.0
-6.0	11.0
260.0	11.0

SUPPORTING ROLLERS	
RADIUS: 10.0 CM	
COORDINATES (CM)	
X	Y
128.0	2.0

TRACK LINK CONTACT AREA			
SINKAGE (CM)		INCRE-MENTAL AREA (CM**2)	PERCENTAGE CAUSING EXTERANL SHEARING
FROM	TO		
.00	.00	76.00	100.0
.00	1.40	64.00	.0
1.40	2.70	71.00	.0
2.70	5.50	351.00	.0

TRACK PARAMETERS FOR THE FRONT UNIT:

WEIGHT PER UNIT LENGTH	.330 KN/M
WIDTH	62.0 CM
PITCH	9.1 CM
HEIGHT OF THE GROUSERS	5.5 CM
THICKNESS	.0 CM
PERCENT EXTERNAL SHEAR AREA FOR COHESIVE SHEARING	13.5 %
LONGITUDINAL ELASTICITY CONSTANT TE (FROM T=TE*E)	10910. KN

NOTE: COORDINATE ORIGIN IS AT THE CENTRE OF THE SPROCKET. POSITIVE X- AND Y-COORDINATES ARE TO THE REAR AND DOWN, RESPECTIVELY.

Table 5.1.1 (continued)

(Expt.) January 9, 1991 Fernie Snow (RSC-2)

VEHICLE PARAMETERS FOR THE REAR UNIT:

SPRUNG WEIGHT	13.45 KN
UNSPRUNG WEIGHT	4.50 KN
SPRUNG WEIGHT CENTRE OF GRAVITY X-COORDINATE	105.00 CM
SPRUNG WEIGHT CENTRE OF GRAVITY Y-COORDINATE	-7.23 CM
INITIAL TRACK TENSION	4.69 KN
DOUBLE PIVOT JOINT X-COORDINATE (AT THE FRONT OF THE UNIT)	-29.00 CM
DOUBLE PIVOT JOINT Y-COORDINATE (AT THE FRONT OF THE UNIT)	3.00 CM
DRAWBAR HITCH X-COORDINATE	265.00 CM
DRAWBAR HITCH Y-COORDINATE	-2.00 CM

FIXED WHEELS

WHEEL RADIUS (CM)	X-COORDINATE OF WHEEL CENTRE (CM)	Y-COORDINATE OF WHEEL CENTRE (CM)	NOTES
19.00	.00	.00	SPROCKET

TORSION BAR SUSPENSION WHEELS

WHEEL RADIUS (CM)	TORSION ARM PIVOTS: X-COORD. (+ IS TO THE REAR) (CM)	TORSION ARM PIVOTS: Y-COORD. (+ IS DOWN) (CM)	TORSION BAR STIFFNESS (KN-M/DEG)	TORSION ARM ANGLES (+ IS CW FROM HORIZONTAL): REBOUND LIMIT (DEG)	FREE POSITION (DEG)	JOUNCE LIMIT (DEG)	TORSION ARM LENGTH (CM)	NOTES
19.00	28.00	7.00	.0530	89.00	76.00	15.00	25.00	T
19.00	68.00	20.00	.0530	89.00	43.00	-15.00	25.00	T
19.00	111.00	20.00	.0530	89.00	33.00	-15.00	25.00	T
19.00	155.00	20.00	.0530	89.00	24.00	-15.00	25.00	T
19.00	214.00	20.00	.0530	17.00	8.00	-20.00	20.00	T

NOTE: T = TRAILING ARM

NOTE: COORDINATE ORIGIN IS AT THE CENTRE OF THE SPROCKET. POSITIVE X- AND Y-COORDINATES ARE TO THE REAR AND DOWN, RESPECTIVELY.

Table 5.1.1 (continued)

(Expt.) January 9, 1991 Fernie Snow (RSC-2)

BELLY SHAPE	
WIDTH: 61.0 CM	
COORDINATES (CM)	
X	Y
-20.0	-3.0
-6.0	11.0
260.0	11.0

SUPPORTING ROLLERS	
RADIUS: 10.0 CM	
COORDINATES (CM)	
X	Y
128.0	2.0

TRACK LINK CONTACT AREA			
SINKAGE (CM) FROM	TO	INCRE-MENTAL AREA (CM**2)	PERCENTAGE CAUSING EXTERANL SHEARING
.00	.00	76.00	100.0
.00	1.40	64.00	.0
1.40	2.70	71.00	.0
2.70	5.50	351.00	.0

TRACK PARAMETERS FOR THE REAR UNIT:

WEIGHT PER UNIT LENGTH	.330 KN/M
WIDTH	62.0 CM
PITCH	9.1 CM
HEIGHT OF THE GROUSERS	5.5 CM
THICKNESS	.0 CM
PERCENT EXTERNAL SHEAR AREA FOR COHESIVE SHEARING	13.5 %
LONGITUDINAL ELASTICITY CONSTANT TE (FROM T=TE*E)	10910. KN

NOTE: COORDINATE ORIGIN IS AT THE CENTRE OF THE SPROCKET. POSITIVE X- AND Y-COORDINATES ARE TO THE REAR AND DOWN, RESPECTIVELY.

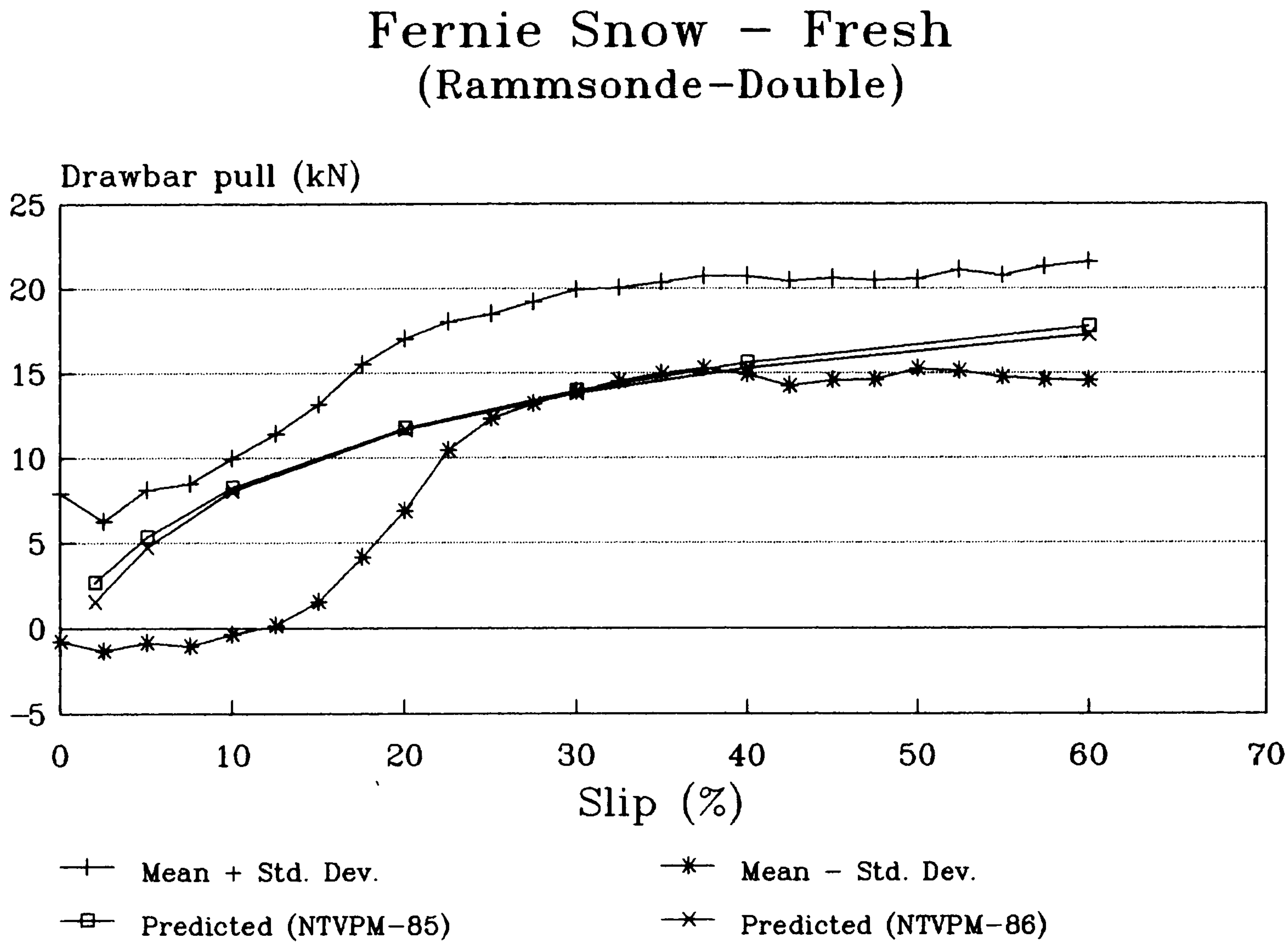

Fig. 5.1.1 Comparison of predictions by NTVPM-85 and NTVPM-86 on undisturbed snow

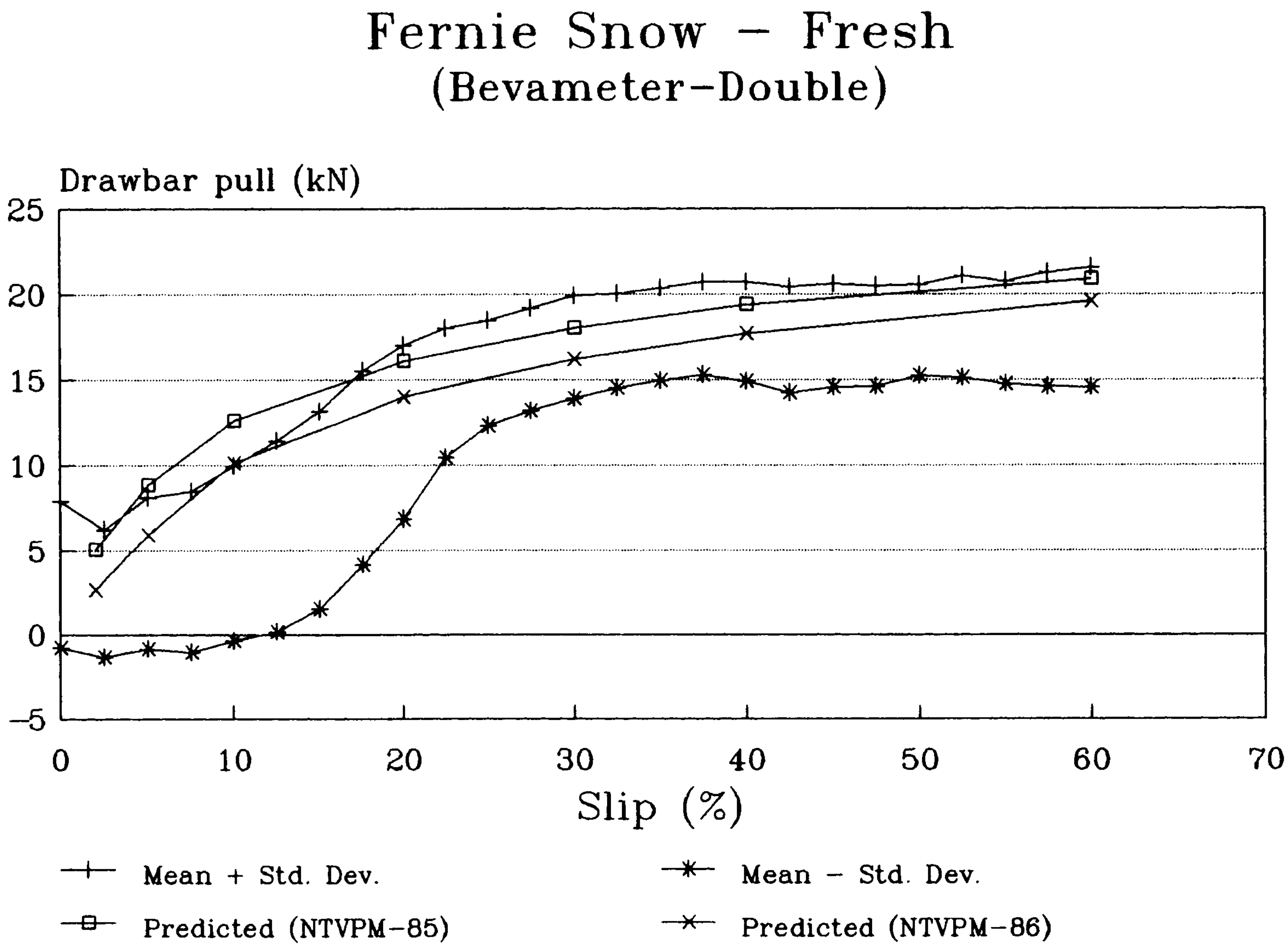

Fig. 5.1.2 Comparison of predictions by NTVPM-85 and NTVPM-86 on undisturbed snow

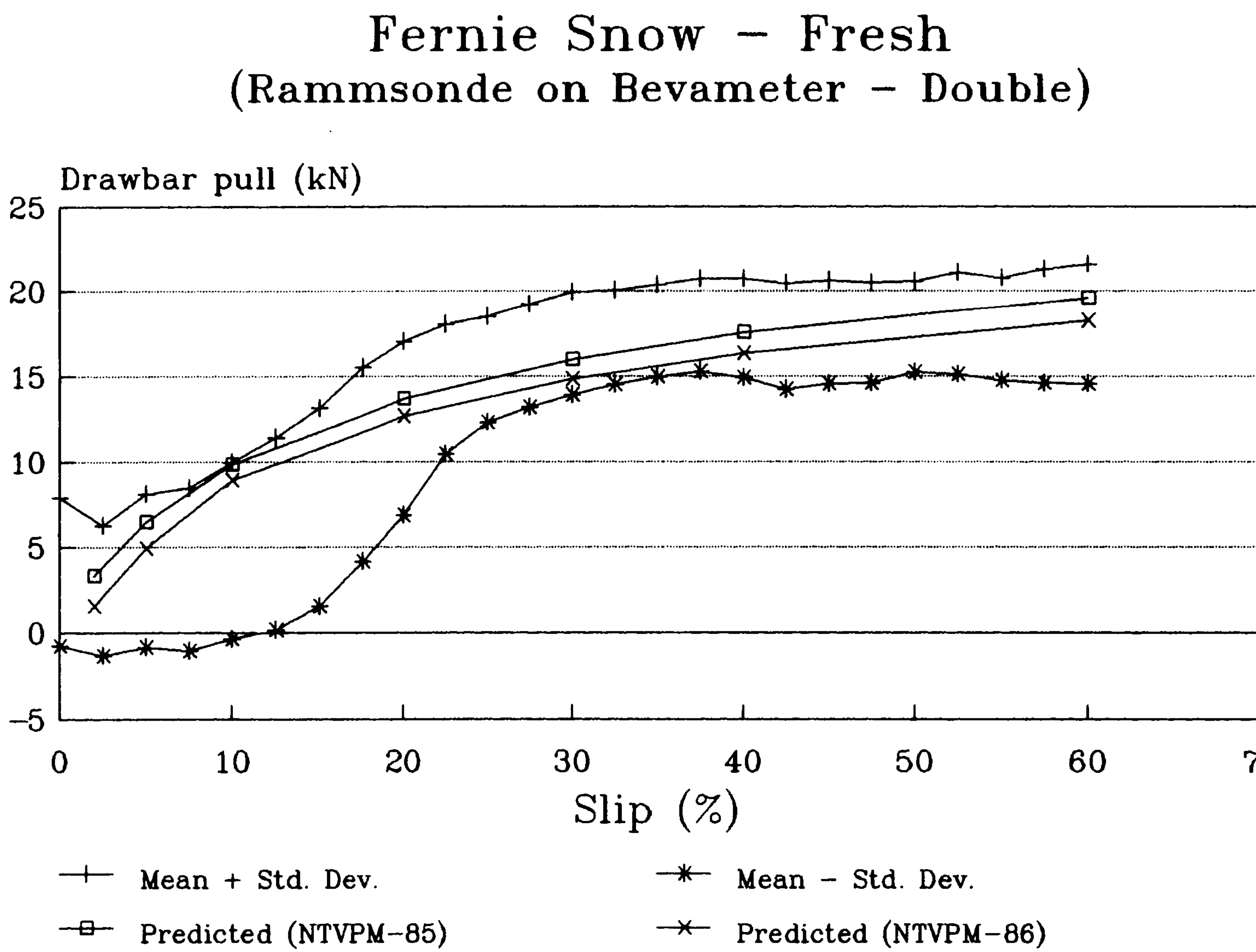

Fig. 5.1.3 Comparison of predictions by NTVPM-85 and NTVPM-86 on undisturbed snow

sinkage data obtained by the Rammsonde, the bevameter and the Rammsonde cone mounted on the bevameter assembly, respectively. In the figures, the performance predicted using NTVPM-85 and the measured one are also shown. Figures 5.1.4 - 5.1.6 and Table 5.1.2 show a comparison of the measured and predicted drawbar pull using NTVPM-85 and NTVPM-86 at slips of 20, 30 and 40%.

Figures 5.1.7 and 5.1.9 show the relationships between the drawbar pull and slip for the test vehicle over undisturbed snow predicted by NTVPM-86 using the average values of the pressure-sinkage parameters of n and k shown in Table 4.2.5 and shear strength parameters c, ϕ and K shown in Table 4.2.6. In the figures, the performance predicted using NTVPM-85 and the measured one are also shown. Figures 5.1.10 - 5.1.12 and Table 5.1.3 show a comparison of the measured and predicted drawbar pulls using NTVPM-85 and NTVPM-86 at slips of 20, 30 and 40%. Sample output from the simulation model NTVPM-86 is given in Appendix C.

It can be seen from the figures and tables that on undisturbed snow, NTVPM-86 provides improved predictions of the performance of the test vehicle in most cases, in comparison with NTVPM-85. For instance, from Table 5.1.3, it can be seen that using the Rammsonde data as input, the average error in the prediction of drawbar pull at slips of 20, 30 and 40%,with respect to the corresponding measured mean values, is 7.82% using NTVPM-86, as against 14.28% using NTVPM-85. Using the bevameter pressure-sinkage data as input, the average error in the prediction of drawbar pull at slips of 20, 30 and 40%, with respect to the corresponding measured mean values, is 8.2% using NTVPM-86, as against 11.37% using NTVPM-85. This is primarily due to the fact that NTVPM-86 provides a significant improvement in the modelling of the suspension system. Over undisturbed snow, the sinkage of the roadwheels was considerable. Therefore, better modelling of the vehicle suspension led to noticeable improvements in the prediction of the interacting forces on the track terrain interface, hence more realistic prediction of tractive performance.

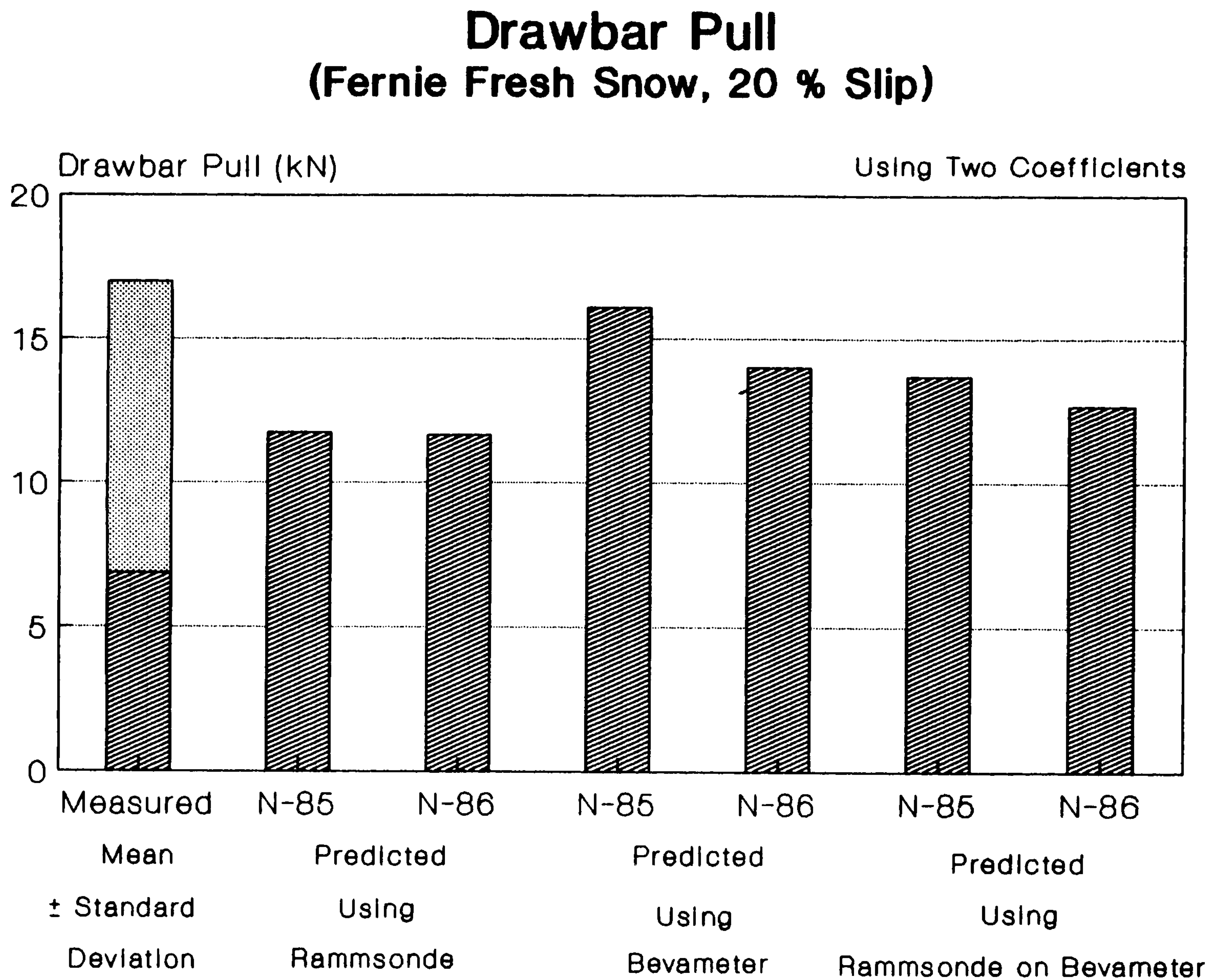

Fig. 5.1.4 Comparison of predicted vehicle performance by NTVPM-85 and NTVPM-86 at 20% slip on undisturbed snow

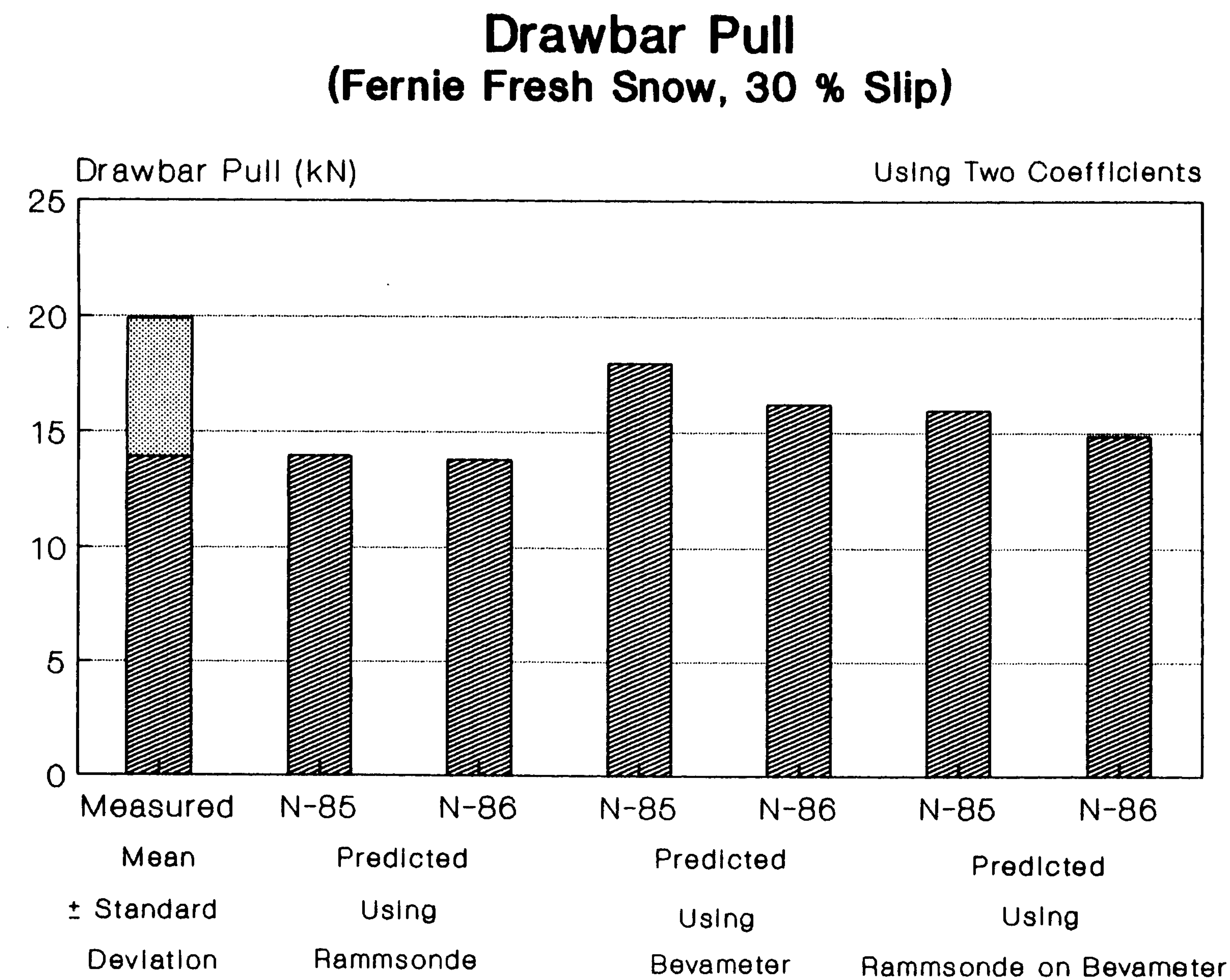

Fig. 5.1.5 **Comparison of predicted vehicle performance by NTVPM-85 and NTVPM-86 at 30% slip on undisturbed snow**

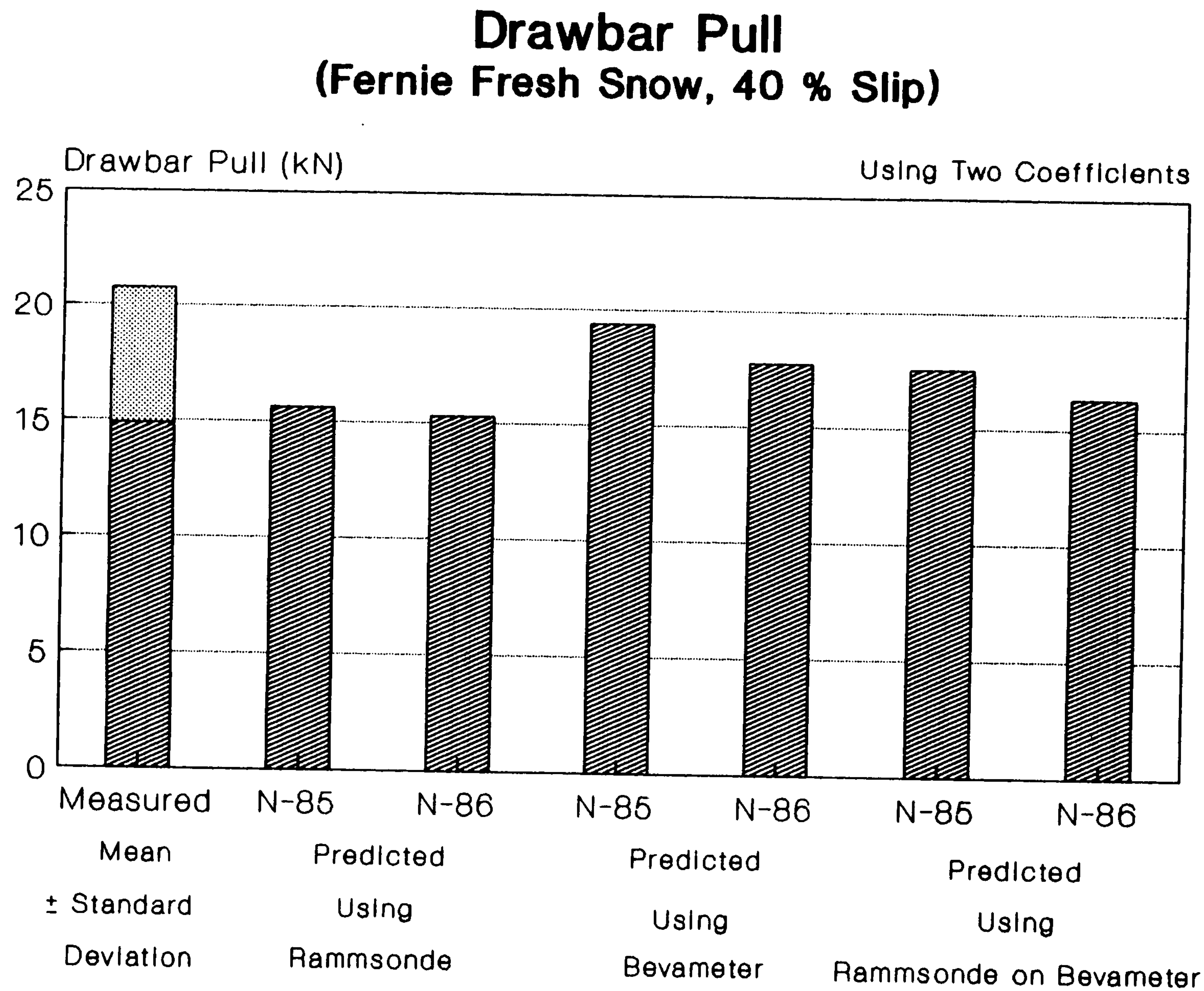

Fig. 5.1.6 Comparison of predicted vehicle performance by NTVPM-85 and NTVPM-86 at 40% on undisturbed snow

Table 5.1.2 **Comparison of the Measured Vehicle Drawbar Pull with the Predicted Ones for Undisturbed Snow (Using Equation: $p = (k_c/b + k_\phi) z^n$)**

Slip (%)	Drawbar Pull (kN)							
	Measured		Predicted					
	Mean	Standard Deviation	Using Rammsonde		Using Bevameter		Using Rammsonde on Bevameter	
			NTVPM -85	NTVPM -86	NTVPM -85	NTVPM -86	NTVPM -85	NTVPM-86
20	11.93	5.06	11.74	11.65	16.09	14.00	13.68	12.67
30	16.92	2.99	13.96	13.80	18.01	16.23	15.96	14.85
40	17.82	2.92	15.62	15.29	19.39	17.71	17.54	16.32

Fernie Snow - Fresh
(Rammsonde-Single)

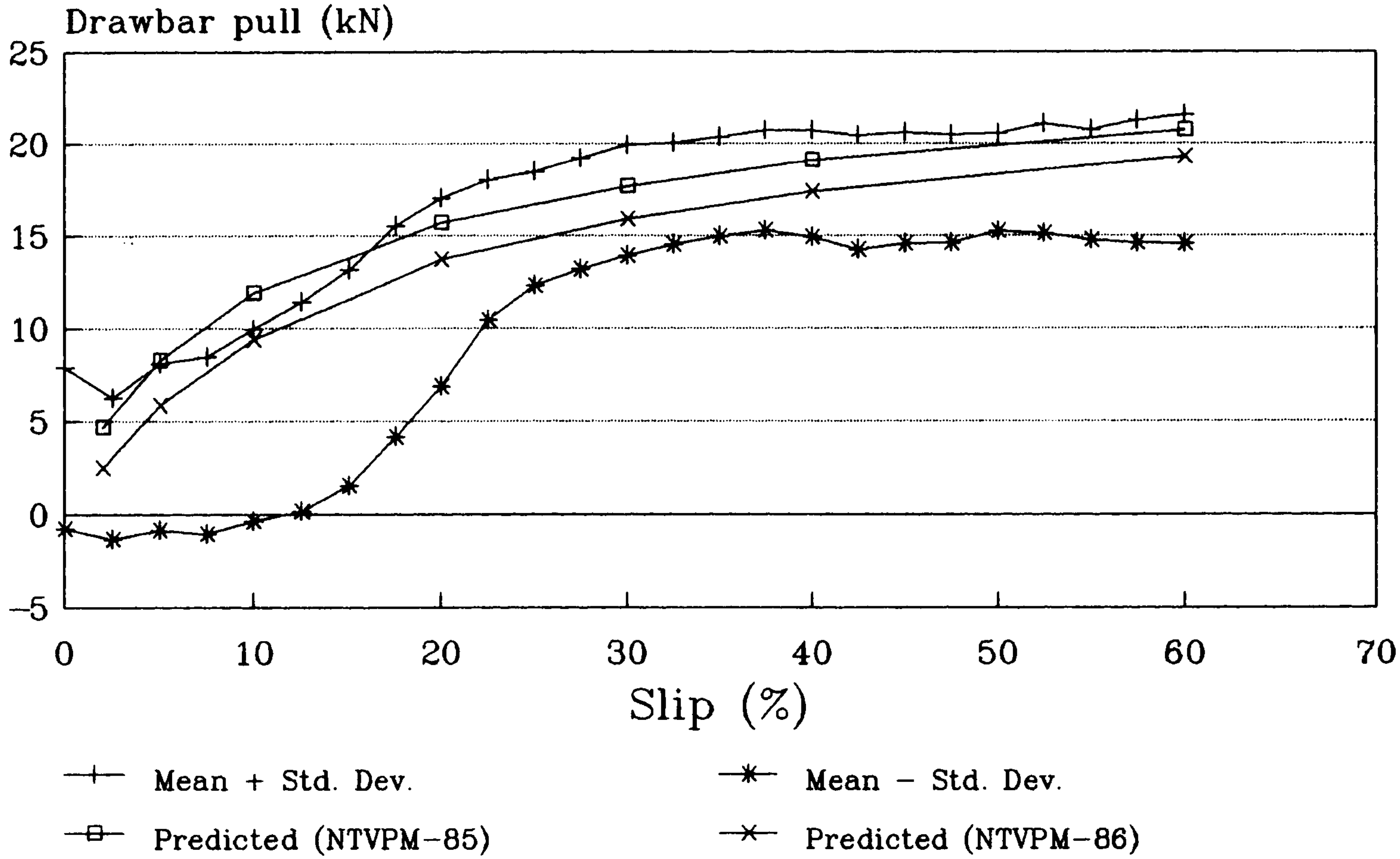

Fig. 5.1.7 Comparison of predictions by NTVPM-85 and NTVPM-86 on undisturbed snow

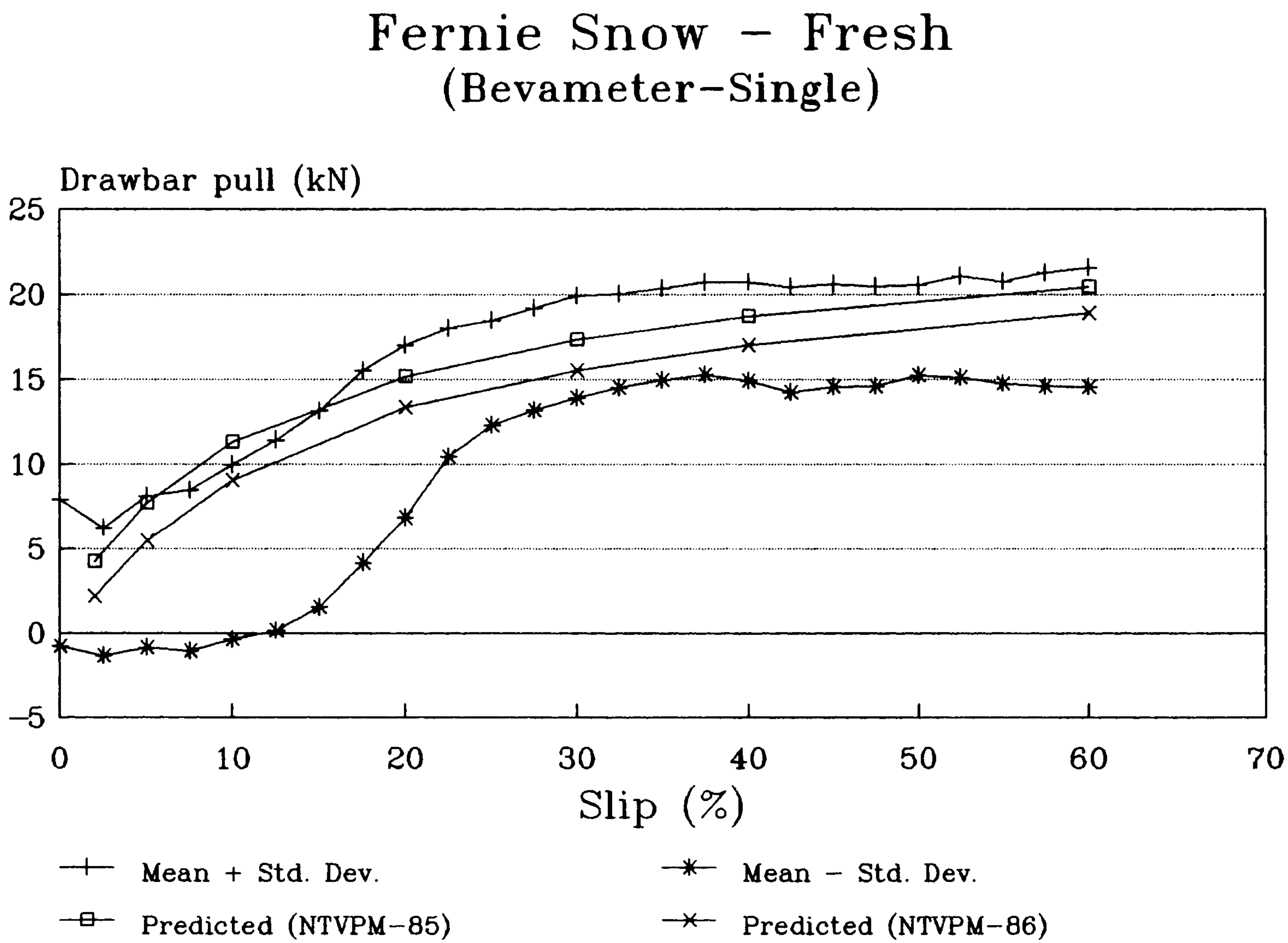

Fig. 5.1.8 Comparison of predictions by NTVPM-85 and NTVPM-86 on undisturbed snow

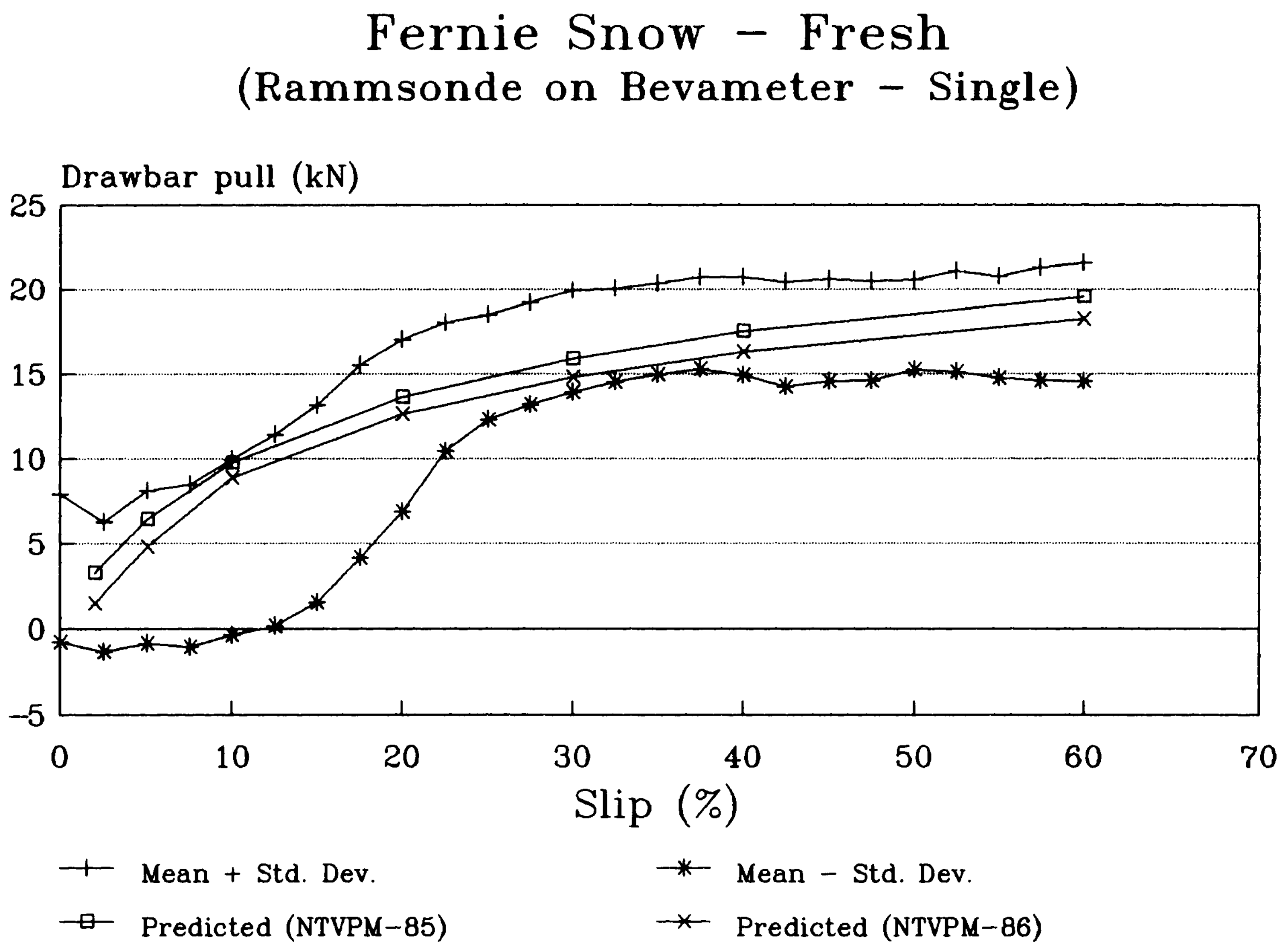

Fig. 5.1.9 Comparison of predictions by NTVPM-85 and NTVPM-86 on undisturbed snow

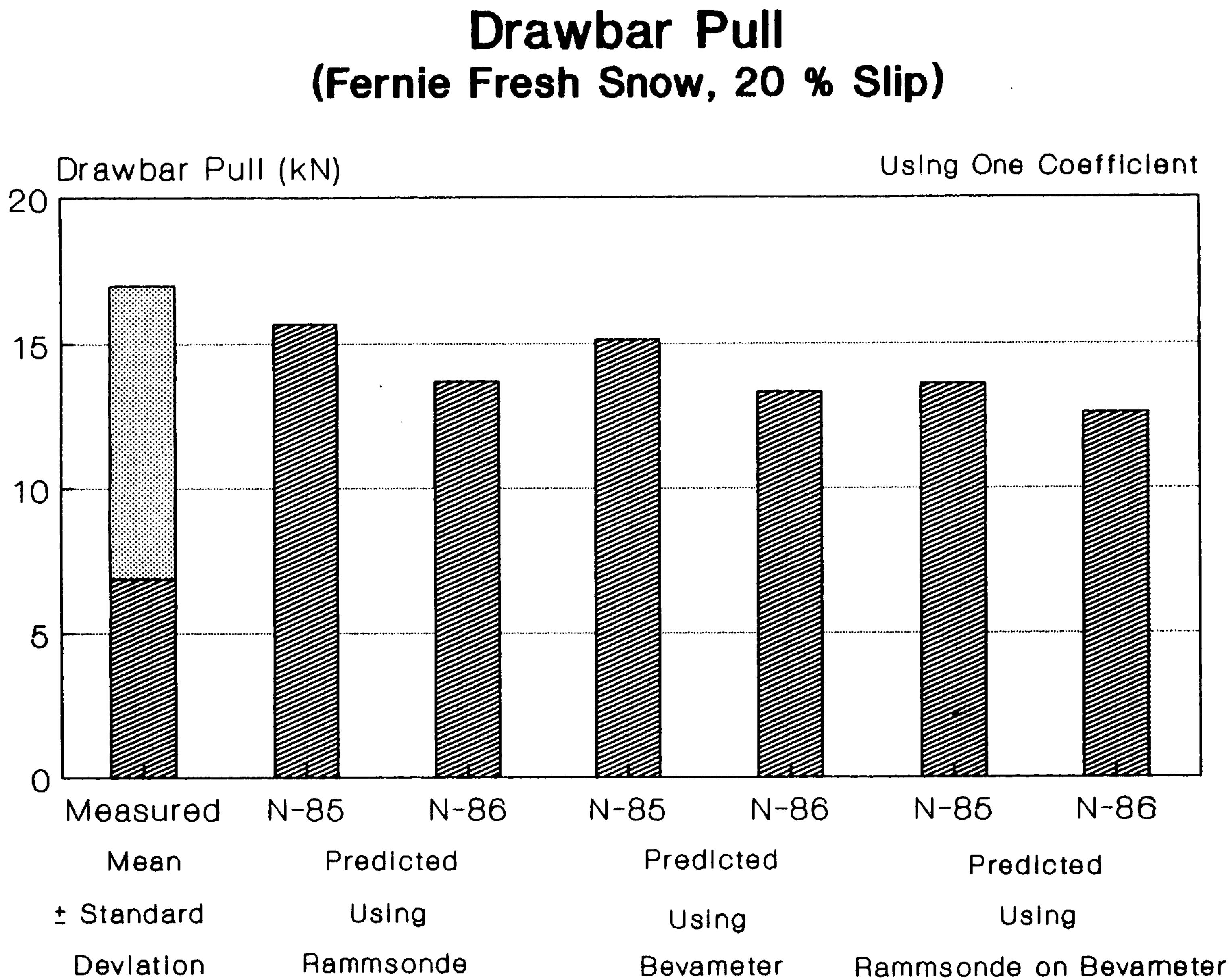

Fig. 5.1.10 Comparison of predicted vehicle performance by NTVPM-85 and NTVPM-86 at 20% slip on undisturbed snow

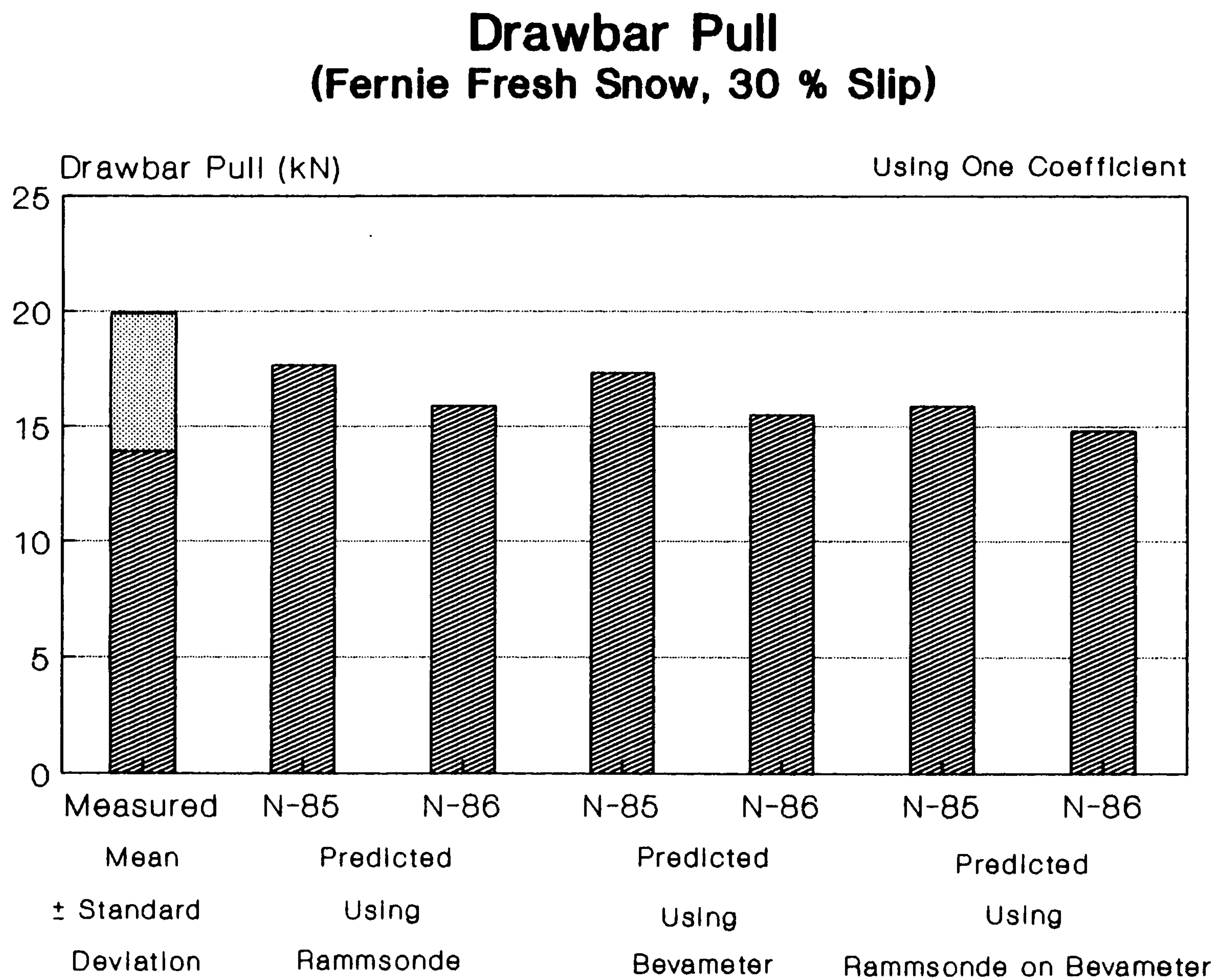

Fig. 5.1.11 Comparison of predicted vehicle performance by NTVPM-85 and NTVPM-86 at 30% slip on undisturbed snow

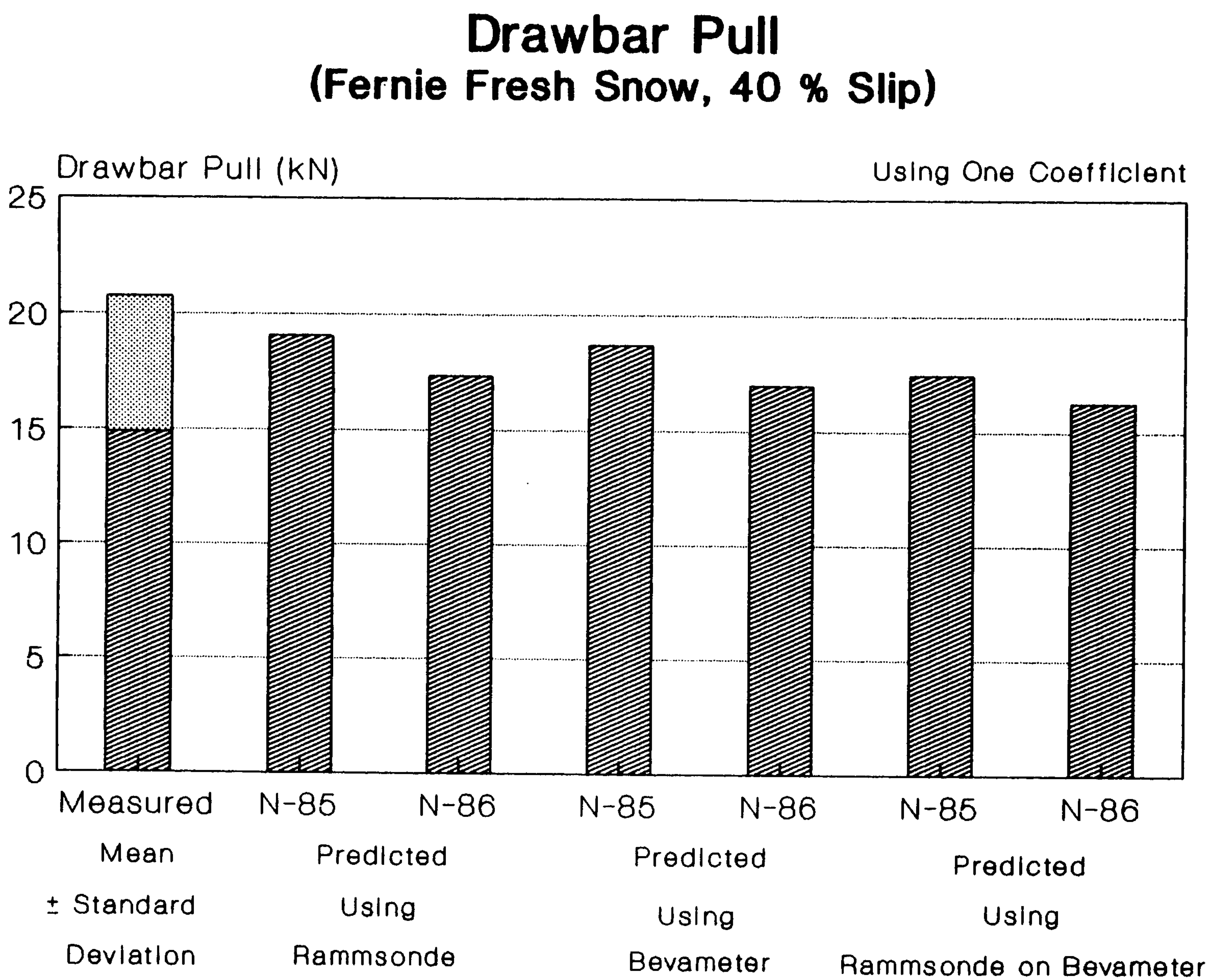

Fig. 5.1.12 Comparison of predicted vehicle performance by NTVPM-85 and NTVPM-86 at 40% slip on undisturbed snow

Table 5.1.3 Comparison of the Measured Vehicle Drawbar Pull with the Predicted Ones for Undisturbed Snow (Using Equation: $p = k z^n$)

Slip (%)	Drawbar Pull (kN)							
	Measured		Predicted					
	Mean	Standard Deviation	Using Rammsonde		Using Bevameter		Using Rammsonde on Bevameter	
			NTVPM -85	NTVPM -86	NTVPM -85	NTVPM -86	NTVPM -85	NTVPM-86
20	11.93	5.06	15.68	13.71	15.16	13.33	13.62	12.63
30	16.92	2.99	17.67	15.90	17.32	15.51	15.90	14.81
40	17.82	2.92	19.08	17.37	18.72	17.01	17.48	16.29

5.2 Correlation of the Measured and Predicted Vehicle Performance on Preconditioned Snow

Using the average values of the pressure-sinkage parameters of n, k_c and k_ϕ shown in Table 4.3.2 and average shear strength parameters, c, ϕ and K shown in Table 4.3.6, the performance of the test vehicle over preconditioned snow was predicted using NTVPM-86. Figures 5.2.1 - 5.2.3 show the relationships between the drawbar pull and slip for the test vehicle over preconditioned snow predicted using NTVPM-86 with the pressure-sinkage data obtained using the three devices. In the figures, the performance predicted using NTVPM-85 and the measured one are also shown. Figures 5.2.4 - 5.2.6 and Table 5.2.1 show a comparison of the measured and predicted drawbar pull using NTVPM-85 and NTVPM-86 at slips of 20, 30 and 40%.

Figures 5.2.7 - 5.2.9 show the relationships between the drawbar pull and slip for the test vehicle over preconditioned snow predicted by NTVPM-86 using the average values of the pressure-sinkage parameters of n and k shown in Table 4.3.4 and average shear strength parameters, c, ϕ and K shown in Table 4.3.6. In the figures, the performance predicted using NTVPM-85 and the measured one are also shown. Figures 5.2.10 - 5.2.12 and Table 5.2.2 show a comparison of the measured and predicted drawbar pulls using NTVPM-85 and NTVPM-86 at slips of 20, 30 and 40%. Sample output from the simulation model NTVPM-86 is given in Appendix D.

It can be seen from the figures and tables that over preconditioned snow while NTVPM-86 provides slightly better predictions than NTVPM-85, the difference in predictions made by the two versions of the simulation model is not very significant, in contrast with the situation over undisturbed snow. This is because after being compacted by a vehicle prior to testing, the preconditioned snow was firmer than the undisturbed snow. As a result, the sinkage of the vehicle was noticeably lower over preconditioned

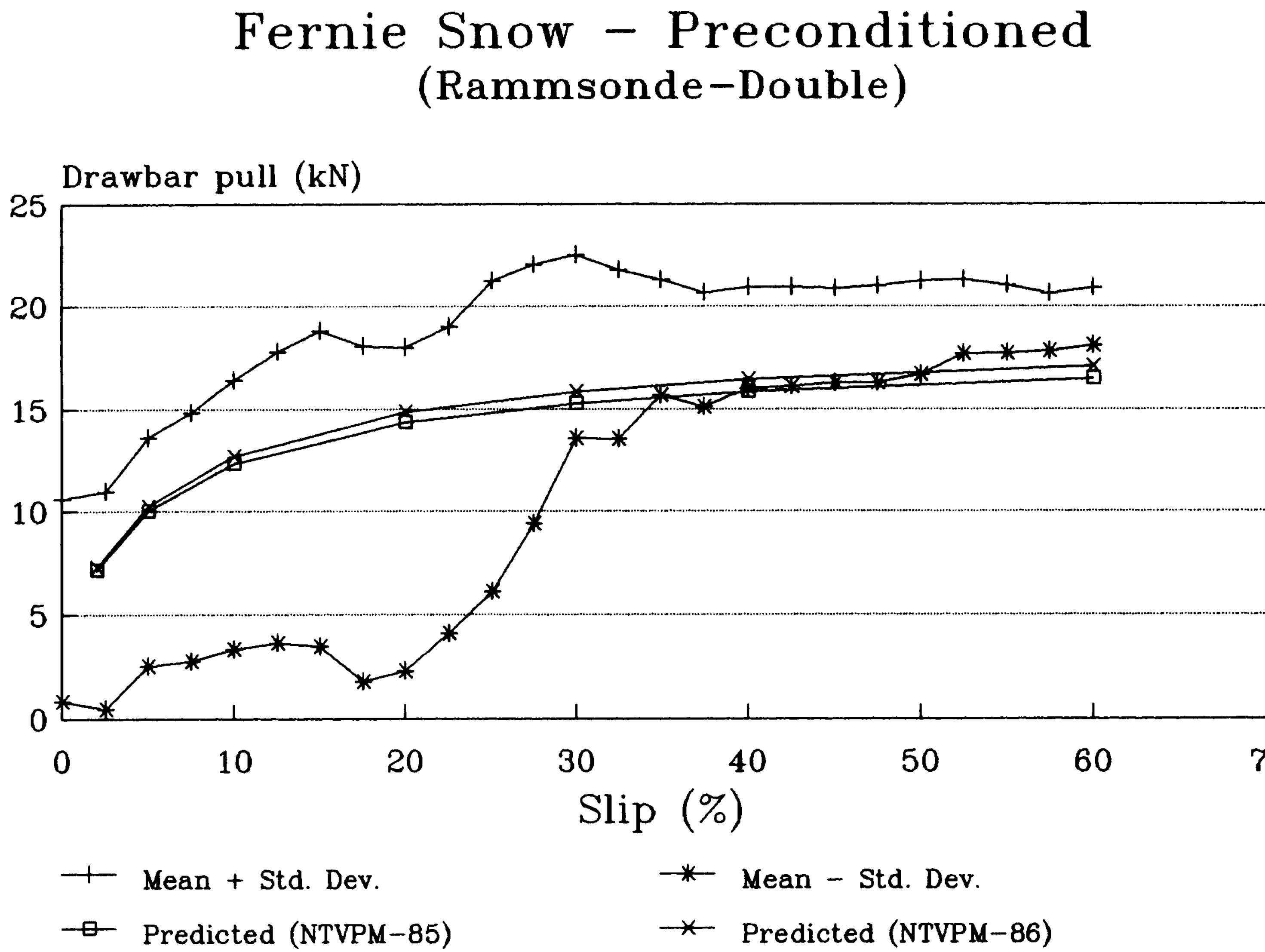

Fig. 5.2.1 Comparison of predictions by NTVPM-85 and NTVPM-86 on preconditioned snow

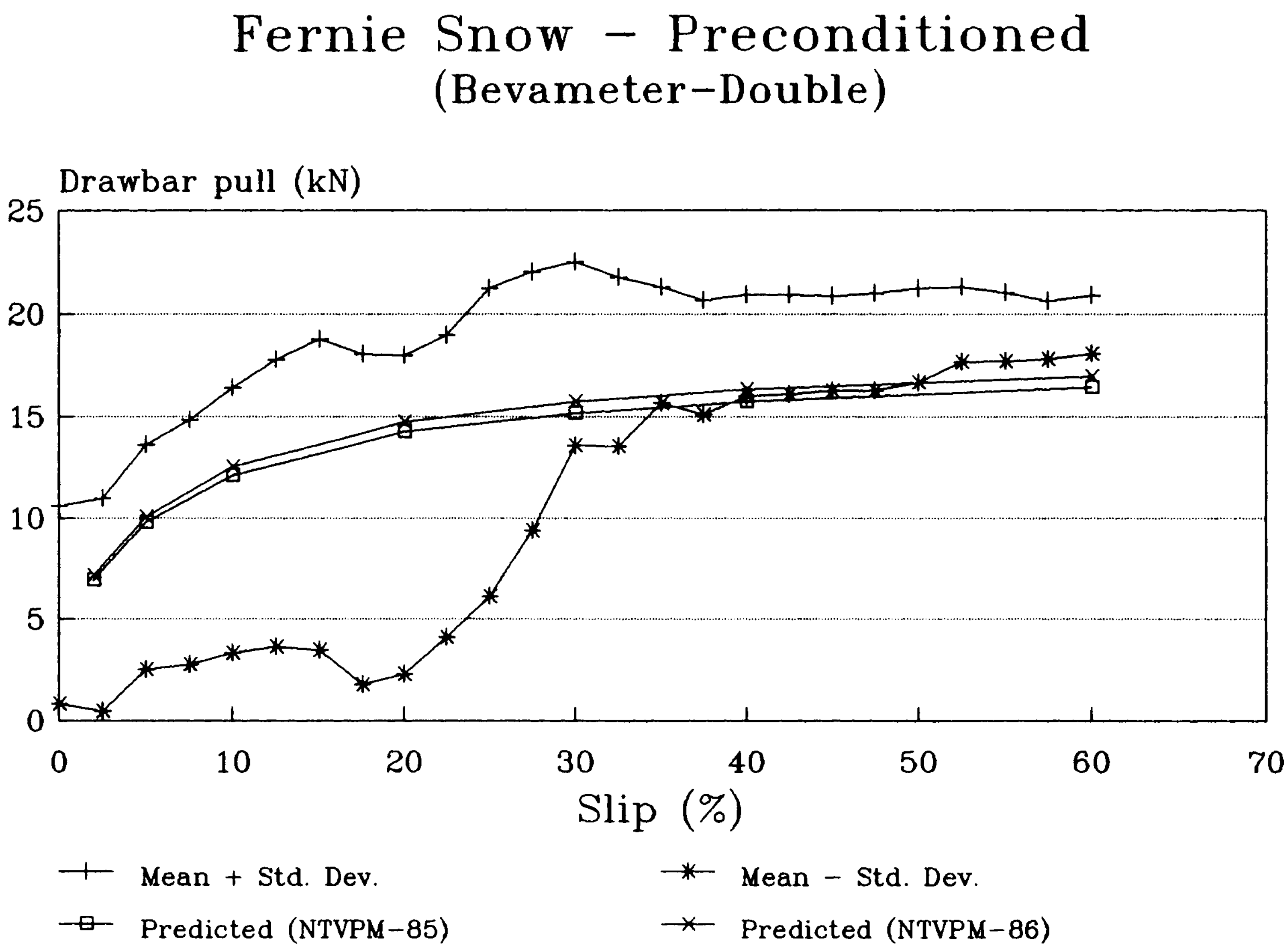

Fig. 5.2.2 Comparison of predictions by NTVPM-85 and NTVPM-86 on preconditioned snow

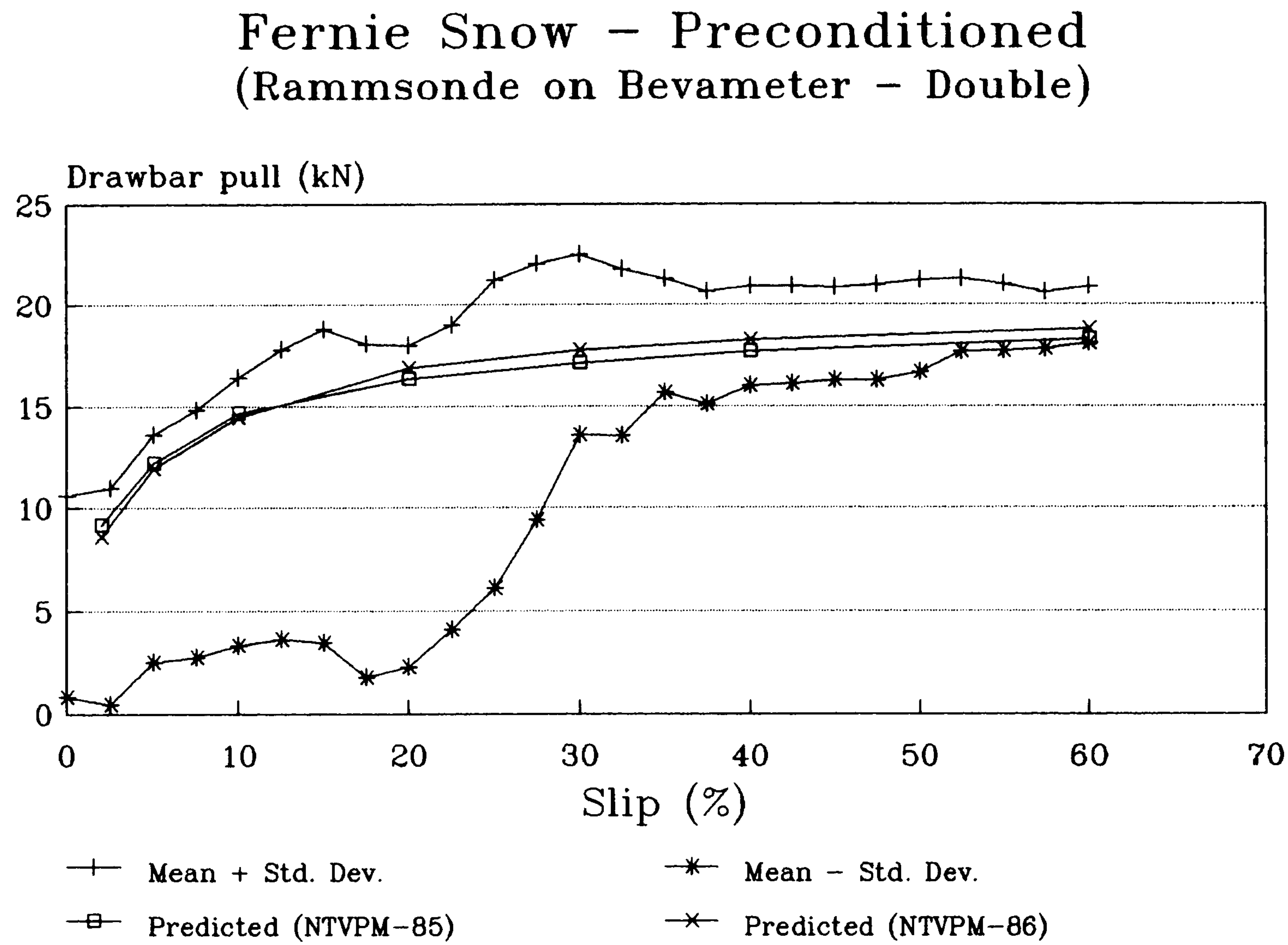

Fig. 5.2.3 Comparison of predictions by NTVPM-85 and NTVPM-86 on preconditioned snow

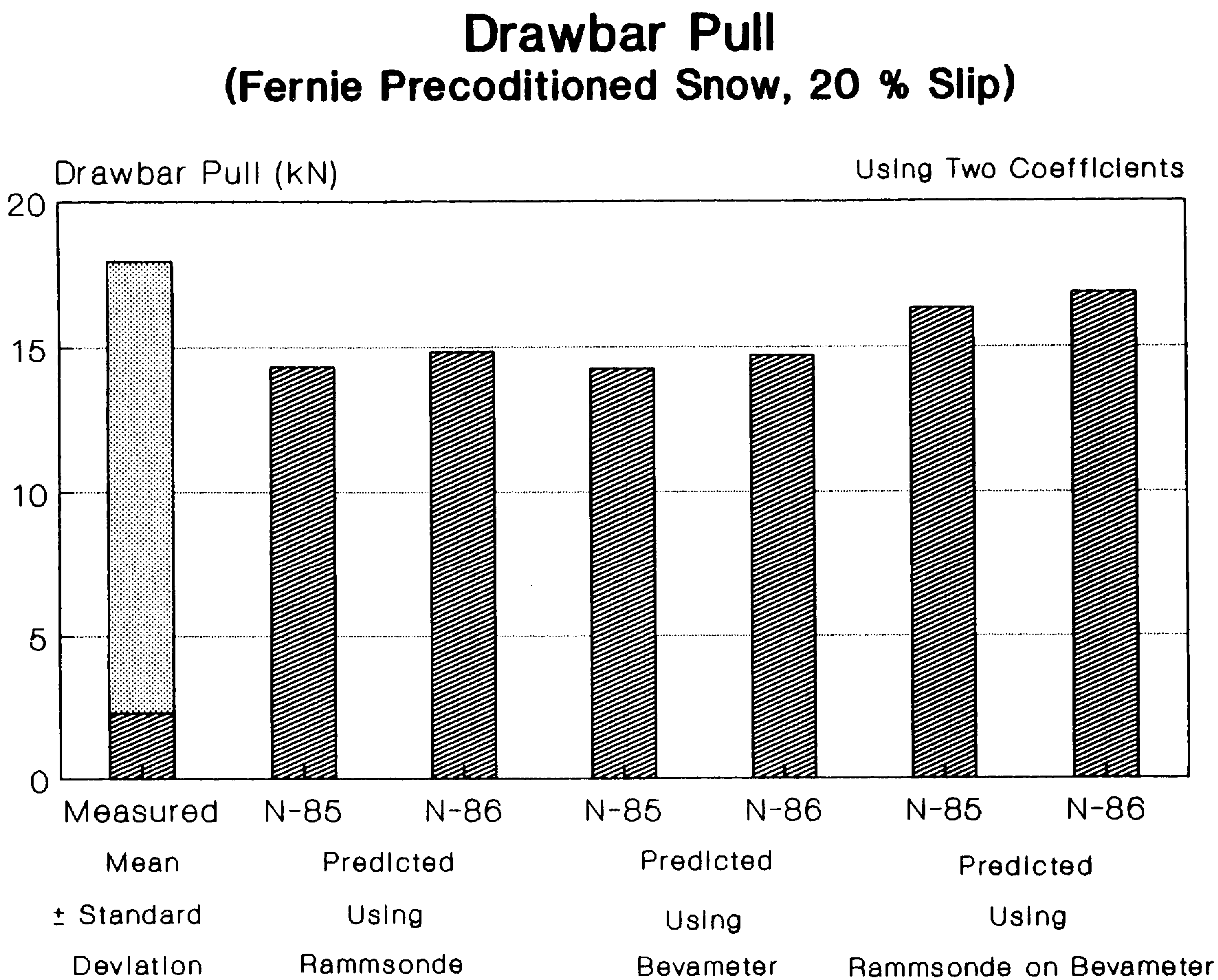

Fig. 5.2.4 Comparison of predicted vehicle performance by NTVPM-85 and NTVPM-86 at 20% slip on preconditioned snow

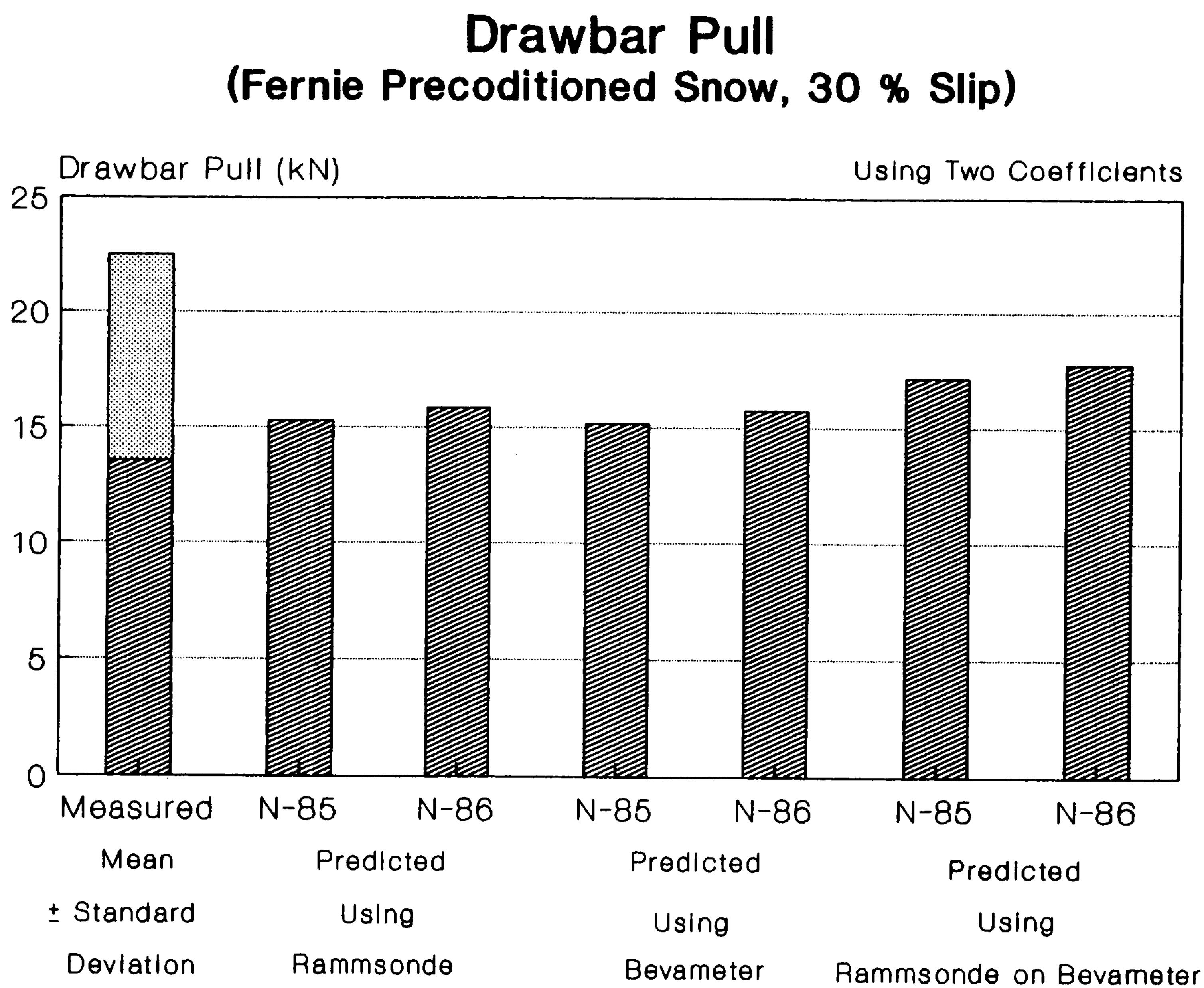

Fig. 5.2.5 Comparison of predicted vehicle performance by NTVPM-85 and NTVPM-86 at 30% slip on preconditioned snow

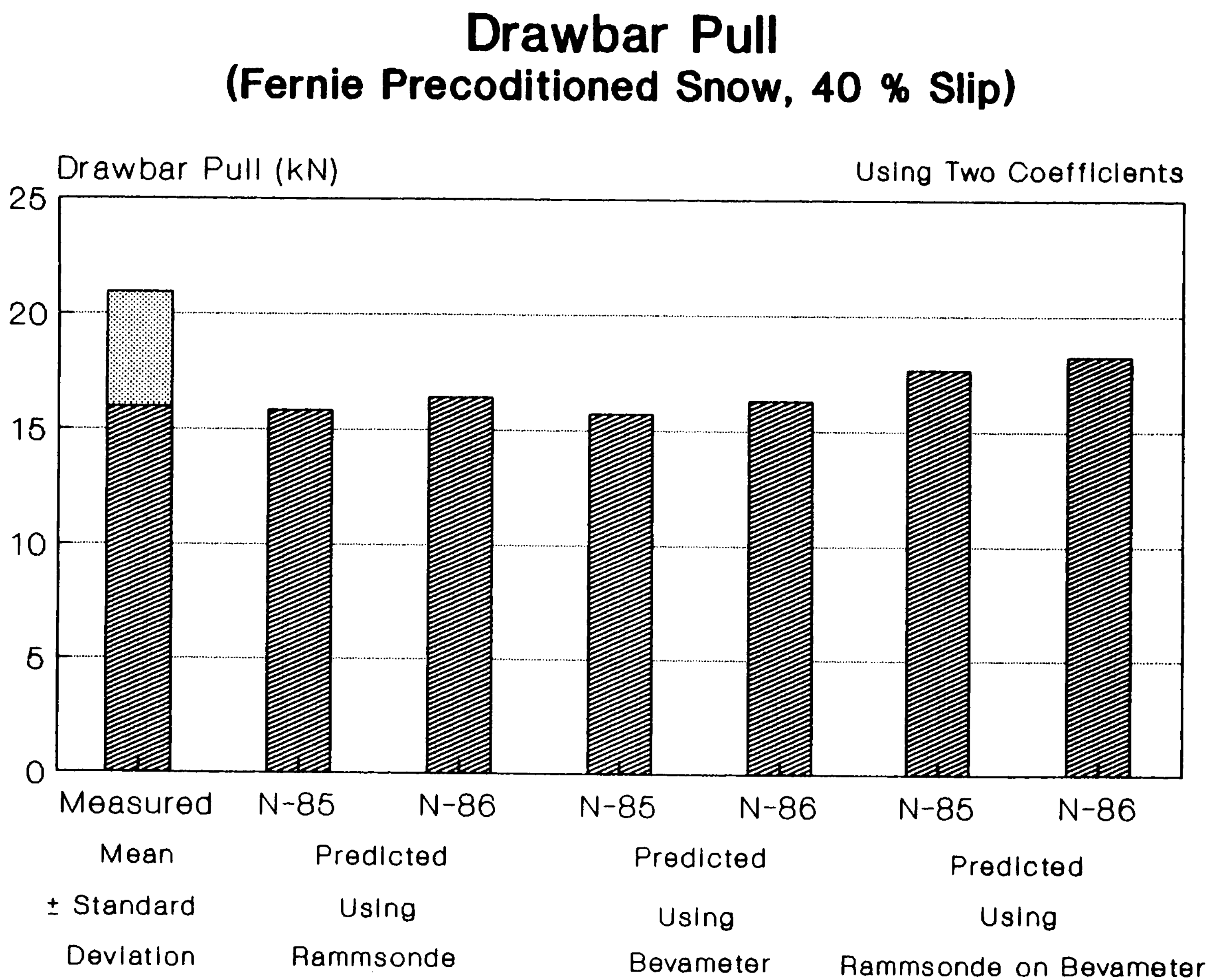

Fig. 5.2.6 Comparison of predicted vehicle performance by NTVPM-85 and NTVPM-86 at 40% slip on preconditioned snow

Table 5.2.1 **Comparison of the Measured Vehicle Drawbar Pull with the Predicted Ones for Preconditioned Snow (Using Equation: $p = (k_c/b + k_\phi) z^n$)**

Slip (%)	Drawbar Pull (kN)							
	Measured		Predicted					
	Mean	Standard Deviation	Using Rammsonde		Using Bevameter		Using Rammsonde on Bevameter	
			NTVPM -85	NTVPM -86	NTVPM -85	NTVPM -86	NTVPM -85	NTVPM-86
20	10.13	7.83	14.34	14.85	14.26	14.71	16.34	16.86
30	18.03	4.46	15.27	15.84	15.17	15.72	17.11	17.73
40	18.46	2.48	15.84	16.42	15.72	16.32	17.67	18.25

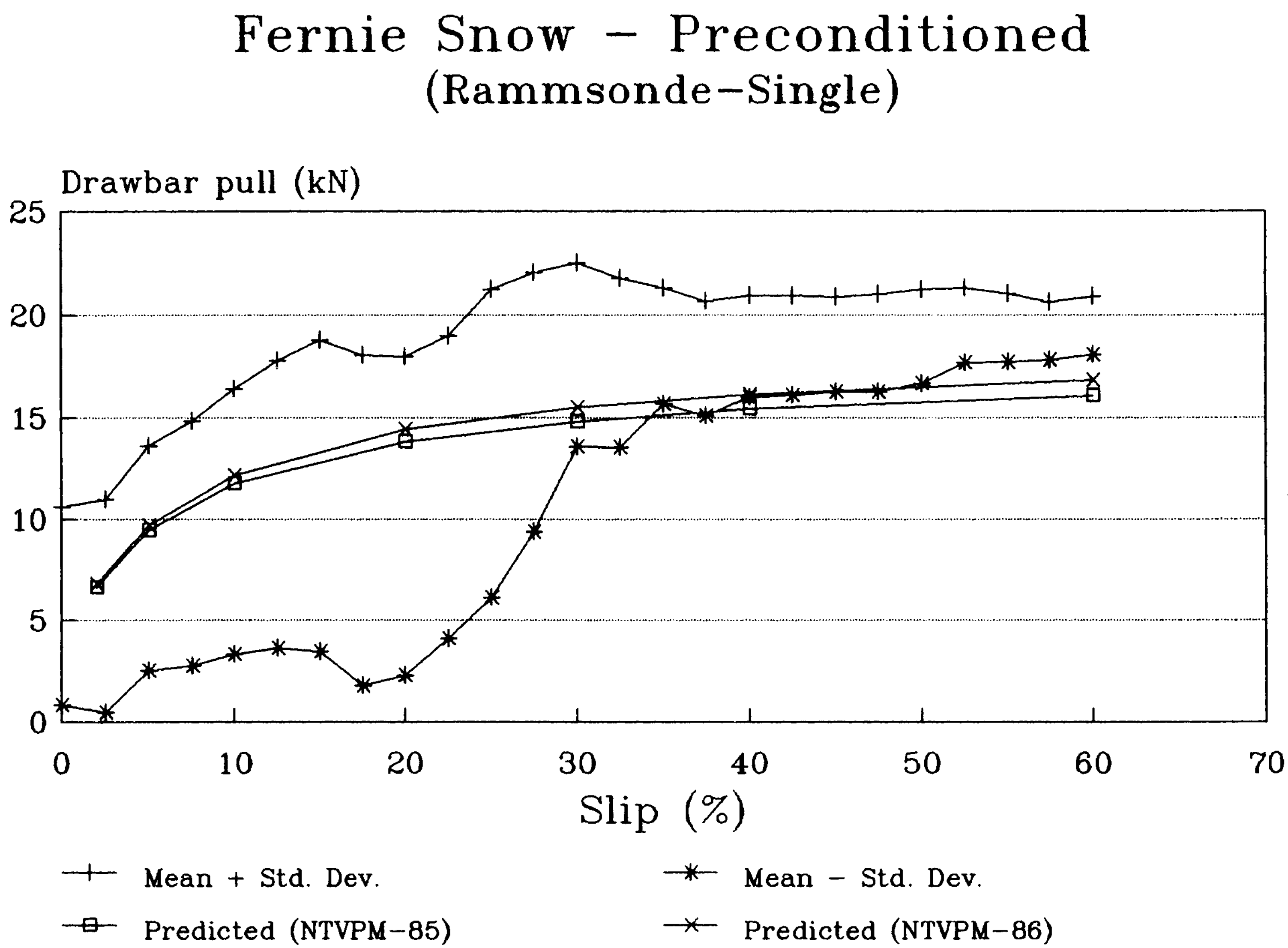

Fig. 5.2.7 Comparison of predictions by NTVPM-85 and NTVPM-86 on preconditioned snow

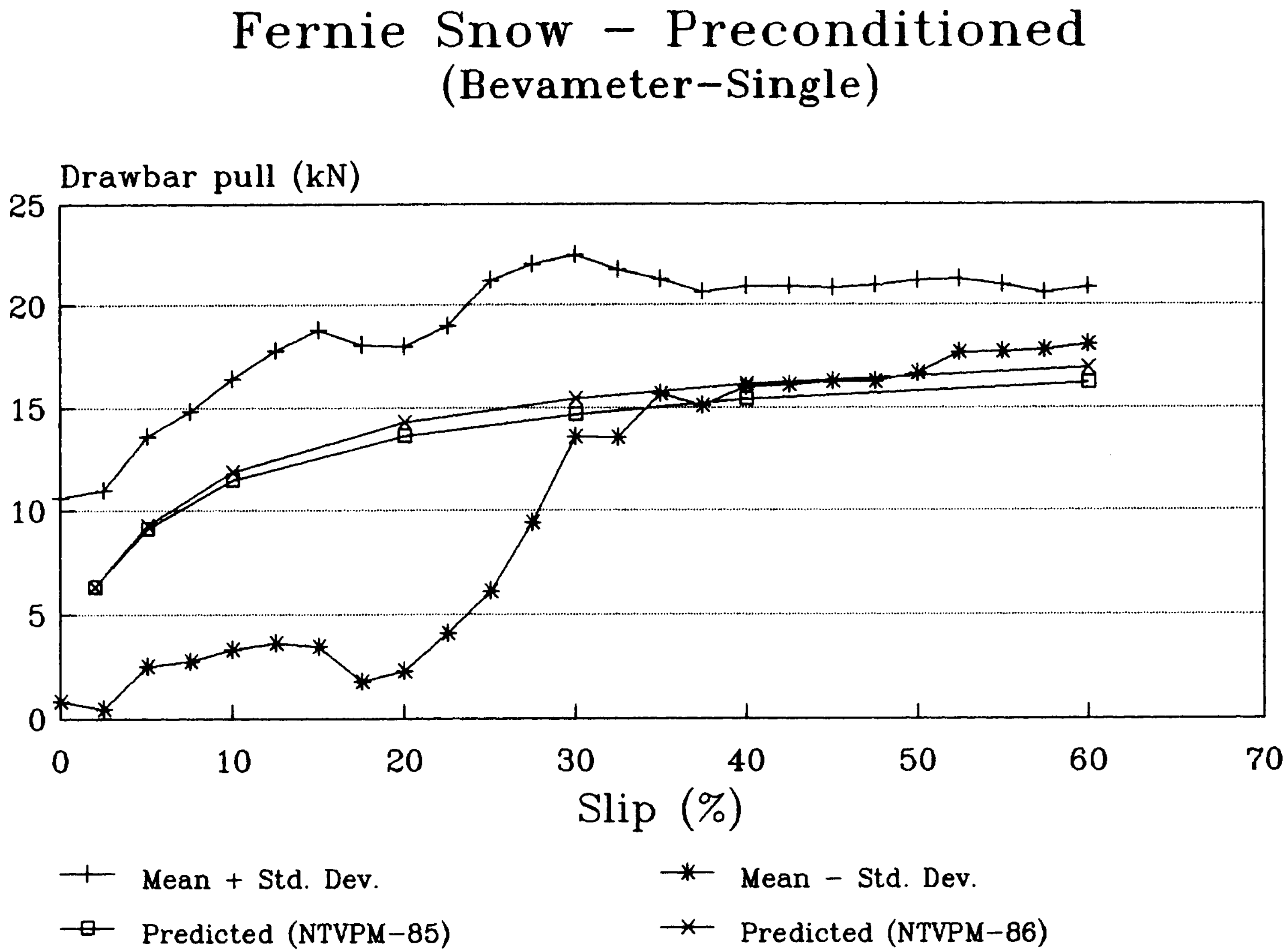

Fig. 5.2.8 Comparison of predictions by NTVPM-85 and NTVPM-86 on preconditioned snow

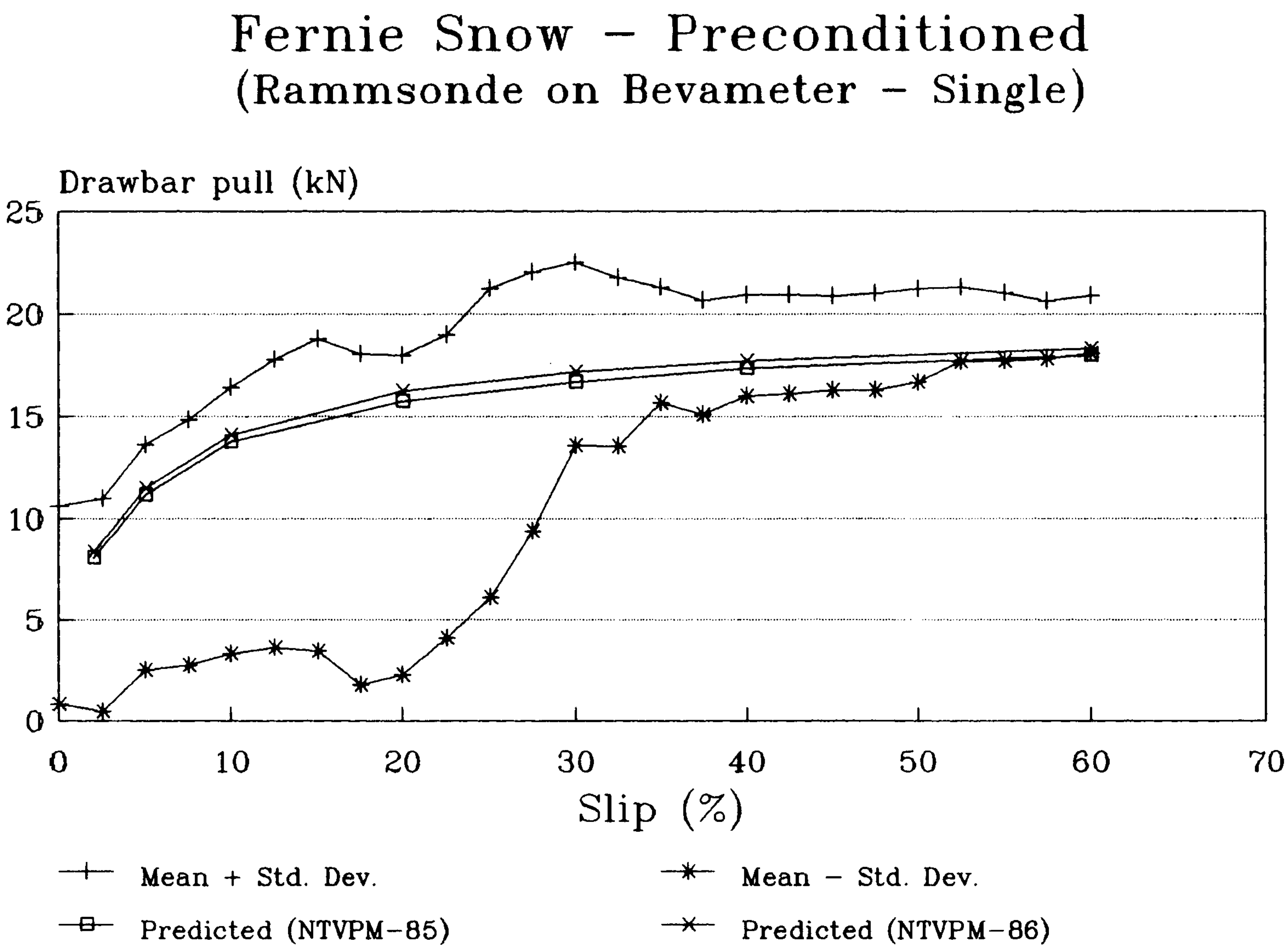

Fig. 5.2.9 Comparison of predictions by NTVPM-85 and NTVPM-86 on preconditioned snow

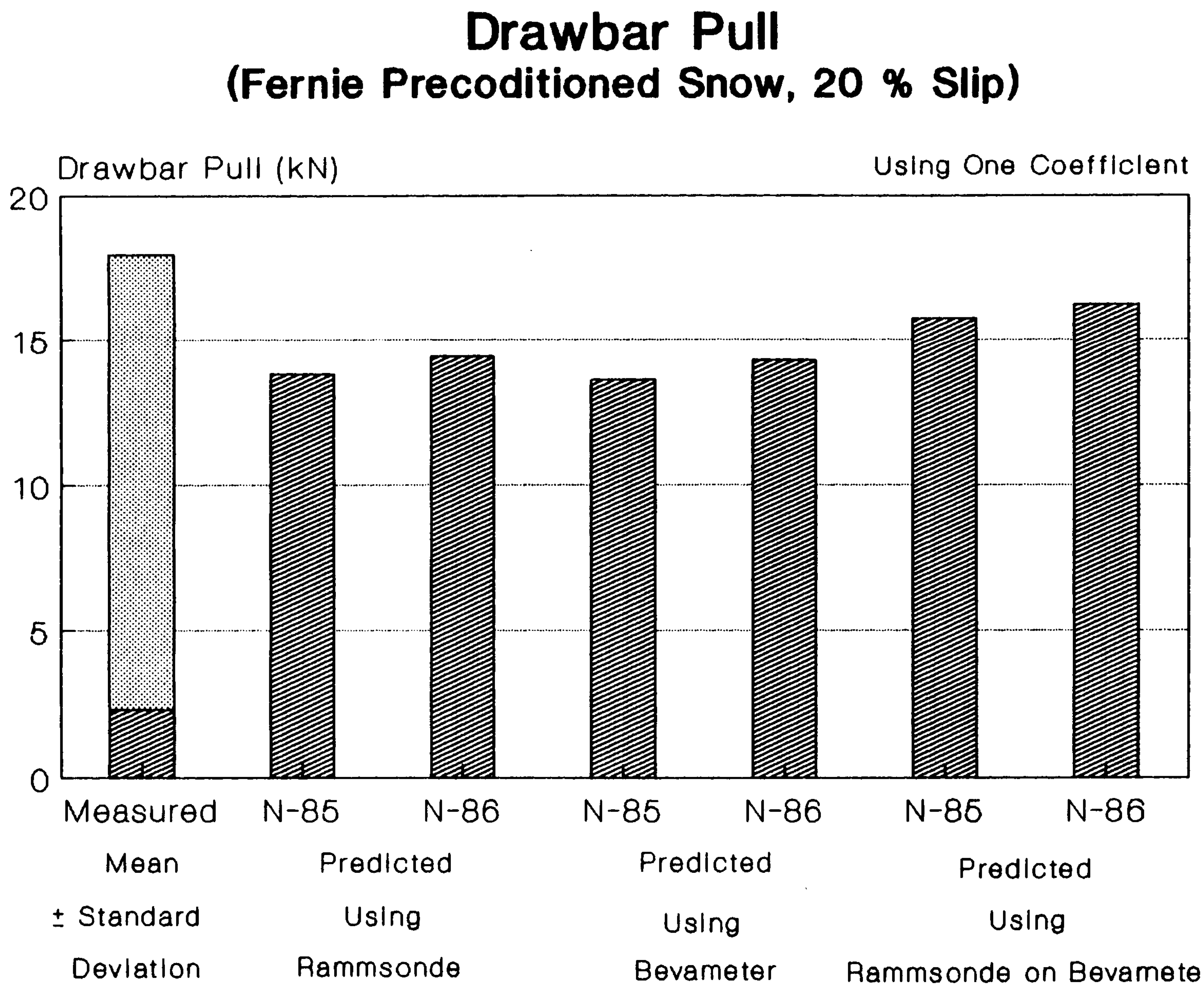

Fig. 5.2.10 Comparison of predicted vehicle performance by NTVPM-85 and NTVPM-86 at 20% slip on preconditioned snow

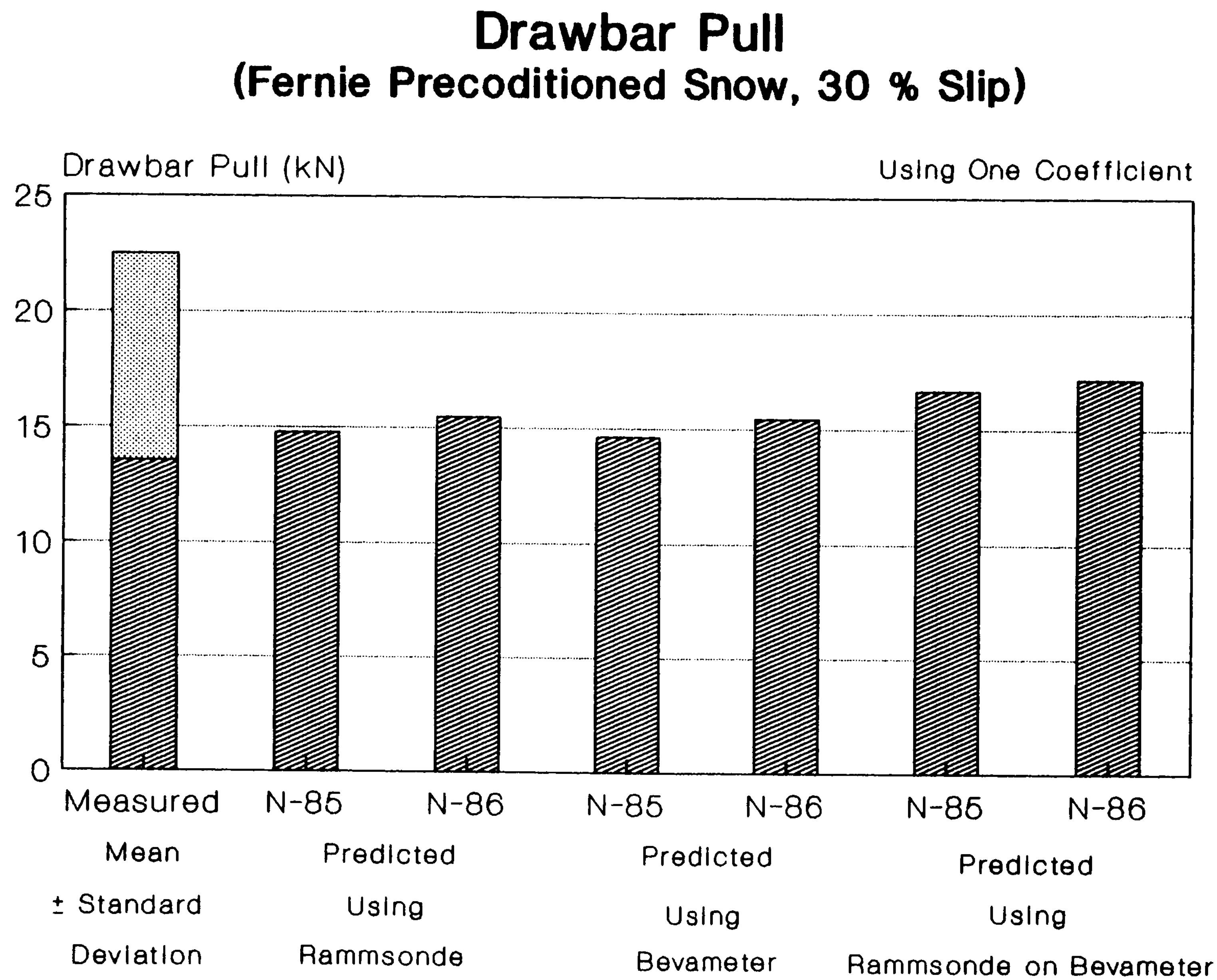

Fig. 5.2.11 Comparison of predicted vehicle performance by NTVPM-85 and NTVPM-86 at 30% slip on preconditioned snow

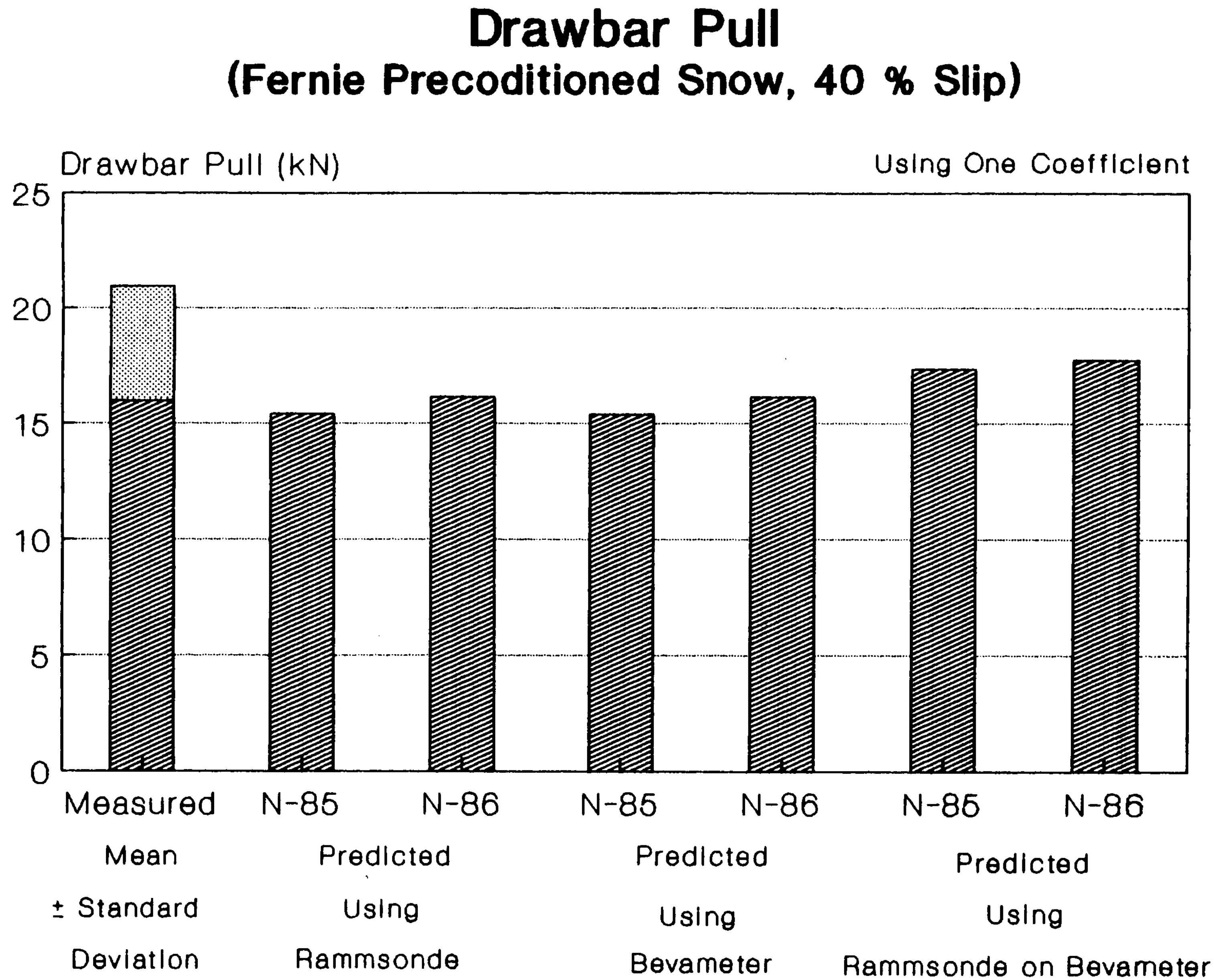

Fig. 5.2.12 Comparison of predicted vehicle performance by NTVPM-85 and NTVPM-86 at 40% slip on preconditioned snow

Table 5.2.2 **Comparison of the Measured Vehicle Drawbar Pull with the Predicted Ones for Preconditioned Snow (Using Equation: $p = k z^n$)**

Slip (%)	Drawbar Pull (kN)							
	Measured		Predicted					
	Mean	Standard Deviation	Using Rammsonde		Using Bevameter		Using Rammsonde on Bevameter	
			NTVPM -85	NTVPM -86	NTVPM -85	NTVPM -86	NTVPM -85	NTVPM-86
20	10.13	7.83	13.82	14.42	13.62	14.28	15.73	16.23
30	18.03	4.46	14.78	15.48	14.65	15.44	16.67	17.17
40	18.46	2.48	15.41	16.13	15.40	16.14	17.33	17.71

snow than over undisturbed snow. This indicates that the modelling technique of the suspension system does not have a significant effect on the results of prediction of tracked vehicle performance over firm terrain.

6. CONCLUSIONS

A. It is shown that on undisturbed snow in Fernie, British Columbia, the performance of a BV 206 predicted using the Nepean Tracked Vehicle Performance Model NTVPM-85, developed by Vehicle Systems Development Corporation, correlates very well with measured data obtained in the field.

Over snow that has been compacted by a single passage of the test vehicle prior to measurement (preconditioned snow), there is also a reasonable correlation between the measured vehicle performance and predicted one using NTVPM-85.

Taking into account the natural variation of terrain conditions in the field and the possible changes in snow conditions during the test period, due to changing atmospheric conditions, it can be concluded that the validity of the basic features of the computer simulation model NTVPM-85 have been further confirmed by the present study.

B. It is shown that predictions of vehicle performance made by NTVPM-85 using pressure-sinkage data obtained with the Rammsonde and with the bevameter are comparable. This confirms that the pressure-sinkage data for both the undisturbed and preconditioned snow obtained by the Rammsonde can be used as input to NTVPM-85 for predicting tracked vehicle performance over snow.

It is found that over undisturbed, fresh snow, the small Rammsonde cone of 4 cm in diameter could not be used to obtain meaningful pressure-sinkage data within a considerable range of snow depth. On undisturbed, fresh snow with density less than 0.2 g/cm^3, the use of the Rammsonde cone with diameter of 10 cm is, therefore, recommended. Over preconditioned snow, however, both the small Rammsonde cone of 4 cm in diameter and the large cone of 10 cm in diameter can be used to obtain pressure-sinkage data over a wide range of depth (Wong, 1990a).

C. It is shown that the latest version of the Nepean Tracked Vehicle Performance Model NTVPM-86, which takes into account fully the characteristics of roadwheel suspension system, provides improved predictions of tracked vehicle performance over snow where track sinkage is considerable.

7. RECOMMENDATIONS

A. Based on the results of this correlation study, it is proposed that the computer simulation model NTVPM-85, using pressure-sinkage data obtained by the Rammsonde (or the bevameter) and shear strength data obtained by a ring type shear device as input, be recommended to the NATO Panel II/GPE6 as an additional module to the existing NATO Reference Mobility model for predicting tracked vehicle performance over snow.

B. To provide the proposed module with the capabilities of comparing and evaluating the over snow performance of tracked vehicles on a common basis, it is recommended that the following sets of terrain data be incorporated into the module as an initial part of the database:

a) For pressure sinkage relationships (using equation: $p = k\ z^n$, where p is pressure and z is sinkage)

Parameters	Undisturbed Snow	Preconditioned Snow
n	0.72	0.61
k (kPa/m^n)	221	927

b) For shear strength (using equation: $s = (c + p \tan \phi)(1 - \exp(-j/K))$, where s is shear stress, p is normal pressure and j is shear displacement of the running gear)

Parameter	Undisturbed Snow		Preconditioned Snow	
	Internal	Rubber-snow	Internal	Rubber-snow
c (kPa)	1.96	0.21	0.32	0.02
ϕ (degrees)	25	11.4	29.4	12.0
K (m)	5.5	0.4	2.5	0.4

As more data on the mechanical properties of different kinds of snow become available, they can be incorporated to form a more comprehensive database for the module.

8 REFERENCES

1. Bekker, M.G., 1956, "Theory of Land Locomotion", The University of Michigan Press.
2. Bekker, M.G., 1969, "Introduction to Terrain-Vehicle Systems", The University of Michigan Press.
3. Chen, S.T. and Wong, J.Y., 1990, "User's guide to the VSDC terrain data analysis software (TDAS)", unpublished report prepared for Vehicle Mobility Section, Defence Research Establishment Suffield, Canadian Department of National Defence.
4. Garber, M. and Wong, J.Y., 1981, "Prediction of ground pressure distribution under tracked vehicles, Parts I and II", Journal of Terramechanics, Vol. 18, No. 1, pp. 1-23 and No. 2, pp. 71-79.
5. Hettiaratchi, D.R.P. and Reece, A.R., 1974, "The calculation of passive soil resistance", Geotechnique, Vol. 24, No. 3, pp. 289-310.
6. Karafiath, L.L. and Nowatzki, E.A., 1978, "Soil Mechanics for Off-Road Vehicle Engineering", Trans Tech Publications, Clausthal, Germany.
7. Karafiath, L.L., 1984, "Finite element analysis of ground deformation beneath moving track loads", Proceedings of the 8th International Conference of the International Society for Terrain-Vehicle Systems, Vol. 1, pp. 277-290.
8. Mining Resource Engineering Limited, 1990, "Validation of a model for track performance in a variety of snow conditions as a module to NATO Reference Mobility Model", unpublished report prepared for Vehicle Mobility Section, Defence Research Establishment Suffield, Canadian Department of National Defence.
9. Rowland, D., 1972, "Tracked vehicle ground pressure and its effect on soil ground performance", Proceedings of the 4th International Conference of the International Society for Terrain-Vehicle Systems, Vol. 1, pp. 353-384.

10. Rula, A.A. and Nuttall, C.J., 1971, "An analysis of ground mobility models (ANAMOB)", Technical Report M-71-4, U.S. Army Engineer Waterways Experiment Station, Vicksburg, Mississippi.

11. Wong, J.Y., 1967, "Behaviour of soil beneath rigid wheels", Journal of Agricultural Engineering Research, Vol. 12, No. 4, pp. 257-269.

12. Wong, J.Y., 1977, "Discussion of 'Prediction of wheel-soil interaction and performance using the finite element method' by Yong and Fattah", Journal of Terramechanics, Vol. 14, No. 4, pp. 249-250.

13. Wong, J.Y., 1978, "Theory of Ground Vehicles", John Wiley, New York. (Russian edition published by Machinostroenie Publishing House, Moscow, U.S.S.R., 1982; Chinese edition published by Machinery Industry Publishing House, Beijing, China, 1985).

14. Wong, J.Y., 1979, "Discussion on 'Soil Mechanics for Off-Road Vehicle Engineering' by Karafiath and Nowatzki", Canadian Geotechnical Journal, Vol. 16, No. 3, pp. 624-626; also Journal of Terramechanics, Vol. 16, No. 4, pp. 191-194.

15. Wong, J.Y., 1980, "Data processing methodology in the characterization of the mechanical properties of terrain", Journal of Terramechanics, Vol. 17, No. 1, pp. 13-41.

16. Wong, J.Y., 1986a, "Computer-aided analysis of the effects of design parameters on the performance of tracked vehicles", Journal of Terramechanics, Vol. 23, No. 2, pp. 95-124.

17. Wong, J.Y., 1986b, "Simulation study of the tractive performance of tracked vehicles with different design features in Dikanas snow", unpublished report prepared for the Vehicle Division, AB Hagglund and Soner, Ornskoldsvik, Sweden (Confidential).

18. Wong, J.Y., 1986c, "Weight parameter analysis of the tractive performance of main battle tanks using the tracked vehicle performance model NTVPM-85", unpublished report prepared for the Director of Combat Mobility Engineering and Maintenance, Canadian Department of National Defence.

19. Wong, J.Y., 1986d, "Simulation and analysis of container handling equipment mobility", unpublished report prepared for the Naval Civil Engineering Laboratory, U.S. Department of the Navy.

20. Wong, J.Y., 1986e, "Technical simulation and analysis of the mobility of a rough terrain container handler and a heavy lift rough terrain crane", unpublished report prepared for the Naval Civil Engineering Laboratory, U.S. Department of the Navy.

21. Wong, J.Y., 1986f, "A comprehensive computer simulation model for the off-road performance of tracked vehicle", Proceedings of the Symposium on Simulation and Control of Ground Vehicles and Transportation Systems, ASME, AMD Vol. 90 (DSC No. 2), Edited by L. Segel, J.Y. Wong, E.H. Law and D.Hrorat, pp. 63-79.

22. Wong, J.Y., 1989a, "Terramechanics and Off-road Vehicles", Elsevier Science Publishers, Amsterdam, the Netherlands.

23. Wong, J.Y., 1989b, "Simulation study of the effects of design modifications on the performance of BV 206", unpublished report prepared for the Light Vehicle Division, Hagglunds Vehicle AB, Ornskoldsvik, Sweden (Confidential).

24. Wong, J.Y., 1990a, "Measurement and characterization of the pressure-sinkage relationships for snow obtained using a Rammsonde and a Bevameter", unpublished report prepared for Vehicle Mobility Section, Defence Research Establishment Suffield, Canadian Department of National Defence.

25. Wong, J.Y., 1990b, "Measurement of the shear strength of snow using a Bevameter and a hand-held shear device", unpublished report prepared for Vehicle Mobility Section, Defence Research Establishment Suffield, Canadian Department of National Defence.

26. Wong, J.Y., 1990c, "Some recent developments in computer-aided methods for design evaluation of off-road vehicles - a summary", Transportation Systems 1990, ASME, AMD Vol. 108, edited by J.Y. Wong, J.J. Moskura and S.A. Velinsky, pp. 183-189.

27. Wong, J.Y. and Reece, A.R., 1966, "Soil failure beneath rigid wheels", Proceedings of the 2nd International Conference of the International Society for Terrain-Vehicle Systems, pp. 425-445.

28. Wong, J.Y. and Preston-Thomas, J., 1986, "Parametric analysis of tracked vehicle performance using an advanced computer simulation model", Proceedings of the Institution of Mechanical Engineers, vol. 200, part D, No. D2, pp. 101-114.

29. Wong, J.Y. and Preston-Thomas, J., 1987a, "A comparison of the mobility of various types of container handling equipment", unpublished report prepared for the Naval Civil Engineering Laboratory, U.S. Department of the Navy.

30. Wong, J.Y and Preston-Thomas, J., 1987b, "Computer simulation study of the mobility of the Armoured Vehicle General Purpose (AVGP) with different tires", unpublished report prepared for the Director of Combat Mobility Engineering and Maintenance, Canadian Department of National Defence.

31. Wong, J.Y. and Preston-Thomas, J., 1987c, "Technical simulation and analysis of the mobility of a logistic vehicle system (LVS) and a Wishbone container handler", unpublished report prepared for the Naval Civil Engineering Laboratory, U.S. Department of the Navy.

32. Wong, J.Y. and Preston-Thomas, J., 1988, "Investigation into the effects of suspension characteristics and design parameters on the performance of tracked vehicles using an advanced computer simulation model", Proceedings of the Institution of Mechanical Engineers, Vol. 202, No. D3, pp. 143-161.

33. Wong, J.Y. and Preston-Thomas, J., 1989, "Simulation study of the tractive performance of the STRV 2000 main battle tank", unpublished report prepared for Hagglunds Vehicle AB, Ornskoldsvik, Sweden (Confidential).

34. Wong, J.Y., Garber, M. and Preston-Thomas, J., 1984, "Theoretical prediction and experimental substantiation of the ground pressure distribution and tractive performance of tracked vehicles", Proceedings of the Institution of Mechanical Engineers, Vol. 198, part D, No. 15, pp. 265-285.

35. Yong, R.N. and Fattah, E.A., 1976, "Prediction of wheel-soil interaction and performance using the finite element method", Journal of Terramechanics, Vol. 13, No. 4, pp. 227-240.

APPENDIX A

SAMPLE OUTPUT OF NTVPM-85 FOR UNDISTURBED SNOW

PREDICTION OF TRACKED VEHICLE PERFORMANCE
(MODEL: NTVPM-85)
VEHICLE SYSTEMS DEVELOPMENT CORPORATION
NEPEAN, ONTARIO, CANADA

SEPTEMBER 11, 1990

VEHICLE TYPE BV206 (Expt.)

VEHICLE PARAMETERS FOR THE FRONT UNIT:

WEIGHT	28.06 KN
CENTRE OF GRAVITY X-COORDINATE	131.50 CM
CENTRE OF GRAVITY Y-COORDINATE	-14.40 CM
SPROCKET RADIUS	19.00 CM
SPROCKET CENTRE X-COORDINATE	.00 CM
SPROCKET CENTRE Y-COORDINATE	.00 CM
TENSIONING WHEEL RADIUS	19.00 CM
TENSIONING WHEEL CENTRE X-COORDINATE	233.13 CM
TENSIONING WHEEL CENTRE Y-COORDINATE	30.50 CM
ROADWHEEL RADIUS	19.00 CM
INITIAL TRACK TENSION	3.53 KN
DOUBLE PIVOT JOINT X-COORDINATE (AT THE REAR OF THE UNIT)	273.00 CM
DOUBLE PIVOT JOINT Y-COORDINATE (AT THE REAR OF THE UNIT)	3.00 CM
LENGTH OF THE INTERCONNECTING LINK	76.00 CM
SUSPENSION HEAVE STIFFNESS	.69 KN/CM

FRONT UNIT -- ROADWHEEL GEOMETRY

X-COORDINATE OF WHEEL CENTRE (CM)	Y-COORDINATE OF WHEEL CENTRE (CM)
34.04	30.50
86.28	30.50
129.28	30.50
173.28	30.50

BELLY SHAPE

WIDTH: 61.0 CM

COORDINATES (CM) X	COORDINATES (CM) Y
-20.0	-3.0
-6.0	11.0
260.0	11.0

SUPPORTING ROLLERS

RADIUS: 10.0 CM

COORDINATES (CM) X	COORDINATES (CM) Y
128.0	2.0

TRACK LINK CONTACT AREA

SINKAGE (CM) FROM	SINKAGE (CM) TO	INCRE-MENTAL AREA (CM**2)	PERCENTAGE CAUSING RUBBER SHEARING
.00	.00	76.00	100.0
.00	1.40	64.00	.0
1.40	2.70	71.00	.0
2.70	5.50	351.00	.0

NOTE: COORDINATE ORIGIN IS AT THE CENTRE OF THE SPROCKET. POSITIVE X- AND Y-COORDINATES ARE TO THE REAR AND DOWN, RESPECTIVELY.

TRACK PARAMETERS FOR THE FRONT UNIT:

WEIGHT PER UNIT LENGTH	.330 KN/M
WIDTH	62.0 CM
PITCH	9.1 CM
HEIGHT OF THE GROUSERS	5.5 CM
PERCENT RUBBER FOR COHESIVE SHEARING	13.5 %
LONGITUDINAL ELASTICITY CONSTANT TE (FROM T=TE*E)	10910. KN

VEHICLE PARAMETERS FOR THE REAR UNIT:

WEIGHT	17.95 KN
CENTRE OF GRAVITY X-COORDINATE	96.50 CM
CENTRE OF GRAVITY Y-COORDINATE	-.40 CM
SPROCKET RADIUS	19.00 CM
SPROCKET CENTRE X-COORDINATE	.00 CM
SPROCKET CENTRE Y-COORDINATE	.00 CM
TENSIONING WHEEL RADIUS	19.00 CM
TENSIONING WHEEL CENTRE X-COORDINATE	233.13 CM
TENSIONING WHEEL CENTRE Y-COORDINATE	30.50 CM
ROADWHEEL RADIUS	19.00 CM
INITIAL TRACK TENSION	4.69 KN
DOUBLE PIVOT JOINT X-COORDINATE (AT THE FRONT OF THE UNIT)	-29.00 CM
DOUBLE PIVOT JOINT Y-COORDINATE (AT THE FRONT OF THE UNIT)	3.00 CM
DRAWBAR HITCH X-COORDINATE	265.00 CM
DRAWBAR HITCH Y-COORDINATE	-2.00 CM
SUSPENSION HEAVE STIFFNESS	.67 KN/CM

REAR UNIT -- ROADWHEEL GEOMETRY

X-COORDINATE OF WHEEL CENTRE (CM)	Y-COORDINATE OF WHEEL CENTRE (CM)
34.04	30.50
86.28	30.50
131.97	30.50
177.84	30.50

NOTE: COORDINATE ORIGIN IS AT THE CENTRE OF THE SPROCKET. POSITIVE X- AND Y-COORDINATES ARE TO THE REAR AND DOWN, RESPECTIVELY.

BELLY SHAPE		SUPPORTING ROLLERS		TRACK LINK CONTACT AREA			
WIDTH: 61.0 CM		RADIUS: 10.0 CM		SINKAGE (CM)		INCRE-MENTAL AREA (CM**2)	PERCENTAGE CAUSING RUBBER SHEARING
COORDINATES (CM) X	COORDINATES (CM) Y	COORDINATES (CM) X	COORDINATES (CM) Y	FROM	TO		
-20.0	-3.0	128.0	2.0	.00	.00	76.00	100.0
-6.0	11.0			.00	1.40	64.00	.0
260.0	11.0			1.40	2.70	71.00	.0
				2.70	5.50	351.00	.0

TRACK PARAMETERS FOR THE REAR UNIT:

WEIGHT PER UNIT LENGTH	.330 KN/M
WIDTH	62.0 CM
PITCH	7.1 CM
HEIGHT OF THE GROUSERS	5.5 CM
PERCENT RUBBER FOR COHESIVE SHEARING	13.5 %
LONGITUDINAL ELASTICITY CONSTANT TE (FROM T=TE*E)	10910. KN

NOTE: COORDINATE ORIGIN IS AT THE CENTRE OF THE SPROCKET. POSITIVE X- AND Y- COORDINATES ARE TO THE REAR AND DOWN, RESPECTIVELY.

FRONT UNIT

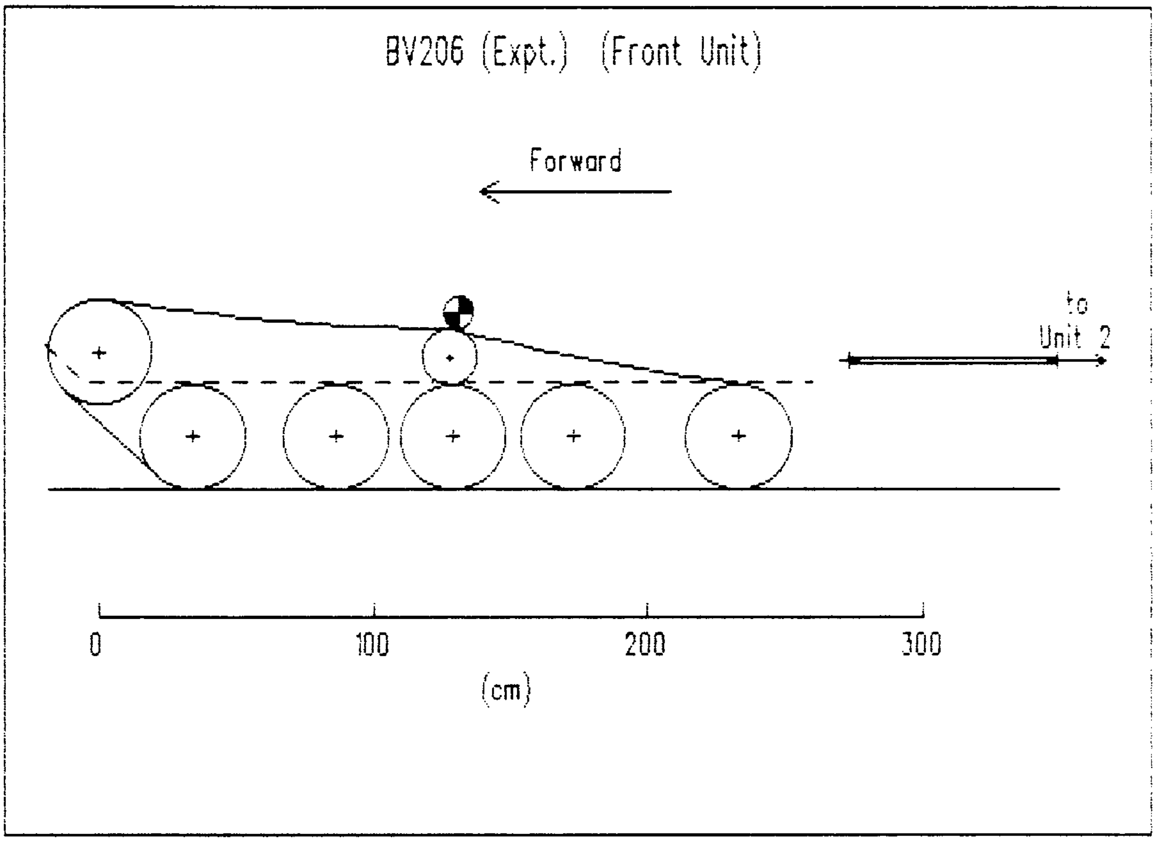

FRONT UNIT - WHEEL LOADS AND GEOMETRY ON LEVEL HARD GROUND

WHEEL	VERTICAL LOADS AT THE WHEEL-GROUND INTERFACE (KN)	WHEEL CENTRE X-COOR-DINATE (CM)	WHEEL CENTRE HEIGHT ABOVE GROUND (CM)
SPROCKET	.00	.00	49.50
1	2.79	34.04	19.00
2	2.80	86.28	19.00
3	2.81	129.28	19.00
4	2.81	173.28	19.00
TEN. WHEEL	2.82	233.13	19.00
TOTAL	14.03		

NOTE: THESE LOADS ARE FOR ONE SIDE OF THE VEHICLE ONLY.

NOTE: COORDINATE ORIGIN IS AT THE CENTRE OF THE SPROCKET OF THE FRONT UNIT.
POSITIVE X-COORDINATES ARE TO THE REAR.

REAR UNIT

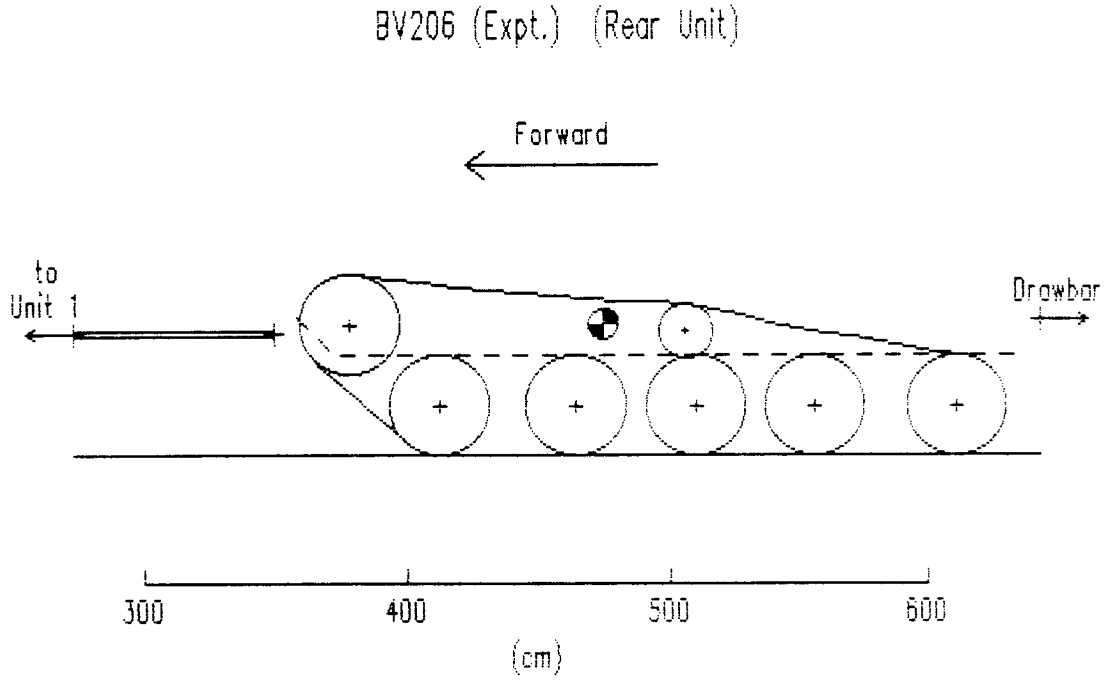

REAR UNIT - WHEEL LOADS AND GEOMETRY ON LEVEL HARD GROUND

WHEEL	VERTICAL LOADS AT THE WHEEL-GROUND INTERFACE (KN)	WHEEL CENTRE X-COORDINATE (CM)	WHEEL CENTRE HEIGHT ABOVE GROUND (CM)
SPROCKET	.00	378.00	49.50
1	3.13	412.04	19.00
2	2.42	464.28	19.00
3	1.80	509.97	19.00
4	1.18	555.84	19.00
TEN. WHEEL	.44	611.13	19.00
TOTAL	8.98		

NOTE: THESE LOADS ARE FOR ONE SIDE OF THE VEHICLE ONLY.

NOTE: COORDINATE ORIGIN IS AT THE CENTRE OF THE SPROCKET OF THE FRONT UNIT. POSITIVE X-COORDINATES ARE TO THE REAR.

TERRAIN TYPE Fernie Snow(RSF-12D)

PRESSURE-SINKAGE PARAMETERS:

KC	FROM EQUATION P=(KC/B+KPHI)*Z**M	8.96	KN/M**(M+1)
KPHI	FROM EQUATION P=(KC/B+KPHI)*Z**M	194.48	KN/M**(M+2)
M	FROM EQUATION P=(KC/B+KPHI)*Z**M	1.004	

PARAMETERS FOR REPETITIVE LOADING:

K0	FROM EQUATION KR=K0+AU*ZU	.0	KPA/M
AU	FROM EQUATION KR=K0+AU*ZU	33333.0	KPA/M**2

SHEAR STRENGTH PARAMETERS:

RUBBER-TERRAIN SHEARING:

PHI	FROM MOHR-COULOMB EQUATION	11.4	DEG.
C	FROM MOHR-COULOMB EQUATION	.21	KPA
K	FROM EXPONENTIAL SHEAR EQUATION	.39	CM

INTERNAL SHEARING OF THE TERRAIN:

PHI	FROM MOHR-COULOMB EQUATION	25.0	DEG.
C	FROM MOHR-COULOMB EQUATION	1.96	KPA
K	FROM EXPONENTIAL SHEAR EQUATION	5.50	CM

SIDE THRUST NOT INCLUDED.

VEHICLE BELLY SHEARING:

PHI	FROM MOHR-COULOMB EQUATION	5.7	DEG.
C	FROM MOHR-COULOMB EQUATION	.00	KPA

FRONT UNIT -- SLIP = 20.00 %

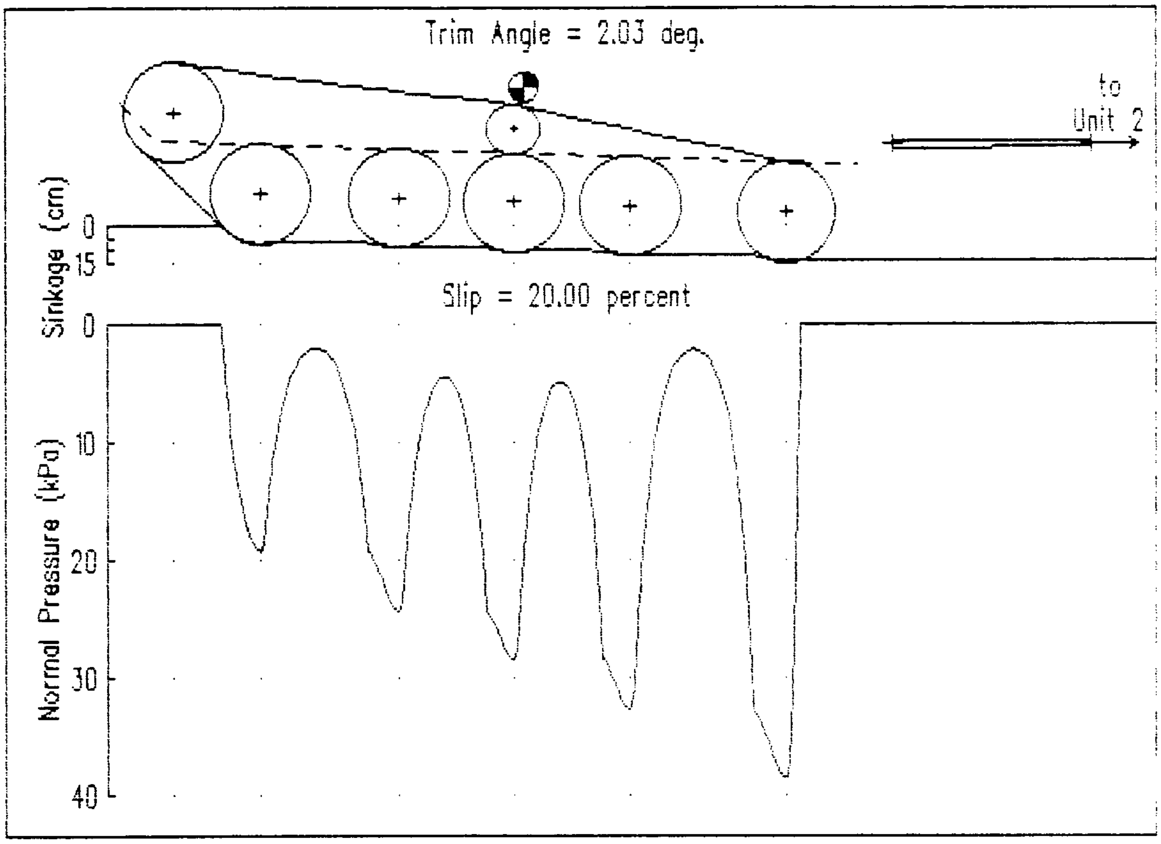

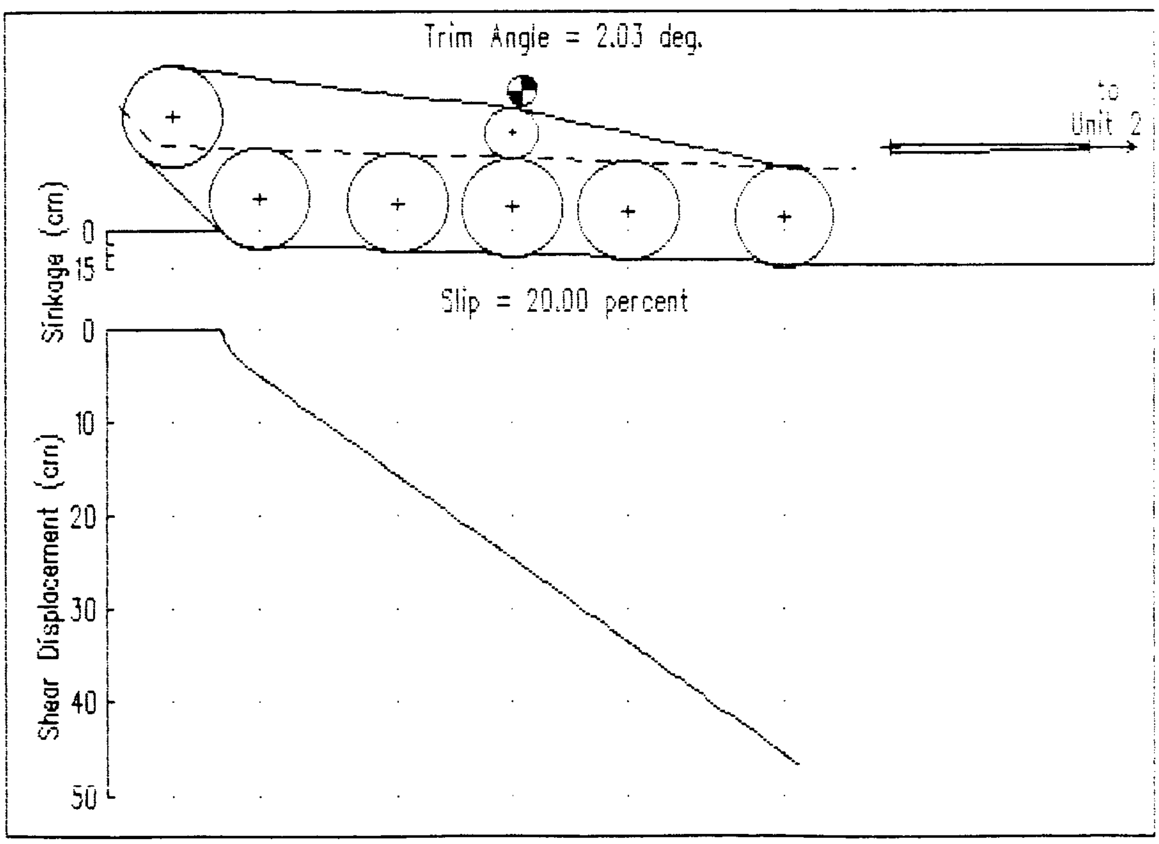

FRONT UNIT -- SLIP = 20.00 %

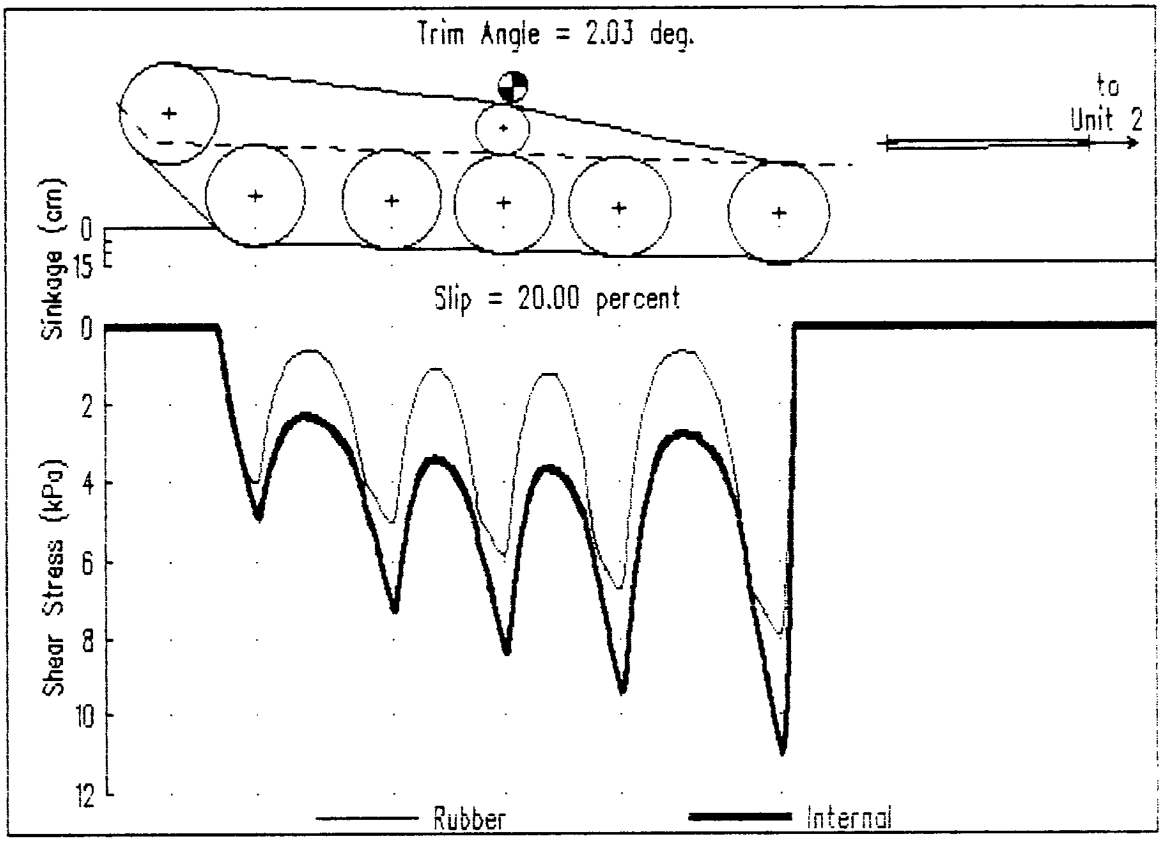

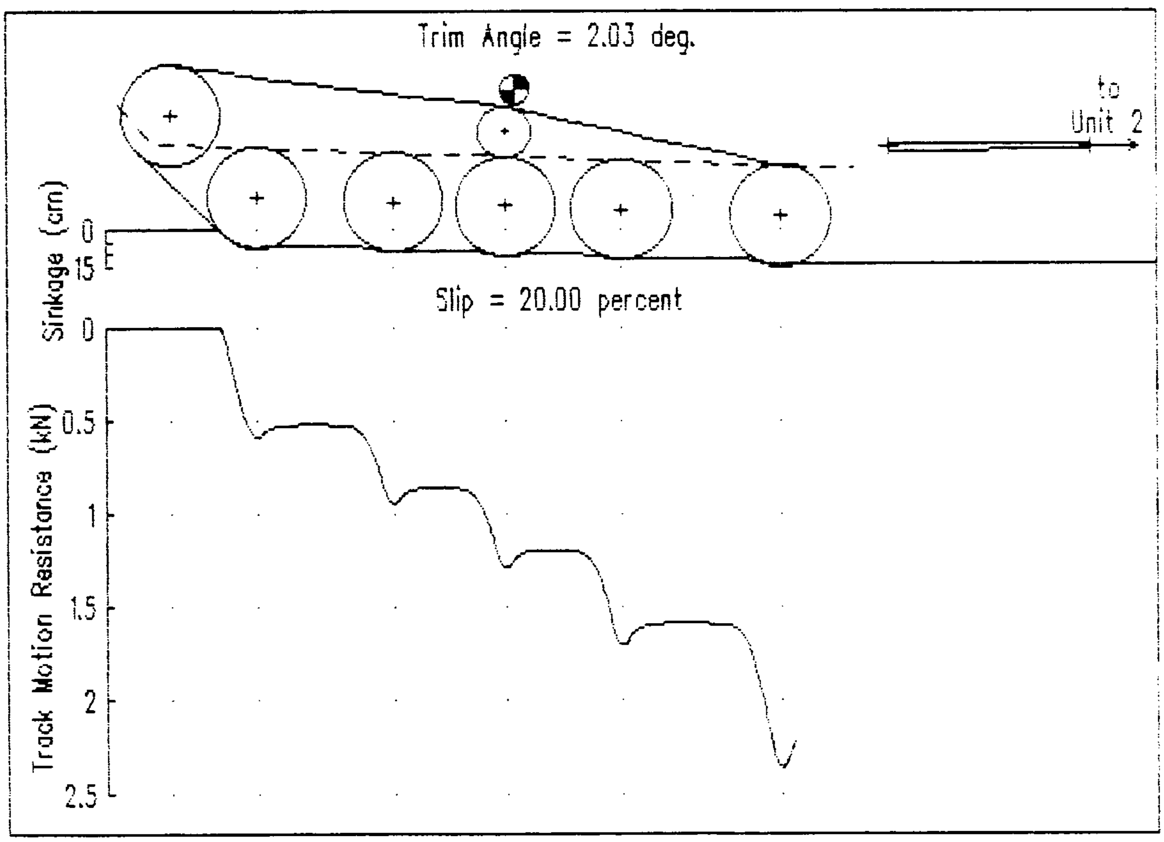

FRONT UNIT -- SLIP = 20.00 %

WHEEL	TRACK CONTACT ANGLE LEFT (+ IS CW FROM BDC) (DEG.)	TRACK CONTACT ANGLE RIGHT (+ IS CCW FROM BDC) (DEG.)	LOADS AT THE WHEEL-TERRAIN INTERFACE X (+ IS FORWARD) (KN)	LOADS AT THE WHEEL-TERRAIN INTERFACE Y (+ IS UP) (KN)	LOADS SUPPORTED BY TRACK BETWEEN WHEELS X (+ IS FORWARD) (KN)	LOADS SUPPORTED BY TRACK BETWEEN WHEELS Y (+ IS UP) (KN)
SPR.	188.27	-43.83	.000	.000		
					-.015	.021
1	44.17	5.90	-.036	1.056		
					.595	1.744
2	14.24	5.95	.157	.694		
					.651	1.986
3	13.26	5.94	.177	.774		
					.721	2.351
4	13.31	5.95	.197	.894		
					.892	3.050
T.W.	15.04	168.75	.391	1.428		
TOTAL			.886	4.846	2.844	9.152

NOTE: THE LOADS IN THIS TABLE ARE FOR ONE SIDE OF THE VEHICLE ONLY.

WHEEL	SINKAGE (CM)	AXLE LOADS X (+ IS FORWARD) (KN)	AXLE LOADS Y (+ IS UP) (KN)	TRACK TENSION AT LEFT CONTACT POINT (KN)	TRACK TENSION MEAN (KN)	TRACK TENSION AT RIGHT CONTACT POINT (KN)
SPR.	-24.58	-12.087	-4.440	9.16		4.23
					4.23	
1	7.11	-1.457	4.468	4.24		4.48
					4.85	
2	8.97	-.182	2.539	5.21		5.42
					5.82	
3	10.49	-.181	2.864	6.21		6.44
					6.88	
4	12.05	-.215	3.365	7.32		7.57
					8.15	
T.W.	14.18	17.852	5.202	8.73		9.16
					9.16	
TOTAL		3.730	13.998			

NOTE: THE LOADS IN THIS TABLE ARE FOR ONE SIDE OF THE VEHICLE ONLY.

FRONT UNIT -- SLIP = 20.00 %

		PER UNIT WEIGHT
BELLY LOAD:	.00 KN	.00 %
BELLY DRAG:	.00 KN	.00 %
TRACK MOTION RESISTANCE:	2.31 KN	8.26 %
TOTAL EXTERNAL MOTION RESISTANCE:	2.31 KN	8.26 %
THRUST:	9.77 KN	34.90 %
HORIZONTAL JOINT FORCE (+ REARWARD):	7.46 KN	26.64 %
VERTICAL JOINT FORCE (+ DOWN):	-.06 KN	-.22 %
TRACTIVE EFFICIENCY:	61.07 %	

CHASSIS TRIM ANGLE:	2.03 DEG
JOINT ANGLE (+ IS CW FROM HORIZONTAL):	-.47 DEG
EFFECTIVE RADIUS OF TRACK:	11.18 CM
RUBBER PAD LOAD / TOTAL TRACK LINK LOAD:	19.4 %

REAR UNIT -- SLIP = 20.00 %

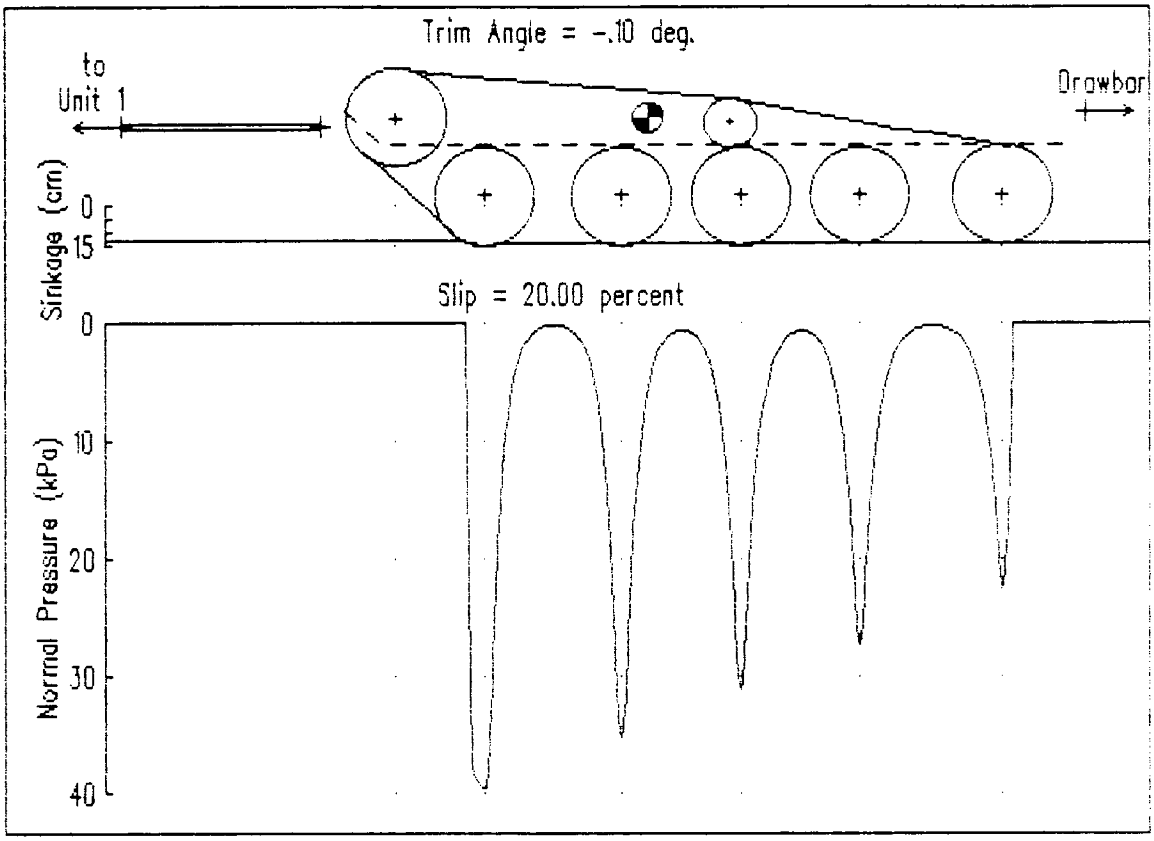

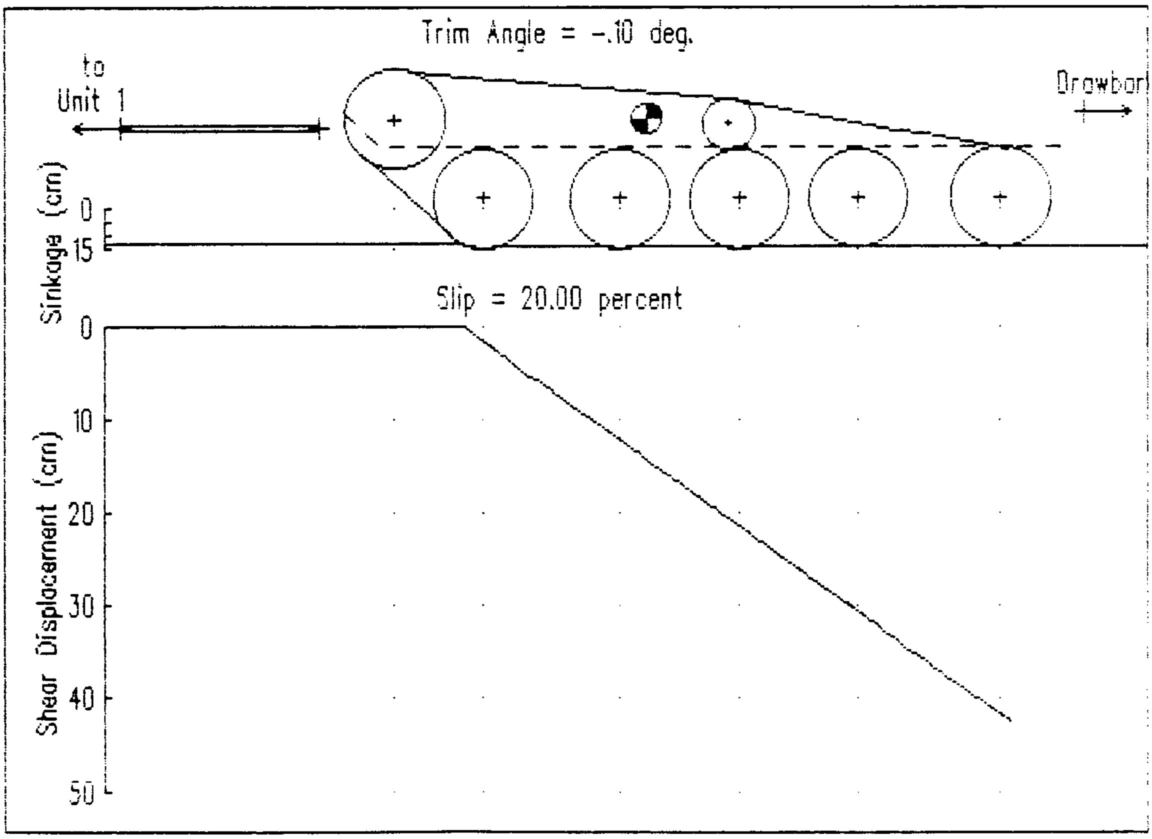

REAR UNIT -- SLIP = 20.00 %

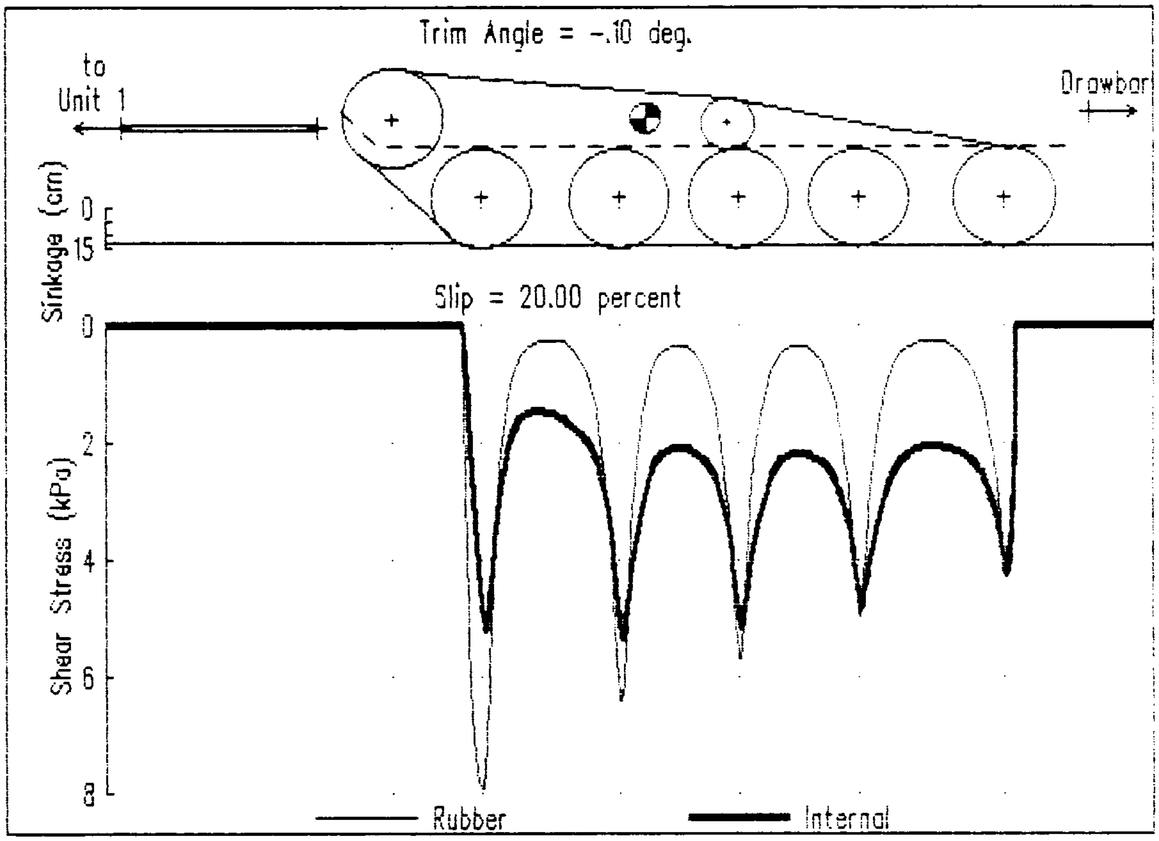

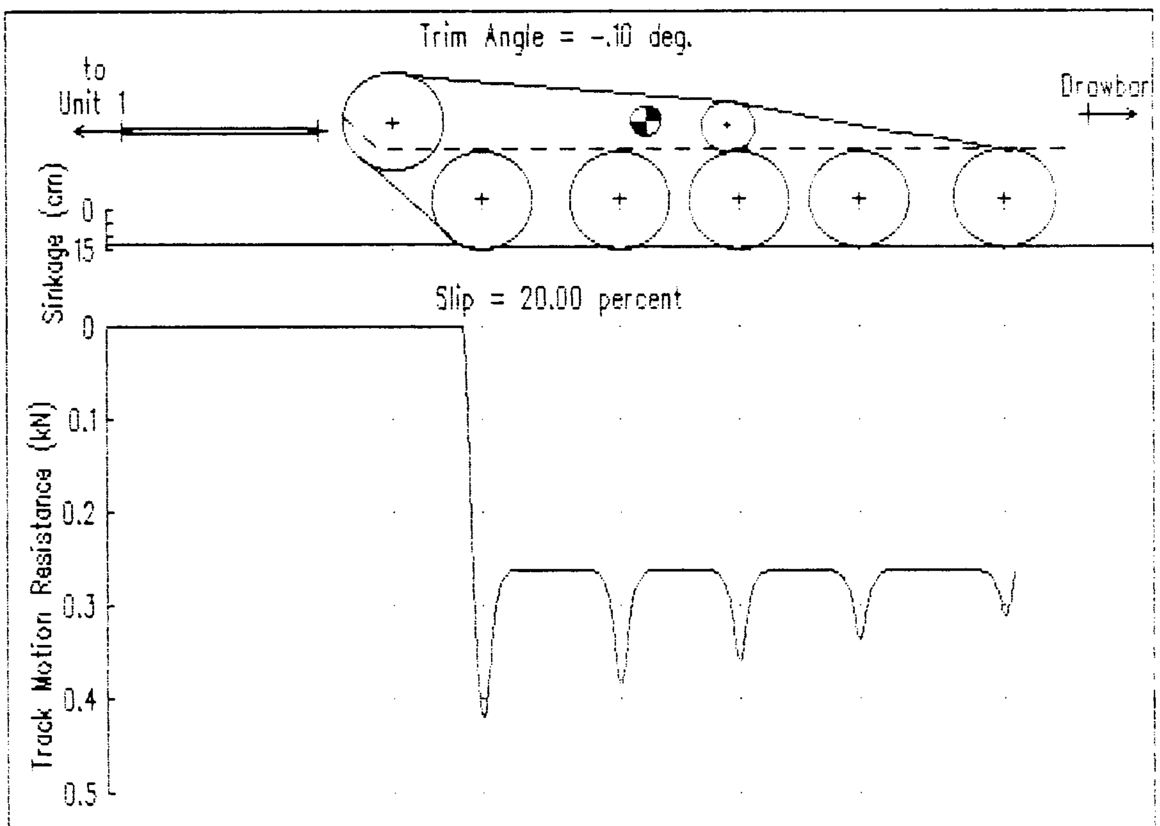

REAR UNIT -- SLIP = 20.00 %

WHEEL	TRACK CONTACT ANGLE LEFT (+ IS CW FROM BDC) (DEG.)	TRACK CONTACT ANGLE RIGHT (+ IS CCW FROM BDC) (DEG.)	LOADS AT THE WHEEL-TERRAIN INTERFACE X (+ IS FORWARD) (KN)	LOADS AT THE WHEEL-TERRAIN INTERFACE Y (+ IS UP) (KN)	LOADS SUPPORTED BY TRACK BETWEEN WHEELS X (+ IS FORWARD) (KN)	LOADS SUPPORTED BY TRACK BETWEEN WHEELS Y (+ IS UP) (KN)
SPR.	186.36	-41.76	.000	.000		
					.000	.000
1	41.76	7.84	.001	1.704		
					.549	1.325
2	7.10	6.80	.122	.750		
					.618	1.307
3	6.14	5.89	.104	.583		
					.644	1.265
4	5.23	5.02	.083	.438		
					.742	1.174
T.W.	4.22	171.05	.133	.451		
TOTAL			.443	3.926	2.553	5.073

NOTE: THE LOADS IN THIS TABLE ARE FOR ONE SIDE OF THE VEHICLE ONLY.

WHEEL	SINKAGE (CM)	AXLE LOADS X (+ IS FORWARD) (KN)	AXLE LOADS Y (+ IS UP) (KN)	TRACK TENSION AT LEFT CONTACT POINT (KN)	TRACK TENSION MEAN (KN)	TRACK TENSION AT RIGHT CONTACT POINT (KN)
SPR.	-15.56	-11.213	-4.101	7.80		4.66
					4.66	
1	14.88	-1.319	5.467	4.66		4.84
					5.11	
2	14.79	-.005	2.067	5.38		5.51
					5.32	
3	14.71	-.004	1.877	6.12		6.23
					6.55	
4	14.63	-.003	1.672	6.87		6.75
					7.32	
T.W.	14.53	15.539	2.016	7.69		7.20
					7.80	
TOTAL		2.996	8.999			

NOTE: THE LOADS IN THIS TABLE ARE FOR ONE SIDE OF THE VEHICLE ONLY.

REAR UNIT -- SLIP = 20.00 %

		PER UNIT WEIGHT
BELLY LOAD:	.00 KN	.00 %
BELLY DRAG:	.00 KN	.00 %
TRACK MOTION RESISTANCE:	.28 KN	1.58 %
TOTAL EXTERNAL MOTION RESISTANCE:	.28 KN	1.58 %
THRUST:	6.28 KN	34.85 %
TRACTIVE EFFICIENCY:	76.37 %	

CHASSIS TRIM ANGLE:	-.10 DEG
EFFECTIVE RADIUS OF TRACK:	11.98 CM
RUBBER PAD LOAD / TOTAL TRACK LINK LOAD:	16.8 %

PERFORMANCE OF THE ARTICULATED VEHICLE -- SLIP = 20.00 %

		PER UNIT WEIGHT
TOTAL BELLY LOAD:	.00 KN	.00 %
TOTAL BELLY DRAG:	.00 KN	.00 %
TOTAL TRACK MOTION RESISTANCE:	2.60 KN	5.65 %
TOTAL EXTERNAL MOTION RESISTANCE:	2.60 KN	5.65 %
TOTAL THRUST:	16.05 KN	34.88 %
TOTAL DRAWBAR PULL:	13.45 KN	29.24 %
TRACTIVE EFFICIENCY:	67.05 %	

SUMMARY
****

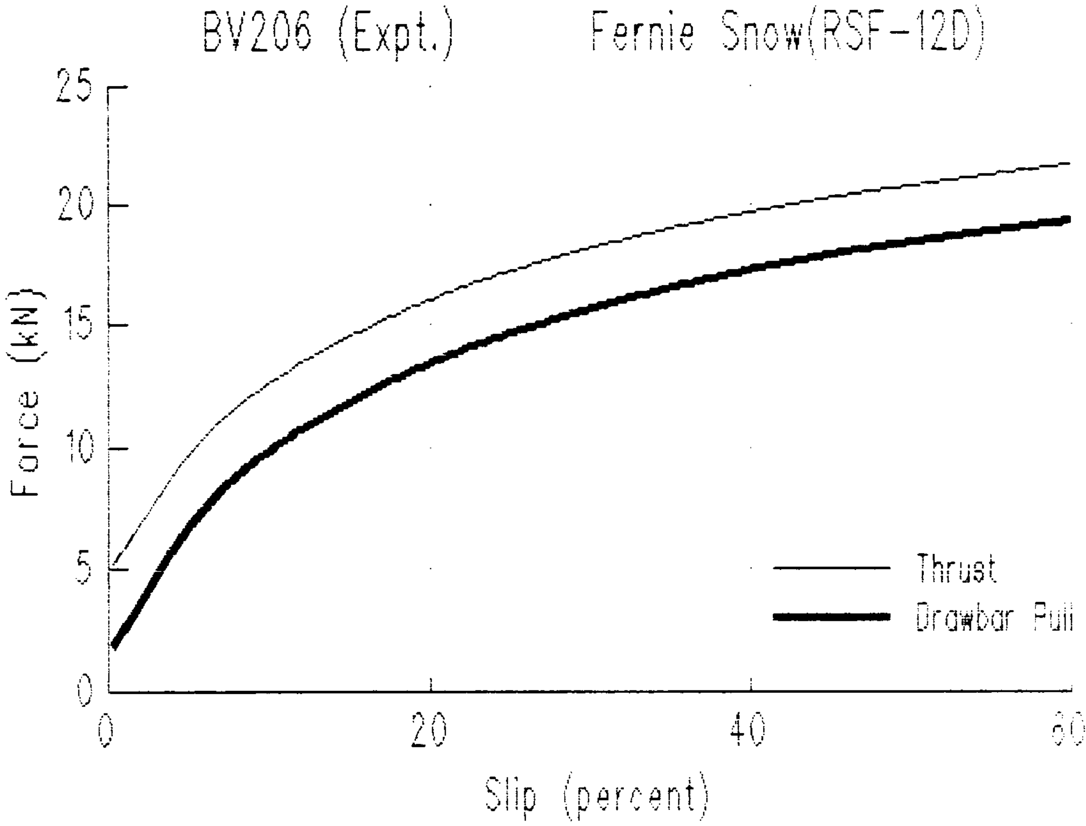
BV206 (Expt.) Fernie Snow(RSF-12D)
Force (kN)
25
20
15
10
5
0
0
20
40
60
Slip (percent)
Thrust
Drawbar Pull

SUMMARY

****

SLIP	BELLY LOAD		BELLY DRAG		TRACK MOTION RESISTANCE	
		PER UNIT VEHICLE WEIGHT		PER UNIT VEHICLE WEIGHT		PER UNIT VEHICLE WEIGHT
(%)	(KN)	(%)	(KN)	(%)	(KN)	(%)
2.00	.00	.00	.00	.00	3.24	7.04
5.00	.00	.00	.00	.00	3.01	6.54
10.00	.00	.00	.00	.00	2.80	6.09
20.00	.00	.00	.00	.00	2.60	5.65
30.00	.00	.00	.00	.00	2.53	5.49
40.00	.00	.00	.00	.00	2.41	5.24
60.00	.00	.00	.00	.00	2.33	5.06

SUMMARY

SLIP (%)	THRUST (KN)	THRUST PER UNIT VEHICLE WEIGHT (%)	TOTAL EXTERNAL MOTION RESISTANCE (KN)	TOTAL EXTERNAL MOTION RESISTANCE PER UNIT VEHICLE WEIGHT (%)	DRAWBAR PULL (KN)	DRAWBAR PULL PER UNIT VEHICLE WEIGHT (%)	TRACTIVE EFFICIENCY (%)
2.00	6.85	14.89	3.24	7.04	3.61	7.85	51.66
5.00	9.68	21.04	3.01	6.54	6.67	14.49	65.45
10.00	12.62	27.42	2.80	6.09	9.81	21.33	70.01
20.00	16.05	34.88	2.60	5.65	13.45	29.24	67.05
30.00	18.19	39.53	2.53	5.49	15.66	34.04	60.28
40.00	19.68	42.78	2.41	5.24	17.27	37.54	52.65
60.00	21.65	47.05	2.33	5.06	19.32	41.99	35.70

WHEEL SINKAGES (cm)

SLIP (%)	FRONT UNIT: FRONT ROADWHEEL	FRONT UNIT: REAR ROADWHEEL	REAR UNIT: FRONT ROADWHEEL	REAR UNIT: REAR ROADWHEEL
2.00	9.28	12.97	16.33	15.99
5.00	8.69	12.71	15.81	15.50
10.00	8.00	12.41	15.33	15.05
20.00	7.11	12.05	14.88	14.63
30.00	6.84	11.94	14.71	14.47
40.00	6.20	11.71	14.49	14.26
60.00	5.78	11.58	14.31	14.10

APPENDIX B

SAMPLE OUTPUT OF NTVPM-85 FOR PRECONDITIONED SNOW

TERRAIN TYPE Fernie Snow(RSC-14D)

PRESSURE-SINKAGE PARAMETERS:

KC	FROM EQUATION P=(KC/B+KPHI)*Z**M	-19.06	KN/M**(M+1)
KPHI	FROM EQUATION P=(KC/B+KPHI)*Z**M	2546.20	KN/M**(M+2)
M	FROM EQUATION P=(KC/B+KPHI)*Z**M	.983	

PARAMETERS FOR REPETITIVE LOADING:

K0	FROM EQUATION KR=K0+AU*ZU	.0	KPA/M
AU	FROM EQUATION KR=K0+AU*ZU	33333.0	KPA/M**2

SHEAR STRENGTH PARAMETERS:

RUBBER-TERRAIN SHEARING:

PHI	FROM MOHR-COULOMB EQUATION	10.7	DEG.
C	FROM MOHR-COULOMB EQUATION	.00	KPA
K	FROM EXPONENTIAL SHEAR EQUATION	.39	CM

INTERNAL SHEARING OF THE TERRAIN:

PHI	FROM MOHR-COULOMB EQUATION	28.0	DEG.
C	FROM MOHR-COULOMB EQUATION	1.16	KPA
K	FROM EXPONENTIAL SHEAR EQUATION	2.50	CM

SIDE THRUST NOT INCLUDED.

VEHICLE BELLY SHEARING:

PHI	FROM MOHR-COULOMB EQUATION	5.7	DEG.
C	FROM MOHR-COULOMB EQUATION	.00	KPA

FRONT UNIT -- SLIP = 20.00 %

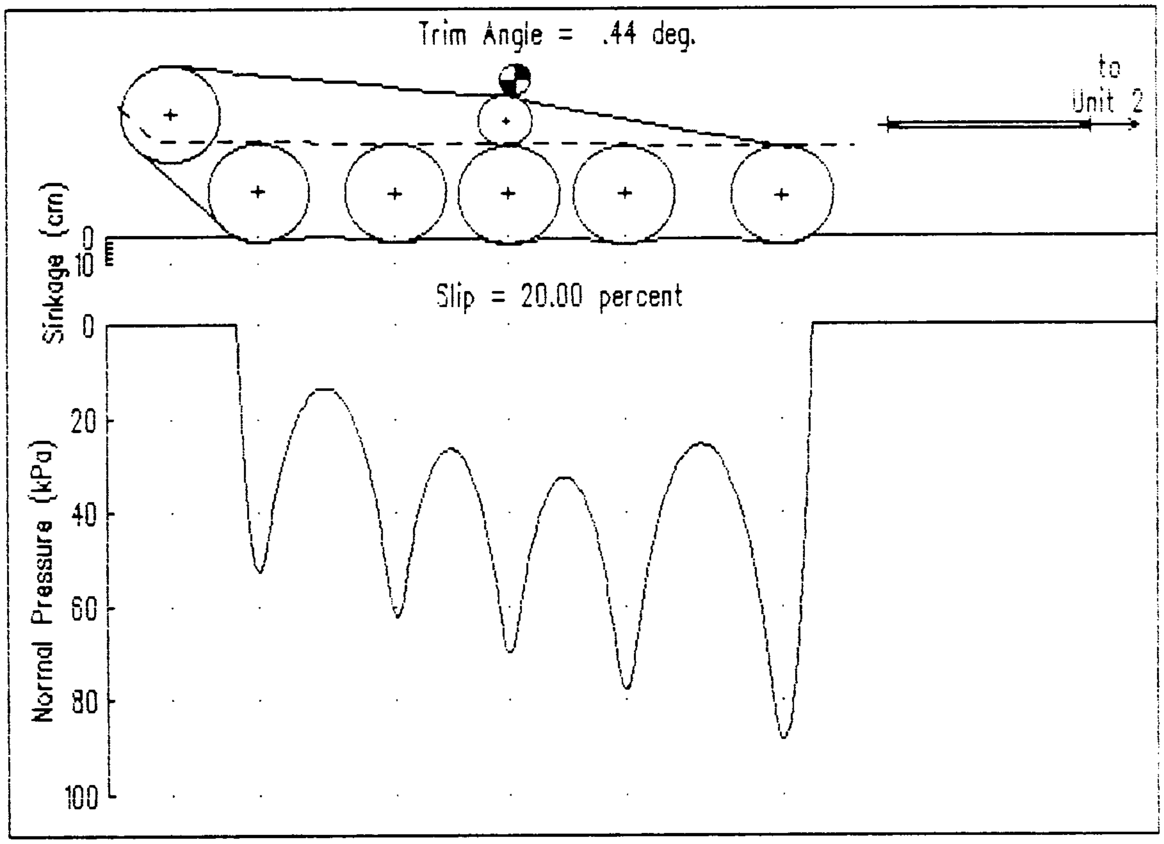

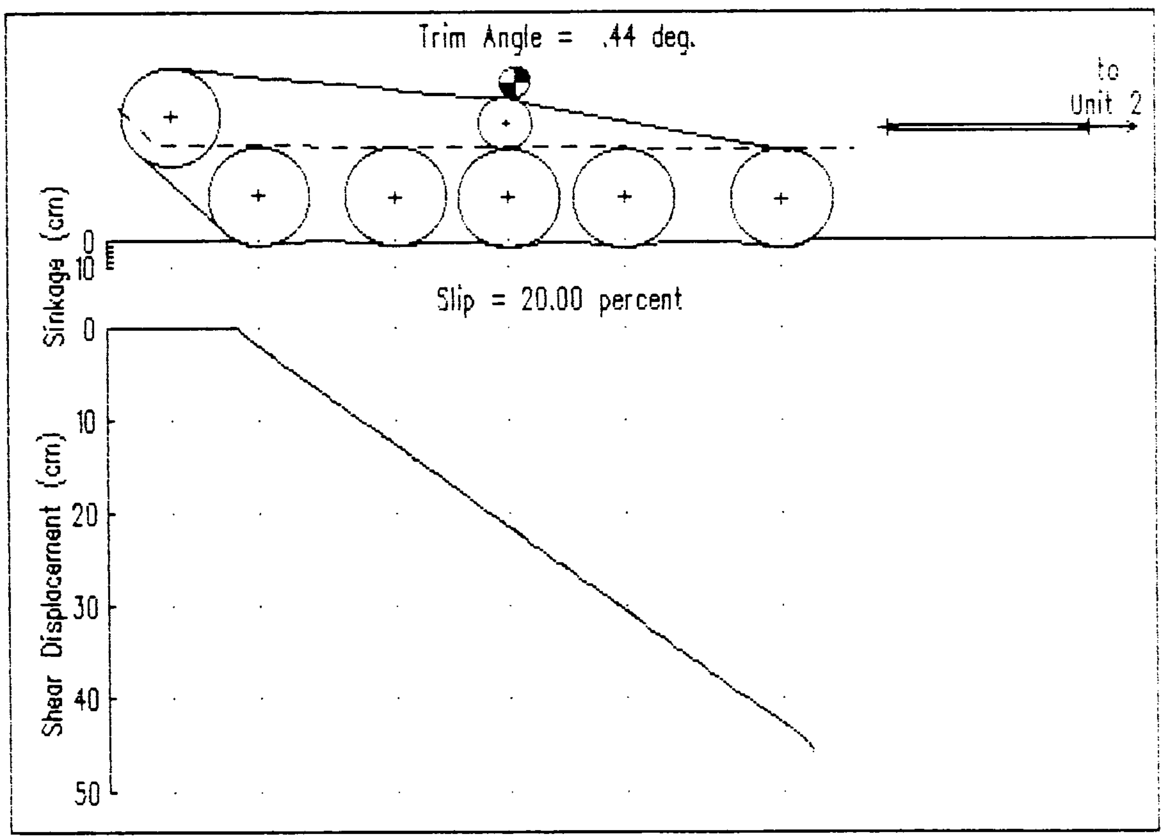

FRONT UNIT -- SLIP = 20.00 %

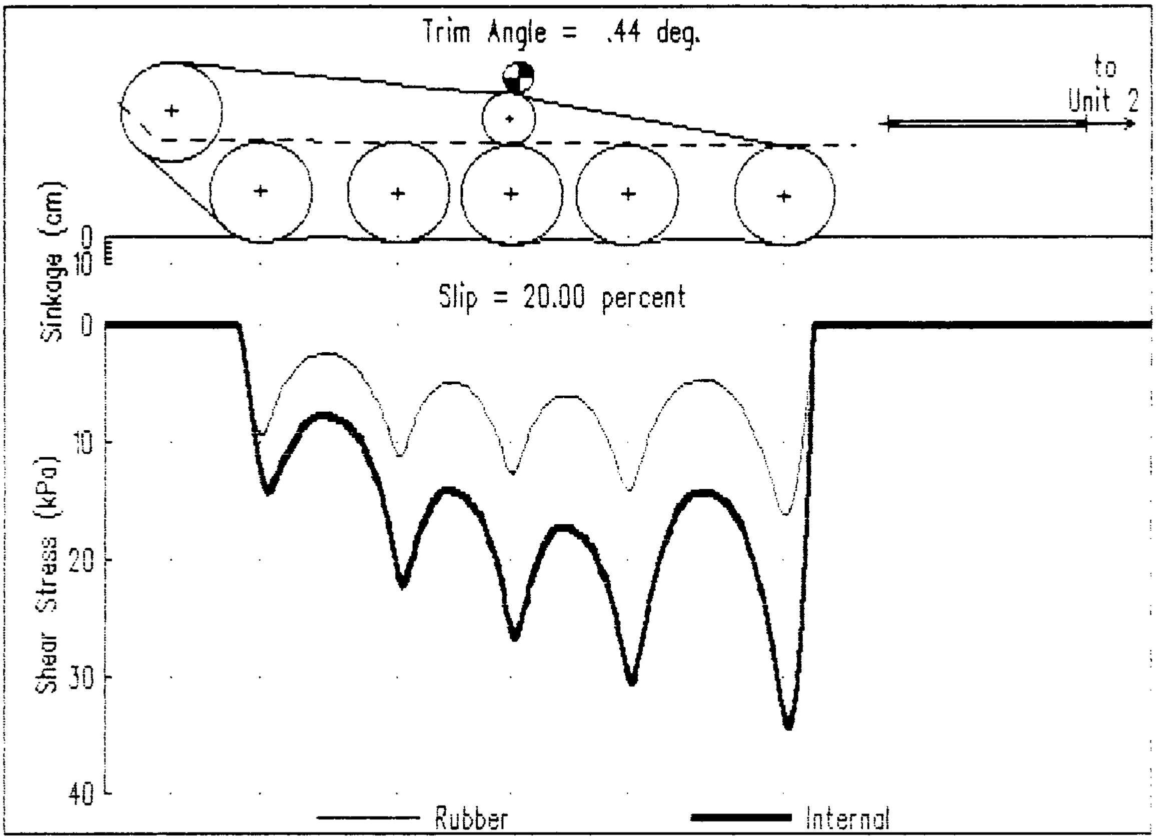

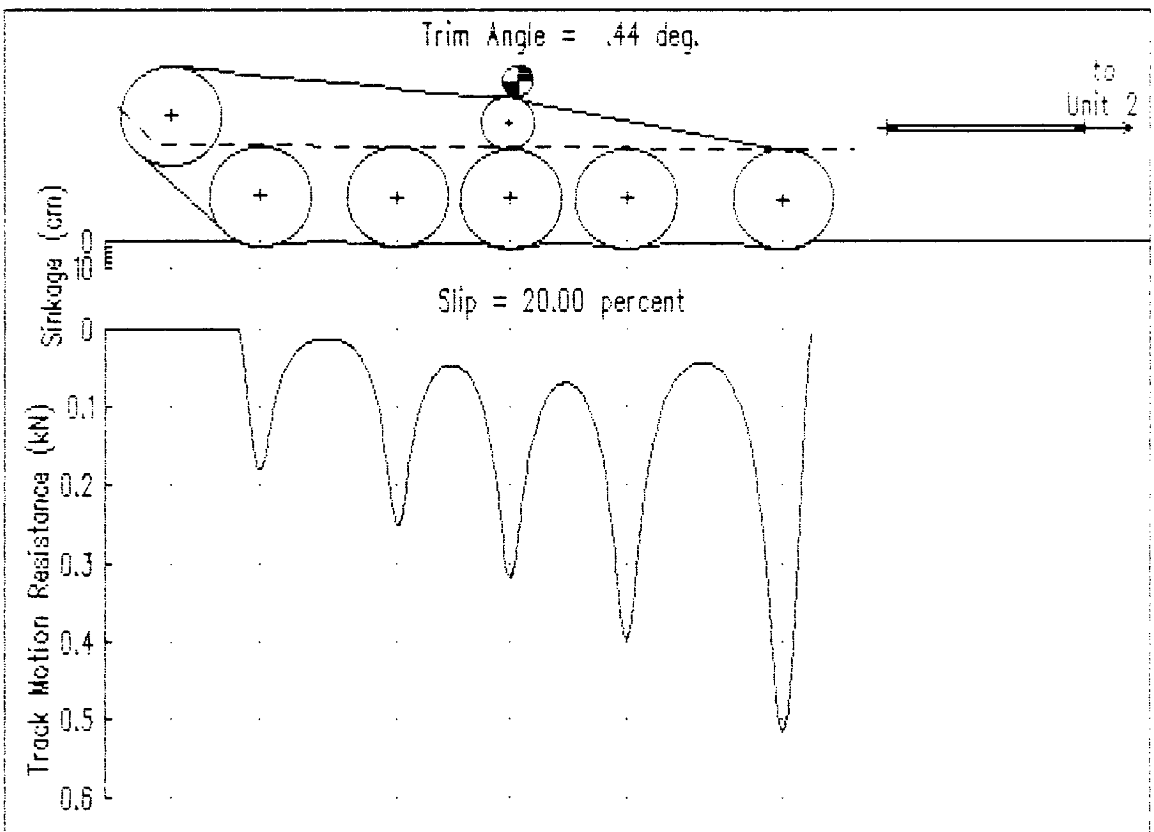

FRONT UNIT -- SLIP = 20.00 %

WHEEL	TRACK CONTACT ANGLE LEFT (+ IS CW FROM BDC) (DEG.)	TRACK CONTACT ANGLE RIGHT (+ IS CCW FROM BDC) (DEG.)	LOADS AT THE WHEEL-TERRAIN INTERFACE X (+ IS FORWARD) (KN)	LOADS AT THE WHEEL-TERRAIN INTERFACE Y (+ IS UP) (KN)	LOADS SUPPORTED BY TRACK BETWEEN WHEELS X (+ IS FORWARD) (KN)	LOADS SUPPORTED BY TRACK BETWEEN WHEELS Y (+ IS UP) (KN)
SPR.	186.58	-42.30	.000	.000		
					.000	.000
1	42.30	9.12	.085	.737		
					.708	1.763
2	10.71	9.24	.184	.614		
					.811	2.097
3	10.54	9.42	.216	.694		
					.956	2.530
4	10.67	10.32	.259	.811		
					1.265	3.333
T.W.	11.79	170.24	.737	1.491		
TOTAL			1.481	4.347	3.740	9.723

NOTE: THE LOADS IN THIS TABLE ARE FOR ONE SIDE OF THE VEHICLE ONLY.

WHEEL	SINKAGE (CM)	AXLE LOADS X (+ IS FORWARD) (KN)	AXLE LOADS Y (+ IS UP) (KN)	TRACK TENSION AT LEFT CONTACT POINT (KN)	TRACK TENSION MEAN (KN)	TRACK TENSION AT RIGHT CONTACT POINT (KN)
SPR.	-28.58	-13.152	-4.425	9.87		4.56
					4.56	
1	2.18	-1.201	4.554	4.56		4.72
					5.09	
2	2.58	-.030	2.537	5.46		5.65
					6.08	
3	2.91	-.026	2.983	6.50		6.72
					7.22	
4	3.24	-.008	3.671	7.72		7.99
					8.65	
T.W.	3.70	19.638	4.750	9.32		9.87
					9.87	
TOTAL		5.221	14.070			

NOTE: THE LOADS IN THIS TABLE ARE FOR ONE SIDE OF THE VEHICLE ONLY.

FRONT UNIT -- SLIP = 20.00 %

		PER UNIT WEIGHT
BELLY LOAD:	.00 KN	.00 %
BELLY DRAG:	.00 KN	.00 %
TRACK MOTION RESISTANCE:	.09 KN	.34 %
TOTAL EXTERNAL MOTION RESISTANCE:	.09 KN	.34 %
THRUST:	10.54 KN	37.68 %
HORIZONTAL JOINT FORCE (+ REARWARD):	10.44 KN	37.34 %
VERTICAL JOINT FORCE (+ DOWN):	-.10 KN	-.36 %
TRACTIVE EFFICIENCY:	79.28 %	

CHASSIS TRIM ANGLE:	.44 DEG
JOINT ANGLE (+ IS CW FROM HORIZONTAL):	-.55 DEG
EFFECTIVE RADIUS OF TRACK:	6.72 CM
RUBBER PAD LOAD / TOTAL TRACK LINK LOAD:	53.6 %

REAR UNIT -- SLIP = 20.00 %

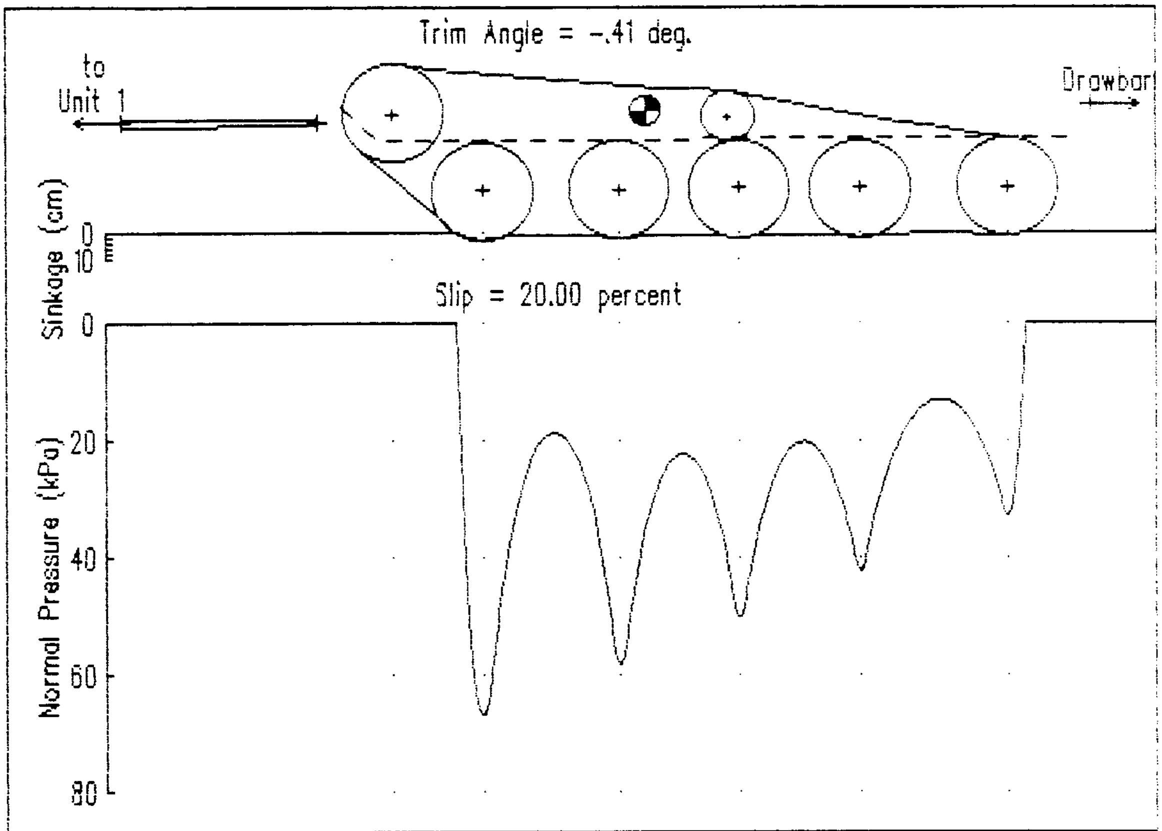

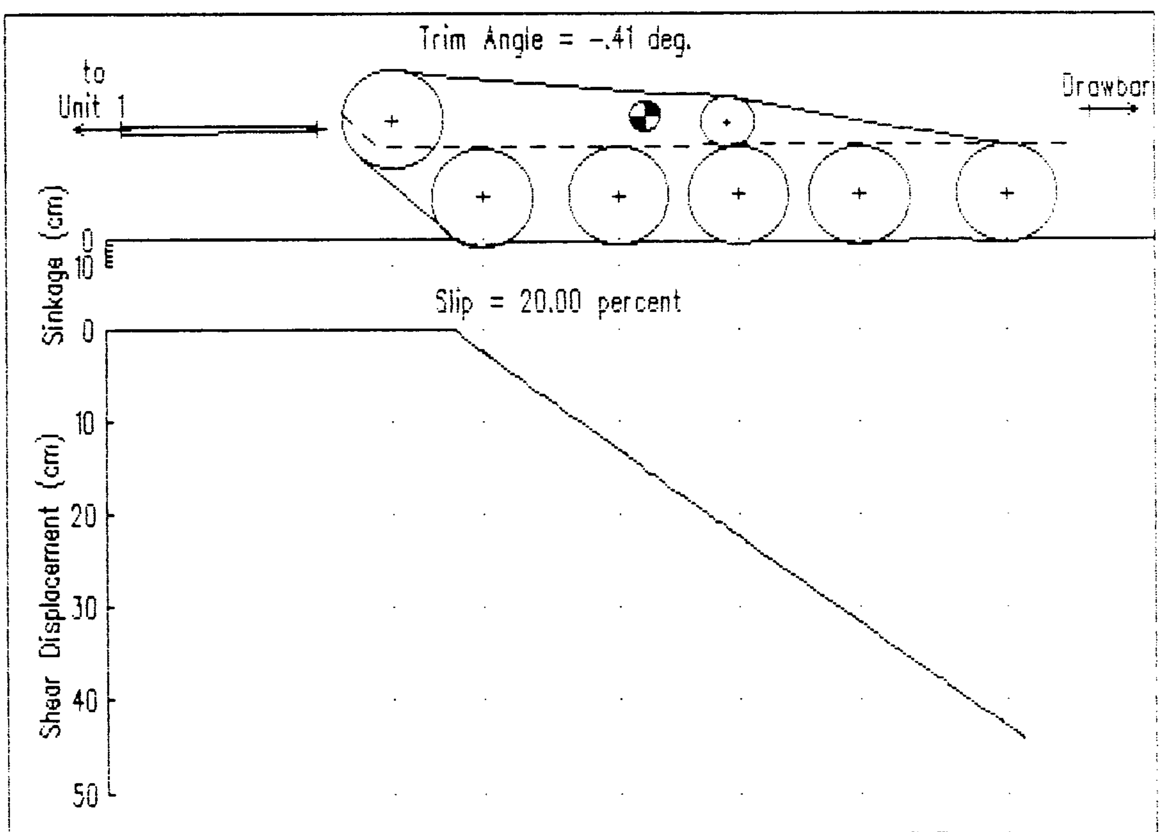

REAR UNIT -- SLIP = 20.00 %

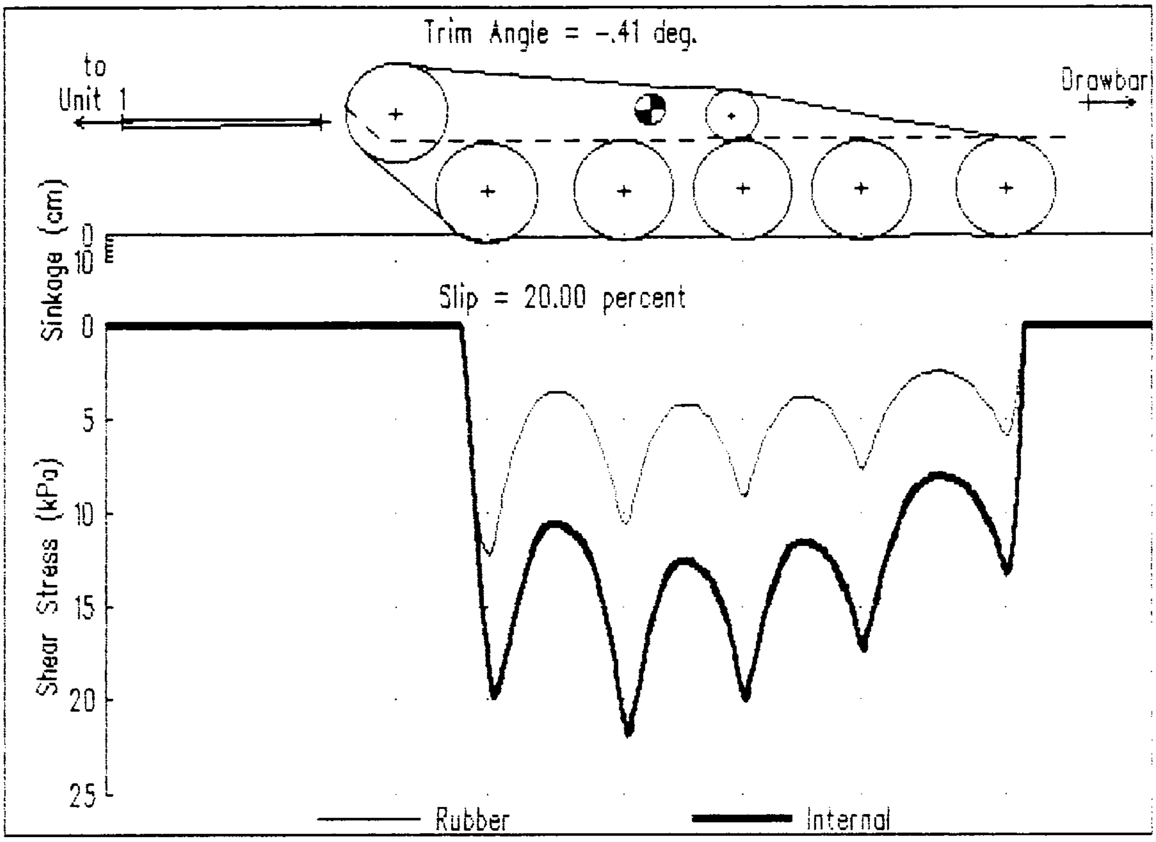

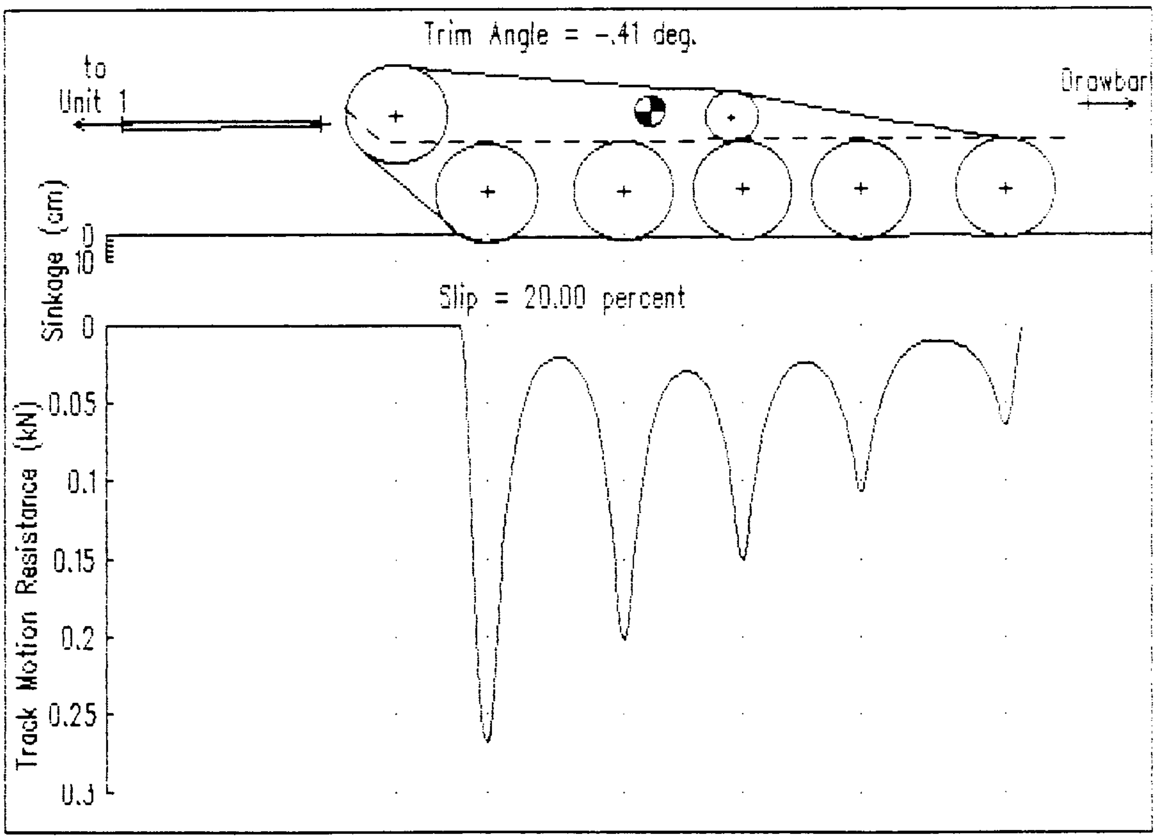

REAR UNIT -- SLIP = 20.00 %

WHEEL	TRACK CONTACT ANGLE LEFT (+ IS CW FROM BDC) (DEG.)	TRACK CONTACT ANGLE RIGHT (+ IS CCW FROM BDC) (DEG.)	LOADS AT THE WHEEL-TERRAIN INTERFACE X (+ IS FORWARD) (KN)	LOADS AT THE WHEEL-TERRAIN INTERFACE Y (+ IS UP) (KN)	LOADS SUPPORTED BY TRACK BETWEEN WHEELS X (+ IS FORWARD) (KN)	LOADS SUPPORTED BY TRACK BETWEEN WHEELS Y (+ IS UP) (KN)
SPR.	185.85	-41.45	.000	.000		
					.000	.000
1	41.45	10.45	.108	.974		
					.821	1.942
2	9.05	8.29	.146	.458		
					.787	1.780
3	7.04	6.83	.110	.320		
					.756	1.629
4	5.59	5.78	.081	.222		
					.776	1.478
T.W.	4.38	171.20	.160	.273		
TOTAL			.605	2.246	3.140	6.829

NOTE: THE LOADS IN THIS TABLE ARE FOR ONE SIDE OF THE VEHICLE ONLY.

WHEEL	SINKAGE (CM)	AXLE LOADS X (+ IS FORWARD) (KN)	AXLE LOADS Y (+ IS UP) (KN)	TRACK TENSION AT LEFT CONTACT POINT (KN)	TRACK TENSION MEAN (KN)	TRACK TENSION AT RIGHT CONTACT POINT (KN)
SPR.	-27.43	-12.702	-4.494	8.92		5.14
					5.14	
1	2.83	-1.308	5.347	5.14		5.36
					5.76	
2	2.45	-.014	2.339	6.17		6.32
					6.70	
3	2.12	-.003	2.045	7.09		7.20
					7.57	
4	1.79	.003	1.803	7.94		8.02
					8.40	
T.W.	1.39	17.770	2.036	8.79		8.92
					8.92	
TOTAL		3.746	9.075			

NOTE: THE LOADS IN THIS TABLE ARE FOR ONE SIDE OF THE VEHICLE ONLY.

REAR UNIT -- SLIP = 20.00 %

		PER UNIT WEIGHT
BELLY LOAD:	.00 KN	.00 %
BELLY DRAG:	.00 KN	.00 %
TRACK MOTION RESISTANCE:	.04 KN	.20 %
TOTAL EXTERNAL MOTION RESISTANCE:	.04 KN	.20 %
THRUST:	7.53 KN	41.71 %
TRACTIVE EFFICIENCY:	79.61 %	

CHASSIS TRIM ANGLE:	-.41 DEG
EFFECTIVE RADIUS OF TRACK:	6.40 CM
RUBBER PAD LOAD / TOTAL TRACK LINK LOAD:	59.1 %

PERFORMANCE OF THE ARTICULATED VEHICLE -- SLIP = 20.00 %

		PER UNIT WEIGHT
TOTAL BELLY LOAD:	.00 KN	.00 %
TOTAL BELLY DRAG:	.00 KN	.00 %
TOTAL TRACK MOTION RESISTANCE:	.13 KN	.29 %
TOTAL EXTERNAL MOTION RESISTANCE:	.13 KN	.29 %
TOTAL THRUST:	18.06 KN	39.26 %
TOTAL DRAWBAR PULL:	17.93 KN	38.98 %
TRACTIVE EFFICIENCY:	79.42 %	

SUMMARY
****

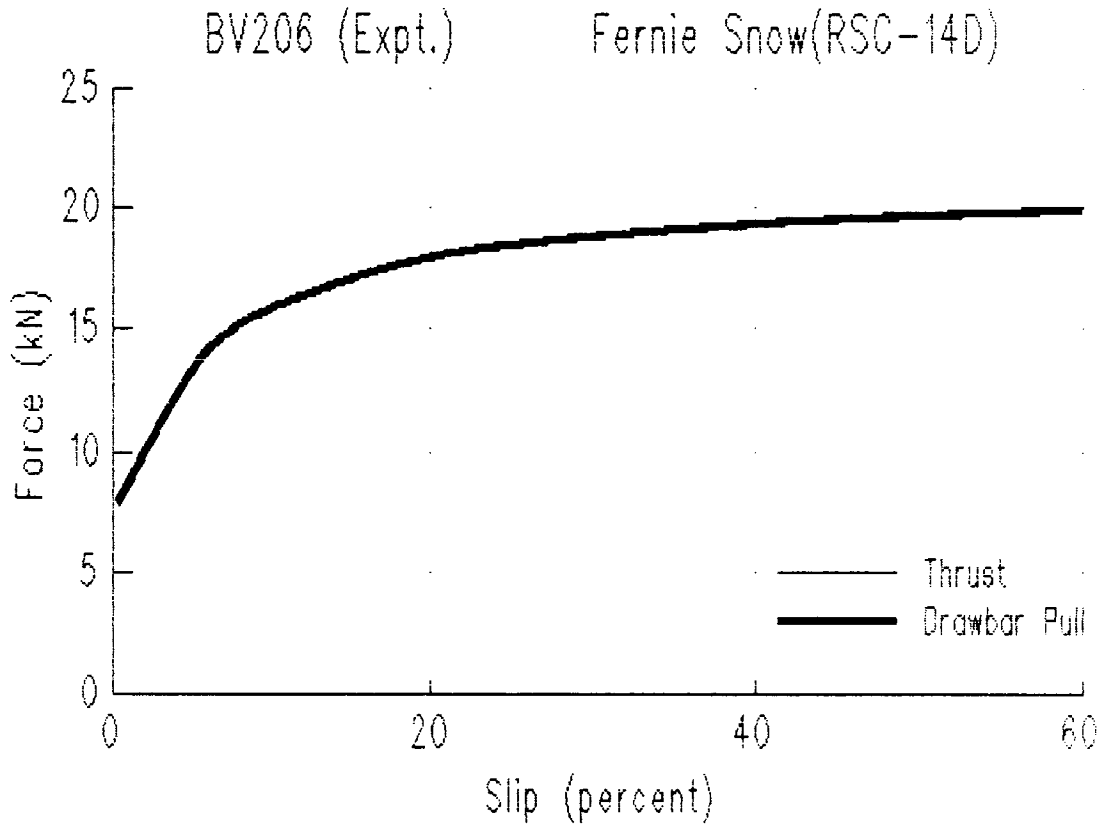
BV206 (Expt.) Fernie Snow(RSC-14D)
25
20
15
10
5
0
Force (kN)
0
20
40
60
Slip (percent)
Thrust
Drawbar Pull

SUMMARY
****

SLIP (%)	BELLY LOAD (KN)	BELLY LOAD PER UNIT VEHICLE WEIGHT (%)	BELLY DRAG (KN)	BELLY DRAG PER UNIT VEHICLE WEIGHT (%)	TRACK MOTION RESISTANCE (KN)	TRACK MOTION RESISTANCE PER UNIT VEHICLE WEIGHT (%)
2.00	.00	.00	.00	.00	.09	.19
5.00	.00	.00	.00	.00	.11	.24
10.00	.00	.00	.00	.00	.12	.27
20.00	.00	.00	.00	.00	.13	.29
30.00	.00	.00	.00	.00	.13	.29
40.00	.00	.00	.00	.00	.14	.29
60.00	.00	.00	.00	.00	.14	.30

SUMMARY

SLIP (%)	THRUST (KN)	THRUST PER UNIT VEHICLE WEIGHT (%)	TOTAL EXTERNAL MOTION RESISTANCE (KN)	TOTAL EXTERNAL MOTION RESISTANCE PER UNIT VEHICLE WEIGHT (%)	DRAWBAR PULL (KN)	DRAWBAR PULL PER UNIT VEHICLE WEIGHT (%)	TRACTIVE EFFICIENCY (%)
2.00	10.00	21.74	.09	.19	9.92	21.55	97.16
5.00	13.45	29.23	.11	.24	13.34	28.99	94.23
10.00	15.96	34.68	.12	.27	15.83	34.41	89.31
20.00	18.06	39.26	.13	.29	17.93	38.98	79.42
30.00	18.93	41.14	.13	.29	18.79	40.84	69.50
40.00	19.44	42.25	.14	.29	19.30	41.95	59.58
60.00	20.01	43.50	.14	.30	19.88	43.20	39.73

WHEEL SINKAGES (cm)

SLIP	FRONT UNIT		REAR UNIT	
(%)	FRONT ROADWHEEL	REAR ROADWHEEL	FRONT ROADWHEEL	REAR ROADWHEEL
2.00	2.50	3.16	3.13	1.63
5.00	2.34	3.20	2.97	1.71
10.00	2.21	3.23	2.86	1.77
20.00	2.18	3.24	2.83	1.79
30.00	2.12	3.26	2.78	1.81
40.00	2.09	3.26	2.76	1.82
60.00	2.06	3.27	2.74	1.83

APPENDIX C

SAMPLE OUTPUT OF NTVPM-86 FOR UNDISTURBED SNOW

PREDICTION OF TRACKED VEHICLE PERFORMANCE
(MODEL: NTVPM-86)
VEHICLE SYSTEMS DEVELOPMENT CORPORATION
NEPEAN, ONTARIO, CANADA

January 11, 1991

VEHICLE TYPE BV206 (Expt.)

VEHICLE PARAMETERS FOR THE FRONT UNIT:

SPRUNG WEIGHT	23.56 KN
UNSPRUNG WEIGHT	4.50 KN
SPRUNG WEIGHT CENTRE OF GRAVITY X-COORDINATE	134.00 CM
SPRUNG WEIGHT CENTRE OF GRAVITY Y-COORDINATE	-20.97 CM
INITIAL TRACK TENSION	3.53 KN
DOUBLE PIVOT JOINT X-COORDINATE (AT THE REAR OF THE UNIT)	273.00 CM
DOUBLE PIVOT JOINT Y-COORDINATE (AT THE REAR OF THE UNIT)	3.00 CM
LENGTH OF THE INTERCONNECTING LINK	76.00 CM

LEADING PIVOT IS UNRESTRICTED
TRAILING PIVOT IS UNRESTRICTED

FIXED WHEELS

WHEEL RADIUS (CM)	X-COORDINATE OF WHEEL CENTRE (CM)	Y-COORDINATE OF WHEEL CENTRE (CM)	NOTES
19.00	.00	.00	SPROCKET

TORSION BAR SUSPENSION WHEELS

WHEEL RADIUS (CM)	TORSION ARM PIVOTS: X-COORD. (+ IS TO THE REAR) (CM)	TORSION ARM PIVOTS: Y-COORD. (+ IS DOWN) (CM)	TORSION BAR STIFFNESS (KN-M/DEG)	TORSION ARM ANGLES (+ IS CW FROM HORIZONTAL): REBOUND LIMIT (DEG)	FREE POSITION (DEG)	JOUNCE LIMIT (DEG)	TORSION ARM LENGTH (CM)	NOTES
19.00	28.00	7.00	.0530	89.00	76.00	15.00	25.00	T
19.00	68.00	20.00	.0530	89.00	43.00	-15.00	25.00	T
19.00	111.00	20.00	.0530	89.00	43.00	-15.00	25.00	T
19.00	155.00	20.00	.0530	89.00	43.00	-15.00	25.00	T
19.00	214.00	20.00	.0530	17.00	17.00	-20.00	20.00	T

NOTE: T = TRAILING ARM

NOTE: COORDINATE ORIGIN IS AT THE CENTRE OF THE SPROCKET. POSITIVE X- AND Y-COORDINATES ARE TO THE REAR AND DOWN, RESPECTIVELY.

BELLY SHAPE	
WIDTH: 61.0 CM	
COORDINATES (CM)	
X	Y
-20.0	-3.0
-6.0	11.0
260.0	11.0

SUPPORTING ROLLERS	
RADIUS: 10.0 CM	
COORDINATES (CM)	
X	Y
128.0	2.0

TRACK LINK CONTACT AREA			
SINKAGE (CM)		INCRE- MENTAL AREA (CM**2)	PERCENTAGE CAUSING EXTERANL SHEARING
FROM	TO		
.00	.00	76.00	100.0
.00	1.40	64.00	.0
1.40	2.70	71.00	.0
2.70	5.50	351.00	.0

TRACK PARAMETERS FOR THE FRONT UNIT:

WEIGHT PER UNIT LENGTH	.330 KN/M
WIDTH	62.0 CM
PITCH	9.1 CM
HEIGHT OF THE GROUSERS	5.5 CM
THICKNESS	.0 CM
PERCENT EXTERNAL SHEAR AREA FOR COHESIVE SHEARING	13.5 %
LONGITUDINAL ELASTICITY CONSTANT TE (FROM T=TE*E)	10910. KN

NOTE: COORDINATE ORIGIN IS AT THE CENTRE OF THE SPROCKET. POSITIVE X- AND Y- COORDINATES ARE TO THE REAR AND DOWN, RESPECTIVELY.

VEHICLE PARAMETERS FOR THE REAR UNIT:

SPRUNG WEIGHT	13.45 KN
UNSPRUNG WEIGHT	4.50 KN
SPRUNG WEIGHT CENTRE OF GRAVITY X-COORDINATE	105.00 CM
SPRUNG WEIGHT CENTRE OF GRAVITY Y-COORDINATE	-7.23 CM
INITIAL TRACK TENSION	4.69 KN
DOUBLE PIVOT JOINT X-COORDINATE (AT THE FRONT OF THE UNIT)	-29.00 CM
DOUBLE PIVOT JOINT Y-COORDINATE (AT THE FRONT OF THE UNIT)	3.00 CM
DRAWBAR HITCH X-COORDINATE	265.00 CM
DRAWBAR HITCH Y-COORDINATE	-2.00 CM

FIXED WHEELS

WHEEL RADIUS (CM)	X-COORDINATE OF WHEEL CENTRE (CM)	Y-COORDINATE OF WHEEL CENTRE (CM)	NOTES
19.00	.00	.00	SPROCKET

TORSION BAR SUSPENSION WHEELS

WHEEL RADIUS (CM)	TORSION ARM PIVOTS: X-COORD. (+ IS TO THE REAR) (CM)	TORSION ARM PIVOTS: Y-COORD. (+ IS DOWN) (CM)	TORSION BAR STIFFNESS (KN-M/DEG)	TORSION ARM ANGLES (+ IS CW FROM HORIZONTAL): REBOUND LIMIT (DEG)	FREE POSITION (DEG)	JOUNCE LIMIT (DEG)	TORSION ARM LENGTH (CM)	NOTES
19.00	28.00	7.00	.0530	89.00	76.00	15.00	25.00	T
19.00	68.00	20.00	.0530	89.00	43.00	-15.00	25.00	T
19.00	111.00	20.00	.0530	89.00	33.00	-15.00	25.00	T
19.00	155.00	20.00	.0530	89.00	24.00	-15.00	25.00	T
19.00	214.00	20.00	.0530	17.00	8.00	-20.00	20.00	T

NOTE: T = TRAILING ARM

NOTE: COORDINATE ORIGIN IS AT THE CENTRE OF THE SPROCKET. POSITIVE X- AND Y-COORDINATES ARE TO THE REAR AND DOWN, RESPECTIVELY.

BELLY SHAPE	
WIDTH: 61.0 CM	
COORDINATES (CM)	
X	Y
-20.0	-3.0
-6.0	11.0
260.0	11.0

SUPPORTING ROLLERS	
RADIUS: 10.0 CM	
COORDINATES (CM)	
X	Y
128.0	2.0

TRACK LINK CONTACT AREA			
SINKAGE (CM)		INCRE-MENTAL AREA (CM**2)	PERCENTAGE CAUSING EXTERANL SHEARING
FROM	TO		
.00	.00	76.00	100.0
.00	1.40	64.00	.0
1.40	2.70	71.00	.0
2.70	5.50	351.00	.0

TRACK PARAMETERS FOR THE REAR UNIT:

WEIGHT PER UNIT LENGTH	.330 KN/M
WIDTH	62.0 CM
PITCH	9.1 CM
HEIGHT OF THE GROUSERS	5.5 CM
THICKNESS	.0 CM
PERCENT EXTERNAL SHEAR AREA FOR COHESIVE SHEARING	13.5 %
LONGITUDINAL ELASTICITY CONSTANT TE (FROM T=TE*E)	10910. KN

NOTE: COORDINATE ORIGIN IS AT THE CENTRE OF THE SPROCKET. POSITIVE X- AND Y-COORDINATES ARE TO THE REAR AND DOWN, RESPECTIVELY.

FRONT UNIT

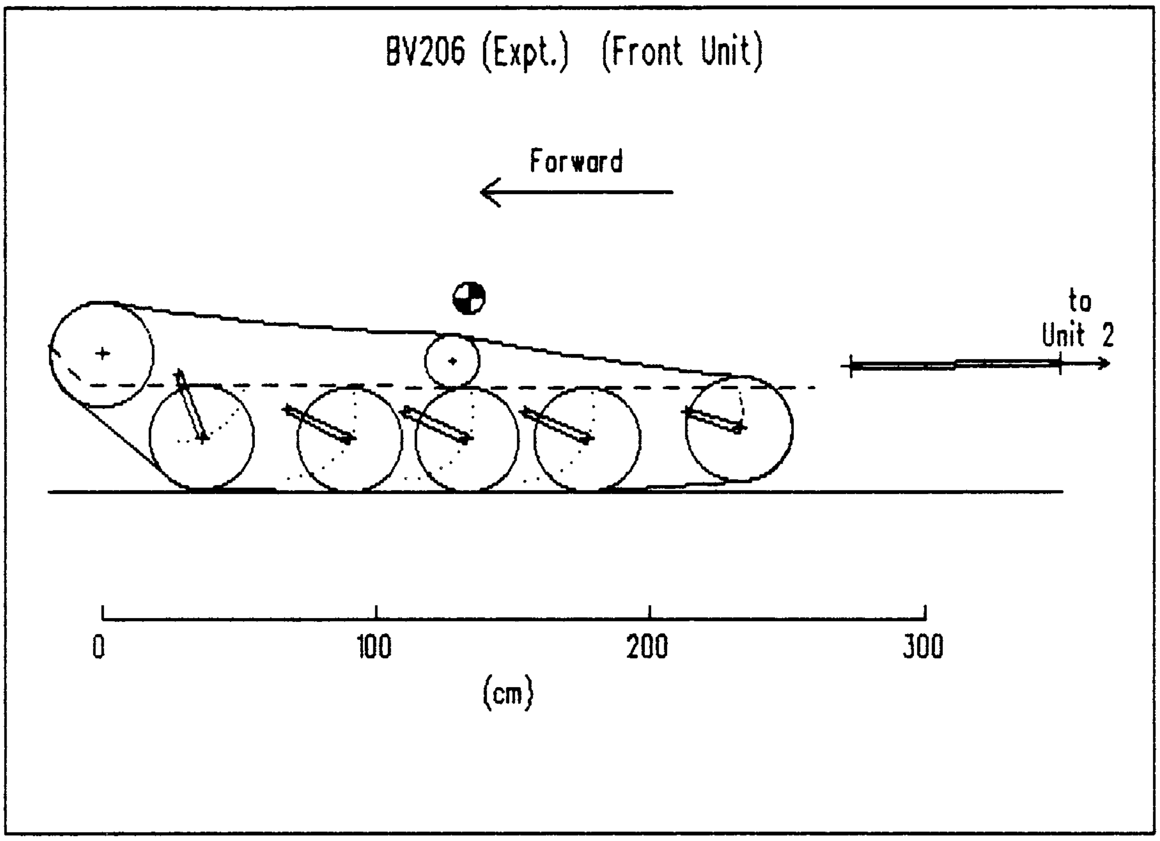

FRONT UNIT - WHEEL LOADS AND GEOMETRY ON LEVEL HARD GROUND

WHEEL	SUSPENSION TYPE	VERTICAL LOADS AT THE TRACK-WHEEL INTERFACE (KN)	TORSION BAR WIND-UP (DEG)	WHEEL CENTRE X-COORDINATE (CM)	WHEEL CENTRE HEIGHT ABOVE GROUND (CM)
SPROCKET	FIXED	.00		.00	50.27
1	TORSION BAR	.00	6.54	36.57	19.61
2	TORSION BAR	4.51	17.75	90.41	19.00
3	TORSION BAR	4.63	18.48	133.54	19.00
4	TORSION BAR	4.60	19.23	177.68	19.00
5	TORSION BAR	.00	.00	232.95	22.86
TOTAL		13.74			

NOTE: THESE LOADS ARE FOR ONE SIDE OF THE VEHICLE ONLY.

CHASSIS TRIM ANGLE (+ IS CW FROM HOR.): .384 DEG
LINK TRIM ANGLE (+ IS CW FROM HOR.): -.725 DEG
VERTICAL FORCE APPLIED TO REAR HITCH (+ IS DOWN): .000 KN
MOMENT APPLIED TO REAR HITCH (+ IS CW): .000 KN-M

NOTE: COORDINATE ORIGIN IS AT THE CENTRE OF THE SPROCKET OF THE FRONT UNIT. POSITIVE X-COORDINATES ARE TO THE REAR.

REAR UNIT

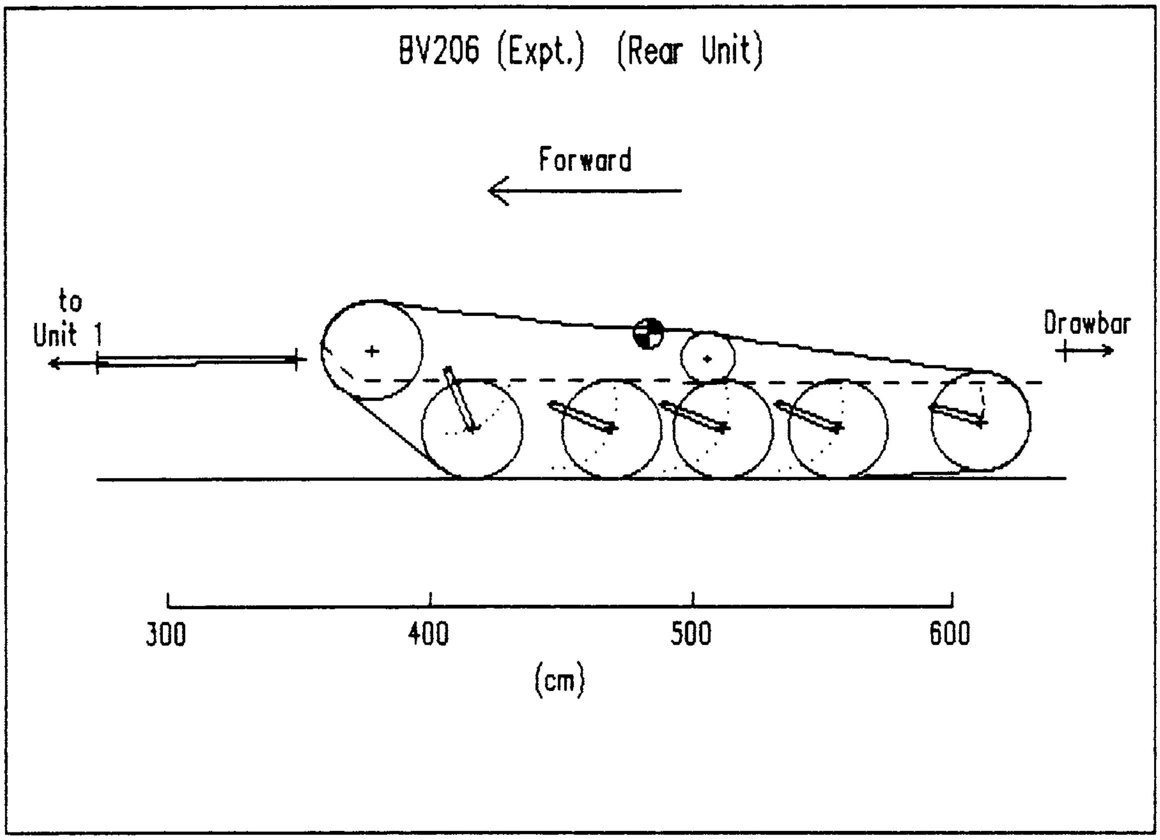

REAR UNIT - WHEEL LOADS AND GEOMETRY ON LEVEL HARD GROUND

WHEEL	SUSPENSION TYPE	VERTICAL LOADS AT THE TRACK-WHEEL INTERFACE (KN)	TORSION BAR WIND-UP (DEG)	WHEEL CENTRE X-COOR-DINATE (CM)	WHEEL CENTRE HEIGHT ABOVE GROUND (CM)
SPROCKET	FIXED	.00		377.99	49.22
1	TORSION BAR	-.01	9.18	415.64	19.00
2	TORSION BAR	4.97	20.29	468.86	19.00
3	TORSION BAR	2.82	10.96	511.98	19.00
4	TORSION BAR	.73	2.64	556.09	19.00
5	TORSION BAR	.00	-9.00	610.95	21.91
TOTAL		8.51			

NOTE: THESE LOADS ARE FOR ONE SIDE OF THE VEHICLE ONLY.

CHASSIS TRIM ANGLE (+ IS CW FROM HOR.): .358 DEG
VERTICAL FORCE APPLIED TO FRONT HITCH (+ IS UP): .000 KN
MOMENT APPLIED TO FRONT HITCH (+ IS CCW): .000 KN-M

NOTE: COORDINATE ORIGIN IS AT THE CENTRE OF THE SPROCKET OF THE FRONT UNIT. POSITIVE X-COORDINATES ARE TO THE REAR.

TERRAIN TYPE Fernie Snow (RSF-1)

PRESSURE-SINKAGE PARAMETERS:

KC	FROM EQUATION P=(KC/B+KPHI)*Z**M	.00 KN/M**(M+1)
KPHI	FROM EQUATION P=(KC/B+KPHI)*Z**M	221.12 KN/M**(M+2)
M	FROM EQUATION P=(KC/B+KPHI)*Z**M	.721

PARAMETERS FOR REPETITIVE LOADING:

KO	FROM EQUATION KR=KO+AU*ZU	.0 KPA/M
AU	FROM EQUATION KR=KO+AU*ZU	33333.0 KPA/M**2

SHEAR STRENGTH PARAMETERS:

EXTERANL SHEARING:

PHI	FROM MOHR-COULOMB EQUATION	11.4 DEG.
C	FROM MOHR-COULOMB EQUATION	.21 KPA
K	FROM EXPONENTIAL SHEAR EQUATION	.39 CM

INTERNAL SHEARING OF THE TERRAIN:

PHI	FROM MOHR-COULOMB EQUATION	25.0 DEG.
C	FROM MOHR-COULOMB EQUATION	1.96 KPA
K	FROM EXPONENTIAL SHEAR EQUATION	5.50 CM

SIDE THRUST NOT INCLUDED.

VEHICLE BELLY SHEARING:

PHI	FROM MOHR-COULOMB EQUATION	5.7 DEG.
C	FROM MOHR-COULOMB EQUATION	.00 KPA

FRONT UNIT -- SLIP = 20.00 %

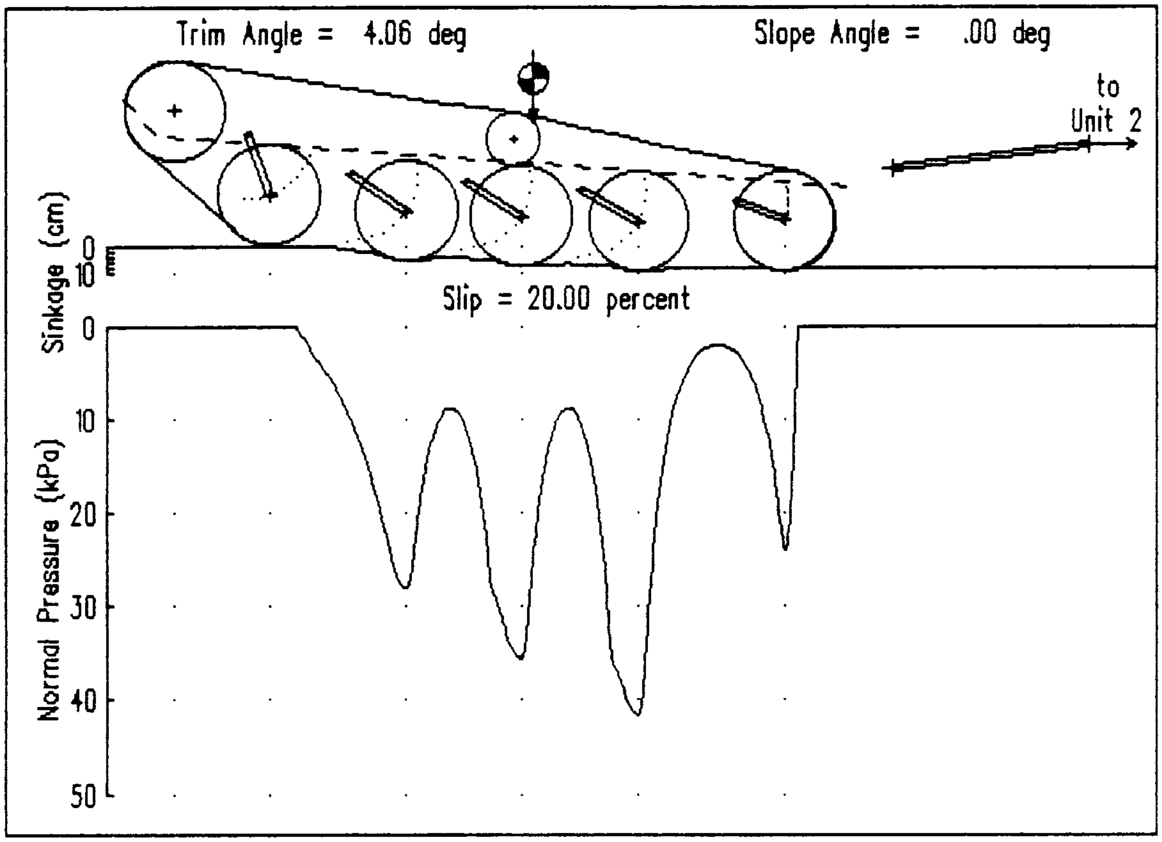

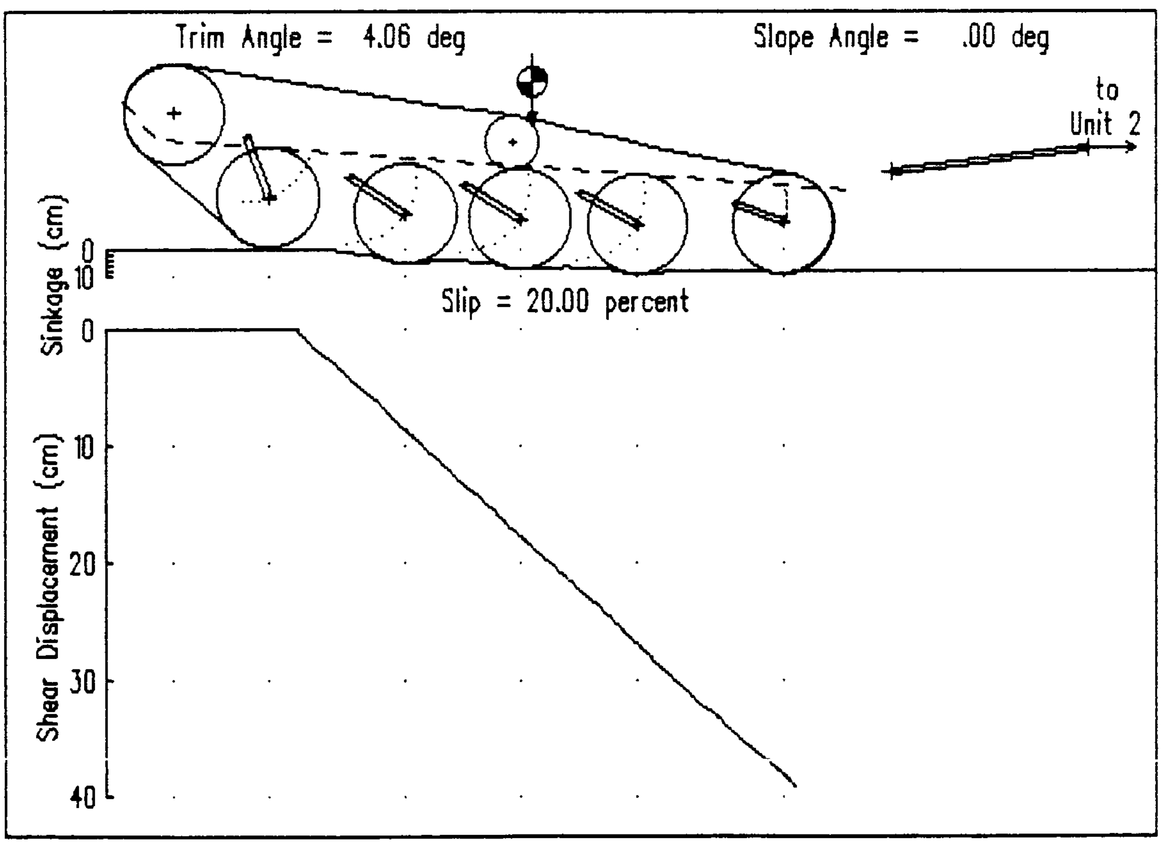

FRONT UNIT -- SLIP = 20.00 %

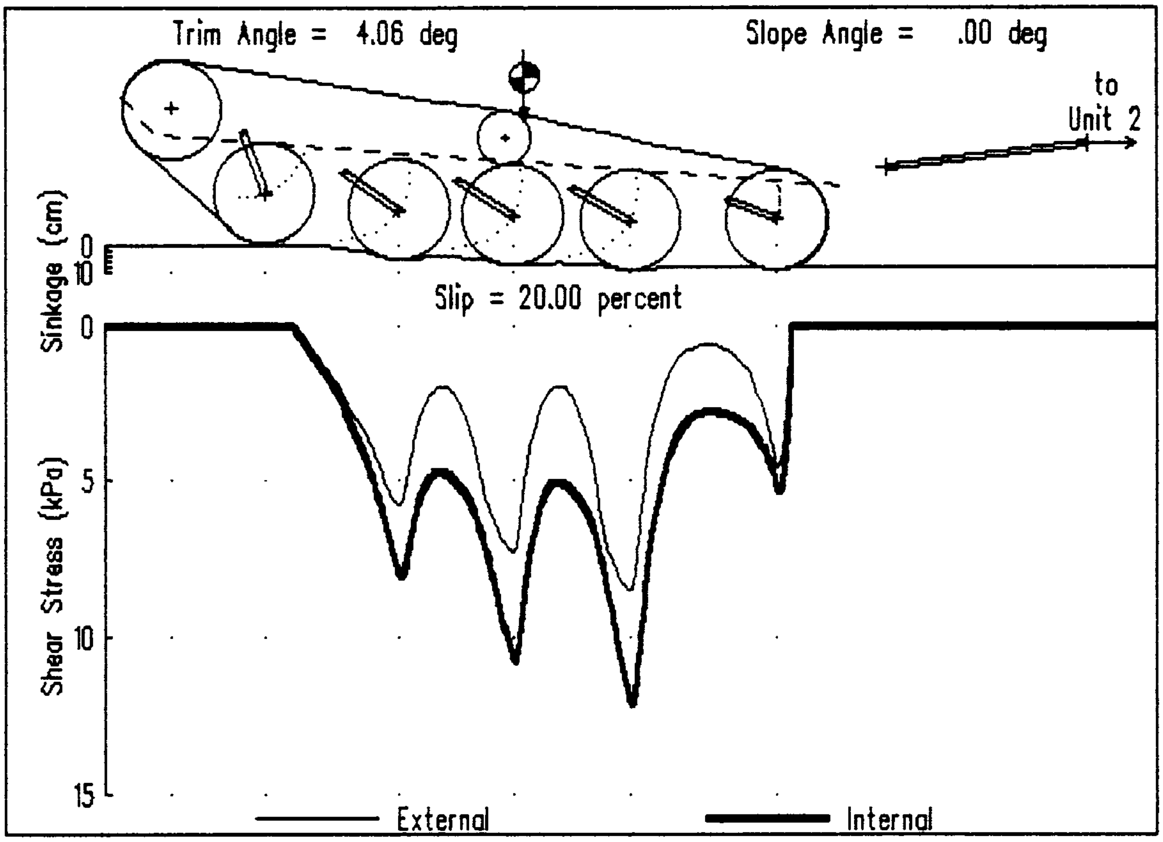

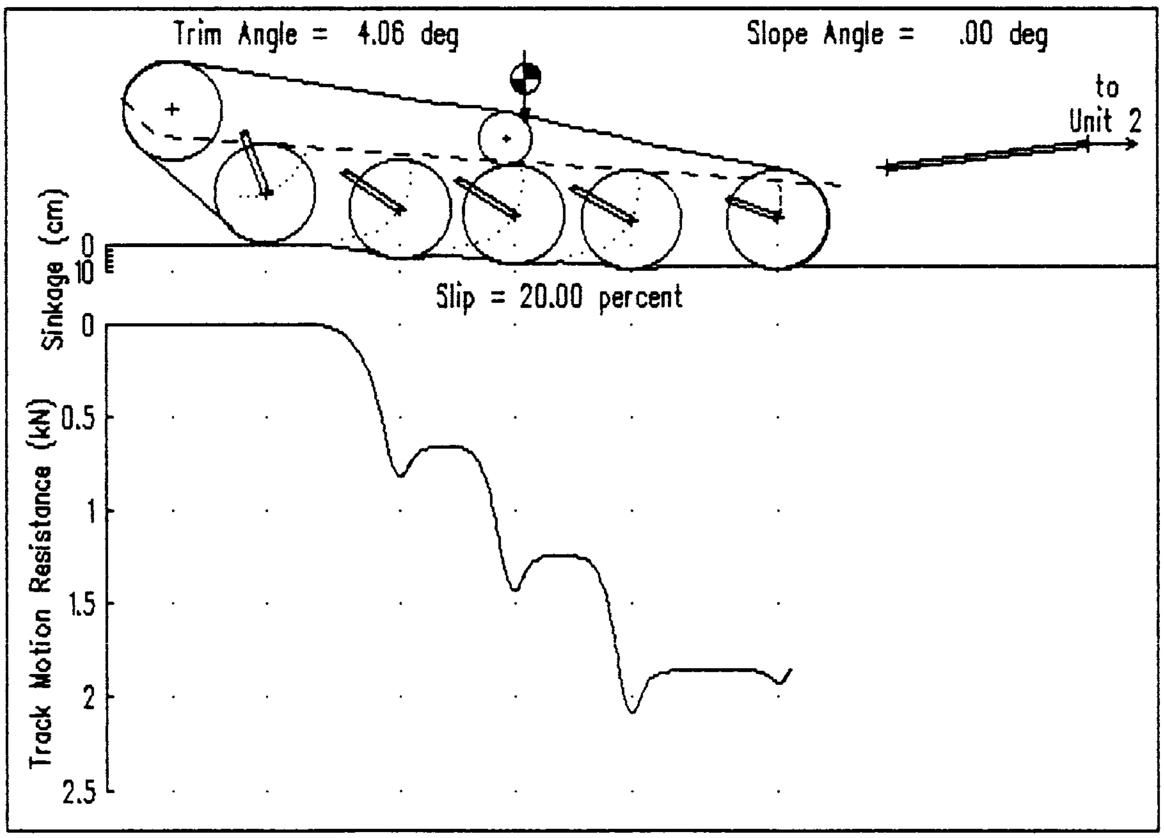

FRONT UNIT -- SLIP = 20.00 %

WHEEL	TRACK CONTACT ANGLE		LOADS AT THE WHEEL-TERRAIN INTERFACE		LOADS SUPPORTED BY TRACK BETWEEN WHEELS	
	LEFT (+ IS CW FROM BDC) (DEG.)	RIGHT (+ IS CCW FROM BDC) (DEG.)	X (+ IS FORWARD) (KN)	Y (+ IS UP) (KN)	X (+ IS FORWARD) (KN)	Y (+ IS UP) (KN)
SPR.	190.38	-42.33	.000	.000		
					.000	.000
1	42.33	-2.23	.000	.000		
					.117	1.540
2	19.63	8.14	.198	1.092		
					.726	2.659
3	17.17	8.00	.272	1.272		
					.866	3.135
4	16.15	7.93	.299	1.425		
					1.080	1.929
5	4.83	169.62	.187	.516		
TOTAL			.955	4.306	2.789	9.263

NOTE: THE LOADS IN THIS TABLE ARE FOR ONE SIDE OF THE VEHICLE ONLY.

WHEEL	SINK-AGE	AXLE LOADS		TORSION BAR WIND-UP	TRACK TENSION		
	(CM)	X (+ IS FORWARD) (KN)	Y (+ IS UP) (KN)	(DEG)	AT LEFT CONTACT POINT (KN)	MEAN (KN)	AT RIGHT CONTACT POINT (KN)
SPR.	-32.97	-12.814	-4.888		9.478		4.722
						4.722	
1	-.42	-1.227	2.546	9.45	4.722		4.722
						4.928	
2	5.72	-.352	3.137	13.21	5.134		5.440
						5.918	
3	7.93	-.323	3.653	15.47	6.397		6.772
						7.327	
4	9.84	-.337	4.312	18.64	7.883		8.287
						8.804	
5	9.31	18.798	2.559	.00	9.321		9.478
						9.478	
TOTAL		3.744	11.319				

NOTE: THE LOADS IN THIS TABLE ARE FOR ONE SIDE OF THE VEHICLE ONLY.

FRONT UNIT -- SLIP = 20.00 %

			PERCENTAGE OF NORMAL LOAD
GRADE:	.00 DEG	.00 %	
BELLY LOAD:		.00 KN	.00 %
BELLY DRAG:		.00 KN	.00 %
TRACK MOTION RESISTANCE:		1.94 KN	7.15 %
TOTAL EXTERNAL MOTION RESISTANCE:		1.94 KN	7.15 %
THRUST:		9.43 KN	34.75 %
HOR. FORCE APPLIED TO REAR HITCH (+ REARWARD):		7.49 KN	27.59 %
VERT. FORCE APPLIED TO REAR HITCH (+ IS DOWN):		-.92 KN	-3.40 %
MOMENT APPLIED TO REAR HITCH (+ IS CW):		-.01 KN-M	
TRACTIVE EFFICIENCY:		63.53 %	

CHASSIS TRIM ANGLE (+ IS CW FROM HOR.):	4.06 DEG
LINK TRIM ANGLE (+ IS CW FROM HOR.):	-7.00 DEG
EFFECTIVE RADIUS OF TRACK:	11.26 CM
LOAD ON EXTERNAL SHEAR AREA / TOTAL TRACK LINK LOAD:	19.1 %

REAR UNIT -- SLIP = 20.00 %

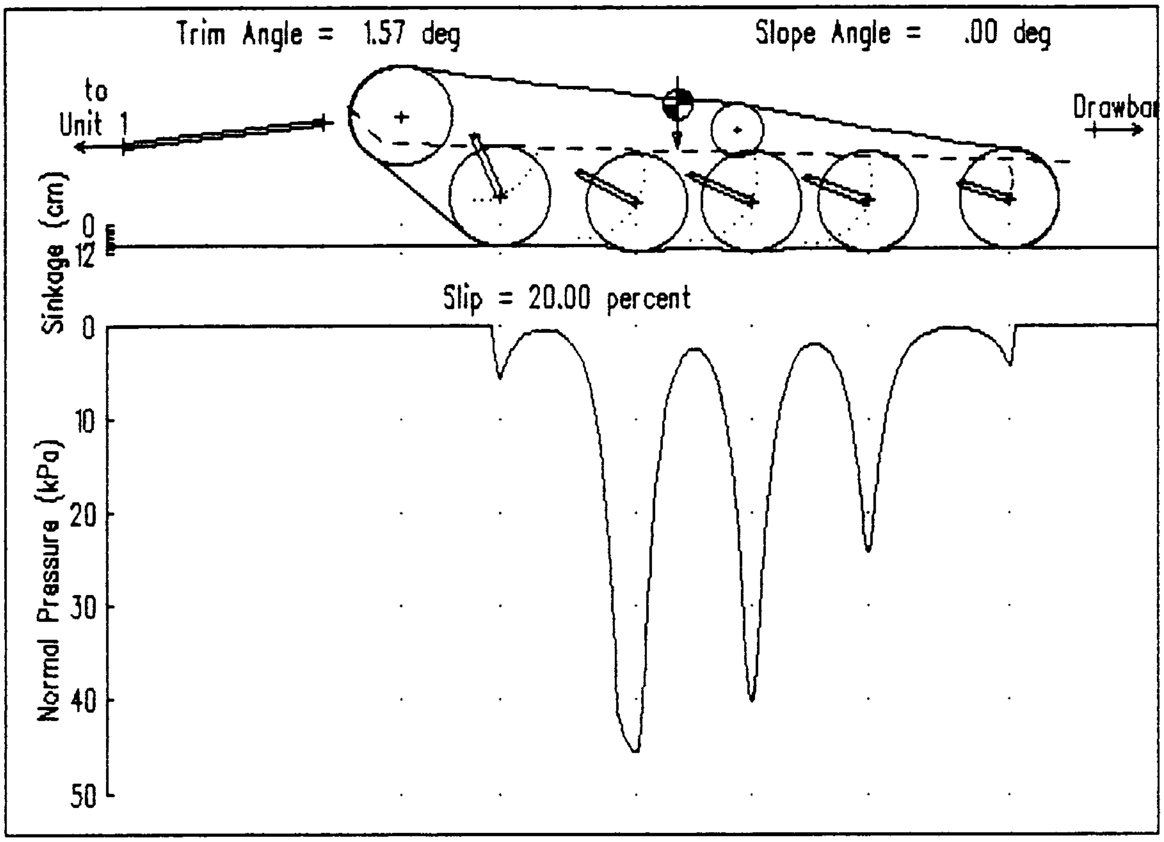

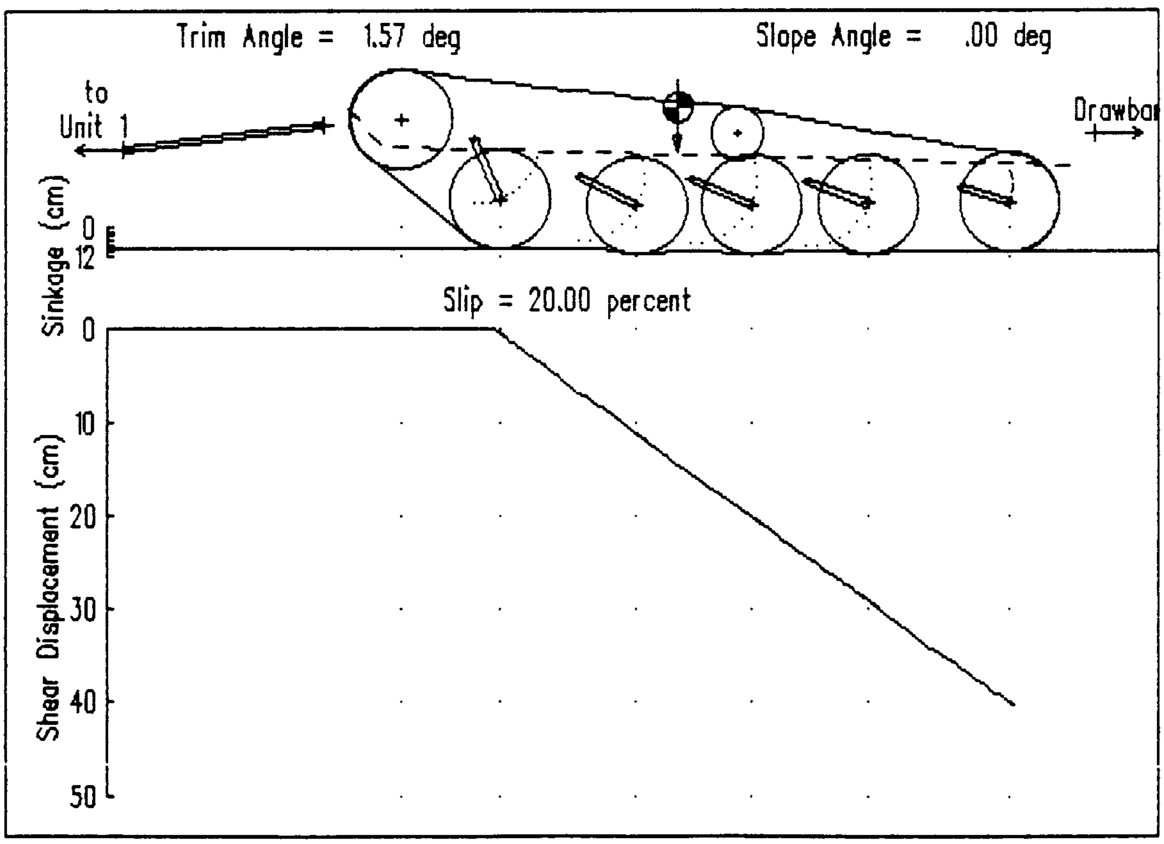

REAR UNIT -- SLIP = 20.00 %

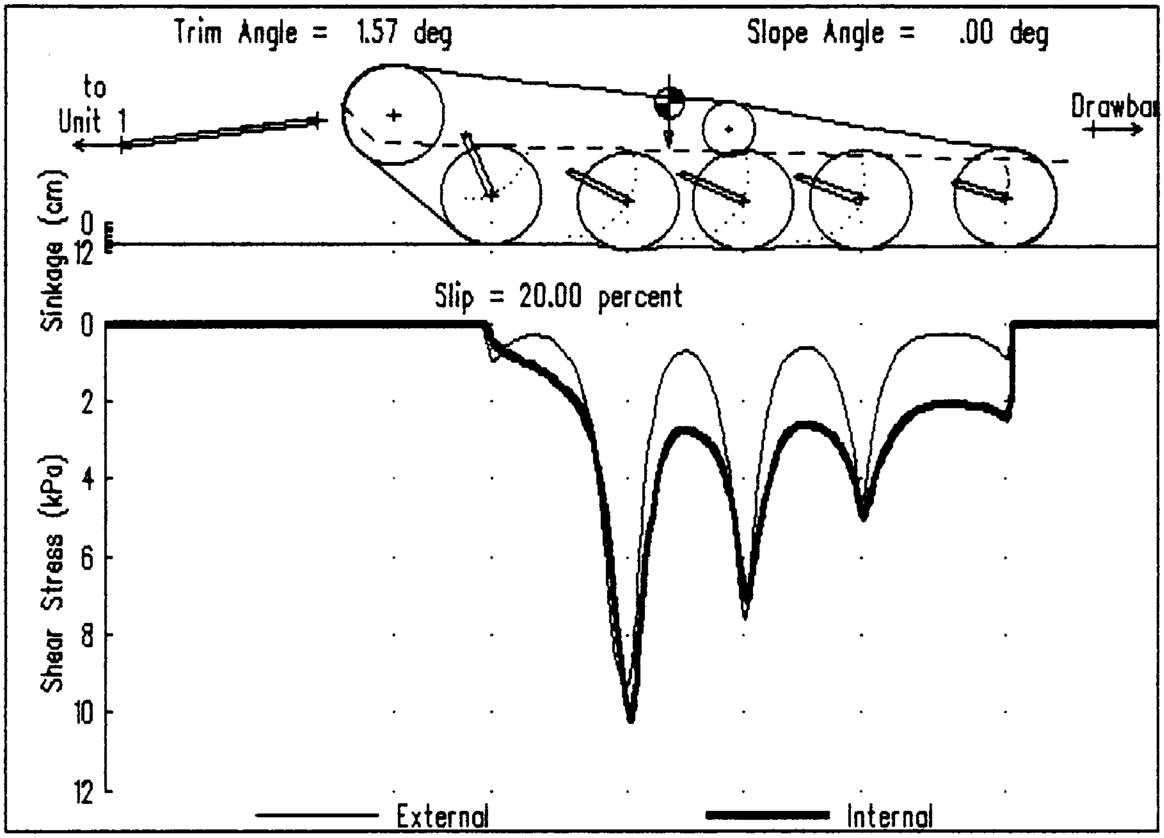

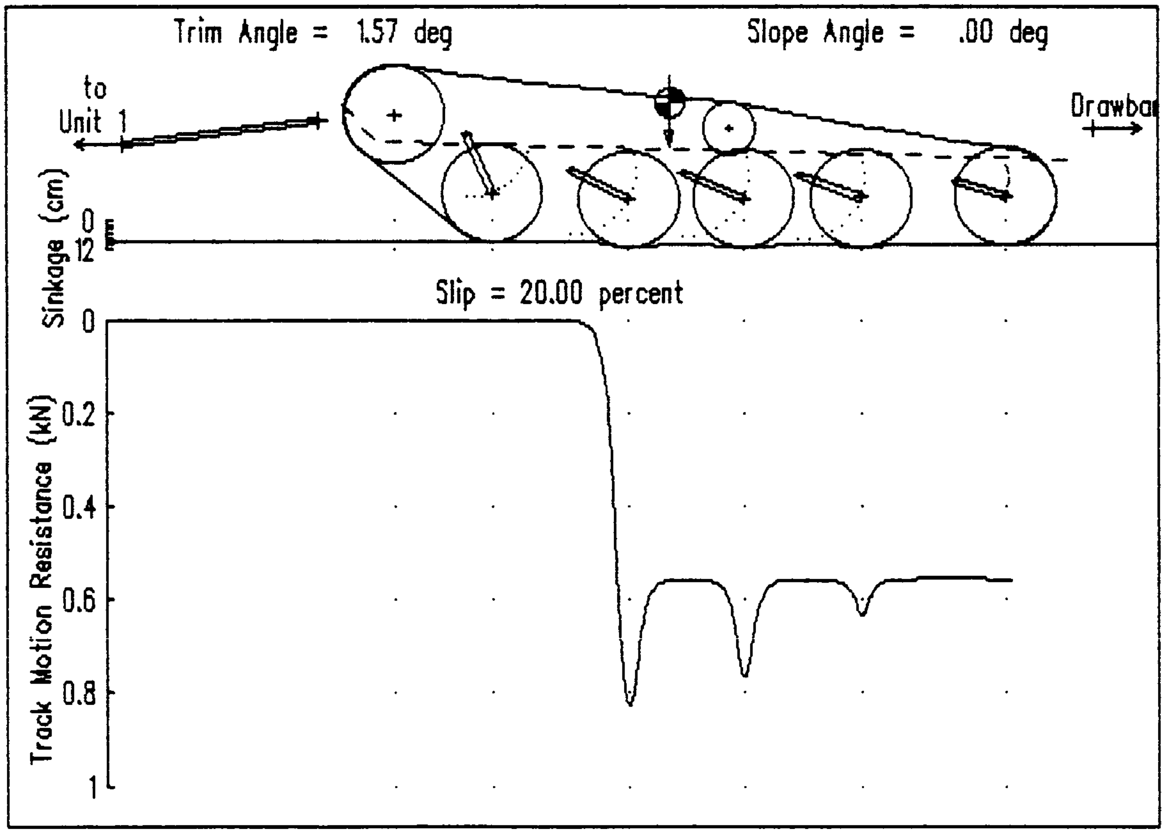

REAR UNIT -- SLIP = 20.00 %

WHEEL	TRACK CONTACT ANGLE		LOADS AT THE WHEEL-TERRAIN INTERFACE		LOADS SUPPORTED BY TRACK BETWEEN WHEELS	
	LEFT (+ IS CW FROM BDC) (DEG.)	RIGHT (+ IS CCW FROM BDC) (DEG.)	X (+ IS FORWARD) (KN)	Y (+ IS UP) (KN)	X (+ IS FORWARD) (KN)	Y (+ IS UP) (KN)
SPR.	187.89	-39.62	.000	.000		
					.000	.000
1	39.62	1.74	.002	.067		
					.245	1.724
2	17.28	9.49	.268	1.895		
					.773	1.904
3	8.53	8.13	.186	1.006		
					.771	1.620
4	5.24	5.04	.085	.387		
					.749	.801
5	1.00	172.11	.032	.036		
TOTAL			.574	3.390	2.538	6.050

NOTE: THE LOADS IN THIS TABLE ARE FOR ONE SIDE OF THE VEHICLE ONLY.

WHEEL	SINK-AGE	AXLE LOADS		TORSION BAR WIND-UP	TRACK TENSION		
	(CM)	X (+ IS FORWARD) (KN)	Y (+ IS UP) (KN)	(DEG)	AT LEFT CONTACT POINT (KN)	MEAN (KN)	AT RIGHT CONTACT POINT (KN)
SPR.	-22.13	-11.884	-4.208		8.246		4.824
						4.824	
1	8.76	-1.108	2.839	9.93	4.824		4.828
						5.070	
2	11.19	-.299	3.965	17.27	5.311		5.717
						6.100	
3	11.05	-.008	2.461	10.63	6.483		6.672
						7.040	
4	10.62	-.003	1.273	5.65	7.408		7.494
						7.855	
5	10.09	16.414	.861	-9.00	8.215		8.246
						8.246	
TOTAL		3.112	7.191				

NOTE: THE LOADS IN THIS TABLE ARE FOR ONE SIDE OF THE VEHICLE ONLY.

REAR UNIT -- SLIP = 20.00 %

GRADE:	.00 DEG	.00 %	PERCENTAGE OF NORMAL LOAD
BELLY LOAD:		.00 KN	.00 %
BELLY DRAG:		.00 KN	.00 %
TRACK MOTION RESISTANCE:		.60 KN	3.16 %
TOTAL EXTERNAL MOTION RESISTANCE:		.60 KN	3.16 %
THRUST:		6.82 KN	36.12 %
DRAWBAR PULL:		13.71 KN	72.62 %
HOR. FORCE APPLIED TO FRONT HITCH (+ FORWARD):		7.49 KN	39.66 %
VERT. FORCE APPLIED TO FRONT HITCH (+ IS UP):		-.93 KN	-4.93 %
MOMENT APPLIED TO FRONT HITCH (+ IS CCW):		.00 KN-M	
TRACTIVE EFFICIENCY:		73.01 %	

CHASSIS TRIM ANGLE (+ IS CW FROM HOR.):	1.57 DEG
EFFECTIVE RADIUS OF TRACK:	11.86 CM
LOAD ON EXTERNAL SHEAR AREA / TOTAL TRACK LINK LOAD:	17.2 %

PERFORMANCE OF THE ARTICULATED VEHICLE -- SLIP = 20.00 %

GRADE:	.00 DEG	.00 %	PERCENTAGE OF NORMAL LOAD
TOTAL BELLY LOAD:		.00 KN	.00 %
TOTAL BELLY DRAG:		.00 KN	.00 %
TOTAL TRACK MOTION RESISTANCE:		2.54 KN	5.52 %
TOTAL EXTERNAL MOTION RESISTANCE:		2.54 KN	5.52 %
TOTAL THRUST:		16.25 KN	35.32 %
TOTAL DRAWBAR PULL:		13.71 KN	29.80 %
TRACTIVE EFFICIENCY:		67.51 %	

SUMMARY

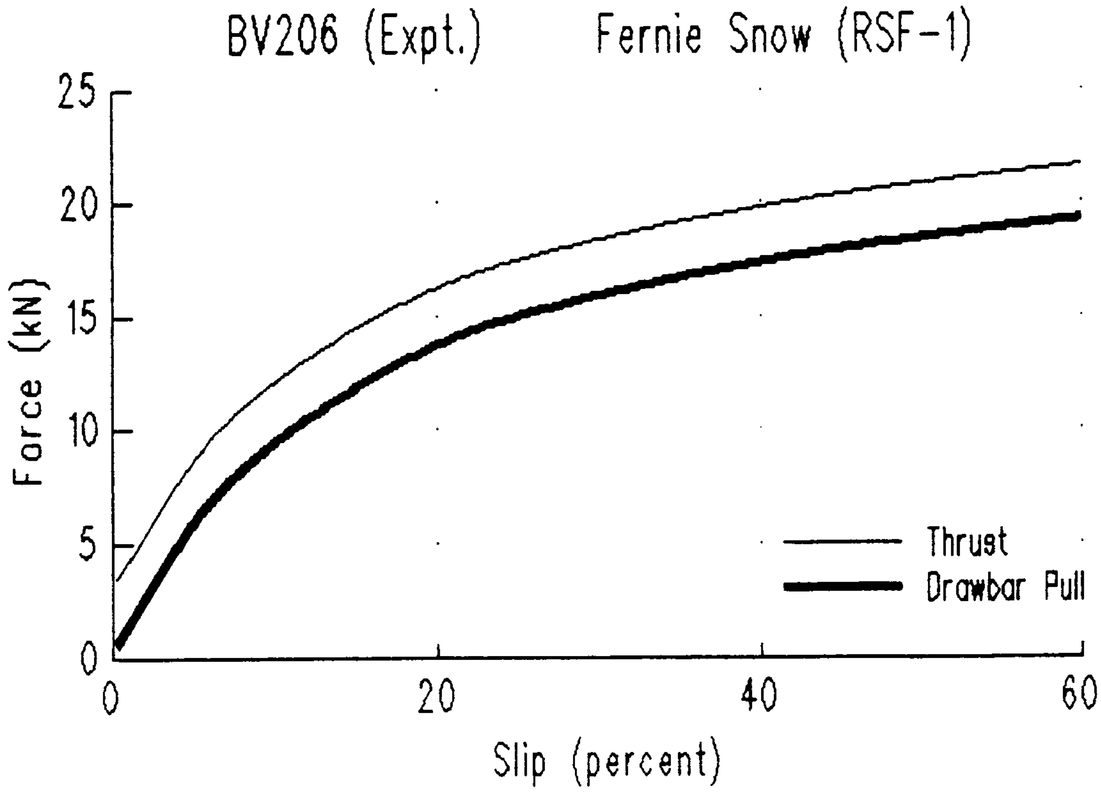
BV206 (Expt.) Fernie Snow (RSF-1)
25
20
15
10
5
0
Force (kN)
0
20
40
60
Slip (percent)
Thrust
Drawbar Pull

SUMMARY

SLIP	BELLY LOAD		BELLY DRAG		TRACK MOTION RESISTANCE	
		PERCENTAGE OF NORMAL LOAD		PERCENTAGE OF NORMAL LOAD		PERCENTAGE OF NORMAL LOAD
(%)	(KN)	(%)	(KN)	(%)	(KN)	(%)
2.00	.00	.00	.00	.00	2.87	6.23
5.00	.00	.00	.00	.00	2.78	6.05
10.00	.00	.00	.00	.00	2.69	5.86
20.00	.00	.00	.00	.00	2.54	5.52
30.00	.00	.00	.00	.00	2.47	5.37
40.00	.00	.00	.00	.00	2.42	5.27
60.00	.00	.00	.00	.00	2.37	5.14

SLIP	THRUST		TOTAL EXTERNAL MOTION RESISTANCE		DRAWBAR PULL		TRACTIVE EFFICIENCY
		PERCENTAGE OF NORMAL LOAD		PERCENTAGE OF NORMAL LOAD		PERCENTAGE OF NORMAL LOAD	
(%)	(KN)	(%)	(KN)	(%)	(KN)	(%)	(%)
2.00	5.37	11.68	2.87	6.23	2.51	5.45	45.72
5.00	8.63	18.76	2.78	6.05	5.85	12.72	64.39
10.00	12.09	26.28	2.69	5.86	9.40	20.42	69.95
20.00	16.25	35.32	2.54	5.52	13.71	29.80	67.51
30.00	18.37	39.92	2.47	5.37	15.90	34.55	60.59
40.00	19.80	43.03	2.42	5.27	17.37	37.76	52.65
60.00	21.63	47.01	2.37	5.14	19.26	41.86	35.62

NOTE: GRADE = .00 DEG = .00 % FOR ALL SLIPS.

SUMMARY

WHEEL SINKAGES (cm)

SLIP	FRONT UNIT		REAR UNIT	
(%)	FRONT ROADWHEEL	REAR ROADWHEEL	FRONT ROADWHEEL	REAR ROADWHEEL
2.00	.43	11.43	10.47	11.94
5.00	.24	11.19	10.21	11.75
10.00	.04	10.96	9.94	11.56
20.00	-.42	9.84	8.76	10.62
30.00	-.64	9.68	8.59	10.46
40.00	-.79	9.57	8.48	10.35
60.00	-.98	9.45	8.34	10.22

APPENDIX D

SAMPLE OUTPUT OF NTVPM-86 FOR PRECONDITIONED SNOW

TERRAIN TYPE Fernie Snow (RSC-2)

PRESSURE-SINKAGE PARAMETERS:

KC	FROM EQUATION P=(KC/B+KPHI)*Z**M	3.74 KN/M**(M+1)
KPHI	FROM EQUATION P=(KC/B+KPHI)*Z**M	1371.70 KN/M**(M+2)
M	FROM EQUATION P=(KC/B+KPHI)*Z**M	.772

PARAMETERS FOR REPETITIVE LOADING:

KO	FROM EQUATION KR=KO+AU*ZU	.0 KPA/M
AU	FROM EQUATION KR=KO+AU*ZU	33333.0 KPA/M**2

SHEAR STRENGTH PARAMETERS:

EXTERANL SHEARING:

PHI	FROM MOHR-COULOMB EQUATION	12.0 DEG.
C	FROM MOHR-COULOMB EQUATION	.02 KPA
K	FROM EXPONENTIAL SHEAR EQUATION	.39 CM

INTERNAL SHEARING OF THE TERRAIN:

PHI	FROM MOHR-COULOMB EQUATION	29.4 DEG.
C	FROM MOHR-COULOMB EQUATION	.32 KPA
K	FROM EXPONENTIAL SHEAR EQUATION	2.50 CM

SIDE THRUST NOT INCLUDED.

VEHICLE BELLY SHEARING:

PHI	FROM MOHR-COULOMB EQUATION	5.7 DEG.
C	FROM MOHR-COULOMB EQUATION	.00 KPA

FRONT UNIT -- SLIP = 20.00 %

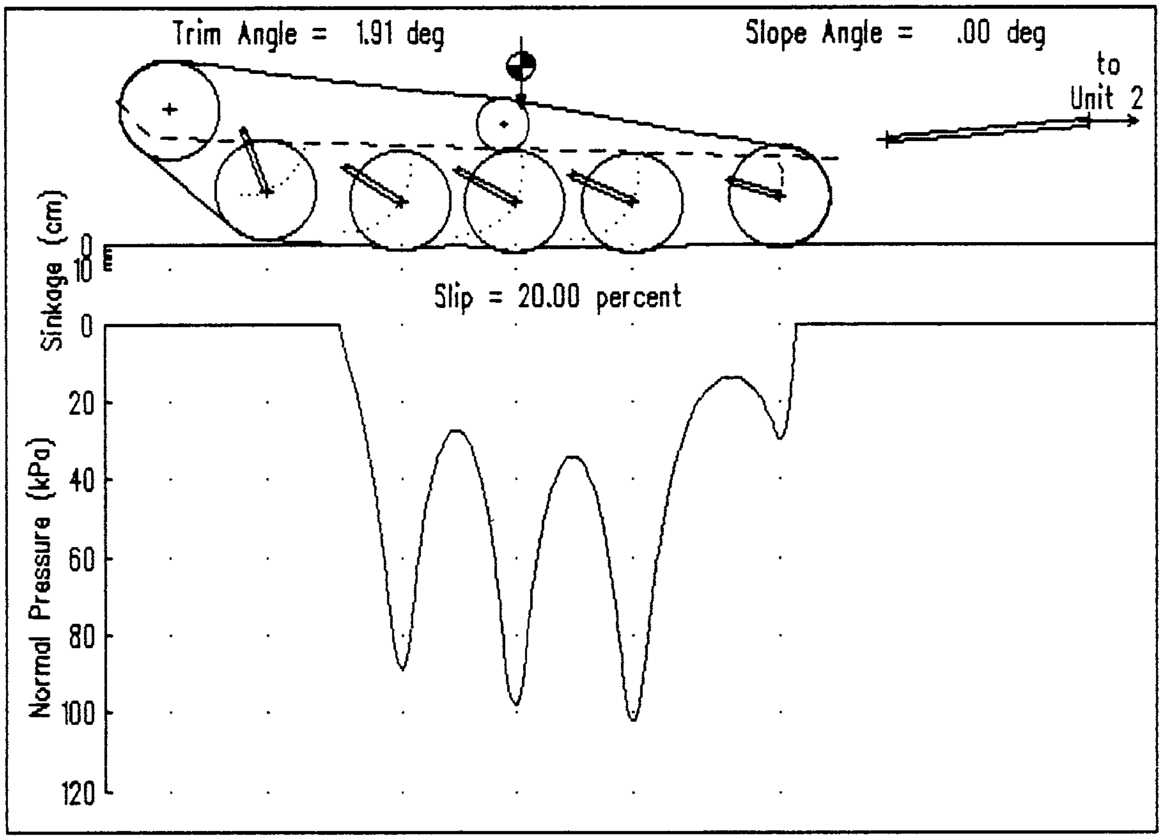

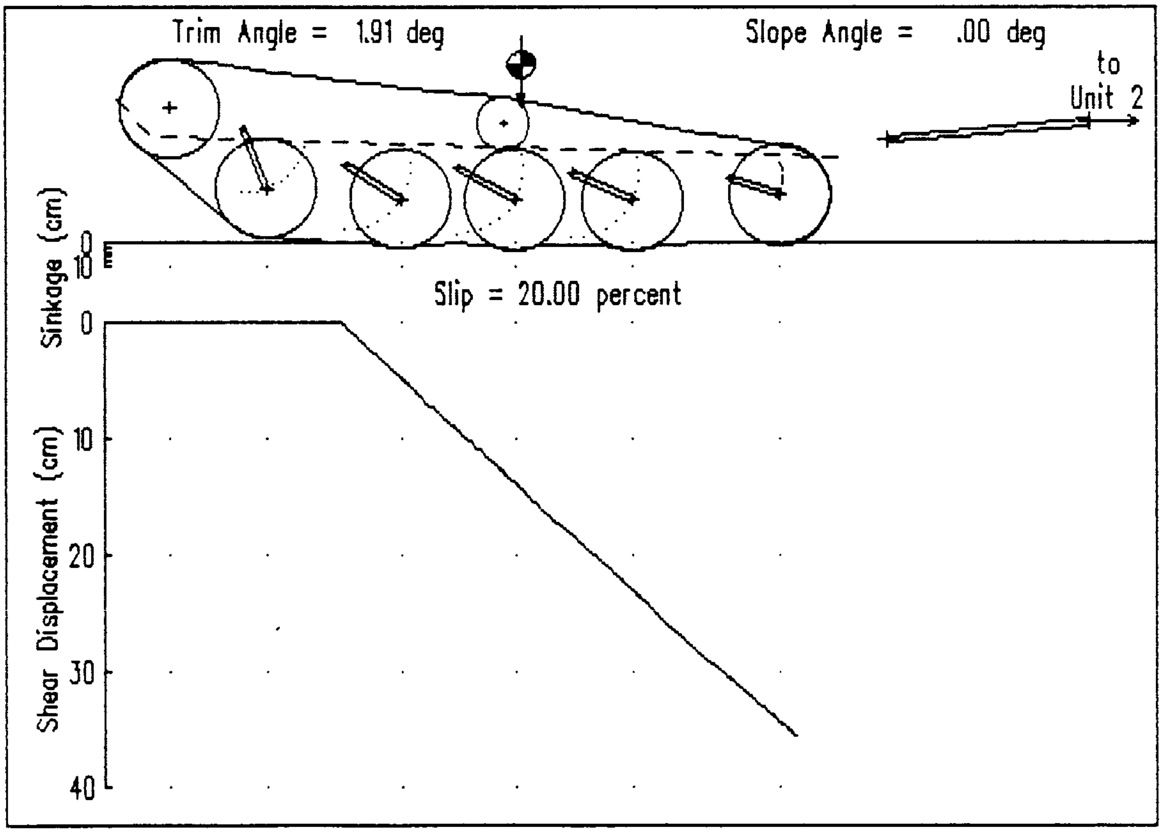

FRONT UNIT -- SLIP = 20.00 %

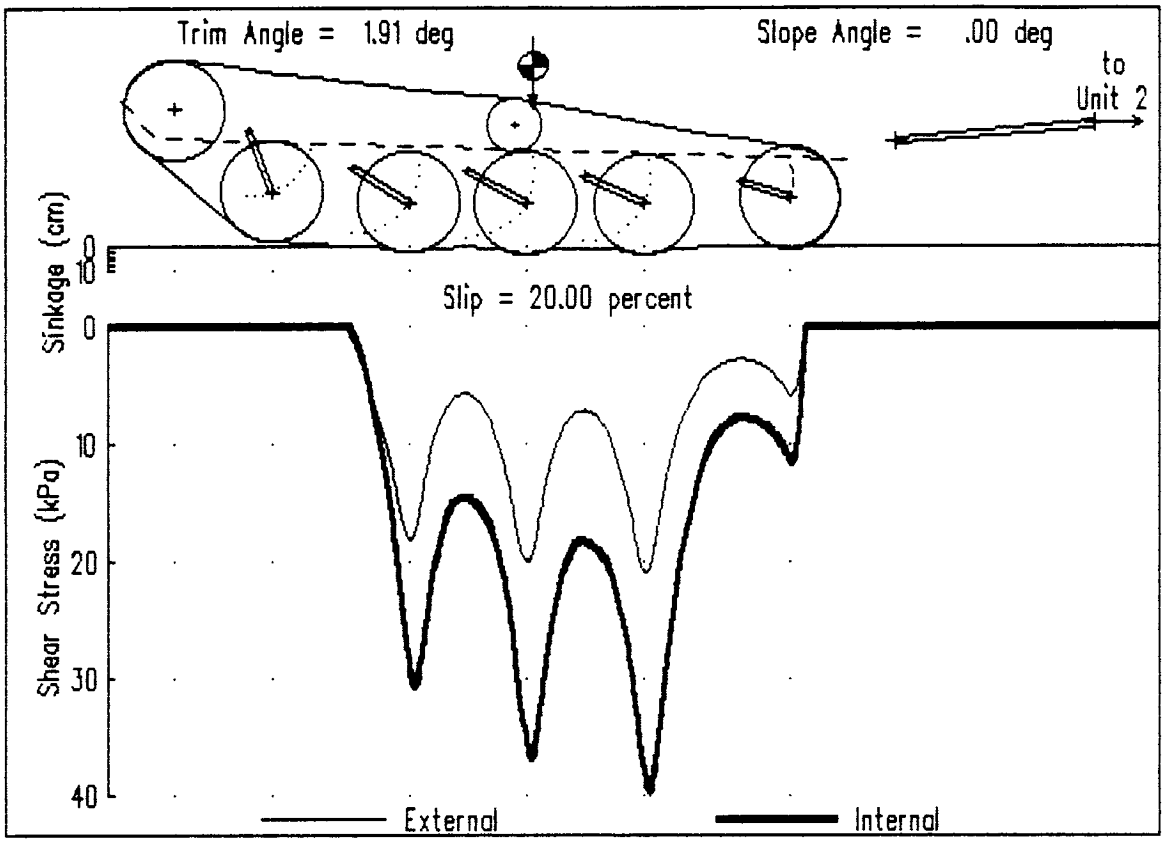

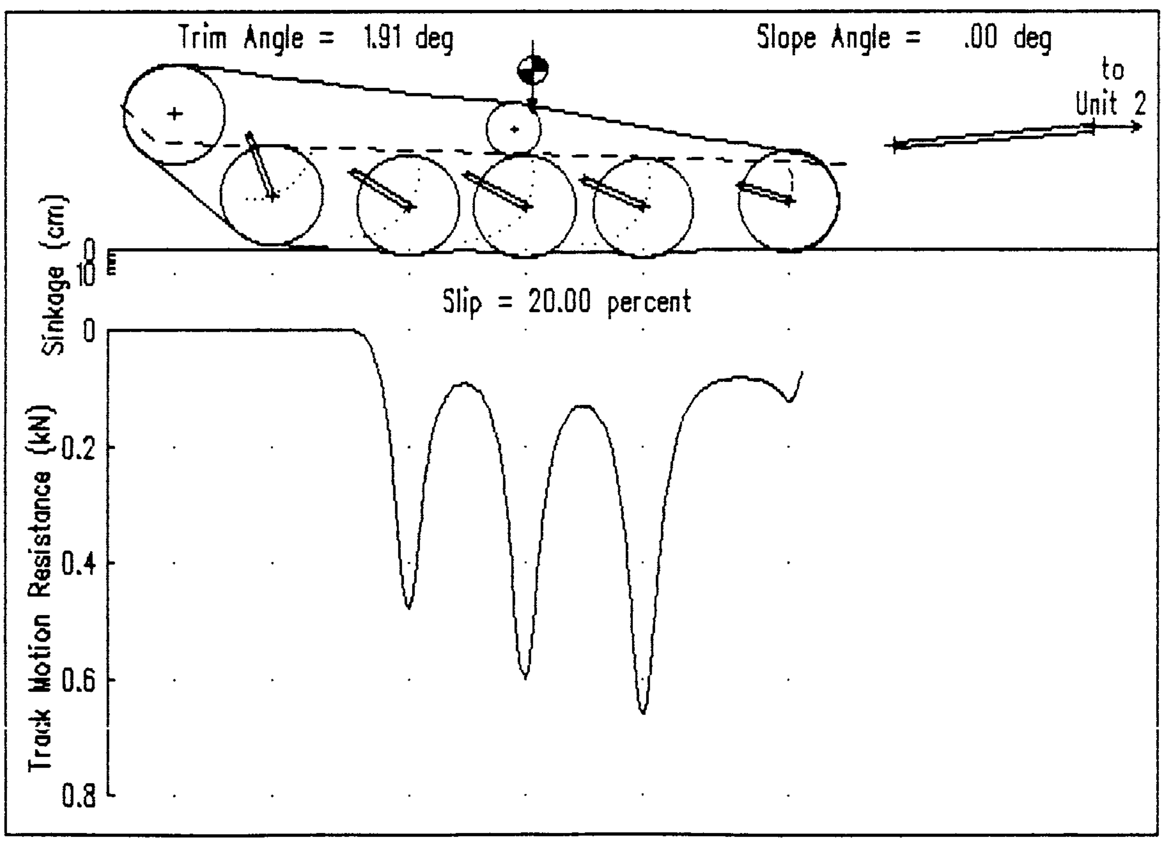

FRONT UNIT -- SLIP = 20.00 %

WHEEL	TRACK CONTACT ANGLE LEFT (+ IS CW FROM BDC) (DEG.)	TRACK CONTACT ANGLE RIGHT (+ IS CCW FROM BDC) (DEG.)	LOADS AT THE WHEEL-TERRAIN INTERFACE X (+ IS FORWARD) (KN)	LOADS AT THE WHEEL-TERRAIN INTERFACE Y (+ IS UP) (KN)	LOADS SUPPORTED BY TRACK BETWEEN WHEELS X (+ IS FORWARD) (KN)	LOADS SUPPORTED BY TRACK BETWEEN WHEELS Y (+ IS UP) (KN)
SPR.	188.23	-40.25	.000	.000		
					.000	.000
1	40.25	-2.83	.000	.000		
					.063	1.040
2	14.53	12.11	.323	1.282		
					.853	2.648
3	13.65	12.18	.387	1.382		
					1.084	3.191
4	12.88	12.59	.425	1.422		
					1.154	2.411
5	3.66	171.77	.118	.263		
TOTAL			1.253	4.349	3.155	9.291

NOTE: THE LOADS IN THIS TABLE ARE FOR ONE SIDE OF THE VEHICLE ONLY.

WHEEL	SINK-AGE (CM)	AXLE LOADS X (+ IS FORWARD) (KN)	AXLE LOADS Y (+ IS UP) (KN)	TORSION BAR WIND-UP (DEG)	TRACK TENSION AT LEFT CONTACT POINT (KN)	TRACK TENSION MEAN (KN)	TRACK TENSION AT RIGHT CONTACT POINT (KN)
SPR.	-32.62	-13.039	-4.503		9.407		4.885
						4.885	
1	-1.42	-1.150	2.465	9.29	4.885		4.885
						4.995	
2	2.75	-.070	3.259	13.26	5.106		5.457
						5.913	
3	3.12	-.048	3.864	16.07	6.368		6.776
						7.341	
4	3.29	-.006	4.551	19.39	7.906		8.339
						8.825	
5	.97	18.721	1.754	.00	9.312		9.407
						9.407	
TOTAL		4.408	11.390				

NOTE: THE LOADS IN THIS TABLE ARE FOR ONE SIDE OF THE VEHICLE ONLY.

FRONT UNIT -- SLIP = 20.00 %

			PERCENTAGE OF NORMAL LOAD
GRADE:	.00 DEG	.00 %	
BELLY LOAD:		.00 KN	.00 %
BELLY DRAG:		.00 KN	.00 %
TRACK MOTION RESISTANCE:		.16 KN	.59 %
TOTAL EXTERNAL MOTION RESISTANCE:		.16 KN	.59 %
THRUST:		8.98 KN	32.90 %
HOR. FORCE APPLIED TO REAR HITCH (+ REARWARD):		8.82 KN	32.31 %
VERT. FORCE APPLIED TO REAR HITCH (+ IS DOWN):		-.78 KN	-2.86 %
MOMENT APPLIED TO REAR HITCH (+ IS CW):		.00 KN-M	
TRACTIVE EFFICIENCY:		78.57 %	

CHASSIS TRIM ANGLE (+ IS CW FROM HOR.):	1.91 DEG
LINK TRIM ANGLE (+ IS CW FROM HOR.):	-5.01 DEG
EFFECTIVE RADIUS OF TRACK:	7.10 CM
LOAD ON EXTERNAL SHEAR AREA / TOTAL TRACK LINK LOAD:	48.0 %

REAR UNIT -- SLIP = 20.00 %

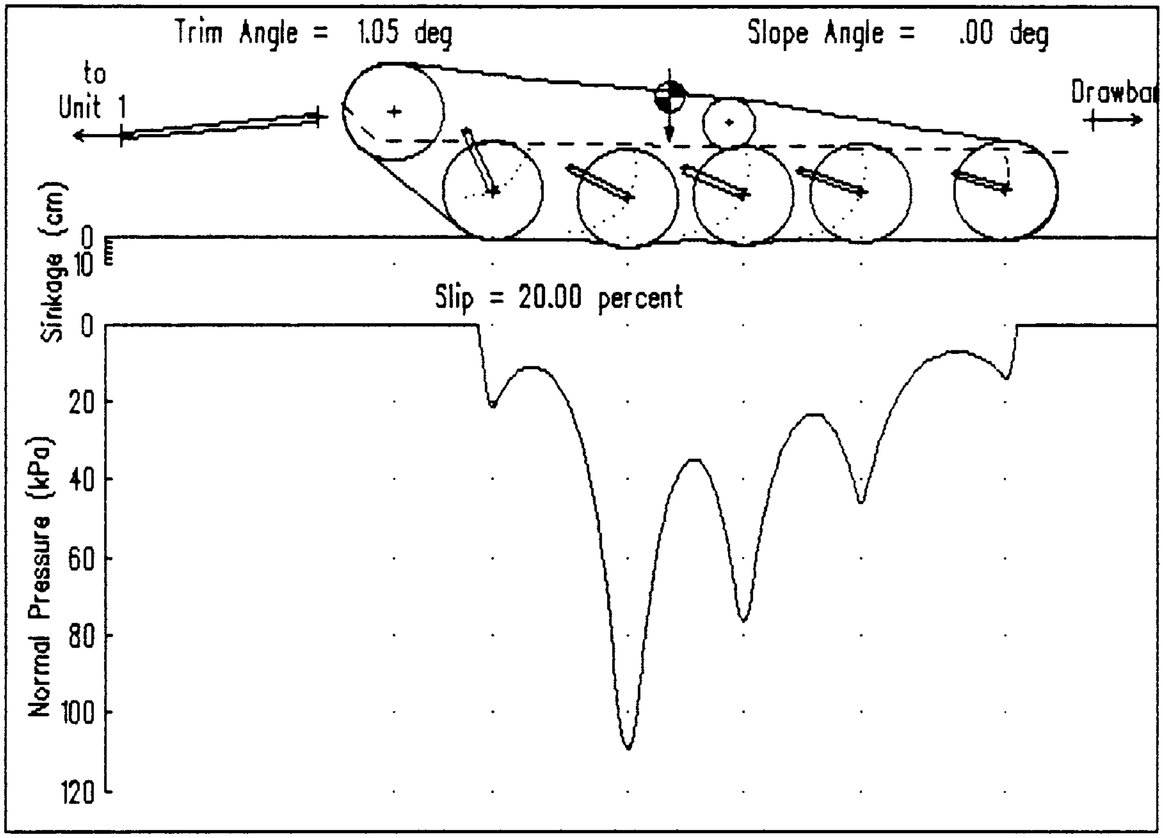

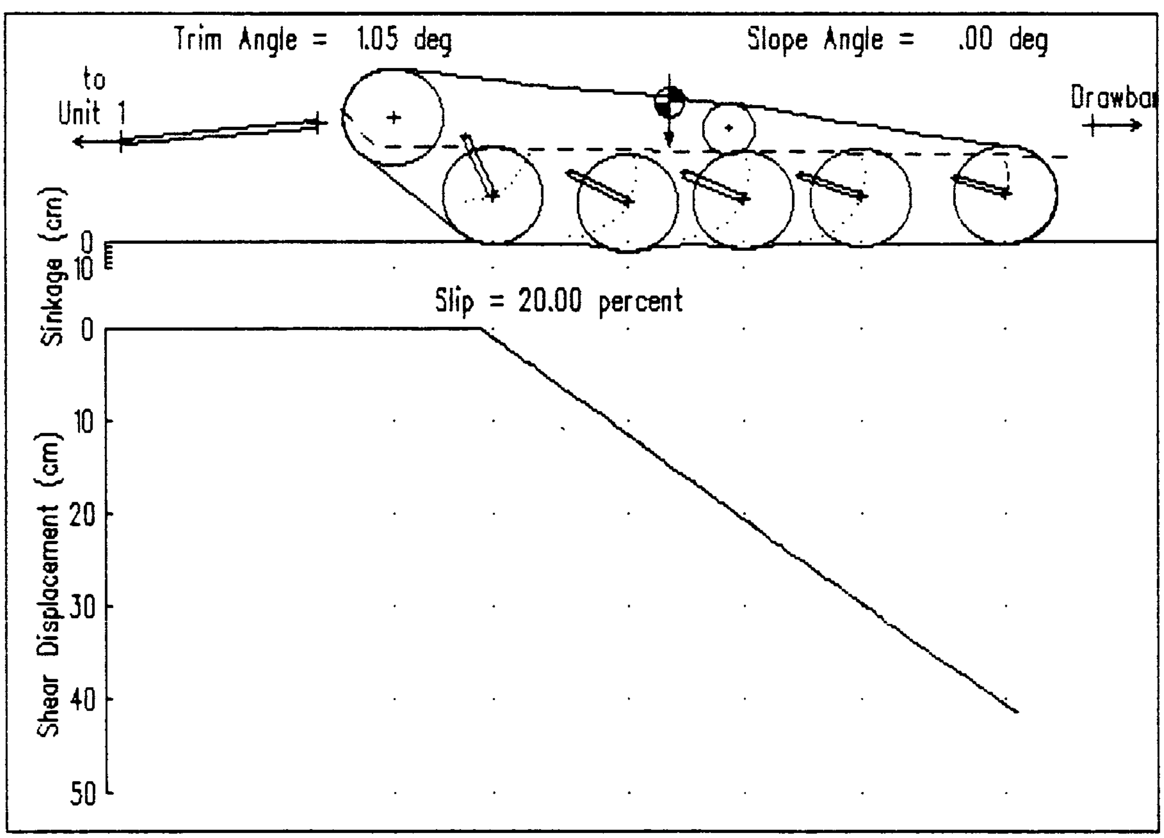

REAR UNIT -- SLIP = 20.00 %

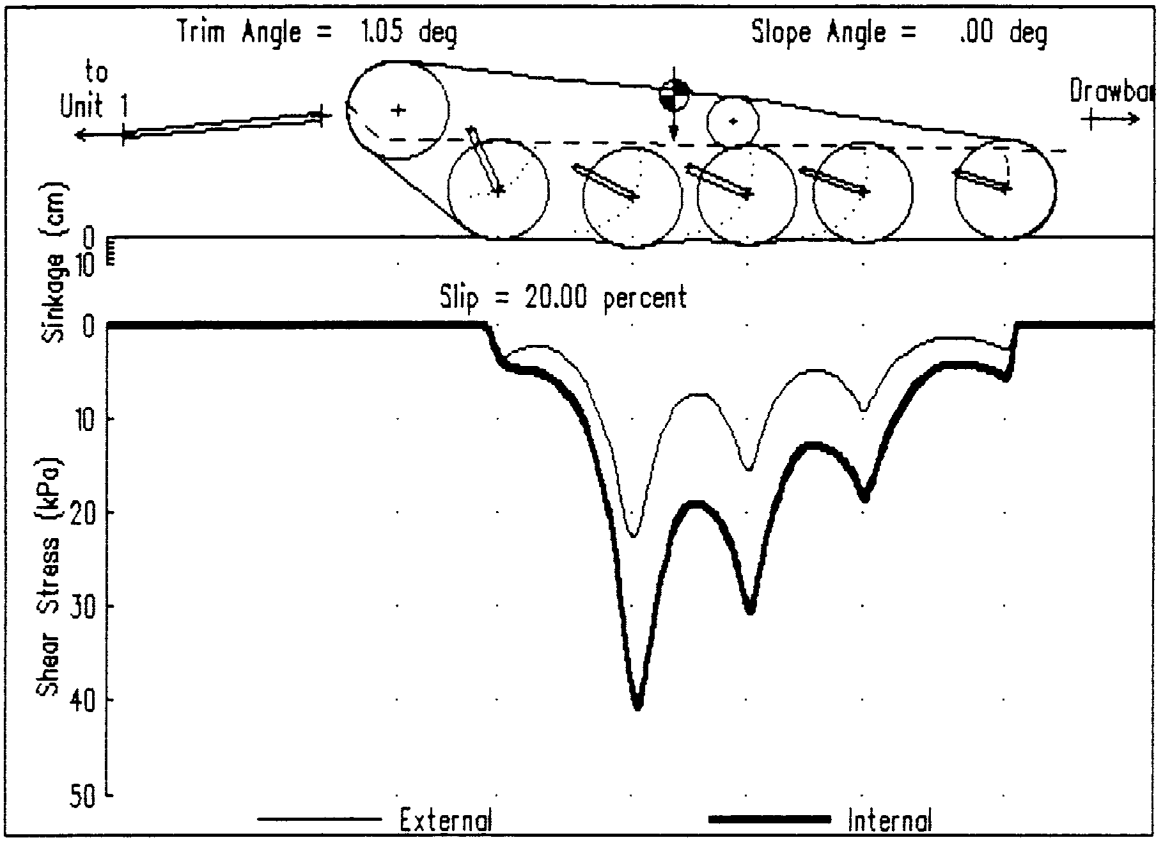

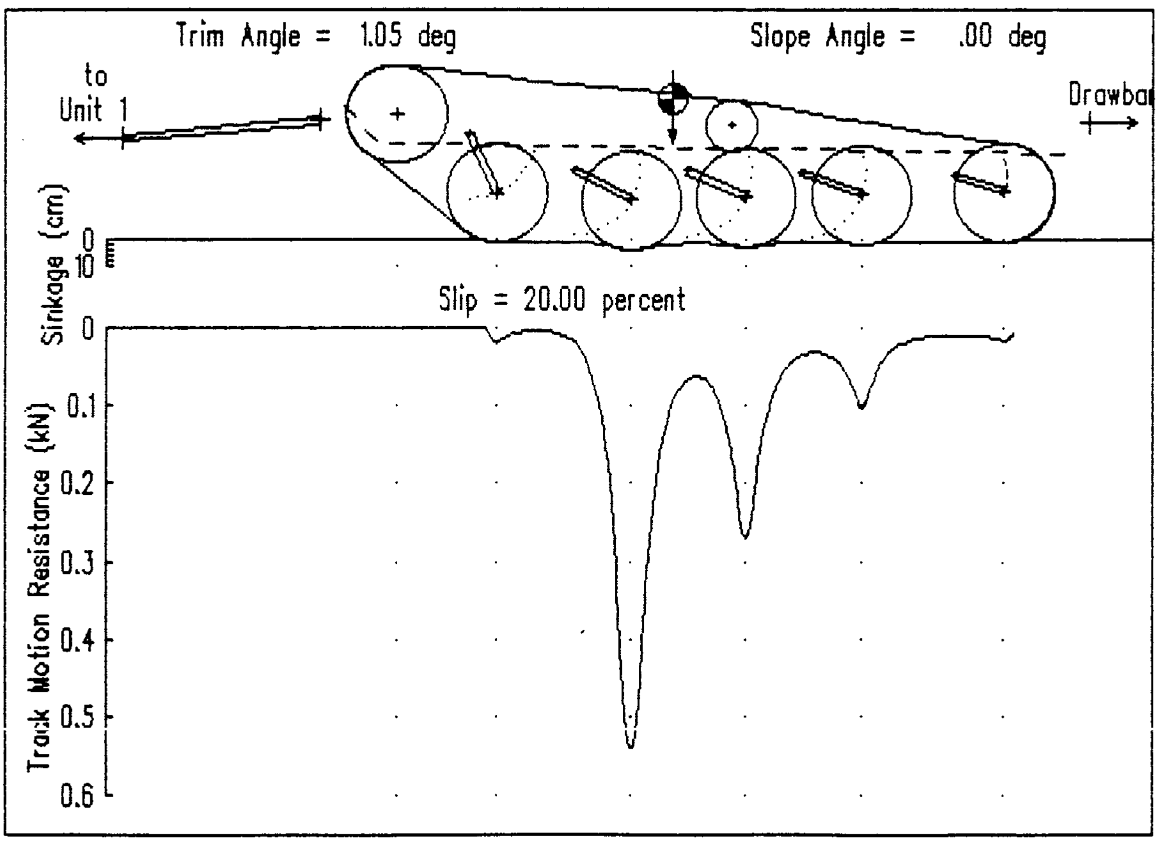

REAR UNIT -- SLIP = 20.00 %

WHEEL	TRACK CONTACT ANGLE		LOADS AT THE WHEEL-TERRAIN INTERFACE		LOADS SUPPORTED BY TRACK BETWEEN WHEELS	
	LEFT (+ IS CW FROM BDC) (DEG.)	RIGHT (+ IS CCW FROM BDC) (DEG.)	X (+ IS FORWARD) (KN)	Y (+ IS UP) (KN)	X (+ IS FORWARD) (KN)	Y (+ IS UP) (KN)
SPR.	187.38	-38.58	.000	.000		
					.000	.000
1	38.58	2.89	.010	.131		
					.310	1.726
2	14.77	13.12	.335	1.303		
					.918	2.464
3	8.97	9.13	.177	.603		
					.714	1.833
4	5.20	5.75	.069	.224		
					.454	1.017
5	1.61	172.62	.030	.062		
TOTAL			.621	2.323	2.396	7.040

NOTE: THE LOADS IN THIS TABLE ARE FOR ONE SIDE OF THE VEHICLE ONLY.

WHEEL	SINK-AGE (CM)	AXLE LOADS X (+ IS FORWARD) (KN)	AXLE LOADS Y (+ IS UP) (KN)	TORSION BAR WIND-UP (DEG)	TRACK TENSION AT LEFT CONTACT POINT (KN)	TRACK TENSION MEAN (KN)	TRACK TENSION AT RIGHT CONTACT POINT (KN)
SPR.	-29.65	-12.294	-4.320		8.280		5.223
						5.223	
1	.70	-1.143	3.202	11.07	5.223		5.242
						5.489	
2	3.57	-.052	3.698	15.43	5.735		6.091
						6.512	
3	2.50	.005	2.363	10.18	6.934		7.111
						7.439	
4	1.51	.008	1.263	5.61	7.767		7.835
						8.044	
5	.46	16.492	.907	-9.00	8.253		8.280
						8.280	
TOTAL		3.016	7.113				

NOTE: THE LOADS IN THIS TABLE ARE FOR ONE SIDE OF THE VEHICLE ONLY.

REAR UNIT -- SLIP = 20.00 %

			Percentage of normal load
GRADE:	.00 DEG	.00 %	PERCENTAGE OF NORMAL LOAD
BELLY LOAD:		.00 KN	.00 %
BELLY DRAG:		.00 KN	.00 %
TRACK MOTION RESISTANCE:		.05 KN	.26 %
TOTAL EXTERNAL MOTION RESISTANCE:		.05 KN	.26 %
THRUST:		6.08 KN	32.47 %
DRAWBAR PULL:		14.85 KN	79.29 %
HOR. FORCE APPLIED TO FRONT HITCH (+ FORWARD):		8.82 KN	47.08 %
VERT. FORCE APPLIED TO FRONT HITCH (+ IS UP):		-.78 KN	-4.17 %
MOMENT APPLIED TO FRONT HITCH (+ IS CCW):		.00 KN-M	
TRACTIVE EFFICIENCY:		79.37 %	

CHASSIS TRIM ANGLE (+ IS CW FROM HOR.):	1.05 DEG
EFFECTIVE RADIUS OF TRACK:	6.29 CM
LOAD ON EXTERNAL SHEAR AREA / TOTAL TRACK LINK LOAD:	61.1 %

PERFORMANCE OF THE ARTICULATED VEHICLE -- SLIP = 20.00 %

GRADE:	.00 DEG	.00 %	PERCENTAGE OF NORMAL LOAD
TOTAL BELLY LOAD:		.00 KN	.00 %
TOTAL BELLY DRAG:		.00 KN	.00 %
TOTAL TRACK MOTION RESISTANCE:		.21 KN	.45 %
TOTAL EXTERNAL MOTION RESISTANCE:		.21 KN	.45 %
TOTAL THRUST:		15.06 KN	32.72 %
TOTAL DRAWBAR PULL:		14.85 KN	32.27 %
TRACTIVE EFFICIENCY:		78.90 %	

SUMMARY

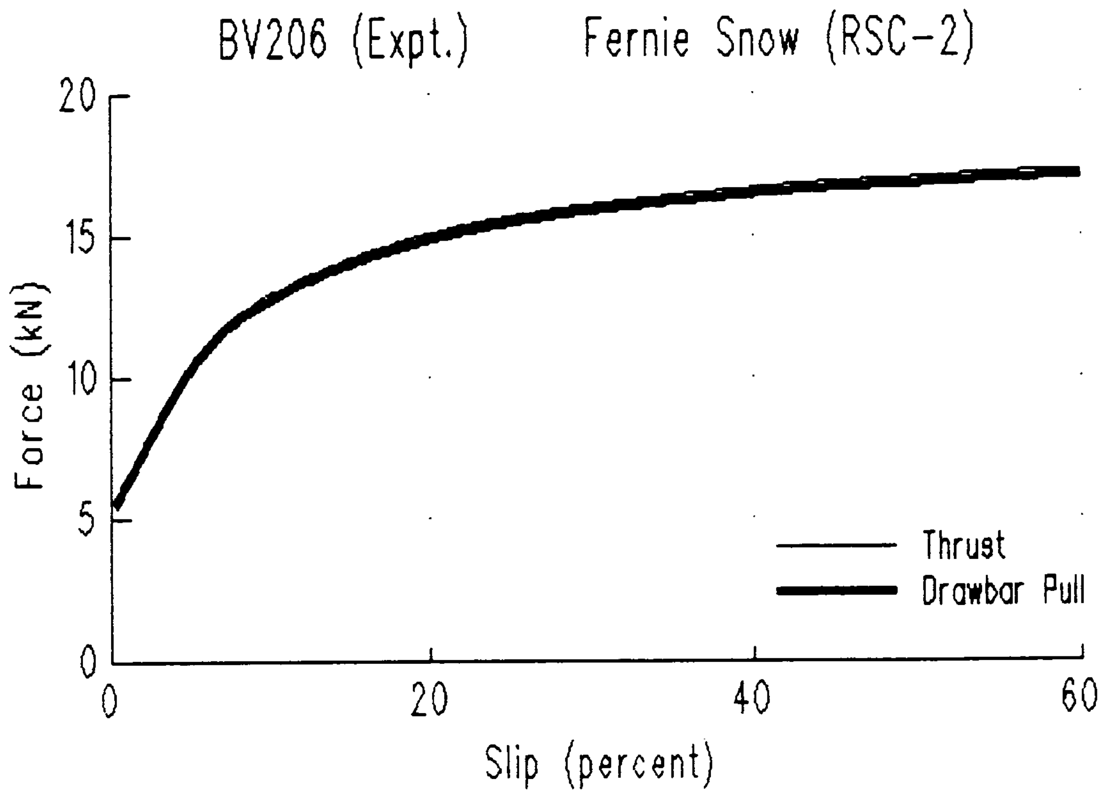
BV206 (Expt.) Fernie Snow (RSC-2)
Force (kN)
Slip (percent)
Thrust
Drawbar Pull
0
5
10
15
20
0
20
40
60

SUMMARY

SLIP (%)	BELLY LOAD (KN)	BELLY LOAD PERCENTAGE OF NORMAL LOAD (%)	BELLY DRAG (KN)	BELLY DRAG PERCENTAGE OF NORMAL LOAD (%)	TRACK MOTION RESISTANCE (KN)	TRACK MOTION RESISTANCE PERCENTAGE OF NORMAL LOAD (%)
2.00	.00	.00	.00	.00	.16	.35
5.00	.00	.00	.00	.00	.18	.39
10.00	.00	.00	.00	.00	.20	.43
20.00	.00	.00	.00	.00	.21	.45
30.00	.00	.00	.00	.00	.21	.46
40.00	.00	.00	.00	.00	.21	.46
60.00	.00	.00	.00	.00	.21	.46

SLIP (%)	THRUST (KN)	THRUST PERCENTAGE OF NORMAL LOAD (%)	TOTAL EXTERNAL MOTION RESISTANCE (KN)	TOTAL EXTERNAL MOTION RESISTANCE PERCENTAGE OF NORMAL LOAD (%)	DRAWBAR PULL (KN)	DRAWBAR PULL PERCENTAGE OF NORMAL LOAD (%)	TRACTIVE EFFICIENCY (%)
2.00	7.44	16.17	.16	.35	7.28	15.82	95.90
5.00	10.43	22.67	.18	.39	10.25	22.27	93.35
10.00	12.90	28.03	.20	.43	12.70	27.61	88.63
20.00	15.06	32.72	.21	.45	14.85	32.27	78.90
30.00	16.05	34.89	.21	.46	15.84	34.43	69.08
40.00	16.64	36.16	.21	.46	16.42	35.70	59.23
60.00	17.27	37.54	.21	.46	17.06	37.08	39.51

NOTE: GRADE = .00 DEG = .00 % FOR ALL SLIPS.

SUMMARY

WHEEL SINKAGES (cm)

SLIP	FRONT UNIT		REAR UNIT	
(%)	FRONT ROADWHEEL	REAR ROADWHEEL	FRONT ROADWHEEL	REAR ROADWHEEL
2.00	-.27	3.42	.78	1.50
5.00	-.69	3.37	.73	1.50
10.00	-1.07	3.33	.71	1.51
20.00	-1.42	3.29	.70	1.51
30.00	-1.58	3.28	.70	1.51
40.00	-1.68	3.27	.70	1.51
60.00	-1.79	3.26	.70	1.51

UNCLASSIFIED

#70566

JUL / JUIL 15 1991

NO. OF COPIES / NOMBRE DE COPIES	COPY NO. / COPIE N°	INFORMATION SCIENTIST'S INITIALS / INITIALES DE L'AGENT D'INFORMATION SCIENTIFIQUE
1	1	JC
AQUISITION ROUTE / FOURNI PAR ▶	DRES	
DATE ▶	02 JULY 1991	
DSIS ACCESSION NO. / NUMÉRO DSIS ▶	91-03375	

DND 1158 (6-87)

National Defence / Défense nationale

PLEASE RETURN THIS DOCUMENT TO THE FOLLOWING ADDRESS:

DIRECTOR
SCIENTIFIC INFORMATION SERVICES
NATIONAL DEFENCE
HEADQUARTERS
OTTAWA, ONT. - CANADA K1A 0K2

PRIÈRE DE RETOURNER CE DOCUMENT À L'ADRESSE SUIVANTE:

DIRECTEUR
SERVICES D'INFORMATION SCIENTIFIQUES
QUARTIER GÉNÉRAL
DE LA DÉFENSE NATIONALE
OTTAWA, ONT. - CANADA K1A 0K2

UNCLASSIFIED